EXPLORATION OF APORPHINES AS MDMA ANTAGONISTS

AND AChE INHIBITORS

by

STEVAN PECIC

A dissertation submitted to the Graduate Faculty in Biochemistry in partial fulfillment of the requirements for the degree of Doctor of Philosophy

The City University of New York

2010

This manuscript has been read and accepted for the
Graduate Faculty in Biochemistry in satisfaction of the dissertation
requirement for the degree of Doctor of Philosophy.

Dr. Wayne W. Harding

Date	Chair of Examining Committee

Dr. Edward J. Kennelly

Date	Executive Officer

Dr. Vanya Quinones

Dr. Akira Kawamura

Dr. Shaneen Singh

Dr. Maarten Reith
Supervision Committee

THE CITY UNIVERSITY OF NEW YORK

Abstract

Exploration of Aporphines as MDMA Antagonists

and AChE Inhibitors

by

Stevan Pecic

Advisor: Dr. Wayne W. Harding

PART A

MDMA (3,4-methylenedioxy methamphetamine) is a psychoactive drug which is thought to act via stimulation of secretion as well as inhibition of re-uptake of large amounts of serotonin, noradrenaline and dopamine in the brain. MDMA also acts directly on a number of receptors, including 5-HT_{2A} receptors. There is considerable evidence that 5-HT_{2A} antagonists can modulate behavioral and physiological effects of MDMA in animals.

Nantenine an aporphine alkaloid ex *Nandina domestica* has been reported to block and reverse a range of behavioral and physiological effects of MDMA in mice. It is known that nantenine has moderate 5-HT_{2A} antagonist activity. However, very little structure-activity relationship (SAR) studies have been performed on nantenine with regards to its activity at the 5-HT_{2A} receptor.

As part of our research focus to develop aporphine-based 5-HT_{2A} antagonists as potential MDMA antagonists, we have prepared a library of novel analogs to investigate the structural requirements for nantenine's 5-HT_{2A} activity. Our studies demonstrate that

the N-methyl group, methylenedioxy ring and structural rigidity of the aporphine nucleus are important for activity, and that appropriate substitutions on the aromatic aporphine core can improve 5-HT_{2A} antagonist activity.

To elucidate possible binding modes of these compounds and to determine the correlation with our binding data, we built a 5-HT_{2A} homology model based on a bovine rhodopsin template and then performed docking/scoring experiments.

Our results suggest that members of the C1 series of nantenine analogs bind to the 5-HT_{2A} receptor in the same orientation but differently than nantenine. In addition to known and important interaction between the protonated nitrogen of the ligands and Asp155 of the receptor, some of these analogs established a hydrogen bond with Ser242 as well as hydrophobic interactions with Phe234 and Gly238. These latter interactions may account for their enhanced activity as compared to nantenine.

Our findings will be useful in the future design of high affinity 5-HT_{2A} ligands based on the nantenine aporphine core structure.

PART B

For the second part of the project, nantenine as well as a number of flexible analogs were evaluated for acetylcholinesterase (AChE) inhibitory activity in a microplate spectrophotometric assays based on Ellman's method. It was found that the rigid aporphine core of nantenine and *N*-methyl substituent are important structural requirements for its anticholinesterase activity. Nantenine showed mixed inhibition kinetics in enzyme assays. Molecular docking experiments suggest that nantenine binds

preferentially to the catalytic site of AChE but is also capable of interacting with the peripheral anionic site (PAS) of the enzyme thus accounting for its mixed inhibition profile. The aporphine core of nantenine may thus be a useful template for the design of novel PAS or dual-site AChE inhibitors; inhibiting the PAS is desirable for prevention of aggregation of the amyloid peptide Aβ a major causative factor in the progression of Alzheimer's disease (AD).

Acknowledgments

I would like to take this opportunity to thank my mentor, Dr. Wayne W. Harding, for his guidance and assistance during my past five years of doctoral studies. His encouragement and support helped me to work as an independent researcher.

I am also grateful to Dr. Vanya Quinones, Dr. Akira Kawamura, Dr. Shaneen Singh and Dr. Maarten Reith for serving on my doctoral committee. I am very grateful to them for their time, great inputs and providing me with valuable advice and suggestions given their individual areas of expertise.

I would like to thank our collaborators, Dr. William E. Fantegrossi, Dr. Hérnan A. Navarro and Dr. Boojala Vijay B. Reddy.

I would also like to express my gratitude to my colleagues and friends at the Chemistry Department at Hunter College for their kind help, encouragement, support and friendship throughout this challenge. Especially I need to thank Professor Klaus Grohmann for not only being my graduate advisor, but also for his valuable professional and personal advice.

Additional thanks go to George Solotchi, for his help with teaching and preparing the procedures for labs and to Dr. Matthew Devany, for his help with NMR.

I also wish to express my warmest thanks to my parents, Ljubinka and Zarko, for their support and appreciation for my studies.

Finally, I am deeply grateful to my wife Jelena for sharing her life with me.

The thesis is dedicated to my parents.

Овај рад посвећујем својим родитељима.

Table of Contents

List of Figures

CHAPTER 1

CHAPTER 3

CHAPTER 3 – Appendix

CHAPTER 4

CHAPTER 4 – Appendix

List of Schemes

CHAPTER 2

CHAPTER 3

CHAPTER 4

List of Tables

CHAPTER 1

CHAPTER 2

CHAPTER 3

CHAPTER 4

Abbreviations

5-HT	5-hydroxytryptamine, serotonin
AChE	acetylcholineesterase
AcOH	acetic acid
AD	Alzheimer's disease
APP	amyloid precursor protein
Asn, N	asparagine
Asp, D	aspartic acid
BACE1	β-site APP cleaving enzyme, β-secretase
BOC	*t*-butoxycarbonyl
BLAST	Basic Local Alignment Search Tool
BRho	bovine rhodopsin
BuChE	butyrylcholinesterase
CDI	1,1`-carbonyldiimidazole
CHO	Chinese hamster ovary
CNS	central nervous system
DAT	dopamine transporters
DCM	dichloromethane, methylene chloride
DEA	Drug Enforcement Agency
DMA	N,N-dimethylacetamide
DMAP	4-(dimethylamino)pyridine
DME	1,2-dimethoxyethane
DMF	dimethylformamide

DMSO	dimethyl sulfoxide
DOR	delta opioid receptor
ee	enantiomeric excess
ESI-MS	electrospray ionization mass spectrometer
FLIPR	fluorometric imaging plate reader
GA	Genetic Algorithm
Gly, G	glycine
GPCR	G-protein-coupled receptor
IBS	irritable bowel syndrome
ICM	Internal Coordinate Mechanics
KOR	kappa opioid receptor
HAda2a	human adenosine A2A receptor
HAdrb2	human β2-adrenergic receptor
HPLC	high-performance liquid chromatography
HTR	head twitch response
MC	Monte Carlo
MDA	3,4-methylenedioxyamphethamine
MDMA	3,4-methylenedioxy-N-metamphetamine
MOR	mu opioid receptor
NET	norepinephrine transporters
NIDA	National Institute on Drug Abuse
PAS	peripheral anionic site
PDB	Protein Data Bank

PDSP	Psychoactive Drug Screening Program
Phe, F	phenylalanine
PIFA	phenyliodine bis-trifluoroacetate
RMSD	root-mean-square deviation
SAR	structure-activity relationship
SAVES	Structural Analysis and Verification Server
Ser, S	serine
SERT	serotonin transporters
SET	single-electron transfer mechanism
SRho	squid rhodopsin
TAdrb1	turkey β1-adrenergic receptor
TFA	trifluoroacetic acid
THF	tetrahydrofuran
TM	transmembrane
TMSCl	*t*-methylsilyl chloride
Trp, W	tryptophan
Tyr, Y	tyrosine
Val, V	valine
ZEGA	Zero Gap
Zrms	Z-score RMS
Zsm	Z-score standard mean
Zstd	Z-score standard deviation

CHAPTER 1: Introduction

1.1 MDMA

MDMA (3,4-methylenedioxy-N-methyl amphetamine), most commonly known by the street names Ecstasy, E, X, or XTC (Figure 1.1) is a semi-synthetic derivative of the phenethylamine family, whose primary effect is stimulating secretion and inhibiting re-uptake of large amounts of serotonin, dopamine and norepinephrine in the brain.[1] MDMA also acts directly on a number of receptors, including α_1-adrenergic and 5-HT_{2A} receptors.[2] According to the 2008 National Survey on Drug Use and Health, 2.1 million Americans age 12 and older had abused "Ecstasy" at least once in the year prior to being surveyed.[3]

Like amphetamine, MDMA is a synthetic substance that does not exist in nature. Both were synthesized many decades ago: amphetamine in 1885 and MDMA in 1912 by a German pharmaceutical firm; the intention was apparently to market MDMA as an appetite inhibitor.[4] In the 1950s, the US military added it to a long list of experimental substances as a possible brainwashing and/or chemical agent.[5] Its rediscovery in the late 1970s is probably due to popularity in the "rave" subculture, because MDMA and related drugs enhance energy, endurance, sociability and sexual arousal.[6] Numerous psychiatric literatures in the 1980's reported that MDMA may have been used as a possible adjunct to psychotherapy.[7] In 1985 it was shown that MDMA and its demethylated metabolite 3,4-methylenedioxyamphetamine (MDA) had long-term neurotoxic effects in laboratory animals. As a result of the study and concern over MDMA's increasing recreational use, the Drug Enforcement Agency (DEA)[8] placed MDMA in Schedule I.[9] MDMA is almost

always taken orally and is prepared as single-dose tablets, stamped with a wide variety of symbols according to the imagination of the maker.[1]

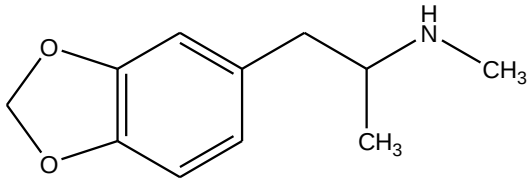

MDMA

Figure 1.1 Chemical structure of MDMA

Based on statistical data provided by National Institute on Drug Abuse (NIDA), the most commonly used illegal drug in the US is marijuana, having more than ten times more users than the MDMA. Cocaine, the second abused drug in US, has much more serious adverse effects and almost double more users comparing with MDMA.[3] Still the availability, attractive design and some short-term "desired" effects of MDMA, place this illicit drug in the top list of popularity among high-school students.[8]

1.1.1 The Effects of MDMA

After 15-30 minutes upon oral intake, *the acute effects* of MDMA become apparent. The first symptoms are anxiety, tachycardia, and elevated blood pressure.[10] They are followed by bruxism, paresthesias, dry mouth, increased psychomotor activity, and blurred vision. Within the first hour upon MDMA intake, these sympathomimetic effects are mostly replaced by feelings of relaxation, euphoria, and increased empathy and communication. These effects last for up to 90 minutes and then decrease over the next 3 to 6 hours.[10] *The desired effects* for which MDMA is used are closely similar to those that account for the continuing popularity of other amphetamines. *Physically*, it

produces a marked increase in wakefulness, endurance and sense of energy, sexual arousal, and postponement of fatigue and sleepiness. The accompanying *psychological effects* are described as a sense of euphoria, well-being, sharpened sensory perception, greater sociability, extraversion, heightened sense of closeness to other people, and greater tolerance of their views and feelings.[1] The latter effects have given rise to the claim that MDMA represents a distinct class of drugs designated “empathogens” or “entactogens” that may be of potential value as an aid in psychotherapy.[11] However, no comparable study has been conducted on patients treated with MDMA, and the recent clinical literature contains almost no reference to its use in psychotherapy.[1] Many users attempt to prolong these “desired effects“ by taking additional doses of the drug. However, when too much addional MDMA is consumed in a single session, individuals report unpleasant symptoms of autonomic hyperarousal associated with feelings of restlessness, paranoia, and anxiety.[10] Tolerance to the psychoactive properties of MDMA develops rapidly, and the user is unable to restore the euphoric effects with repeated doses. Instead, sympathomimetic effects predominate, placing the patient at risk for cardiovascular instability, arrhythmias, and hyperthermia. In addition, following the acute effects of MDMA, users often report a 24- to 48-hour period characterized by lethargy, anorexia, and dysphoria. This period of lethargy is known as “the blues” and is dangerous because other drugs often are co-ingested to help ease the "crash" after psychostimulant administration.[10] Like amphetamines, MDMA also has *adverse effects* on many physical functions, even when taken in moderate doses for the recreational purposes described earlier. Because the basic action of the amphetamines involves increased arousal and alertness, it is usually accompanied by an increase in tension, which is manifested

physically as muscular tension, jaw clenching, nausea, blurred vision, faintness, tooth grinding (bruxism) and constant restless movement of the legs.[1] The increased muscle activity, together with the drug's direct effect on the thermoregulatory system in the brain, leads to an increase in body temperature. The occurrence of hyponatremia after MDMA use is multifactorial, stemming from increased water intake, excessive sweating with physical exertion, and the release of vasopressin leading to the syndrome of inappropriate antidiuretic hormone secretion (SIADH).[12] Various cases of seizure and death secondary to hyponatremia have been reported. Undesired *psychological acute effects* commonly reported during the drug experience similarly represent an exaggeration of the effects for which the drug is taken. These effects include confusion, depression, sleep problems (insomnia), drug craving, severe anxiety, paranoia, agitation, panic attacks, and delirium.[1] MDMA has similar stimulant properties as methamphetamine (known by street name "crystal meth") and the use of MDMA can cause also similar serious organ failure, hospitalization and in extreme cases, death.[13-16]

The long-term effects of MDMA include massive serotonin release. Numerous case reports link MDMA toxicity to serotonin syndrome. Serotonin syndrome is a condition in which central 5-HT receptor hyperstimulation results in classic findings of hyperthermia, mental status changes, autonomic instability, and altered muscle tone and/or rigidity.[7,10] Hyperthermia can in turn lead to heart failure, hypertension, muscle degeneration and renal failure.[17,18] The long term effects after the use of MDMA are all adverse. They are all thought to arise from a neurotoxic action of the methylenedioxy derivatives of the amphetamines.[19] The ability of MDMA to increase the concentration of serotonin in the synapse probably underlies its production of improved mood and of

sensory alterations. However, at higher doses the massive release of serotonin not only gives rise to acute psychotic symptoms (as described earlier) but also causes chemical damage to the cells that released it.[1,20] Chemical and microscopic studies have shown reduced serotonin content of the brain, decreased numbers of identifiable serotonin-containing neurons and serotonin transporter molecules, and numerous degenerating serotonergic axons and axon terminals in the brains of animals treated with MDMA.[21,22] It has been suggested that the demonstrated neurotoxic effects of MDMA on the serotonin system may be the possible cause of a variety of mental and behavioural problems that outlast the actual drug experience by months or years.[1] Patients have reported symptoms of depression, anxiety, panic attacks, and insomnia after ending MDMA use. Further studies report that patients using MDMA have difficulty concentrating and exhibit short-term memory impairment.[23]

Addiction: Several reports[24-26] have pointed to the addictive properties of MDMA. A survey of MDMA users found that 43 percent of those who reported "ecstasy" use met the accepted diagnostic criteria for dependence, withdrawal effects and tolerance, and 34 percent met the criteria for drug abuse.[3]

Although, one of the most cited significant mechanisms for MDMA-induced toxicity is a release of serotonin via serotonin transporters, still this postulate does not clarify completely the apparent mechanism. Several groups tried to correlate MDMA high efficacy for serotonin neurons with its neurotoxicity.[27-30] The most noticeable findings were reductions in the level of brain serotonin, 5-hydroxyindoleacetic acid (serotonin`s major metabolite), the serotonin transporters and tryptophan hydroxylase. These results suggested that exposure to MDMA will lead to serotonin neurotoxicity.[31]

Findings that selective effects of MDMA on serotonin neurons are species-dependent[19,32], led to even more controversy. Other mechanism had been also proposed, including carrier-dependant transport of MDMA[33], metabolic toxic products[34], oxidative stress[35], hyperthermia, apoptosis[36] and increased extracellular concentrations of dopamine and serotonin.[27] Even though, there are many incomplete evidences and missing data, still the conventional hypothesis, that MDMA is toxic to human serotonin neurons due to high-selective affinity of MDMA for serotonin transporters, is explored the most.

Clearly, MDMA is a dangerous drug that displays many adverse physiological and cognitive effects.

1.1.2 MDMA - Pharmacology

The typical dose range of MDMA for recreational use varies from 50 to 150 mg. MDMA is readily absorbed from the intestinal tract and reaches its peak concentration in the plasma about 2 hours after oral administration.[37] The drug is broken down metabolically, mainly in the liver. Elimination of the drug from the body is moderately slow, and some of the metabolites of MDMA are still pharmacologically active, so that the duration of action may be somewhat longer than the duration of MDMA itself in the body. This may explain the persistence of troublesome after-effects for one or two days after use.[1] There is now a lot of evidence, both experimental and clinical, that MDMA and the other ring-substituted amphethamine derivatives act by increasing the net release of the monoamine neurotransmitters (serotonin, noradrenaline and, to a smaller extent, dopamine) from their axon terminals.[1,12] MDMA does not act by directly releasing serotonin but, rather, by binding to, and reversing the normal directional flow of the

transporter involved in its reuptake.[1] Recent experiments show that MDMA self-administration is abolished in serotonin transporter (SERT) knockout mice.[38] Additionally, rats trained to discriminate between the effects of saline and those of serotonin in an operant task, respond to MDMA as if it were serotonin.[39]

It is clear however, that the increase in the net release of serotonin (and possibly dopamine) is the major mechanism of action underlying the distinctive mental effects of MDMA, whereas the increased release of noradrenaline is mainly responsible for the physical effects that it shares with amphetamine.[1] It has been shown that 5-HT receptors mediate the effects of MDMA such as hallucinations, mood and hyperactivity.[40] Activation of 5-HT_{2A} receptors by direct agonists raises body temperature and produces hallucinations in humans.[41] Dopamine receptors mediate stimulant effects of MDMA.[42] MDMA releases dopamine directly by reversing the action of dopamine transporters, and indirectly by activation of the 5-HT_{2A} receptors.[43,44] This released dopamine will produce similar euphoric effects as other psychostimulants (cocaine, amphethamine, etc) are producing.[40]

1.2 G-Protein-Coupled Receptors

The G-protein-coupled receptor (GPCR) superfamily forms the largest family of receptors in the cell, plays an important role in many physiological and pathophysiological processes, and is responsible for mediating the effects of over 50% of drugs on the market today.[45] GPCRs are integral membrane proteins characterized by the presence of seven α-helical hydrophobic domains, having an intracellular C-terminal and an extracellular N-terminal, three intracellular loops, and three extracellular loops.

Mammalian GPCRs are grouped into three major families: family A (rhodopsin-like or adrenergic-receptor-like family), family B (glucagon-receptor-like or secretin-receptor-like family), and family C (metabotropic glutamate receptors).[46] Within each family a certain sequence pattern (so-called fingerprint) and several structural features beyond the generally shared membrane topology are conserved.[47] Family A is by far the largest, displaying short amino-terminal tails and having highly-conserved amino acid residues within each transmembrane helix. Members of the GPCR superfamily can be activated by a wide range of small molecules.[48] Activation of the GPCR results in a conformational change followed by a signal cascade that passes information to the inside of the cell via interaction of the receptor with G-proteins. The ligand binding site is localized within the seven transmembrane (7TM) region.[49] The high-resolution crystal structures of five GPCRs are currently available: bovine rhodopsin (PDB code: 1U19), squid rhodopsin (PDB code: 2Z73), human β2-adrenergic (PDB code: 2RH1), human adenosine A2A (PDB code: 3EML) and turkey β1-adrenergic receptor (PDB code: 2VT4).

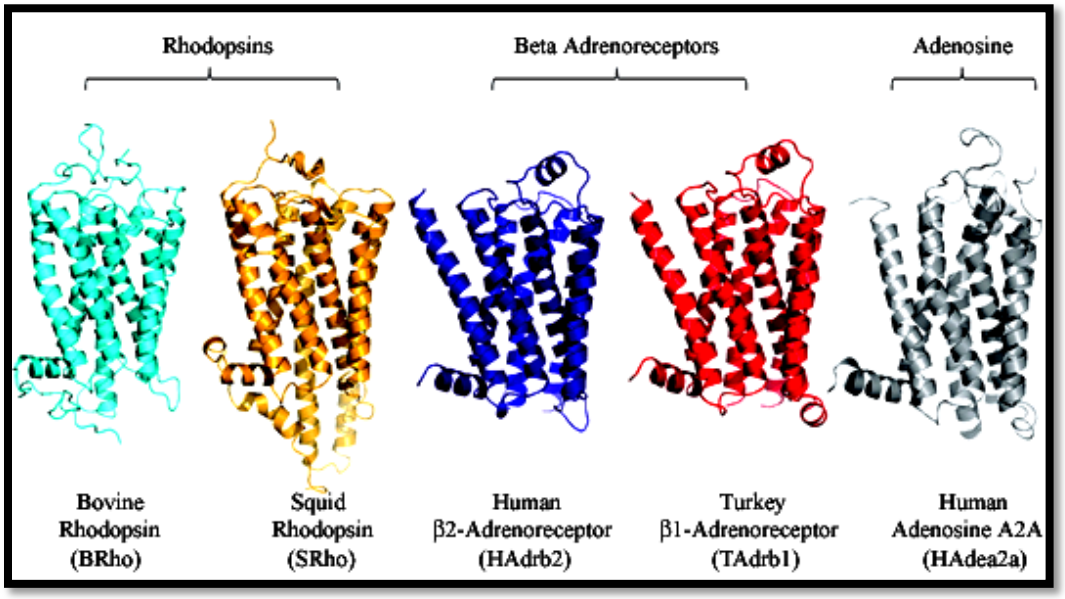

Figure 1.2 Resolved GPCRs crystal structures and subfamilies they belong (Mobarec et al, *J Med Chem* **2009**, *52*, 5207-5216)

1.2.1 Serotonin (5-HT) Receptors: Structure and Function

At present there are at least seven classes of serotonin (5-HT) receptors, 5-HT_1 to 5-HT_7 based on pharmacology, amino acid sequences, gene organization and second messenger coupling pathways.[50] The 5-HT receptors are classified into subfamilies dependent upon operational, transductional and structural characteristics. All of the known serotonin receptors with the exception of the 5-HT_3 receptors (which are ligand-gated ion channels) belong to the superfamily of GPCRs.[51] Over the past few years, all of the 5-HT receptor subtypes have been cloned and sequenced.[52-57]

The 5-HT_1 family is divided in five subfamilies: 5-HT_{1A}, 5-HT_{1B}, 5-HT_{1D}, 5-HT_{1E} and 5-HT_{1F}. Preclinical studies showed that agonists at these receptors have antiaxiety and antidepressant properties,[58] while 5-HT_{1A} receptor antagonists may be of benefit in weight reduction.[59]

Serotonin 5-HT_2 receptors were first identified in 1979 and at present there are three known 5-HT_2 receptor subpopulations, 5-HT_{2A}, 5-HT_{2B}, and 5-HT_{2C}. This subfamily of serotonin receptors utilize a phospholipase C second messenger system (Figure 1.3).[60] Today, there is evidence that 5-HT_2 receptors might be involved in schizophrenia, depression, anxiety, appetite control and cardiovascular function.[61,62]

As we mentioned above 5-HT_3 receptors do not belong to GPCRs; they are nonselective Na^+/K^+ ion channel receptors, found in both, periphery and in the CNS. 5-HT_3 receptors have high structural and functional similarity to nicotinic acetylcholinergic receptors[63] and it was found that they modulate release of serotonin, but also dopamine, acetylcholine and GABA.[64]

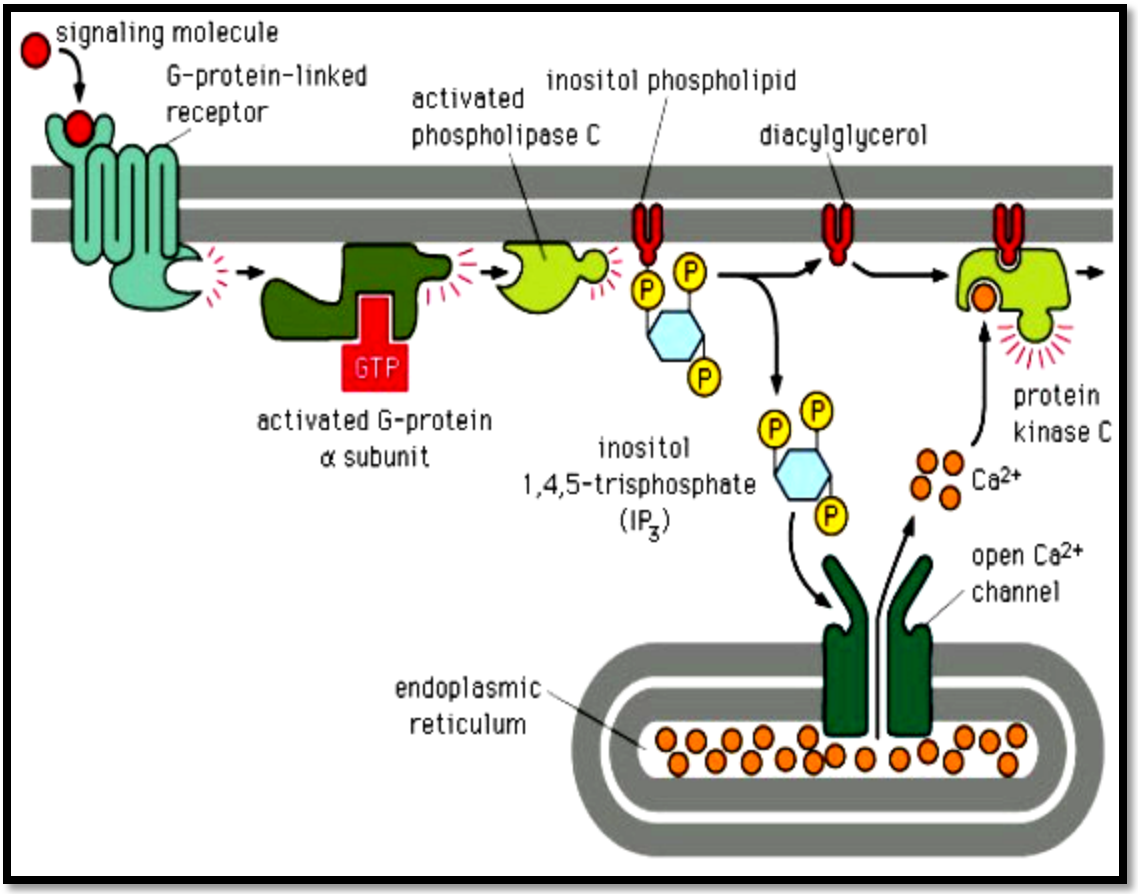

Figure 1.3 Mechanism of receptor-mediated activation of phospholipase C (http://nlp.postech.ac.kr/Research/POSBIOTM/content/common.html)

5-HT_4 receptors belong to recently discovered serotonergic receptors, having low transmembrane sequence homology (<50%) with other serotonin receptors. They are mostly localized in the brain on neurons, and probably responsible for slow excitatory responses to the neurotransmitter serotonin.[65]

Two types of 5-HT_5 receptors have been identified: 5-HT_{5A} and 5-HT_{5B} receptors; but only 5-HT_{5A} in humans.[66] Immunolabelling studies have revealed a potential autoreceptor function and possible role in circadian rhythm control.[67]

The 5-HT_6 receptor was first cloned in 1993.[68] It has been known that human 5-HT_6 receptors are positively coupled to adenylate cyclase second messenger pathway. These receptors are predominantly expressed in the central nervous system.[69]

Four different isoforms of 5-HT_7 receptor have been identified: 5-HT_{7a}, 5-HT_{7b}, 5-HT_{7c} and 5-HT_{7d}. These receptors are mainly expressed in the CNS.[70]

The direct determination, by X-ray crystallography or electron microscopy, of the atomic structure of any member of serotonin family of membrane proteins has not yet been achieved. For the moment, useful structural insights can be obtained by combining sequence and other information with the high-resolution of several GPCRs for which crystal structures are currently available.

1.2.2 Serotonin Receptors: Clinical Implications

Serotonin agonists and antagonists for different 5-HT receptor subfamilies are useful drug targets for the treatment of numerous diseases, and many of them are already commercially available for clinical use.

Current evidence indicates that the 5-HT_1 receptor family might be involved in sleep, impulsivity, alcoholism, sexual behavior, appetite control, thermoregulation and cardiovascular function.[61] The most well-known clinically available compounds (Figure 1.4) are the 5-HT_{1A} receptor agonist buspirone (an antidepressant), and the 5-HT_{1D} receptor agonist sumatriptan (for treatment of migraine).

5-HT_2 receptor family is divided into three subfamilies and these receptors appear to play a role in thermoregulation and sleep, and might be involved in appetite control and learning.[61] Along with other serotonergic receptors they are involved also in cardiovascular function and muscle contraction. Ketanserin, ritanserin and spiperone (Figure 1.4), all 5-HT_{2A} receptor antagonists, are already marketed for treatment of

different psychoses.[71] Clozapine, the tricyclic antipsychotic, also binds at 5-HT_{2A} receptors.[72]

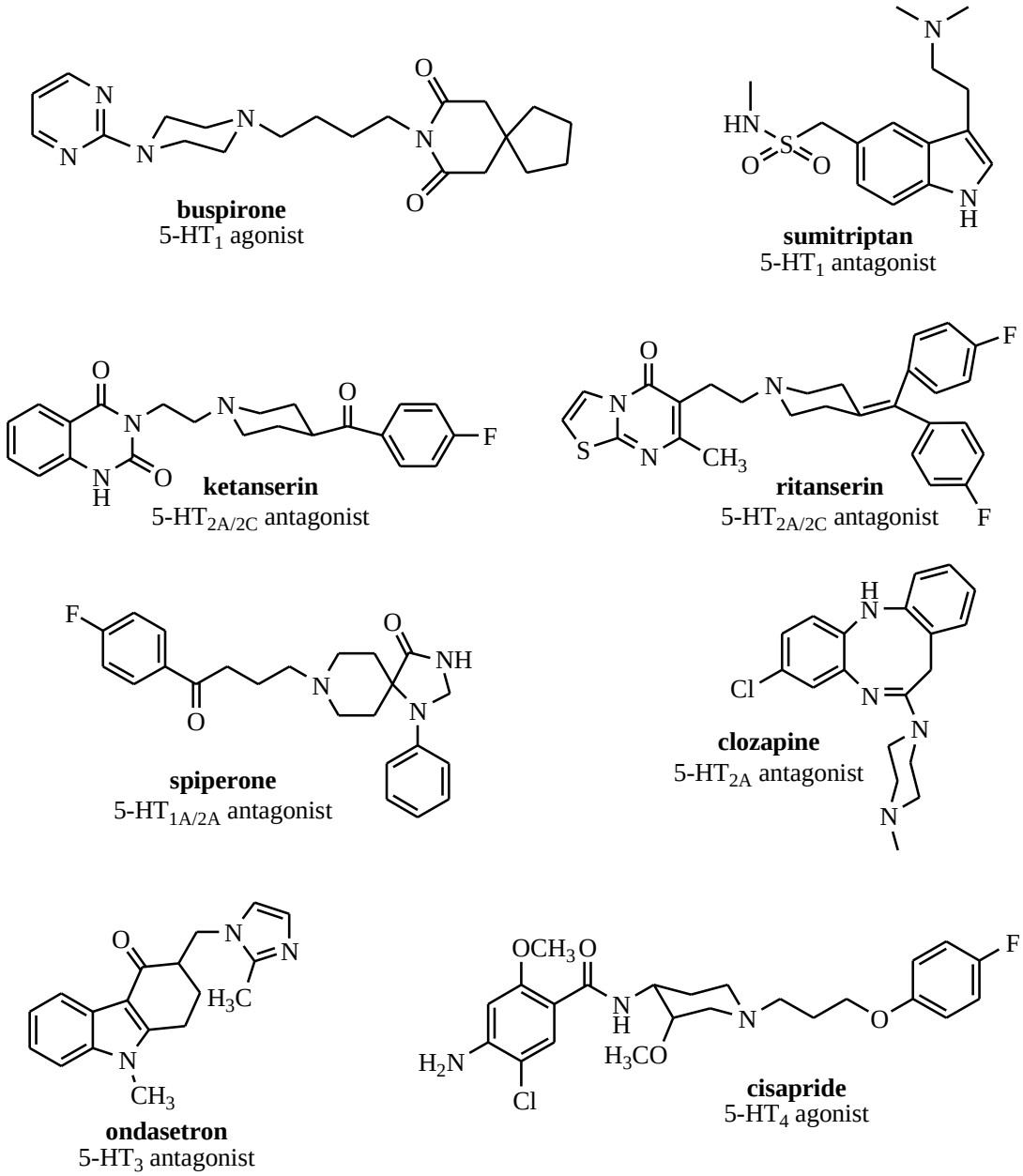

Figure 1.4 Clinically available 5-HT agonists and antagonists

Preclinical studies suggest that 5-HT_3 receptor antagonists may enhance memory and thus may be useful in the treatment of dementia.[73] Antagonists at these receptors have already been used clinically as antiemetics (eg. Ondasetron- Zofran®).[74]

Some of the 5-HT_4 receptor agonists also have clinical uses, eg. Cisaprid - currently being used for the treatment of irritable bowel syndrome (IBS).[75]

Corbett et al. have been reported in 2005 the first selective 5-HT_{5A} receptor antagonist SB-699551-A, being at least 30-fold more selective for this receptor than for the other 5-HT receptor subtypes.[76] A number of experimental and clinical findings have provided evidence for a relationship between this receptor and sleep disturbances.[67] It is also speculated that 5-HT_{5A} receptors are implicated in schizophrenia.[77] Further studies are required to investigate these possibilities.

The brain selective location of 5-HT_6 receptor suggested that this receptor may have potential therapeutic utility for anxiety, depression, schizophrenia, epilepsy, obesity and most importantly cognitive dysfunction.[78] Recently many research efforts in this area led to the discovery of a number of potent and selective 5-HT_6 receptor antagonists. SAM-531 is already in Phase IIb clinical trials in people with mild to moderate Alzheimer's.[79] Continued clinical research will further explore the potential utility of ligands at this receptor for the treatment of Alzheimer's disease, schizophrenia and other cognitive disorders.

The therapeutic potential of 5-HT_7 agonists is treatment of hypertension and use as analgesics (AS-19).[80] Some 5-HT_7 antagonists (SB-258719) can be used as antidepressants, antimigraine agents, analgesics, and for the treatment of IBS.[81]

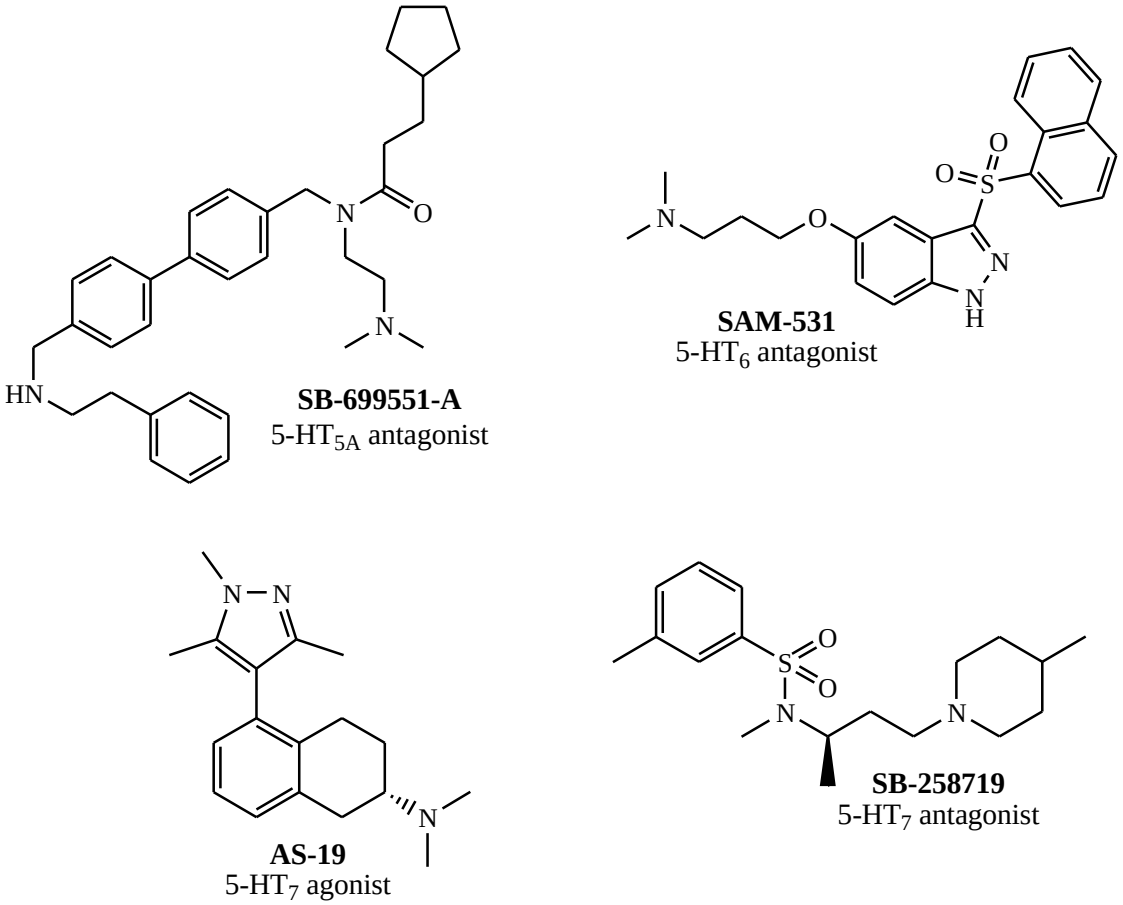

Figure 1.5 Selective ligands for the 5-HT_5, 5-HT_6 and 5-HT_7 receptors

1.3 The 5-HT_{2A} Receptor: Structure, Pharmacophore and Ligands

Previous receptor modeling studies have identified two possible binding sites for 5-HT_{2A} ligands, as shown schematically in Figure 1.6. Site 1 is flanked primarily by transmembrane helices TM3, TM5 and TM6, and has been proposed as the binding site for agonists, partial agonists, and antagonists. Site 2 is an alternative binding site and is flanked by TM1, TM2, TM3, and TM7. Ketanserin, a prototypical 5-HT_{2A} antagonist has been proposed to simultaneously bind in both sites.[82]

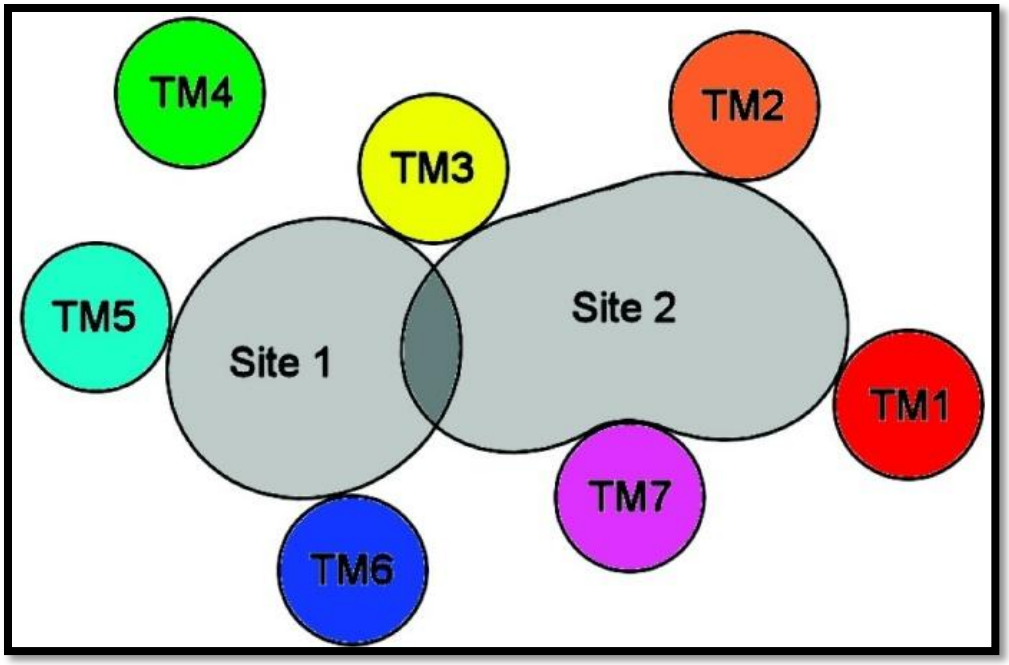

Figure 1.6 Two possible binding sites for 5-HT_{2A} ligands
(Dewkar et al, *Bioorg Med Chem Lett*, **2008**, *18*, 5268)

The mutagenesis data, now available, provides valuable information on 5-HT_{2A} receptor modeling and binding sites. Mutation data has proved a vital tool in model construction, determination of ligand binding sites and in the validation of the final models. Mutagenesis work has implicated a number of the transmembrane residues in ligand binding most notably an aspartate residue of helix 3 which is conserved in all monoamine receptors and is generally accepted to act as the counter ion for the cationic amine group characteristic of the endogenous ligands.[83] Mutation of this residue (Asp155Asn) and the conserved aspartate of helix 2 (Asp120Asn) in the 5-HT_{2A} receptor both gave a decrease in affinity for 5-HT.[84] Helix 2 mutant exhibited a decreased and GTP-insensitive binding of agonists suggesting that the helix 3 aspartate (Asp155) was required for high affinity binding and the aspartate of helix 2 was necessary for activation of the G-protein. The work concerning the two conserved aspartates has been used as a starting point in almost all 5-HT receptor models where ligands have been docked into

receptor models allowing interaction between the cationic amine and one or both of the aspartate residues. It was proposed that helices 3, 5, 6 and 7 interact with each other presenting the aromatic residues to the central cleft of the receptor. [83] Investigation of the binding orientation of serotonin, the endogenous ligand for this receptor, gave multiple potential docking results, probably due to ligand flexibility. In order to develop new selective drugs including receptor antagonists, it is necessary to understand the molecular interactions involved in ligand binding to the receptor.

The pharmacophore concept is a common approach in medicinal chemistry. The pharmacophore of a drug molecule can be defined as a portion of that molecule containing the essential organic functional groups that directly interact with the receptor active site(s) and, therefore, correlate to the molecule biological activity. Because drug-receptor interactions can be very specific, the pharmacophore may constitute a small portion of molecule.[60]

To develop a pharmacophore model, one can use two different approaches: to calculate only the ligand involvements (ligand-based approach), and/or, a receptor binding site approach (receptor-based approach).[72] A *ligand-based approach* (also known as pharmacophore-based drug design) is generally used when the receptor structure is unknown but the ligand structures are known. This situation represents the most common case. The ligand-based approach is basically an indirect method of pharmacophore identifications. The docking *receptor-based approach* is used when both, receptor and ligand structures are known. The ligand can be docked into the known receptor site and molecular mechanics are used to simulate receptor-ligand interactions and dynamics. Even though second approach looks like the most ideal situation, there can be surprises in

the results obtained, mostly due to alternative modes of binding and conformational changes in the receptor structures.[60]

The first attempts at determining the pharmacophoric features of 5-HT_2 ligands were made in 1991 by two groups of investigators: Glennon *et al.*[85] and Höltje *et al.*[86]. Three years later, Andersen *et al.*[87] and Mokrosz *et al.*[88] published, independently of each other similar three-point pharmacophore models for 5-HT_{2A} antagonists (Figure 1.7).

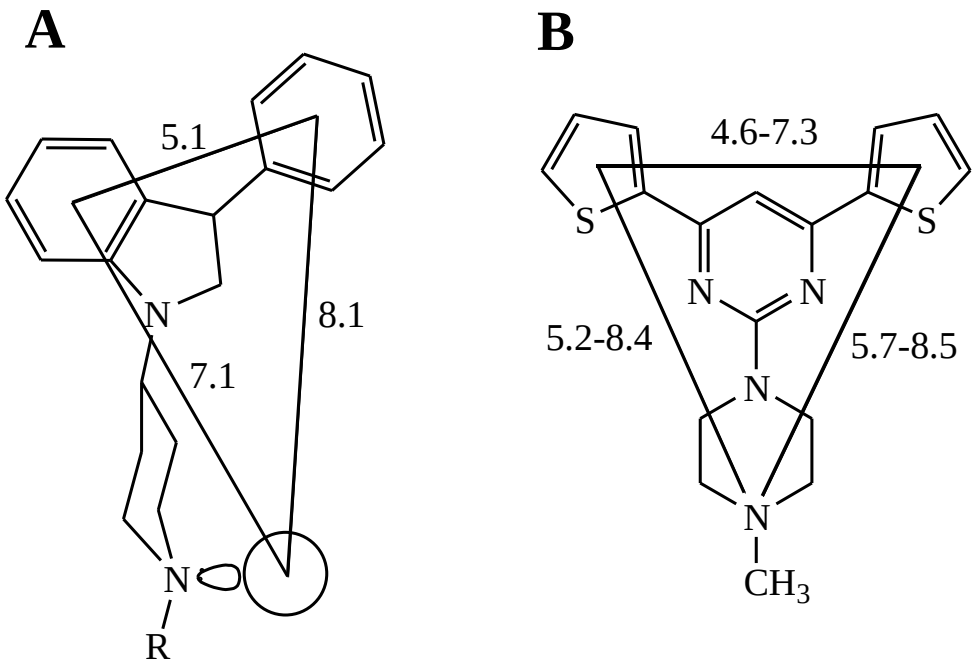

Figure 1.7 Pharmacophore models of 5-HT_{2A} receptor antagonists, defined by: (A) Anderson et al. and (B) Mokrosz et al.

They investigated structurally diverse classes of 5-HT_{2A} ligands and found a triangular arrangement of pharmacophoric elements. The distances between groups crucial for activity (two aromatic centers and a basic nitrogen atom) determined in both studies, slightly differed. The pharmacophore model proposed by Mokorosz was further developed with an extended group of some tricyclic 5-HT_{2A} antagonists (cyproheptadine,

mianserin and pizotifen) and then distance ranges between respective points were defined.[88]

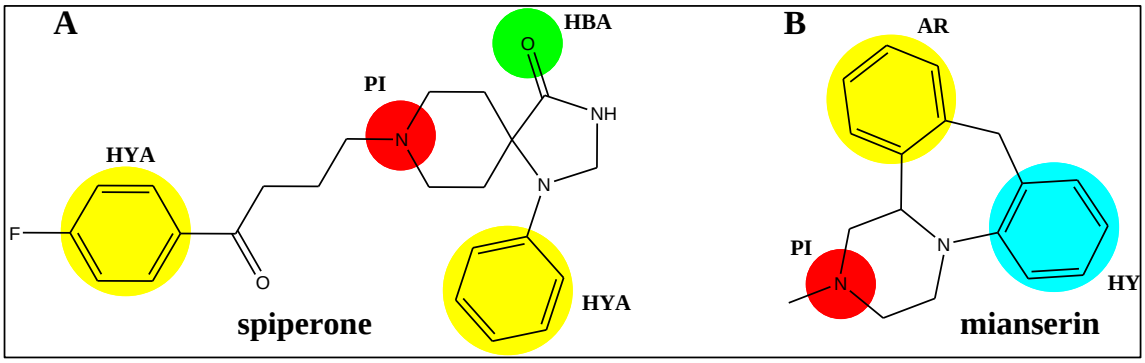

Figure 1.8 Common features pharmacophores for 5-HT_{2A} receptor antagonists: (A) class I pharmacophore aligned to spiperone; (B) class II pharmacophore aligned to mianserin (Klabunde et al, *Chembiochem*, **2005**, *6*, 876)

A different strategy for the development of pharmacophore models was reported in 2005 by Klabunde and Evers.[89] From a database of GPCR ligands, nine 5-HT_{2A} receptor antagonists with K_i values lower than 10 nM were extracted. The results clearly showed that these antagonists can be divided in two structural classes; hence two separate pharmacophore hypotheses were generated. Class I pharmacophore described four essential features required for the binding to 5-HT_{2A} receptor: a protonated nitrogen atom (PI), two hydrophobic aromatic features (HYA) and a hydrogen bond acceptor (HBA), whereas class II pharmacophore was defined by three points: PI, an aromatic ring (AR) and a hydrophobic group (HY) (Figure 1.8).

Comparison of these models indicated that both types of antagonists only partly utilized the same points of interaction, and suggested their different binding mode in the receptor pocket. Some typical 5-HT_{2A} receptor antagonists, their affinity and classes to which they belong are shown in Figure 1.9 below.[89]

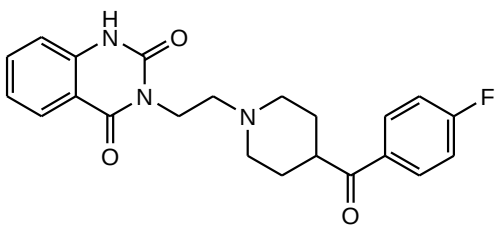

ketanserin
K_i=0.9 nM
class I

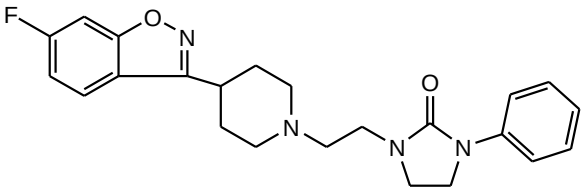

S 18327
K_i=3.2 nM
class I

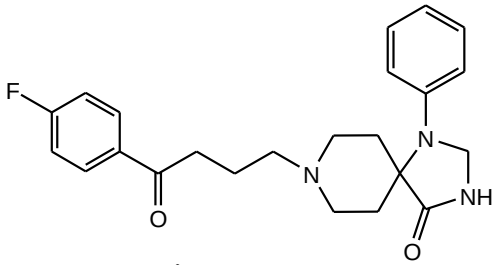

spiperone
K_i=1.0 nM
class I

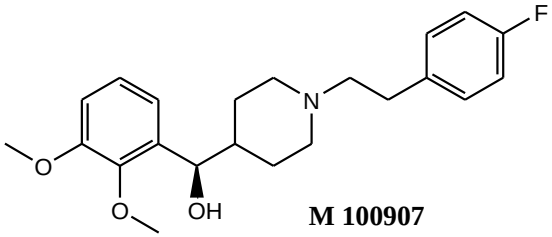

M 100907
K_i=0.8 nM
class I

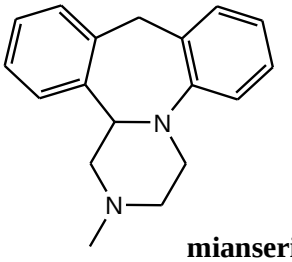

mianserin
K_i=3.0 nM
class II

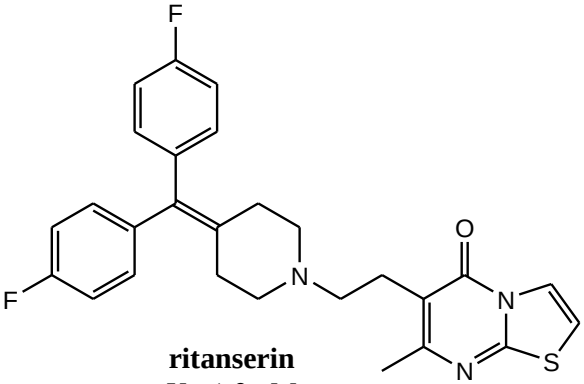

ritanserin
K_i=1.0 nM
class II

Figure 1.9 Class I and class II 5-HT_{2A} receptor antagonists and their affinities[90]

1.4 Aporphines

1.4.1 Occurrence and Biological Activity

More than 500 structures of aporphine alkaloids are reported to date and categorized in several sub-families: aporphines, proaporphines, secoaporphines, oxoaporphines, dehydroaporphines, 7-hydroxyaporphines, aporphine dimers, and aristolactams (Figure 1.10).[91] There are many natural sources of the aporphines including plant families: *Annonaceae, Lauraceae, Monimiaceae, Menispermaceae, Hernandiaceae, Ranunculaceae,* and others.[92] Plant sources of aporphines are mostly characterized by the tetracyclic skeleton, in which relevant features are the presence of an isoquinoline core, together with a biaryl subunit, and one stereogenic center at C-6a (Figure 1.11).[93]

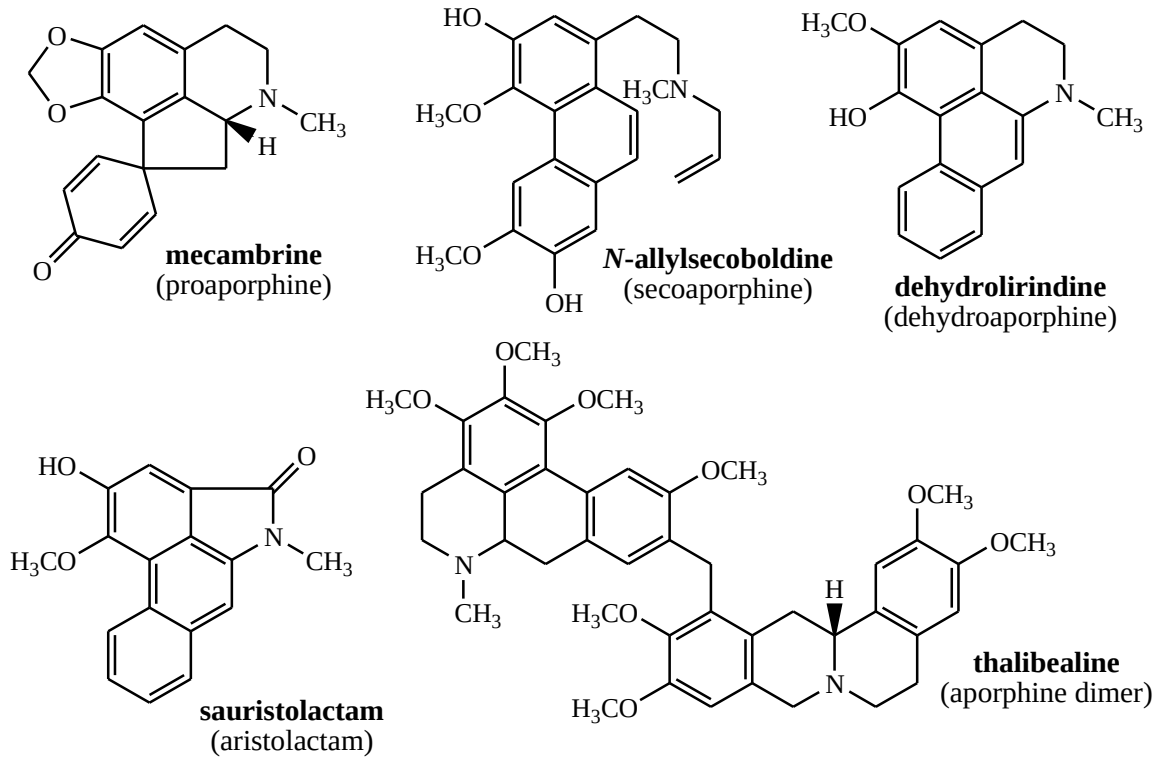

Figure 1.10 Representative members and sub-families of aporphine alkaloids

These natural products and their synthetic derivates have been used for many years because of their antioxidative, antiprotozoal,[94] antimalarial,[95] and cytoprotective properties.[96] Also, they act as dopamine agonists and antagonists in vivo[97], have shown antagonist activity at 5-HT_{2C} serotonergic receptors[98], and some of them have potential uses in cancer treatment.[99]

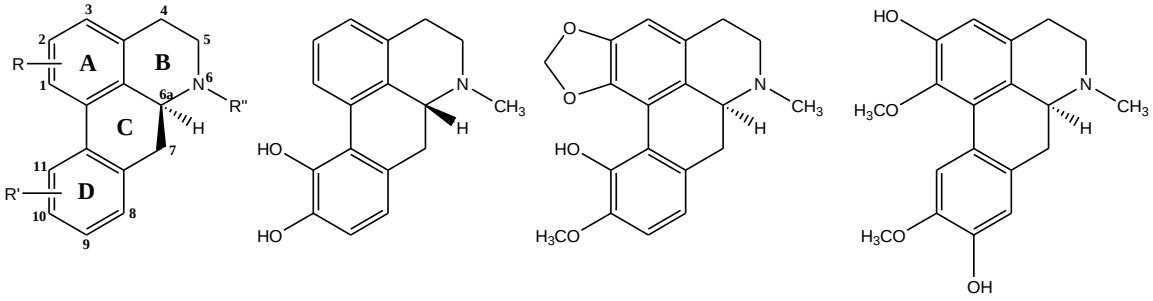

Figure 1.11 Aporphine skeleton, (*R*)-apomorphine, (*S*)-bulbocapnine and (*S*)-boldine

A recent study showed that some aporphine alkaloids from *Fumaria* and *Corydalis* species have significant antifungal and antiviral activity.[100] Several oxoaporphines are reported to have anticholinesterase activity in the micromolar range.[101]

1.4.2 SAR studies at CNS receptors

An SAR study on 10 naturally occurring aporphines, previously shown to possess moderate activity towards dopamine transporters (DAT), revealed that substitutions on ring A will increase affinity at DAT sites, while substituents on ring D will decrease DAT affinity.[102] Three aporphines, (*R*)-apomorphine, (*S*)-bulbocapnine and (*S*)-boldine (Figure 1.11), are the most explored naturally occurring aporphines, with the most SAR studies performed on them. It is known that (*R*)-apomorphine is a potent dopamine D_2 receptor agonist[103], while (*S*)-bulbocapnine is a weak antagonist[104] at the same receptor. (*S*)-boldine, on the other hand, shows α_{1A}-adrenergic antagonistic activity and some moderate

antagonistic effects at both D_1 and D_2 dopamine receptors.[105] Since these three alkaloids had nonselective and weak or moderate activities, many synthetic aporphines were synthesized based on their structures in order to enhance their pharmacological activities.

The SAR study on (*R*)-apomorphine showed that configuration of C-6a is critical for dopaminergic activity; namely the (*R*)-enantiomer (the naturally occurring apomorphine) is potent dopamine agonist, while (*S*)-antipodes usually have dopamine antagonistic activity.[106] Screening of (*R*)- and (*S*)-apomorphine analogs at over 40 different receptors, transporters and ion channels, showed that only noticeable affinity was for dopamine and α-adrenoceptors; whereas (*R*)-isomers were active at α_2-adrenoreceptors, (*S*)-aporphines showed interactions with α_1 adrenergic and D_2 receptor.[107]

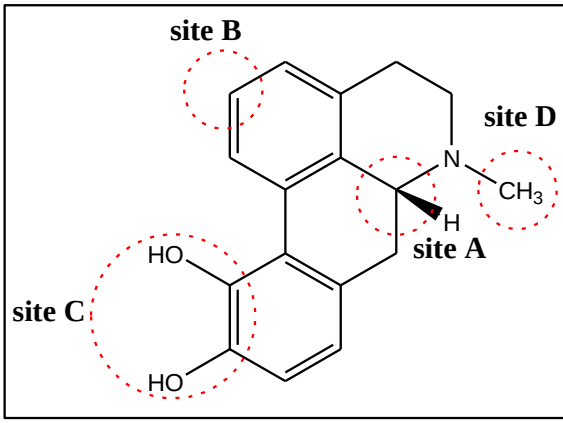

Site A: *R*-enatiomer is potent D_2 receptor antagonist; *S*-enatiomer is partial agonist at D_2 receptor.
Site B: A placement of electronegative group will enhance activity and selectivity for D_2 receptor.
Site C: Removing of any of hydroxyl groups will reduce D_2 activity.
Site D: Replacement of methyl group with hydrogen will reduce the activity; ethyl and propyl groups willenhance the activity for D_2 receptor.

Figure 1.12 SAR study on *R*-apomorphine

C2 analogs of (*R*)-apomorphine showed that D_2 binding affinity and D_2/D_1 receptor selectivity can be increased by adding electronegative group (eg. 2F-apomorphine), suggesting that there might be a lipophilic cleft on D_2 receptor that can interact with 2-substituents on the A ring of apomorphines. Cannon and co-workers showed that 10- and 11-hydroxy group are both important for affinity at dopamine

receptor, since neither (*R*)- nor (*S*)- 10 or 11 dehydroxy apomorphines showed significant activity at these receptors.[108]

However, (*R*)-derivatives were also potent 5-HT_{1A} receptor agonists, while (*S*)-enantiomers showed an antagonistic activity at this receptor. Some racemic compounds lacked affinity at serotonin receptors.[109] SAR on *N*6 position showed that the methyl group can be replaced by ethyl and even a propyl group, giving more potent agonists at D_2 receptor, while norapomorphine lacked affinity at this receptor.[110] Summarized SAR study on (*R*)-apomorphine is shown in Figure 1.12.

Other groups designed, synthesized and evaluated series of bridged aporphines. Interestingly, binding studies of these aporphines indicated their high affinities for 5-HT_{1A} and 5-HT_7 receptors as well as D_2 receptors.[111,112]

Information obtained from SAR study, highly characterized structural skeleton of (*R*)-apomorphine and number of its analogs and derivatives are already being used in development of potent dopaminergic agents as potential treatments of Parkinson's disease and psychotic disorders.[91] Also, (*R*)-apomorphine itself is commercially available drug used for the treatment of Parkinson disease.[113]

1.5 Nantenine

(+)-Nantenine [(+)-9,10-methylendioxy-1,2-dimethoxyaporphine] is an aporphine alkaloid isolated from several different sources: the fruit of *Nandina domestica* Thunberg (Berberidaceae),[114] leaves of *Ocotea macrophylla* (Lauraceae),[115] young leaves of *Guatteria dumetorum*[116] and others family (Figure 1.13). The fruit of

Nandina domestica has been used in Japan for many years to treat asthma, whooping cough, pharynx tumors and uterine bleeding.[117]

It was found that (±)-nantenine competitively inhibited the contraction by phenylephrine and 5-HT in the rat thoracic aorta.[118] These results suggested that (±)-nantenine exerted competitive antagonistic activity at the α_1-adrenoceptor and 5-HT_{2A} receptor.

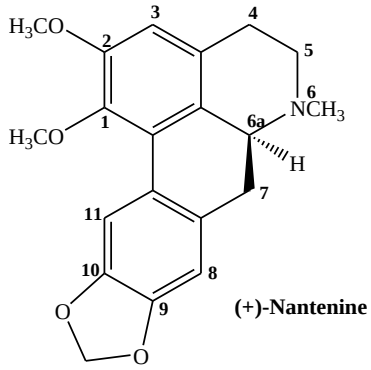

Figure 1.13 Chemical structure of (+)-nantenine

1.5.1 MDMA antagonistic activity

Experiments conducted by our collaborator, Dr. Fantegrossi, have shown that the selective 5-HT_{2A} antagonist M100907 did not reverse (±)-MDMA induced hyperthermia.[119] Additionally, the selective α_1-adrenoceptor antagonist prazosin blocked but did not reverse (±)-MDMA-induced hyperthermia. Thus, neither 5-HT_{2A} antagonism nor α_1-adrenoceptor antagonism individually seem to be sufficient for reversal of (±)-MDMA induced hyperthermia, a concept which is clinically relevant for treatment of MDMA overdose.

Table 1-1. Nantenine effects on MDMA induced hyperthermia, locomotor stimulation, headtwitch response and lethality

	Prazosin (α_1)	**M100907 (5-HT_{2A})**	**Nantenine (α_1/ 5-HT_{2A})**
Hyperthermia	+block/-reverse	-reverse	+block/+reverse
Locomotor Stimulation	Reduce	reduce[119]	reduce
Head twitch	Reduce	block	reduce
Lethality	Reduce	Not tested	reduce

However, it was shown that natural (+)-nantenine blocked and reversed MDMA-induced hyperthermia and also antagonized a wide range of other MDMA-induced effects in mice (Table 1-1).[120]

Dr. Fantegrossi studied the antagonist effects of nantenine and the selective α_1 antagonist prazosin against the induction of racemic MDMA-induced hyperthermia, locomotor stimulation, and lethality in male NIH Swiss mice. Further hyperthermia experiments were conducted with these compounds and the selective 5-HT_{2A} antagonist M100907 (formerly MDL100907) in order to gauge the capacity of these agents to reverse MDMA-induced hyperthermia once established. Finally, experiments were also conducted to assess the actions of nantenine, prazosin, and M100907 against the headtwitch response (HTR) elicited by (*S*)- and (*R*)-MDMA.[120] The HTR is a selective behavioral model for 5-HT_2 activity in rodents, as a wide range of direct and indirect 5-HT_2 agonists have been shown to induce this effect. Further, HTR can be selectively blocked by 5-HT_2 receptor antagonists and the potency with which an antagonist blocks HTR is highly correlated with its affinity for 5-HT_2 receptors.[121]

Pretreatment with either 10 mg/kg nantenine or 1 mg/kg prazosin completely abolished the hyperthermic effects of MDMA (Figure 1.14, top left). In addition to

blocking the induction of hyperthermia produced by MDMA, 10 mg/kg nantenine was also able to reverse MDMA-induced hyperthermia when administered 30-min after MDMA (Figure 1.14, top right). Neither prazosin (1 mg/kg, Figure 1.14, bottom left) nor M100907 (1 mg/kg, Figure 1.14, bottom right) reversed MDMA-induced hyperthermia.[120]

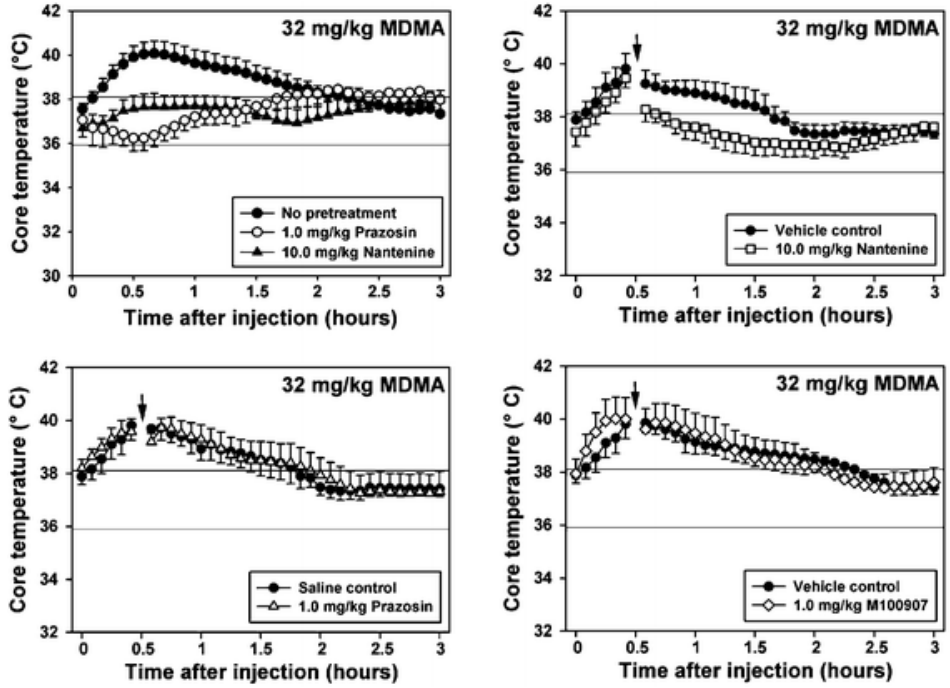

Figure 1.14 Blockade of induction of MDMA-induced hyperthermia (top left) and reversal of MDMA-induced hyperthermia by nantenine (top right), prazosin (bottom left) and M100907 (bottom right)

Racemic MDMA also produced a long-lasting stimulation of locomotor activity, peaking at approximately 175 activity counts 1 h after administration (Figure 1.15, filled circles). Pretreatment with 1 mg/kg prazosin attenuated MDMA-induced locomotor stimulation, while pretreatment with 10 mg/kg nantenine had similar, but more pronounced effects (Figure 1.15).

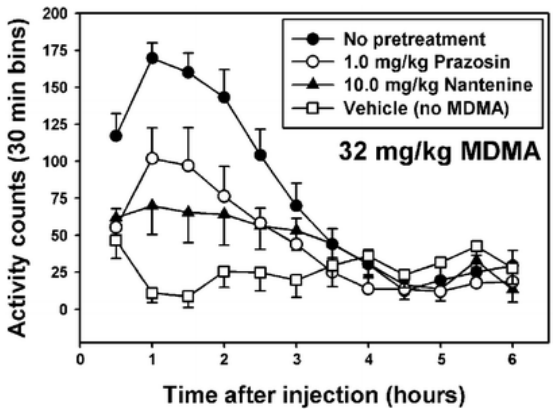

Figure 1.15 Blockade of induction of MDMA-induced locomotor stimulation by prazosin and nantenine

(*S*)-MDMA induced a dose-dependent HTR in mice, producing a maximum of approximately five twitches in 10-min at a dose of 0.32 mg/kg (Figure 1.16, closed circles). Pretreatment with 0.001 mg/kg M100907, 0.1 mg/kg prazosin, or 1 mg/kg nantenine reduced the HTR for all doses of (*S*)-MDMA to saline-like levels. Similarly (*R*)-MDMA produced a significant HTR at a dose of 1.0 mg/kg (Figure 1.17, closed circles).

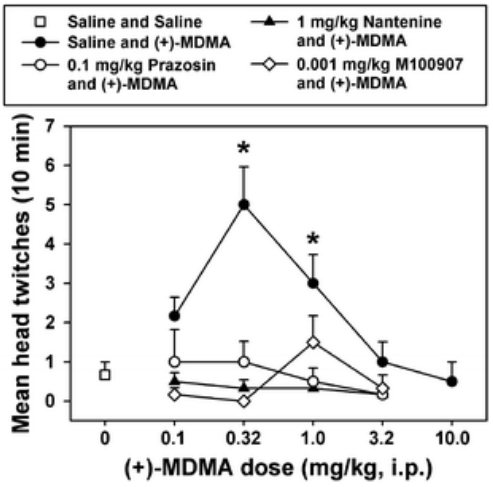

Figure 1.16 Blockade of induction of S(+)-MDMA-induced HTR by M100907, prazosin and nantenine

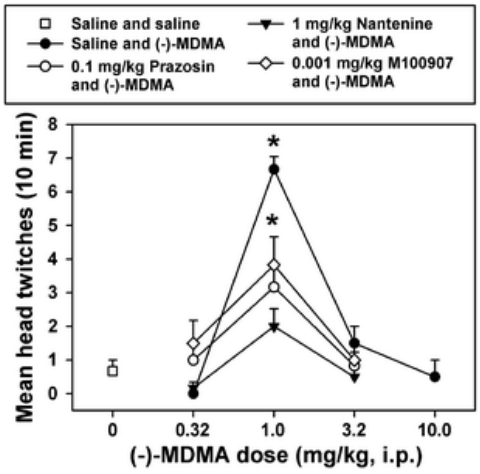

Figure 1.17 Blockade of induction of R(-)-MDMA induced HTR by M100907, prazosin and nantenine

It was demonstrated (Table 1-1) that (+)-nantenine antagonizes physiological and behavioral effects of MDMA and shows promise for the development of MDMA-specific therapeutic agents. It is possible that nantenine exerts its MDMA antagonist activity via antagonism of 5-HT_{2A} and α_1 receptors.

1.5.2 SAR studies at CNS receptors

Only a few reports have been done on the structure-activity relationships (SAR) of nantenine at CNS recepotrs.[118,122] These SAR studies showed that substitution of a methyl group at *N*-6 for an ethyl group reduces α_1 and 5-HT_{2A} activity, while amide derivatives at *N*-6 and demethylation at *N*-6 caused a loss of activity (Figure 1.18-Site B). Also, introduction of a hydroxyl group at C-4 lowers both, 5-HT_{2A} and α_1 activity (Figure 1.18-Site C). Demethylation at C-1 reduces activity at 5-HT_{2A}, but increases α_1 activity (Figure 1.18-Site A).

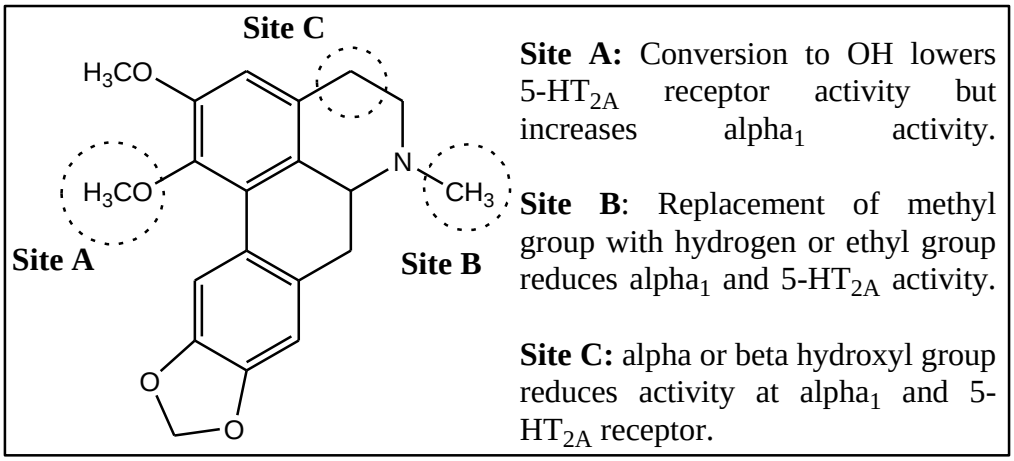

Figure 1.18 SAR studies of (±)-nantenine analogs at 5-HT_{2A} and α_1 receptors done by Indra et al.[122]

1.6 Proposed binding mode of Nantenine at the 5-HT_{2A} receptor

Figure 1.19 shows a binding mode of (±)-nantenine at the binding cleft of the homology model of the 5-HT_{2A} receptor proposed by Indra *et al*.[122] A homology model of the rat 5-HT_{2A} receptor was built based on a bovine rhodopsin as a template using homology program Insight II. After energy minizimation procedures, nantenine was manually docked into the ligand-binding cleft.

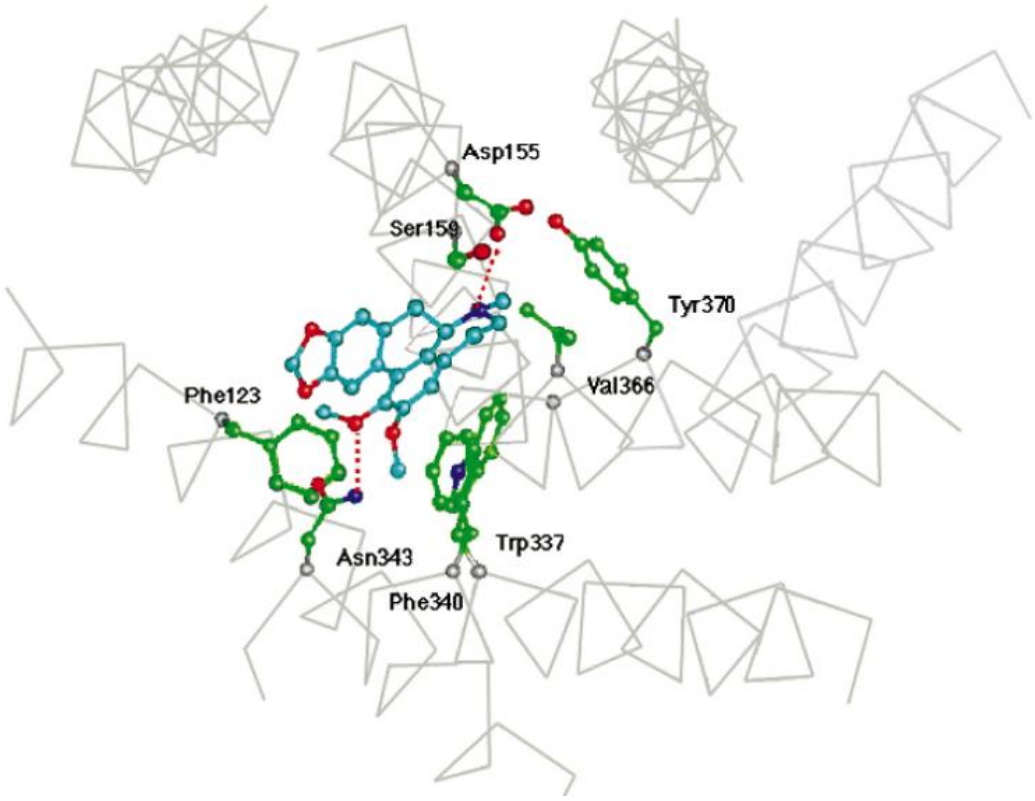

Figure 1.19 Structure of (±)-nantenine at the binding cleft of 5-HT_{2A} receptor model (Indra et al, *Can J Physiol Pharmacol* **2002**, *80*, 198-204)

This model shows that Asp155, a residue in transmembrane helix 3 that is strongly conserved across the family of serotonin receptors, forms a strong ionic bond with *N*-6 of nantenine. The oxygen atom of the C-1 methoxy group interacts with Asn343, a residue from transmembrane helix 6, also strongly conserved in many

GPCRs.[122] It is hypothesized that this interaction may be directly involved in 5-HT_{2A} receptor antagonism.[123] This hydrogen bond probably lowers the motion of transmembrane helix 6, and hence prevents normal activation of the receptor. The *N*-methyl group fits into a pocket that is formed by Val366 and Tyr370, both residues from transmembrane helix 7.[122]

1.7 MDMA and the serotonergic system

No selective antagonists for the physiological and behavioral effects of MDMA have yet been identified. According to the National Institute on Drug Abuse the most effective treatments for methamphetamine addiction are cognitive behavioral interventions.[3]

MDMA acts directly on a number of receptors and transporters in the CNS; still it is shown that serotonin neurotransmission is one of the highly affected.[1,10-12] There is evidence that MDMA does not directly release serotonin from the presynaptic neuron, but rather binds to the serotonin transporters (SERT) and not just blocks the reuptake of excess serotonin from a synaptic cleft, but also reverses the action of these transporters, which will eventually lead to an overall abnormal increased net amount of serotonin.[1] Briefly, in these experiments, radiolabeled [^{3}H] 5-HT was used as a substrate for the serotonin transporter and efflux of serotonin caused by MDMA and other SERT inhibitors was measured. It was shown that MDMA stimulates efflux from these cells at concentrations similar to those that inhibited transport.[124,125]

There is evidence that the adrenergic system is also involved in MDMA's effects. Several groups have shown that α_1 adrenoreceptor antagonists can block MDMA-induced hyperthermia.[120,126,127]

Research in animals showed that pretreatment with the non-selective 5-$HT_{2A/2C}$ antagonist ketanserin attenuate neurochemical and behavioral effects of MDMA.[128] Clozapine, a 5-HT_{2A} antagonist, reverses hyperthermia and sympathetically mediated vasoconstriction induced by MDMA in rabbits and rats.[129] M100907, a selective 5-HT_{2A} antagonist, blocked, but did not reverse MDMA induced hyperthermia in mice.[120] These results suggest a contributing role for 5-HT_2 receptors in the actions of MDMA.

Finally, risperidone, an atypical antipsychotic, was shown to attenuate and reverse MDMA-induced hyperthermia in rats.[130] Risperidone is a potent 5-HT_{2A} receptor antagonist, but it also blocks other 5-HT receptor subtypes and shows weak antagonistic activity at the dopamine D_1 receptor.[131] In this later study, several other antagonists at different 5-HT subtype receptors were also used, and it has been shown that risperidone antagonism at 5-HT_{2A} receptor plays a major role in reversing MDMA-induced hyperthermia in rats.[130]

Although it is evident that physiological and behavioral effects of MDMA are mediated via multiple receptors, still it appears that 5-HT_{2A} receptors play a major role and therefore modulation of this receptor can be expected to play a significant part in a therapeutic strategy.

From a medicinal chemistry standpoint, there are two plausible approaches that one can use to develop a potential therapeutic agent to treat these MDMA-induced effects resulting from impared serotonin neurotransmission.

The first approach is based on a role of the SERT in MDMA-induced neurotoxicity that has been shown in several studies. An experiment in 2007 showed that SERT knockout mice have abolished MDMA self-administration.[38] It was also shown that fluoxetine (Figure 1.20), a selective serotonin reuptake inhibitor (SSRI), completely blocked MDMA-induced serotonin release[132] and attenuates MDMA-induced serotonin neurotoxicity.[133-135] Fluoxetine has lower IC_{50} value than MDMA for inhibition of human SERT,[132,136] which means that fluoxetine has a higher affinity than MDMA for binding to the SERT to produce acute and long-term pharmacologic responses.[35,137] Although binding of SSRIs to SERT will also lead to decreased reuptake of serotonin back to presynaptic neuron, this will still prevent binding of MDMA to SERT and the net amount of serotonin in synaptic cleft will be much lower as compared with the one when MDMA is bound to SERT (since SSRIs do not reverse the action of SERT). However, this strategy has several drawbacks, since it has been known that fluoxetine and other SSRIs have significant side effects and are known for some common drug-drug interactions, which have potential to produce the "serotonin syndrome".[60,138] Fluoxetine and its derivatives are also potent inhibitors of the CYP450 2D6 (an enzyme that is responsible for metabolic breakdown of MDMA in liver),[139,140] and therefore may inhibit MDMA metabolism and substantially increase the toxicity of MDMA.[141,142]

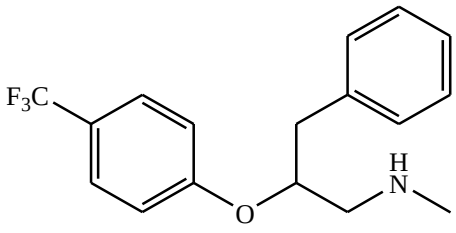

Figure 1.20 Fluoxetine-the selective serotonin reuptake inhibitor

Since several preclinical studies have shown that potent 5-HT_{2A} receptor antagonists (clozapine, ketanserin, M100907, risperidone) can block or reverse various MDMA-induced adverse effects,[120,128-130] we decided to use this, second approach, where we will try to develop potent 5-HT_{2A} receptor antagonists (explained in detail in Chapter 2) which will prevent binding of both serotonin and MDMA for these receptors (the excess serotonin will be eventually degradated by the enzymes present in synaptic cleft, and MDMA will be metabolized by enzymes in liver).

Besides antagonism at the 5-HT_{2A} receptor, it has been shown also that α_1 receptor antagonists can block and/or reverse some of the MDMA-induced adverse effects.[143] However, neither 5-HT_{2A} antagonism nor α_1-adrenoreceptor antagonism seems to be individually sufficient for reversal of a range of MDMA-induced behavioral and physiological effects. Risperidone, a 5-HT_{2A} antagonist with significant α_1 antagonistic activity has been shown to antagonize effects of MDMA. It is therefore apparent that a dual 5-HT_{2A}/α_1 profile may be desirable in a MDMA antagonism. Up to the present time, there is no experiment performed showing that coadministration of 5-HT_{2A} and α_1 receptor antagonists together will be of therapeutic benefit in the treatment of MDMA-caused adverse effects. Even so, such a strategy, using two different drugs that targets two different receptors has significant risk in development of drug-drug interactions, and higher possibility of side effects for each compound.[144] One possible alternative approach is to develop a dual antagonist, at both 5-HT_{2A}/α_1 receptors, that might be used as a potential therapeutic agent for treatment of MDMA-induced intoxication. To accomplish this strategy one first needs to know the particular involment of each receptor in

mediating MDMA-induced effects, and then to design a molecule that will have certain, desired the ratio for antagonism at these two receptors.

Nantenine, an aporphine alkaloid, is an antagonist at both, 5-HT_{2A} and α_1 receptors. Experiments have shown that nantenine blocked and reversed a wide range of behavioral and psychological MDMA-induced effects in mice.[120] We decided to synthesize nantenine and a library of nantenine analogs and submit the compounds for biological evaluation at human 5-HT_{2A} receptors, as a first step in the design of 5-HT_{2A}/α_1 antagonists as potential MDMA antagonists.

In the following chapter (Chapter 2), we describe our approach for the design and synthesis of nantenine and nantenine analogs. In order to better understand the binding mode of nantenine and nantenine analogs at the binding cleft of the 5-HT_{2A} receptor, in a separate approach (Chapter 3), we performed a molecular modeling study. We first built a homology model of the 5-HT_{2A} receptor, and then we docked nantenine and selected nantenine analogs.

Further details of our rationale and hypothesis for this project as well as results and comprehensive experimental data are presented in the two chapters which follow.

1.8 References

(1) Kalant, H. *Cmaj* **2001**, *165*, 917.

(2) Gouzoulis-Mayfrank, E.; Hermle, L.; Kovar, K.; Sass, H. *Fortschr Neurol Psychiatr* **1999**, *67*, 574.

(3) http://www.drugabuse.gov/.

(4) Nichols, D. E.; Oberlender, R. *NIDA research monograph* **1989**, *94*, 1.

(5) Hardman, H. F.; Haavik, C. O.; Seevers, M. H. *Toxicol Appl Pharmacol* **1973**, *25*, 299.

(6) Cuomo, M. J.; Dyment, P. G.; Gammino, V. M. *J Am Coll Health* **1994**, *42*, 271.

(7) Meyer, J. S.; Ali, S. F. *Annals of the New York Academy of Sciences* **2002**, *965*, 373.

(8) http://www.justice.gov/dea/ 2010.

(9) Parrott, A. C. *Psychopharmacology* **2004**, *173*, 234.

(10) Burgess C, O. D. A., Gill M. *Eur Psychiatry* **2000**, *15*, 287.

(11) Nichols, D. E. *Pharmacology & therapeutics* **2004**, *101*, 131.

(12) Ferigolo, M.; Machado, A. G.; Oliveira, N. B.; Barros, H. M. *Revista do Hospital das Clinicas* **2003**, *58*, 332.

(13) Wijetunga, M.; Bhan, R.; Lindsay, J.; Karch, S. *Hawaii Med J* **2004**, *63*, 8.

(14) Karch, S. B. *The Pathology of Drug Abuse*; CRC Press, 1993.

(15) Henry, J. A.; Jeffreys, K. J.; Dawling, S. *Lancet* **1992**, *340*, 384.

(16) Nielsen, S.; Lundemose, J. B.; Simonsen, M. S.; Dragsholt, C. *Ugeskr Laeger* **2001**, *163*, 2253.

(17) Vollenweider, F. X.; Gamma, A.; Liechti, M.; Huber, T. *Neuropsychopharmacology* **1998**, *19*, 241.

(18) Mallick, A.; Bodenham, A. R. *Journal of accident & emergency medicine* **1997**, *14*, 336.

(19) Ricaurte, G. A.; McCann, U. D. *Annals of the New York Academy of Sciences* **1992**, *648*, 371.

(20) Christophersen, A. S. *Toxicol Lett* **2000**, *112-113*, 127.

(21) Boot, B. P.; McGregor, I. S.; Hall, W. *Lancet* **2000**, *355*, 1818.

(22) Colado, M. I.; Granados, R.; O'Shea, E.; Esteban, B.; Green, A. R. *Pharmacology & toxicology* **1999**, *84*, 261.

(23) Parrott, A. C.; Lasky, J. *Psychopharmacology* **1998**, *139*, 261.

(24) Soar, K.; Parrott, A. C.; Fox, H. C. *Psychol Rep* **2004**, *95*, 192.

(25) Robledo, P.; Balerio, G.; Berrendero, F.; Maldonado, R. *Naunyn-Schmiedeberg's archives of pharmacology* **2004**, *369*, 338.

(26) Cottler, L. B.; Womack, S. B.; Compton, W. M.; Ben-Abdallah, A. *Hum Psychopharmacol* **2001**, *16*, 599.

(27) Ricaurte, G. A.; DeLanney, L. E.; Irwin, I.; Langston, J. W. *Brain Res* **1988**, *446*, 165.

(28) Taffe, M. A.; Davis, S. A.; Yuan, J.; Schroeder, R.; Hatzidimitriou, G.; Parsons, L. H.; Ricaurte, G. A.; Gold, L. H. *Neuropsychopharmacology* **2002**, *27*, 993.

(29) Ricaurte, G. A.; Martello, A. L.; Katz, J. L.; Martello, M. B. *The Journal of pharmacology and experimental therapeutics* **1992**, *261*, 616.

(30) McCann, U. D.; Szabo, Z.; Seckin, E.; Rosenblatt, P.; Mathews, W. B.; Ravert, H. T.; Dannals, R. F.; Ricaurte, G. A. *Neuropsychopharmacology* **2005**, *30*, 1741.

(31) Parrott, A. C. *Hum Psychopharmacol* **2001**, *16*, 557.

(32) Slikker, W., Jr.; Ali, S. F.; Scallet, A. C.; Frith, C. H.; Newport, G. D.; Bailey, J. R. *Toxicol Appl Pharmacol* **1988**, *94*, 448.

(33) Green, A. R.; Mechan, A. O.; Elliott, J. M.; O'Shea, E.; Colado, M. I. *Pharmacol Rev* **2003**, *55*, 463.

(34) Sanchez, V.; Camarero, J.; Esteban, B.; Peter, M. J.; Green, A. R.; Colado, M. I. *Br J Pharmacol* **2001**, *134*, 46.

(35) Shankaran, M.; Yamamoto, B. K.; Gudelsky, G. A. *European journal of pharmacology* **1999**, *385*, 103.

(36) Simantov, R.; Tauber, M. *FASEB J* **1997**, *11*, 141.

(37) Mas, M.; Farre, M.; de la Torre, R.; Roset, P. N.; Ortuno, J.; Segura, J.; Cami, J. *The Journal of pharmacology and experimental therapeutics* **1999**, *290*, 136.

(38) Trigo, J. M.; Renoir, T.; Lanfumey, L.; Hamon, M.; Lesch, K. P.; Robledo, P.; Maldonado, R. *Biol Psychiatry* **2007**.

(39) Glennon, R. A.; Young, R. *Pharmacology, biochemistry, and behavior* **2000**, *66*, 483.

(40) Bankson, M. G.; Cunningham, K. A. *Neuropsychopharmacology* **2002**, *26*, 40.

(41) Mazzola-Pomietto, P.; Aulakh, C. S.; Wozniak, K. M.; Hill, J. L.; Murphy, D. L. *Psychopharmacology* **1995**, *117*, 193.

(42) Liechti, M. E.; Vollenweider, F. X. *Hum Psychopharmacol* **2001**, *16*, 589.

(43) Gerra, G.; Zaimovic, A.; Moi, G.; Giusti, F.; Gardini, S.; Delsignore, R.; Laviola, G.; Macchia, T.; Brambilla, F. *Behav Brain Res* **2002**, *134*, 403.

(44) Bubar, M. J.; Cunningham, K. A. *Curr Top Med Chem* **2006**, *6*, 1971.

(45) Cavasotto, C. N.; Orry, A. J.; Abagyan, R. A. *Proteins* **2003**, *51*, 423.

(46) Klabunde, T.; Hessler, G. *Chembiochem* **2002**, *3*, 928.

(47) Attwood, T. K. *Trends Pharmacol Sci* **2001**, *22*, 162.

(48) Bockaert, J.; Pin, J. P. *EMBO J* **1999**, *18*, 1723.

(49) Wess, J. *FASEB J* **1997**, *11*, 346.

(50) Kroeze, W. K.; Kristiansen, K.; Roth, B. L. *Curr Top Med Chem* **2002**, *2*, 507.

(51) Probst, W. C.; Snyder, L. A.; Schuster, D. I.; Brosius, J.; Sealfon, S. C. *DNA Cell Biol* **1992**, *11*, 1.

(52) Lovenberg, T. W.; Erlander, M. G.; Baron, B. M.; Sutcliffe, J. G. *Int Clin Psychopharmacol* **1993**, *8 Suppl 2*, 19.

(53) Saudou, F.; Hen, R. *Neurochem Int* **1994**, *25*, 503.

(54) Gerald, C.; Adham, N.; Kao, H. T.; Olsen, M. A.; Laz, T. M.; Schechter, L. E.; Bard, J. A.; Vaysse, P. J.; Hartig, P. R.; Branchek, T. A.; et al. *EMBO J* **1995**, *14*, 2806.

(55) Plassat, J. L.; Boschert, U.; Amlaiky, N.; Hen, R. *EMBO J* **1992**, *11*, 4779.

(56) Monsma, F. J., Jr.; Shen, Y.; Ward, R. P.; Hamblin, M. W.; Sibley, D. R. *Molecular pharmacology* **1993**, *43*, 320.

(57) Bard, J. A.; Zgombick, J.; Adham, N.; Vaysse, P.; Branchek, T. A.; Weinshank, R. L. *J Biol Chem* **1993**, *268*, 23422.

(58) De Vry, J. *Psychopharmacology* **1995**, *121*, 1.

(59) Grignaschi, G.; Invernizzi, R. W.; Fanelli, E.; Fracasso, C.; Caccia, S.; Samanin, R. *Br J Pharmacol* **1998**, *124*, 1781.

(60) Lemke, T. W., David *Foye`s Principles of Medicinal Chemistry*; Sixth ed., 2008.

(61) Nichols, D. E.; Nichols, C. D. *Chem Rev* **2008**, *108*, 1614.

(62) Roth, B. L. *Ann Clin Psychiatry* **1994**, *6*, 67.

(63) Lummis, S. C. *Biochem Soc Trans* **2004**, *32*, 535.

(64) Farber, L.; Haus, U.; Spath, M.; Drechsler, S. *Scand J Rheumatol Suppl* **2004**, 2.

(65) Bockaert, J.; Claeysen, S.; Compan, V.; Dumuis, A. *Curr Drug Targets CNS Neurol Disord* **2004**, *3*, 39.

(66) Nelson, D. L. *Curr Drug Targets CNS Neurol Disord* **2004**, *3*, 53.

(67) Thomas, D. R. *Pharmacology & therapeutics* **2006**, *111*, 707.

(68) Woolley, M. L.; Marsden, C. A.; Fone, K. C. *Curr Drug Targets CNS Neurol Disord* **2004**, *3*, 59.

(69) Mitchell, E. S.; Neumaier, J. F. *Pharmacology & therapeutics* **2005**, *108*, 320.

(70) Glennon, R. A. *J Med Chem* **2003**, *46*, 2795.

(71) Westkaemper, R. B.; Glennon, R. A. *Curr Top Med Chem* **2002**, *2*, 575.

(72) Bojarski, A. J. *Curr Top Med Chem* **2006**, *6*, 2005.

(73) Greenshaw, A. J. *Trends in pharmacological sciences* **1993**, *14*, 265.

(74) de Wit, R.; Aapro, M.; Blower, P. R. *Cancer Chemother Pharmacol* **2005**, *56*, 231.

(75) Bockaert, J.; Ansanay, H.; Letty, S.; Marchetti-Gauthier, E.; Roman, F.; Rondouin, G.; Fagni, L.; Soumireu-Mourat, B.; Dumuis, A. *C R Acad Sci III* **1998**, *321*, 217.

(76) Corbett, D. F.; Heightman, T. D.; Moss, S. F.; Bromidge, S. M.; Coggon, S. A.; Longley, M. J.; Roa, A. M.; Williams, J. A.; Thomas, D. R. *Bioorg Med Chem Lett* **2005**, *15*, 4014.

(77) Birkett, J. T.; Arranz, M. J.; Munro, J.; Osbourn, S.; Kerwin, R. W.; Collier, D. A. *Neuroreport* **2000**, *11*, 2017.

(78) Hirst, W. D.; Stean, T. O.; Rogers, D. C.; Sunter, D.; Pugh, P.; Moss, S. F.; Bromidge, S. M.; Riley, G.; Smith, D. R.; Bartlett, S.; Heidbreder, C. A.; Atkins, A. R.; Lacroix, L. P.; Dawson, L. A.; Foley, A. G.; Regan, C. M.; Upton, N. *European journal of pharmacology* **2006**, *553*, 109.

(79) Haydar, S. N.; Yun, H.; Andrae, P. M.; Mattes, J.; Zhang, J.; Kramer, A.; Smith, D. L.; Huselton, C.; Graf, R.; Aschmies, S.; Schechter, L. E.; Comery, T. A.; Robichaud, A. J. *J Med Chem* **2010**, *53*, 2521.

(80) Cushing, D. J.; Zgombick, J. M.; Nelson, D. L.; Cohen, M. L. *The Journal of pharmacology and experimental therapeutics* **1996**, *277*, 1560.

(81) Lovenberg, T. W.; Baron, B. M.; de Lecea, L.; Miller, J. D.; Prosser, R. A.; Rea, M. A.; Foye, P. E.; Racke, M.; Slone, A. L.; Siegel, B. W.; et al. *Neuron* **1993**, *11*, 449.

(82) Dewkar, G. K.; Peddi, S.; Mosier, P. D.; Roth, B. L.; Westkaemper, R. B. *Bioorg Med Chem Lett* **2008**, *18*, 5268.

(83) Wishart, G.; Bremner, D. H.; Sturrock, K. R. *Receptors & channels* **1999**, *6*, 317.

(84) Wang, C. D.; Gallaher, T. K.; Shih, J. C. *Molecular pharmacology* **1993**, *43*, 931.

(85) Westkaemper, R. B.; Glennon, R. A. *Pharmacology, biochemistry, and behavior* **1991**, *40*, 1019.

(86) Holtje, H. D.; Batzenschlager, A.; Briem, H.; Bruggmann, J. *Pharmazie in unserer Zeit* **1991**, *20*, 59.

(87) Andersen, K.; Liljefors, T.; Gundertofte, K.; Perregaard, J.; Bogeso, K. P. *Journal of medicinal chemistry* **1994**, *37*, 950.

(88) Mokrosz, J. L.; Strekowski, L.; Duszynska, B.; Harden, D. B.; Mokrosz, M. J.; Bojarski, A. J. *Die Pharmazie* **1994**, *49*, 801.

(89) Klabunde, T.; Evers, A. *Chembiochem* **2005**, *6*, 876.

(90) http://www.pdsp.med.unc.edu/.

(91) Zhang, A.; Zhang, Y.; Branfman, A. R.; Baldessarini, R. J.; Neumeyer, J. L. *J Med Chem* **2007**, *50*, 171.

(92) Shamma, M.; Guinaudeau, H. *Nat Prod Rep* **1986**, *3*, 345.

(93) Anakabe, E. *Synthesis* **2004**, *7*, 1093.

(94) Mahiou, V.; Roblot, F.; Hocquemiller, R.; Cave, A.; Rojas de Arias, A.; Inchausti, A.; Yaluff, G.; Fournet, A.; Angelo, A. *J Nat Prod* **1994**, *57*, 890.

(95) Munoz, V.; Sauvain, M.; Mollinedo, P.; Callapa, J.; Rojas, I.; Gimenez, A.; Valentin, A.; Mallie, M. *Planta Med* **1999**, *65*, 448.

(96) Cassels, B. K. A., M.; Cognet, P.; Speisky, H *Pharmacol. Res.* **1995**, *31*, 103.

(97) Loghin, F.; Chagraoui, A.; Asencio, M.; Comoy, E.; Speisky, H.; Cassels, B. K.; Protais, P. *Eur J Pharm Sci* **2003**, *18*, 133.

(98) Zhelyazkova-Savova, M. D.; Zhelyazkov, D. K. *J Pharm Pharmacol* **2003**, *55*, 125.

(99) Wang. B.H.; Lu, Z. X. P., G.-M. *Planta Med.* **1997**, *63*, 494.

(100) Orhana, I.; Ozcelik, B.; Karaoglu, T.; Sener, B. *Z Naturforsch C* **2007**, *62*, 19.

(101) Tang, H.; Wei, Y. B.; Zhang, C.; Ning, F. X.; Qiao, W.; Huang, S. L.; Ma, L.; Huang, Z. S.; Gu, L. Q. *Eur J Med Chem* **2009**, *44*, 2523.

(102) Protais, P.; Arbaoui, J.; Bakkali, E. H.; Bermejo, A.; Cortes, D. *J Nat Prod* **1995**, *58*, 1475.

(103) Gao, Y.; Zong, R.; Campbell, A.; Kula, N. S.; Baldessarini, R. J.; Neumeyer, J. L. *J Med Chem* **1988**, *31*, 1392.

(104) Schaus, J. M.; Titus, R. D.; Foreman, M. M.; Mason, N. R.; Truex, L. L. *J Med Chem* **1990**, *33*, 600.

(105) Sobarzo-Sanchez, E. M.; Arbaoui, J.; Protais, P.; Cassels, B. K. *J Nat Prod* **2000**, *63*, 480.

(106) Neumeyer, J. L. *Synthesis and Structure-Activity Relationships of Aporphines as Dopamine Receptor Agonists and Antagonists*; Springer-Verlag: Berlin, 1985.

(107) Baldessarini, R. J.; Marsh, E. R.; Kula, N. S.; Zong, R.; Neumeyer, J. L. *European journal of pharmacology* **1994**, *254*, 199.

(108) Cannon, J. G.; Mohan, P.; Bojarski, J.; Long, J. P.; Bhatnagar, R. K.; Leonard, P. A.; Flynn, J. R.; Chatterjee, T. K. *J Med Chem* **1988**, *31*, 313.

(109) Cannon, J. G.; Moe, S. T.; Long, J. P. *Chirality* **1991**, *3*, 19.

(110) Csutoras, C.; Zhang, A.; Zhang, K.; Kula, N. S.; Baldessarini, R. J.; Neumeyer, J. L. *Bioorg Med Chem* **2004**, *12*, 3553.

(111) Linnanen, T.; Brisander, M.; Unelius, L.; Sundholm, G.; Hacksell, U.; Johansson, A. M. *J Med Chem* **2000**, *43*, 1339.

(112) Linnanen, T.; Brisander, M.; Mohell, N.; Johansson, A. M. *Bioorg Med Chem Lett* **2001**, *11*, 367.

(113) Hayes, M. W.; Fung, V. S.; Kimber, T. E.; O'Sullivan, J. D. *Med J Aust* **2010**, *192*, 144.

(114) Tsukiyama, M.; Ueki, T.; Yasuda, Y.; Kikuchi, H.; Akaishi, T.; Okumura, H.; Abe, K. *Planta Med* **2009**, *75*, 1393.

(115) Barrera, C.; Ericsson, D.; Suarez, C.; Enrique, L. *Biochemical Systematics and Ecology* **2009**, *37*, 522.

(116) Correa, J. E.; Rios, C. H.; del Rosario Castillo, A.; Romero, L. I.; Ortega-Barria, E.; Coley, P. D.; Kursar, T. A.; Heller, M. V.; Gerwick, W. H.; Rios, L. C. *Planta Med* **2006**, *72*, 270.

(117) Shoji, N.; Umeyama, A.; Takemoto, T. *Journal of pharmaceutical sciences* **1984**, *73*, 568.

(118) Indra, B.; Matsunaga, K.; Hoshino, O.; Suzuki, M.; Ogasawara, H.; Ohizumi, Y. *European journal of pharmacology* **2002**, *437*, 173.

(119) Fantegrossi, W. E.; Godlewski, T.; Karabenick, R. L.; Stephens, J. M.; Ullrich, T.; Rice, K. C.; Woods, J. H. *Psychopharmacology* **2003**, *166*, 202.

(120) Fantegrossi, W. E.; Kiessel, C. L.; Leach, P. T.; Van Martin, C.; Karabenick, R. L.; Chen, X.; Ohizumi, Y.; Ullrich, T.; Rice, K. C.; Woods, J. H. *Psychopharmacology* **2004**, *173*, 270.

(121) Peroutka, S. J.; Lebovitz, R. M.; Snyder, S. H. *Science (New York, N.Y* **1981**, *212*, 827.

(122) Indra, B.; Matsunaga, K.; Hoshino, O.; Suzuki, M.; Ogasawara, H.; Ishiguro, M.; Ohizumi, Y. *Canadian journal of physiology and pharmacology* **2002**, *80*, 198.

(123) Chambers, J. J.; Nichols, D. E. *Journal of computer-aided molecular design* **2002**, *16*, 511.

(124) Wall, S. C.; Gu, H.; Rudnick, G. *Molecular pharmacology* **1995**, *47*, 544.

(125) Rothman, R. B.; Baumann, M. H.; Dersch, C. M.; Romero, D. V.; Rice, K. C.; Carroll, F. I.; Partilla, J. S. *Synapse* **2001**, *39*, 32.

(126) Sprague, J. E.; Brutcher, R. E.; Mills, E. M.; Caden, D.; Rusyniak, D. E. *Br J Pharmacol* **2004**, *142*, 667.

(127) Bexis, S.; Docherty, J. R. *Br J Pharmacol* **2008**, *153*, 591.

(128) Liechti, M. E.; Saur, M. R.; Gamma, A.; Hell, D.; Vollenweider, F. X. *Neuropsychopharmacology* **2000**, *23*, 396.

(129) Blessing, W. W.; Seaman, B.; Pedersen, N. P.; Ootsuka, Y. *J Neurosci* **2003**, *23*, 6385.

(130) Shioda, K.; Nisijima, K.; Yoshino, T.; Kuboshima, K.; Iwamura, T.; Yui, K.; Kato, S. *Neurotoxicology* **2008**, *29*, 1030.

(131) Schmidt, A. W.; Lebel, L. A.; Howard, H. R., Jr.; Zorn, S. H. *European journal of pharmacology* **2001**, *425*, 197.

(132) Verrico, C. D.; Miller, G. M.; Madras, B. K. *Psychopharmacology* **2007**, *189*, 489.

(133) Schmidt, C. J. *The Journal of pharmacology and experimental therapeutics* **1987**, *240*, 1.

(134) Malberg, J. E.; Sabol, K. E.; Seiden, L. S. *The Journal of pharmacology and experimental therapeutics* **1996**, *278*, 258.

(135) Aguirre, N.; Ballaz, S.; Lasheras, B.; Del Rio, J. *European journal of pharmacology* **1998**, *346*, 181.

(136) Mortensen, O. V.; Kristensen, A. S.; Wiborg, O. *J Neurochem* **2001**, *79*, 237.

(137) Berger, U. V.; Gu, X. F.; Azmitia, E. C. *European journal of pharmacology* **1992**, *215*, 153.

(138) Bordet, R.; Thomas, P.; Dupuis, B. *Am J Psychiatry* **1998**, *155*, 1346.

(139) Maurer, H. H.; Bickeboeller-Friedrich, J.; Kraemer, T.; Peters, F. T. *Toxicol Lett* **2000**, *112-113*, 133.

(140) Tucker, G. T.; Lennard, M. S.; Ellis, S. W.; Woods, H. F.; Cho, A. K.; Lin, L. Y.; Hiratsuka, A.; Schmitz, D. A.; Chu, T. Y. *Biochem Pharmacol* **1994**, *47*, 1151.

(141) Oesterheld, J. R.; Armstrong, S. C.; Cozza, K. L. *Psychosomatics* **2004**, *45*, 84.

(142) Upreti, V. V.; Eddington, N. D. *Journal of pharmaceutical sciences* **2008**, *97*, 1593.

(143) Bexis, S.; Docherty, J. R. *Br J Pharmacol* **2009**, *158*, 259.

(144) Morphy, R.; Rankovic, Z. *J Med Chem* **2006**, *49*, 4961.

CHAPTER 2: Nantenine - Synthesis and SAR Study

2.1 Introduction

As we mentioned in previous chapter MDMA is clearly a dangerous drug with numerous adverse physiological and cognitive effects. There is no specific agent to treat MDMA abuse and overdose. It has been shown by our collaborator Dr. William E. Fantegrossi that aporphine alkaloid nantenine blocked and reversed a range of behavioral and physiological effects induced by MDMA, such as head-twitch response, locomotor stimulation and hyperthermia.[1] When we started this project, very little was known about the receptor binding profile of nantenine, although a number of studies indicated that nantenine is antagonist at both, serotonin 5-HT_{2A} and α_1 receptor.[2,3] These studies together with some recent studies where risperidone, a potent dual 5-HT_{2A}/α_1 antagonist, attenuated and reversed MDMA-induced hyperthermia, suggested that dual 5-HT_{2A}/α_1 antagonism may be good mechanistic strategy towards MDMA antagonism in vivo. We decided to further investigate receptor-binding profile of nantenine as a first step in correlating that with its in vivo MDMA-antagonism.

The central hypothesis of our project is that nantenine may be structurally modified to give more potent antagonists at the 5-HT_{2A} receptor. In order to test this hypothesis, research at this project will focus on the synthesis of nantenine analogs and screening them in a 5-HT_{2A} assay for affinity and antagonist activity.

To accomplish this, our first aim was to synthesize nantenine in high-yield route and submit it for multi-receptor screening. The information we obtain will allow us to get some insight into which receptors are involved in MDMA antagonism of nantenine. Our second aim was to synthesize a library of nantenine analogs (Figure 2.1), that will be

useful for understanding which structural features of nantenine are required for its activity at 5-HT_{2A} receptor. The rationale for design of each nantenine analog is described later in this chapter.

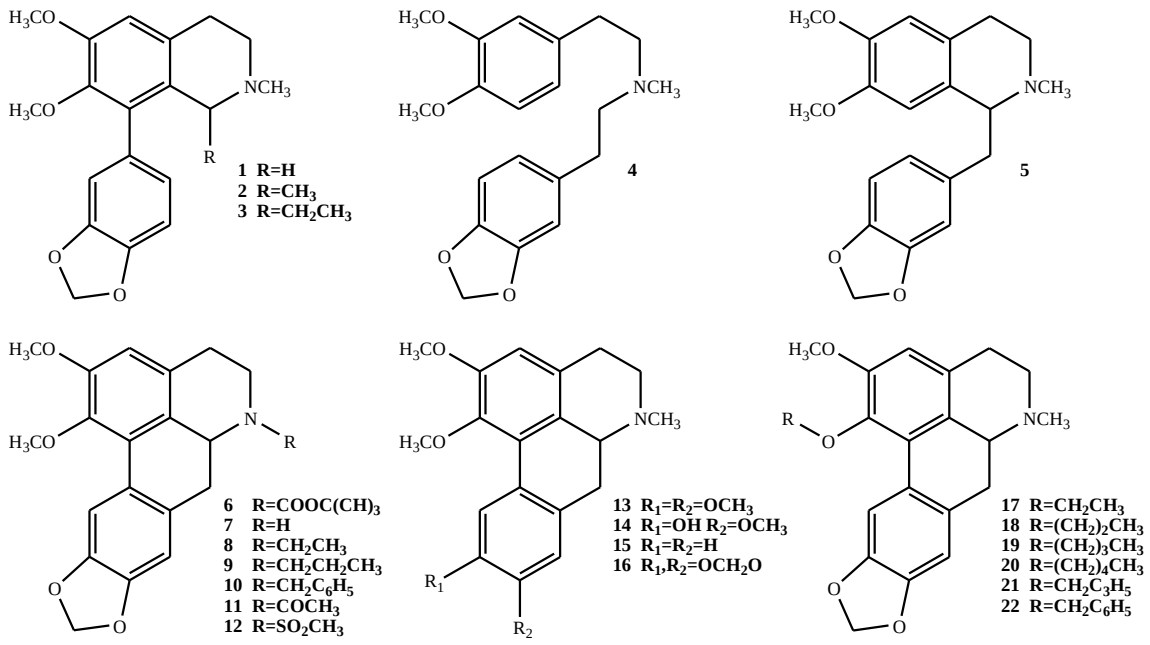

Figure 2.1 Nantenine target analogs

Our third aim was to evaluate the synthesized nantenine analogs using molecular docking experiments. Such molecular modeling experiments will provide a good insight into the possible antagonist-receptor binding mode. To achieve this aim we built the homology model of 5-HT_{2A} receptor, validated it and then performed docking experiments. This aim is explained in detail in Chapter 3.

The competition of these aims provides a platform for us to understand the mechanistic functions and utility of molecules structurally related to nantenine in the antagonism of MDMA's effects. Furthermore these experiments will enable the design and synthesis of novel and potent 5-HT_{2A} receptor antagonists based on nantenine. Such molecules may be useful to study potential MDMA antagonists.

2.2 Synthesis of Nantenine

In order to accomplish our first proposed aim - synthesis of nantenine in high-yielding route, we directed our first efforts towards this synthesis. A commonly used route to synthesize aporphines involves oxidative biaryl coupling of phenolic or phenol ether benzyltetrahydroisoquinoline intermediates in an essentially biomimetic process.[4] In the past, the oxidizing agents commonly used for this reaction included $VOCl_3$, VOF_3, $Pb(OAc)_4$ and $Tl(OCOCF_3)_3$.[5-8] These reagents are toxic and furthermore the yields obtained in these reactions were often quite low.

2.2.1 PIFA-mediated oxidative biaryl coupling

2.2.1.1 PIFA in aporphine synthesis

The reagent phenyliodine bis-trifluoroacetate (PIFA) is an environmentally-friendly alternative reagent for these biaryl cyclizations, providing aporphines in good yields (Figure 2.2).[9,10] Additional advantages of this reaction are shorter reaction times (30 min) and lower temperature that is used.[11] Since others have reported good yields in the synthesis of aporphines via biaryl coupling with PIFA at the outset of the project we decided to use this method to prepare nantenine.

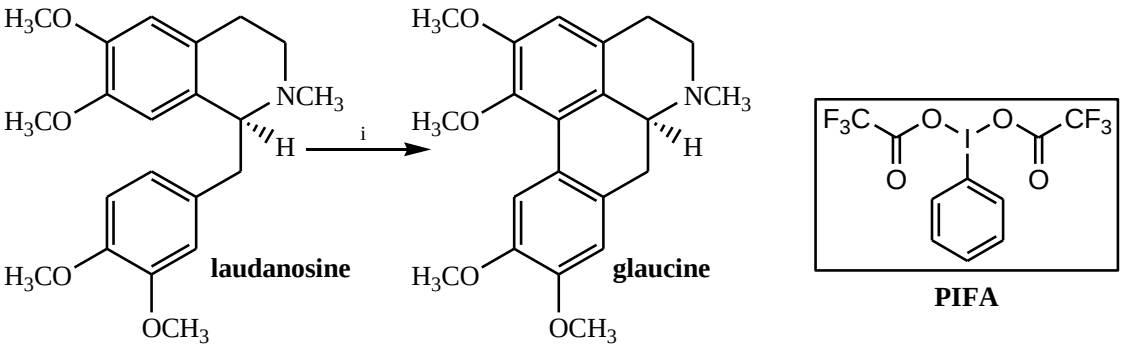

Reagents and conditions: (i) PIFA, BF_3OEt_2, CH_2Cl_2, 30 min, -20 ^oC, **75%**.

Figure 2.2: Example of aporphine synthesis with PIFA done by Anakabe et al.[11]

As it is shown in our retrosynthetic route (Scheme 2.1), we designed synthesis of nantenine, using well-established reactions. We planned to prepare nantenine from 1-benzoisoquinoline **28** using PIFA-oxidative C-C biaryl coupling. This precursor can in turn be obtained from amide **25**, which may be prepared from the commercially available amine **24** and acid **23** shown. We also envisaged that this route would allow us to synthesize a number of nantenine analogs by appropriate structural modifications of the starting materials **23** and **24**.

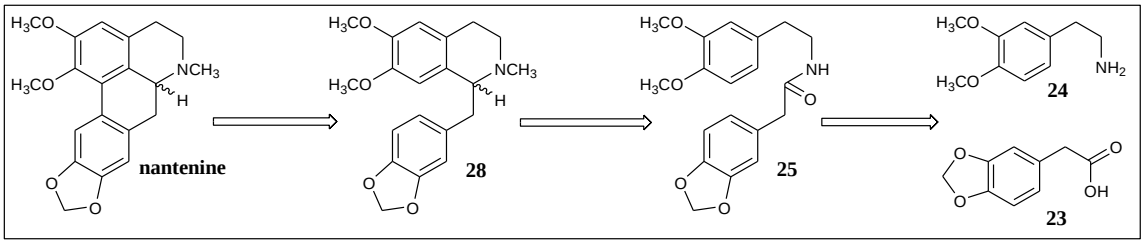

Scheme 2.1 PIFA retrosynthetic route

2.2.1.2 Mechanism of PIFA-mediated biaryl coupling

It is postulated that PIFA generates radical-cations through a single-electron transfer mechanism (SET).[12] There are two proposed mechanisms how this coupling might occur: direct *p-p* coupling and bridgehead *p-p* coupling.[13]

According to direct *p-p* coupling postulate, PIFA will first generate a radical cation of one aromatic ring by SET, followed by nucleophilic attack by the other aromatic ring. This will furnish eventually, via a six-membered transition state, the desired coupled biaryl product (Figure 2.3).

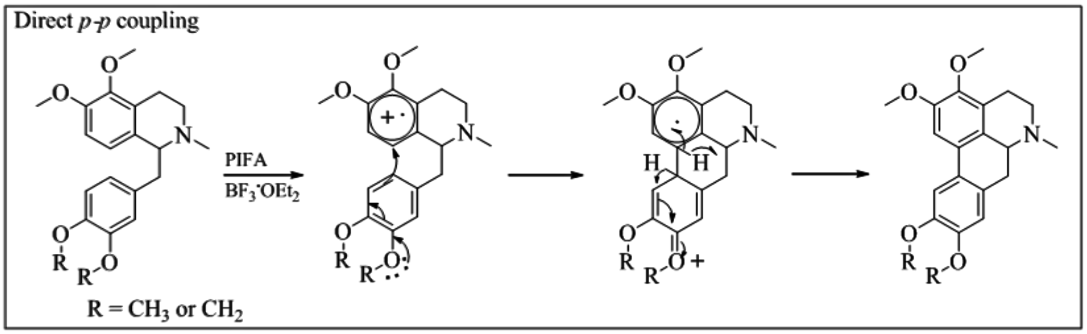

Figure 2.3 Proposed PIFA-mediated direct *p-p* coupling mechanism

On the other hand, mechanism for PIFA-mediated biaryl coupling for second proposed possible coupling starts with PIFA-generation of radical cation in one aromatic ring, and the second aromatic ring serves as starting point for the nucleophilic reaction (Figure 2.4), forming an intermediate through the participation of the free electron-pair on nitrogen.

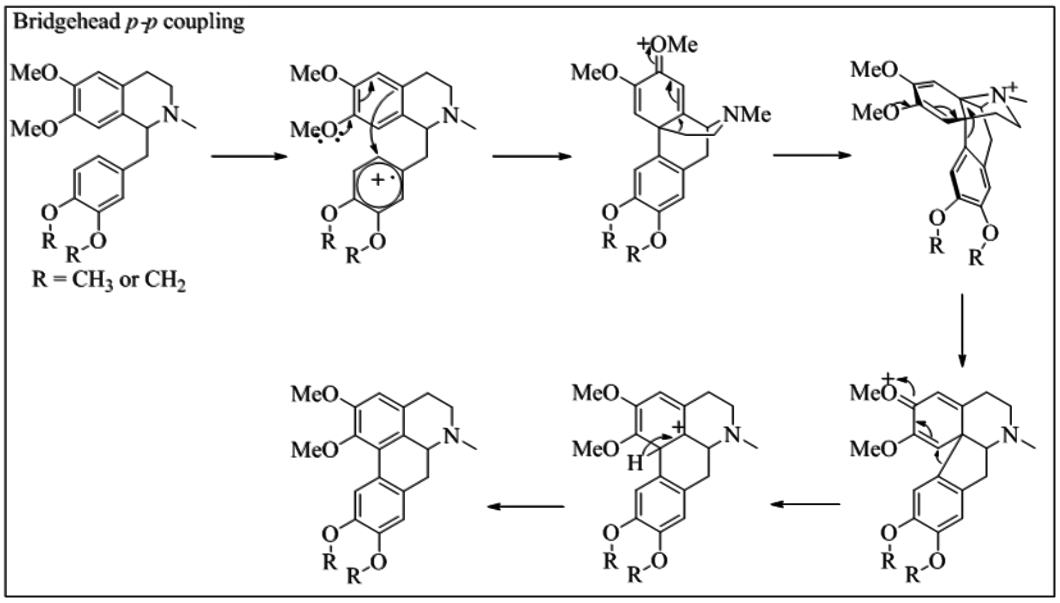

Figure 2.4 Proposed PIFA-mediated bridgehead *p-p* coupling mechanism
(Pingaew et al, *Synlett*, **2007**, *15*, 2363)

In this case bond formation occurs para to an electron releasing group forming a 6-mebered bridgehead intermediate. Further aryl migration is governed probably by stereolectronic factor and after some rearrangements the final coupled biaryl product should be obtained. Besides PIFA, BF_3 is used, probably to activate the PIFA.[13]

2.2.1.3 Synthesis of nantenine with PIFA

We started synthesis of nantenine as shown in Scheme 2.2. Reaction of commercially available amine **23** and carboxylic acid **24** with the peptide coupling reagent CDI, gave the amide **25** in excellent yield. Cyclization of **25** was conducted under Bischler-Napieralski conditions[14] to give imine **26**.

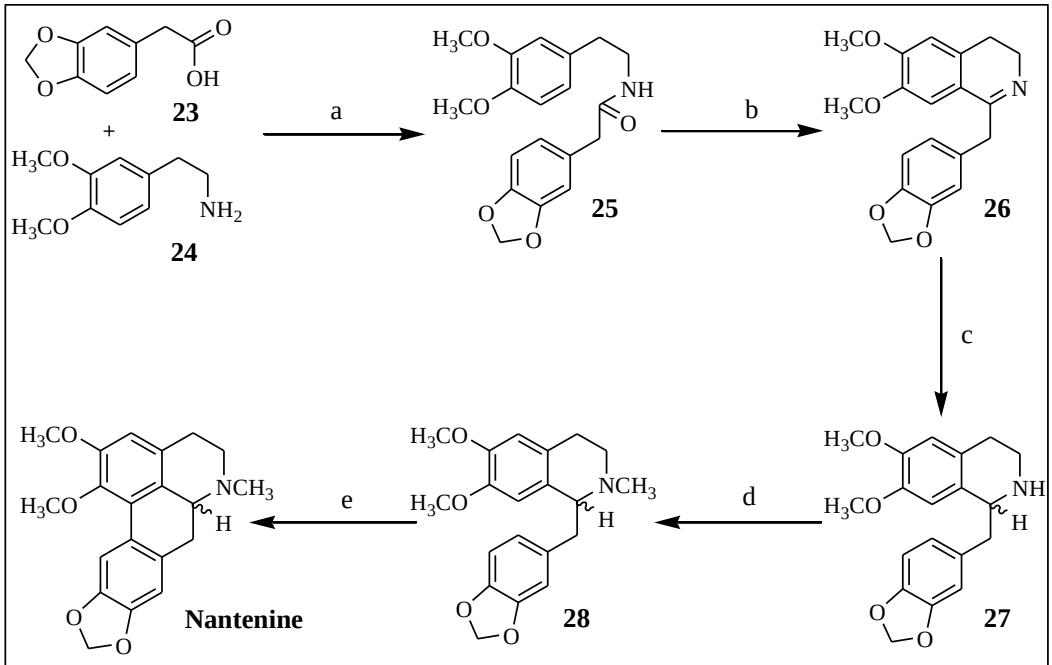

Reagents and conditions: (a) CDI, THF, **96%** (b) $POCl_3$, CH_2Cl_2 (c) $NaBH_4$, MeOH -78 ^oC (d) DCM, HCHO, $Na(OAc)_3BH$, 1.5 h, **75%** over three steps (e) PIFA, $BF_3.OEt_2$, DCM, -40 ^oC 30 min, **10%**.

Scheme 2.2 PIFA-route for synthesis of nantenine

The imine **26** was immediately reduced (since it tends to decompose) and the resulting secondary amine **27** subsequently methylated to give the tetrahydroisoquinoline **28**. Cyclization of **28** to nantenine was then carried out with PIFA at -40 °C in DCM. Unfortunately, we obtained only 10% yield under these conditions. We found also that variations in temperature (-78 °C, -20 °C and rt) did not improve this outcome in yield (no product was observed).

2.2.2 Direct biaryl coupling

2.2.2.1 Direct biaryl coupling for synthesis of aporphines

Nevertheless, given the low yield of PIFA-mediated biaryl coupling, we started to pursue other routes to synthesize nantenine and nantenine analogs. The direct biaryl coupling procedure is very useful for construction of biaryl bonds, in both inter- and intra-molecular reactions, and has been used in the synthesis of a number of bioactive molecules including aporphines. This coupling has been reported to occur in high yield using Pd(II)-acetate and various ligands (Figure 2.7).[15]

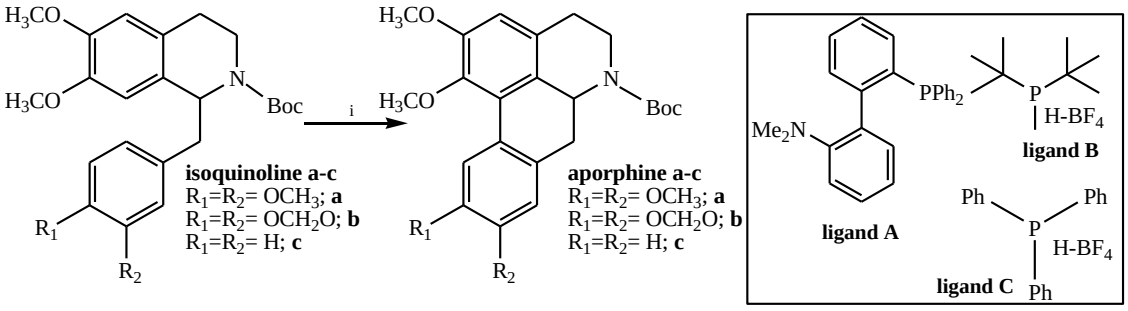

Reagents and conditions: (i) $Pd(OAc)_2$, Ligand, K_2CO_3, DMA, 130 °C.

Figure 2.5 Example of aporphine synthesis via direct biaryl coupling (LaFrance et al, *Eur J Org Chem*, **2007**, 811-825)

2.2.2.2 Mechanism of direct biaryl coupling

Direct biaryl coupling is similar to the Heck reaction in terms of substrates used. However, whereas the Heck reaction couples an activated arene (such as an aryl halide or aryl triflate) and an alkene, direct biaryl coupling uses an activated arene and an aromatic ring as substrates.[16] There is evidence that the Heck and direct biaryl coupling reactions are mechanistically dissimilar, with direct biaryl coupling likely proceeding via a concerted metalation–deprotonation pathway.[17] The proposed proton-abstraction mechanism in the palladium-catalyzed intramolecular arylation is shown in Figure 2.8

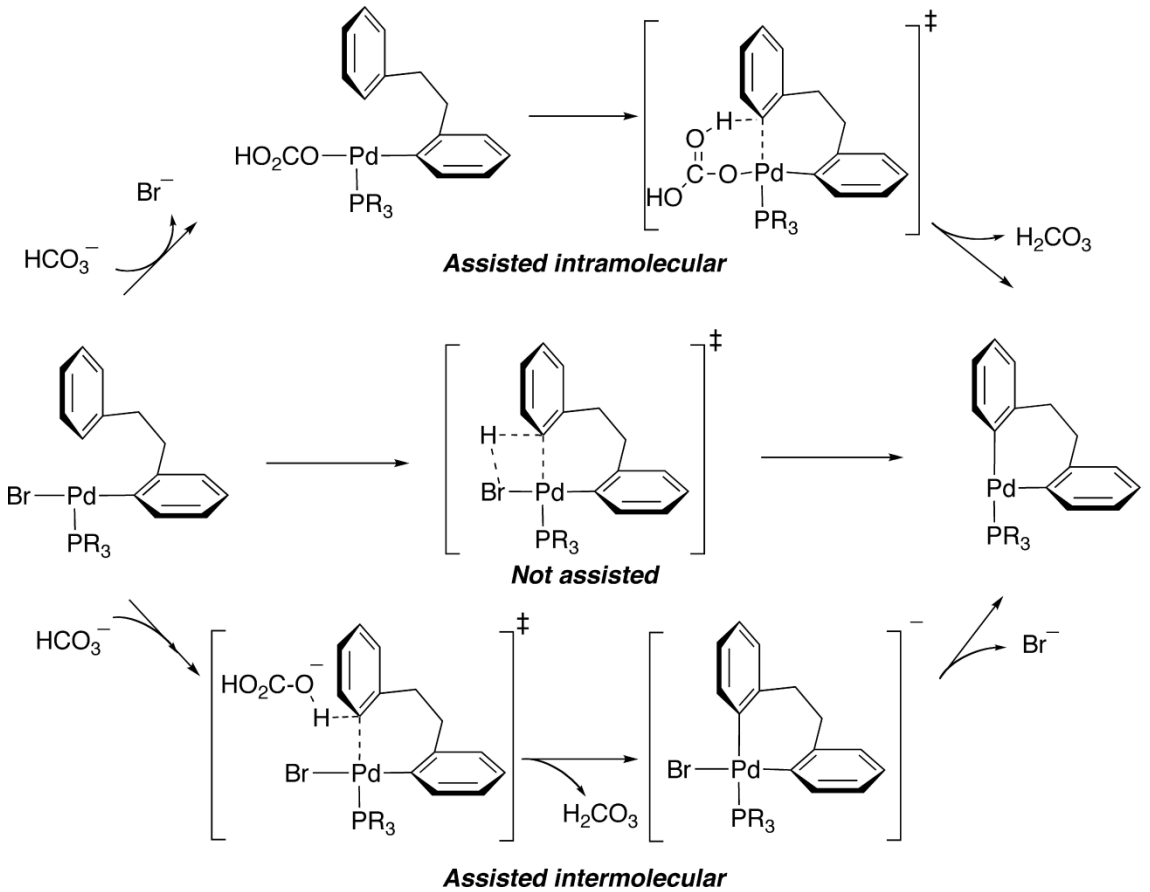

Figure 2.6 Proposed mechanism for direct biaryl coupling
(Garcia-Cuadrado et al., *J. Am. Chem. Soc.*, **2007**, *129*, 6880)

It is postulated that the formation of the metal–carbon bond is concerted with the breaking of the carbon-hydrogen bond, with the hydrogen being transferred to a basic

center. Since the existence of this step is not fully defined, three possible variations are proposed. Proton can be transferred either to the bromide ligand (not assisted path), or to another base (assisted paths). In the assisted intramolecular mechanism, the external base can coordinate to the metal, previously displacing bromide.

2.2.2.3 Synthesis of nantenine via direct biaryl coupling

We decided to synthesize nantenine via direct biaryl coupling route under thermal conditions. (Scheme 2.3) According to our retrosynthetic route nantenine can be obtained from Boc-protected tetrahydroisoquinoline **33** using direct biaryl coupling conditions, while this intermediate may be prepared from the amide **30** which is in turn readily accessible from the commercially available amine **24** and readily available bromoacid **29**.

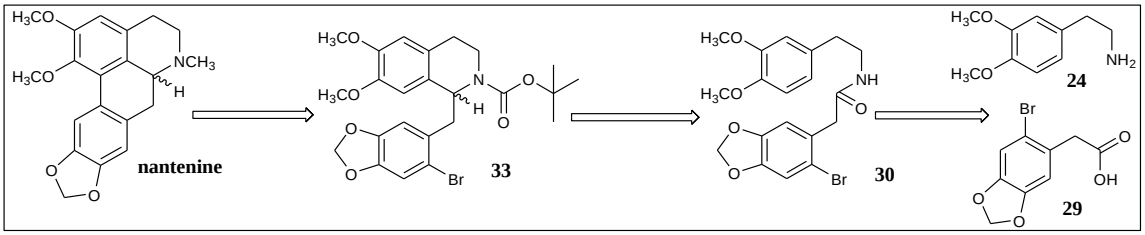

Scheme 2.3 Direct biaryl coupling - retrosynthetic route

Preparation of nantenine using this approach is shown in Scheme 2.4. 3,4-Dimethoxy phenethylamine **24** was condensed with bromoacid **29** under standard CDI coupling conditions. The amide **30** was then cyclized under Bischler-Napieralski conditions[14] to afford imine **31**, which was immediately reduced to give **32** without purification. Following protection of amine with the tert-butoxy carbonyl group we obtained compound **33**, an intermediate that was used for the direct biaryl cyclization. Although this cyclization was reported to give desired products in excellent yields (above 90%),[15] in our hands only 48% of aporphine **6** was obtained using the previously reported thermal conditions. We noticed that a significant amount of starting material remained

after reacting for 24 h. Even after reacting for 48 h, the reaction did not proceed to completion. Addition of pivalic acid, which has been reported to enhance some biaryl coupling reactions and overall yields,[18] did not result in any improvement in the yield of **6** under thermal conditions.

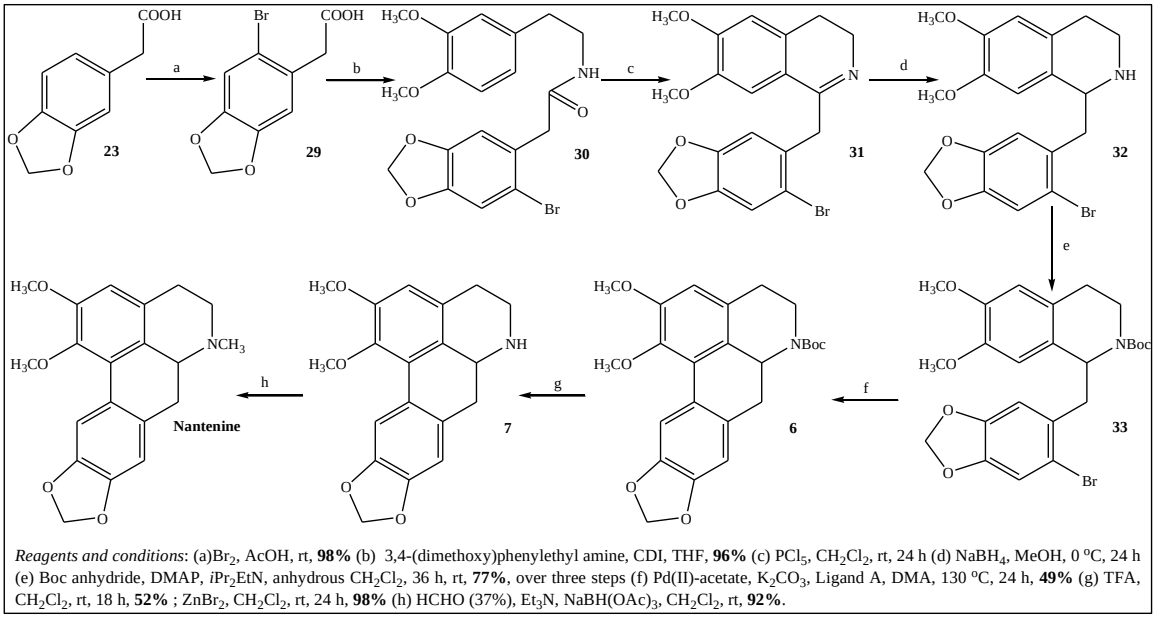

Reagents and conditions: (a)Br_2, AcOH, rt, **98%** (b) 3,4-(dimethoxy)phenylethyl amine, CDI, THF, **96%** (c) PCl_5, CH_2Cl_2, rt, 24 h (d) $NaBH_4$, MeOH, 0 ^oC, 24 h (e) Boc anhydride, DMAP, iPr_2EtN, anhydrous CH_2Cl_2, 36 h, rt, **77%**, over three steps (f) Pd(II)-acetate, K_2CO_3, Ligand A, DMA, 130 ^oC, 24 h, **49%** (g) TFA, CH_2Cl_2, rt, 18 h, **52%** ; $ZnBr_2$, CH_2Cl_2, rt, 24 h, **98%** (h) HCHO (37%), Et_3N, $NaBH(OAc)_3$, CH_2Cl_2, rt, **92%**.

Scheme 2.4 Direct-biaryl coupling route

At this point, we decided to attempt to improve the yield of this biaryl cyclization and increase the overall efficiency of our synthesis through the use of microwaves. We succeeded to increase the yield of **6** up to 90%.[19] The boc-protecting group of aporphine **6** was removed under typical acidic conditions (TFA/DCM). Disappointingly, this reaction gave only a moderate yield (52%) of the aporphine **7**. Given the apparent sensitivity of the aporphine nucleus to acidic conditions, we decided to use weak Lewis acid, $ZnBr_2$/DCM, and that gave us excellent yield (98%) of compound **7**. This compound served as a key intermediate for synthesis of nantenine and other *N*-substituent nantenine analogs. Upon *N*-alkylation of aporphine **7** we obtained racemic nantenine in

good yield. The racemic compound was subsequently resolved into its two enantiomers. (*R*)-(-)-Nantenine was obtained by resolving with (+)-2,3-di-*p*-toluoyl-d-tartaric acid (Scheme 2.5), having 96% ee (as determined by chiral HPLC) and $[\alpha]_D^{24}$ -117.0 (c=0.58, $CHCl_3$).

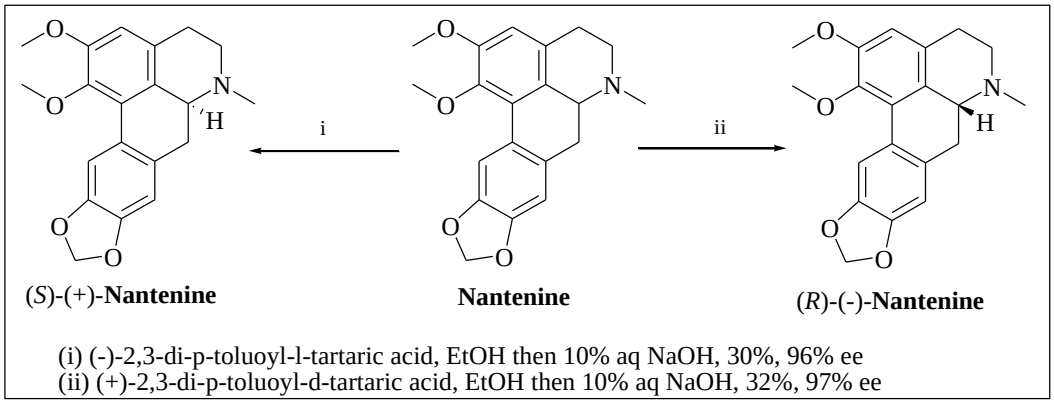

Scheme 2.5 Resolution of nantenine enantiomers

The (*S*)-enantiomer was obtained by resolution of the racemate with (-)-2,3-di-*p*-toluoyl-l-tartaric acid; having 97% ee (by chiral HPLC) and $[\alpha]_D^{24}$ +115.5 (c=0.51, $CHCl_3$). Racemic nantenine and these two enantiomers were sent for further biological evaluation.

2.3 Synthesis of Nantenine Analogs for SAR Study at 5-HT_{2A} Receptor

For this section our focus was on the synthesis of different nantenine analogs and screening them for a 5-HT_{2A} antagonist activity. This was done in order to better understand what structural features of nantenine are important for binding and antagonism at the 5-HT_{2A} receptor. This will allow us to design more potent 5-HT_{2A} antagonists which may function in vivo as antagonists of the effects of MDMA and which may therefore be useful to treat MDMA abuse and overdose.

We designed 4 groups of nantenine analogs for this SAR study: flexible analogs, N-substituted analogs, methylenedioxy analogs and C-1 analogs.

2.3.1 Synthesis of flexible analogs

This group of analogs (Figure 2.9) was designed to examine the role of the structural rigidity of the nantenine aporphine skeleton in binding and antagonist activity at human 5-HT_{2A} receptors. When we started this project no such information was available. This well-explored medicinal chemistry tactic is useful, since if any of these compounds retain the activity for 5-HT_{2A} receptor, it will produce some degree of structural simplification of the pharmacophore. Less rigid compounds and their analogs are also more easily prepared so that any follow-up SAR study would be more readily conducted.

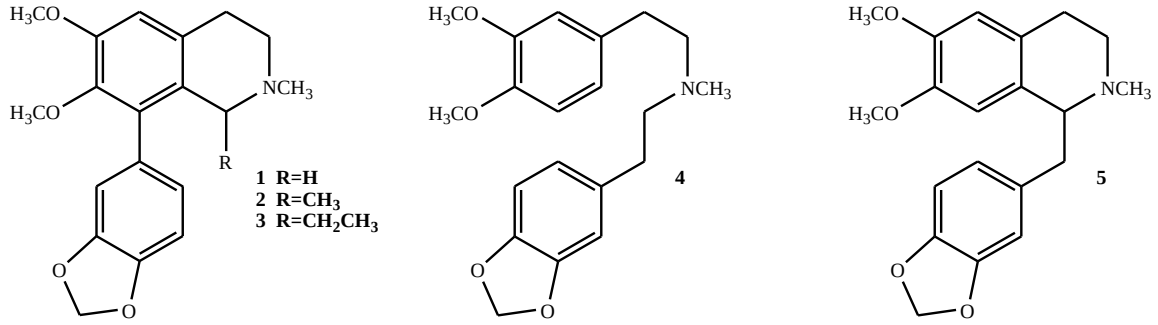

Figure 2.7 Flexible nantenine target analogs

Analogs **1-3** are flexible analogs without ring C that is present in aporphines (*seco*-ring C derivates of nantenine), hence they have increased degrees of freedom between two aromatic rings (A and D) that increase number of potential conformers. They are designed to provide the information of the importance of the ring C in antagonizing 5-HT_{2A} receptor.

Analogs **4** and **5** are designed with other flexible analogs in order to test the importance of the structural rigidity of the nantenine aporphine skeleton in antagonistic activity at 5-HT_{2A} receptor. The biaryl bond of nantenine is absent in both analogs. Analog **4** represents the most flexible analog that will be designed in this project, since

two rings, B and C are truncated, hence it has a lot possible rotations around several bonds. On the other hand, analog **5** has less flexible conformers, since it has only ring C absent. Taken together, these flexible analogs may indicate whether ring C and/or B are required to be intact in aporphine skeleton in antagonistic activity towards 5-HT_{2A} receptor.

Analogs **1-3** were synthesized as shown in Scheme 2.6 below.

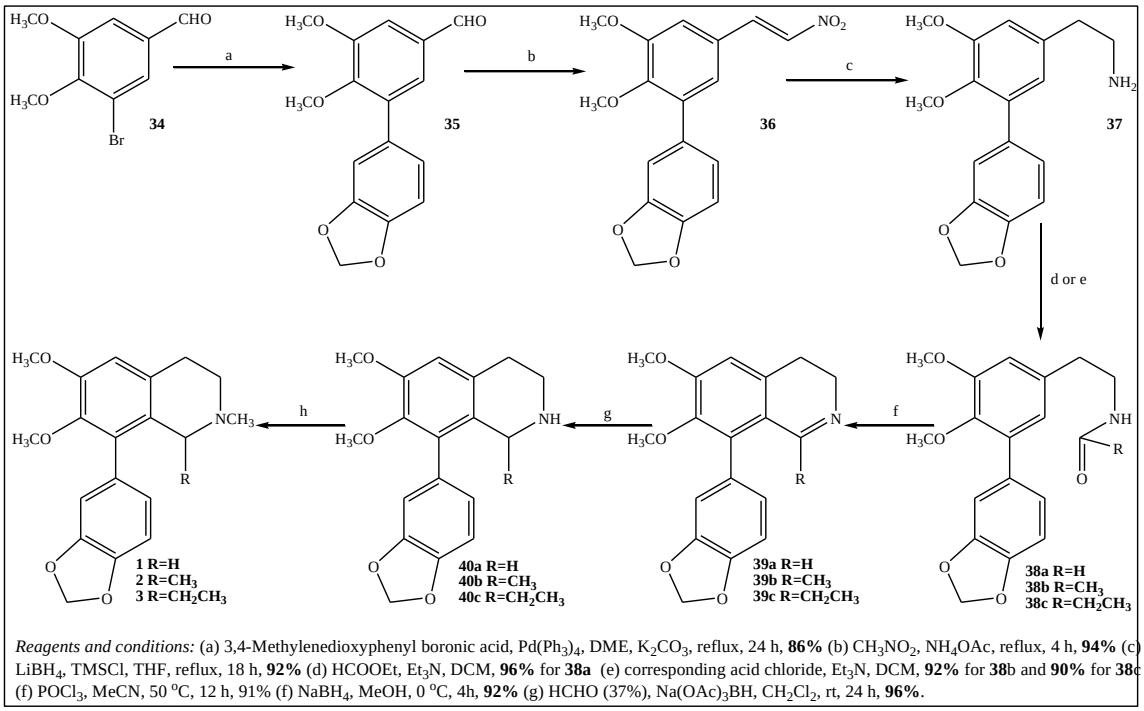

Reagents and conditions: (a) 3,4-Methylenedioxyphenyl boronic acid, $Pd(Ph_3)_4$, DME, K_2CO_3, reflux, 24 h, **86%** (b) CH_3NO_2, NH_4OAc, reflux, 4 h, **94%** (c) $LiBH_4$, TMSCl, THF, reflux, 18 h, **92%** (d) HCOOEt, Et_3N, DCM, **96%** for **38a** (e) corresponding acid chloride, Et_3N, DCM, **92%** for **38**b and **90%** for **38**c (f) $POCl_3$, MeCN, 50 ^oC, 12 h, 91% (f) $NaBH_4$, MeOH, 0 ^oC, 4h, **92%** (g) HCHO (37%), $Na(OAc)_3BH$, CH_2Cl_2, rt, 24 h, **96%**.

Scheme 2.6 Synthesis of nantenine analogs **1-3**

Using Suzuki cross coupling,[20] 3,4-(methylenedioxy) boronic acid was coupled with the commercially available 5-bromoveratraldehyde **34**. Upon nitro-aldol reaction on **35**, nitrostyrene **36** was obtained, which on reduction with lithium borohydride gave the amine **37**. Ethyl formate, acetyl chloride or propionyl chloride, were added to the amine **37**, yielding amides **38a**, **38b** and **38c**, respectively. The amides were cyclized under Bischler-Napieralski reaction conditions to afford the corresponding

dihydroisoquinolines **39a-c**. The dihydroisoquinolines **39a-c** were immediately reduced with sodium borohydride yielding tetrahydroisoquinolines **40a-c**. The methylation under reductive amination conditions[21] of **40a-c** with formaldehyde and sodium triacetoxy-borohydride gave the target analogs **1**-**3**.

The major difficulty during the synthesis of these analogs was the Bischler-Napieralski cyclization of compounds **38a-c**. Using the standard reaction conditions ($POCl_3/CH_2Cl_2$, reflux)[22] we couldn't obtain the desired imines **39a-c**. Probably it was due to steric bulk of the biphenyl system. This problem was solved by changing the solvent to acetonitrile, a polar protic solvent that probably stabilized the iminium ion intermediate en route to **39a-c**.

Analogs **4** and **5** were synthesized via the same intermediate amide **25**, as it is shown in Scheme 2.7 below.

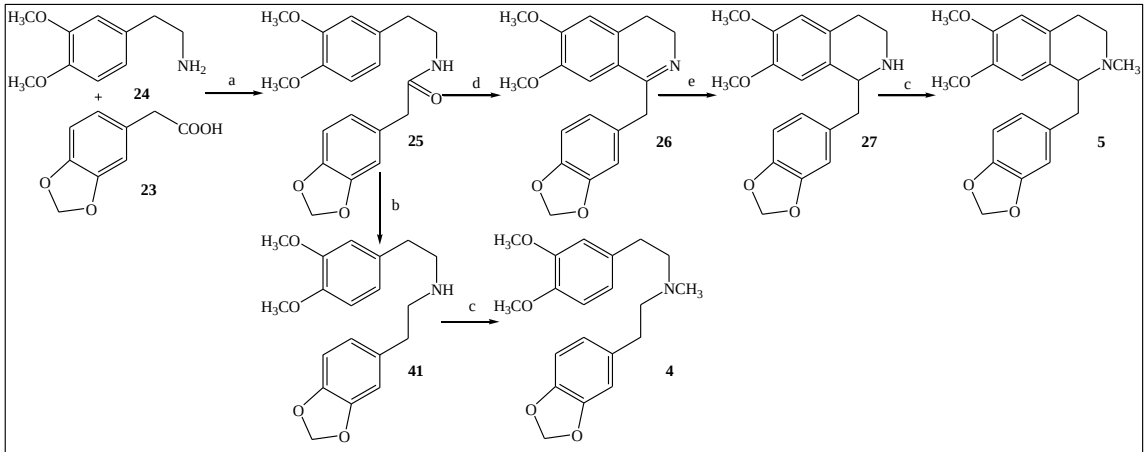

Scheme 2.7 Synthesis of nantenine analogs **4** and **5**

Commercially available 3,4-(dimethoxy)-phenethylamine, **24** and the 3,4-(methylenedioxy) phenylacetic acid, **23** were condensed under CDI peptide coupling conditions to afford amide **25**. The compound **25** was reduced by BF_3-etherate and 1M

BH_3-THF solution, and afforded amine **41** which was subsequently *N*-methylated in order to give analog **4**. Analog **5** was obtained from intermediate amide **25**, in three steps. The amide **25** was first cyclized under Bischler-Napieralski reaction condition to yield the isoquinoline **26**. The imine **26** was reduced with sodium borohydride and that furnished the compound **27**. Reductive amination of **27** yielded analog **5**.

2.3.2 Synthesis of *N*-substituent analogs

This group of nantenine analogs were designed containing various *N*-substituents. Seven different analogs were synthesized and were evaluated for affinity and antagonist activity at 5-HT_{2A} receptor. This group of compounds was synthesized in order for us to understand the importance of the *N*-methyl group of nantenine in antagonizing 5-HT_{2A} receptors:

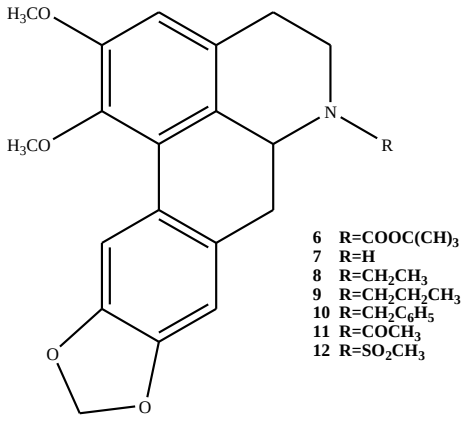

Figure 2.8 Target *N*-methyl substituent nantenine analogs

Previous work done by Indra *et* al. proposed that basic nitrogen makes ionic bond with Asp155 of helix 3 in 5-HT_{2A} receptor[2]and is important for antagonistic activity.[23] In order to indicate if basic nitrogen of nantenine is required for affinity and activity at 5-HT_{2A} receptor, we design analogs **6**, **11** and **12**. The methyl group of nantenine at *N*-6, has been substituted with Boc group in analog **6**, acetyl group in analog **11** and methanesulfonyl group in analog **12**. These groups will on the other hand introduce

additional hydrogen bond acceptor sites. *In vitro* assay for activity and affinity at 5-HT_{2A} receptor will clarify the impact of non-basic nitrogen and presence of these potential hydrogen bonds centers.

The *N*-6 analogs were synthesized following Scheme 2.8 below. Starting from aporphine **7**, a key intermediate in synthesis of nantenine (previously described in Scheme 2.5 above), we obtained analogs **8-12** in a single step reaction. Thus, analog **7** was alkylated via reductive amination to give analogs **8-10**. Addition of acetyl chloride to compound **7**, yielded analog **11**. Analog **12** was prepared by addition of methanesulfonyl chloride[24] to aporphine **7**.

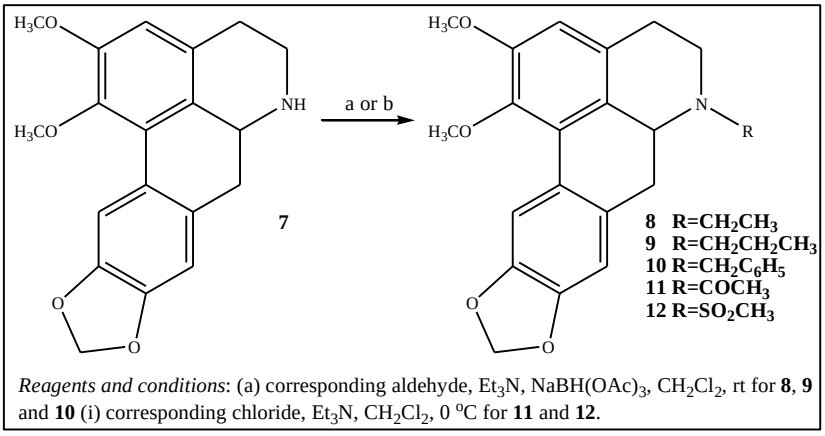

Scheme 2.8 Synthesis of nantenine analogs **6-12**

2.3.3 Synthesis of Ring A and Ring D nantenine analogs

In order to evaluate the role of the methylenedioxy ring we designed a small library of 4 analogs (Figure 2.10) to probe effects of structural variations of the C9 and C10 alkoxy substituents as well as ring A substituents of nantenine on its *in vitro* 5-HT_{2A} activity. Thus, analogs **13-16** were synthesized and evaluated for antagonist activity at 5-HT_{2A} receptors.

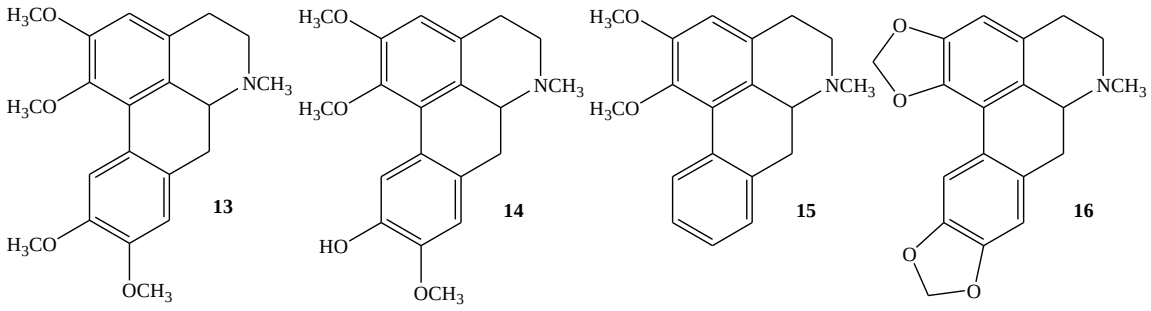

Figure 2.9 Methylenedioxy nantenine analogs

The purpose of synthesis of analog **13** is to evaluate how the replacement of methylenedioxy ring in nantenine structure with the two methoxy groups will affect the antagonism at 5-HT_{2A} receptor. The synthesis and evaluation of analog **14** will also show us the role of methylenedioxy ring of nantenine in antagonizing the 5-HT_{2A} receptor. This analog has hydroxy group in position 10, and hence it is more polar than nantenine and analog **13**. Furthermore, *in vitro* evaluation of this analog will indicate how introducing of this additional hydrogen bond donor will impact the activity at 5-HT_{2A} receptor. *In vitro* evaluation of analog **15** will demonstrate the consequences on antagonistic activity of nantenine when methylenedioxy ring is completely removed from nantenine core. The results we get from *in vitro* screening of analog **16** will clearly show the importance of the dimethoxy substituent in ring A of nantenine in antagonizing the 5-HT_{2A} receptor.

Analogs **13**, **14** and **16** were synthesized starting form commercially available alkaloid boldine **42** using the semi-synthetic route as it is described in Scheme 2.9 below. Upon *O*-methylation of **42**, we obtained analog **13**. Analog **14** was obtained after treating of analog **13** with gaseous hydrogen bromide in glacial acetic acid, the obtained residue contained mixture of products.[25] Using flash chromatography analog **14** was separated and purified.

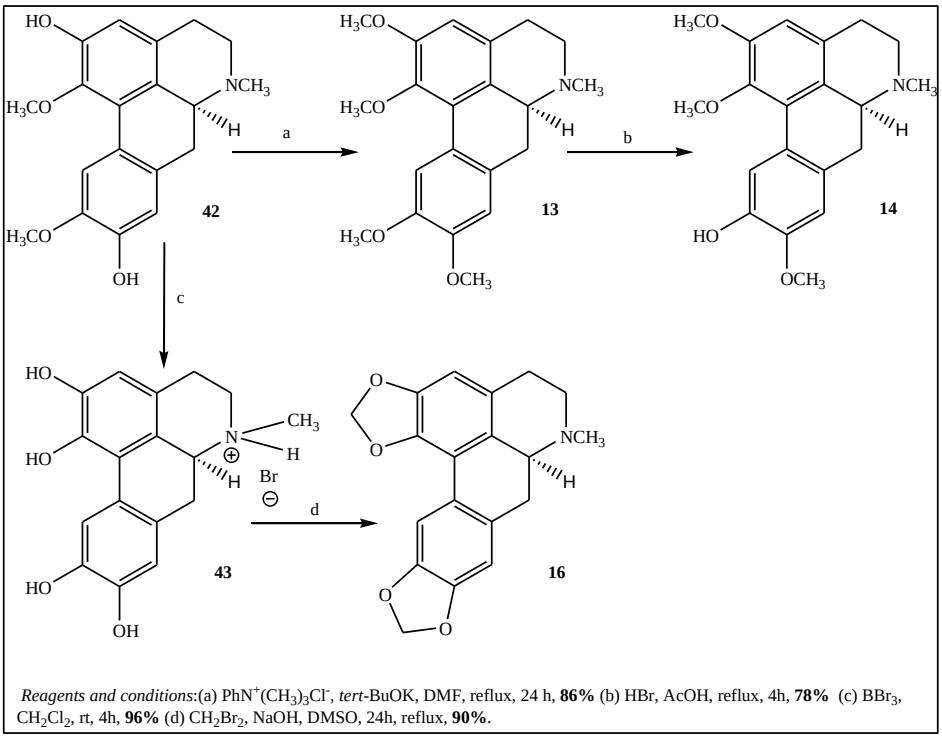

Reagents and conditions:(a) $PhN^{+}(CH_3)_3Cl^{-}$, *tert*-BuOK, DMF, reflux, 24 h, **86%** (b) HBr, AcOH, reflux, 4h, **78%** (c) BBr_3, CH_2Cl_2, rt, 4h, **96%** (d) CH_2Br_2, NaOH, DMSO, 24h, reflux, **90%**.

Scheme 2.9 Synthesis of nantenine analogs **13**,**14** and **16**

Analog **16** was obtained in two-steps. First the methoxy groups of boldine **42** were cleaved using BBr_3, and then the treatment with dibromomethane yielded analog **16**.

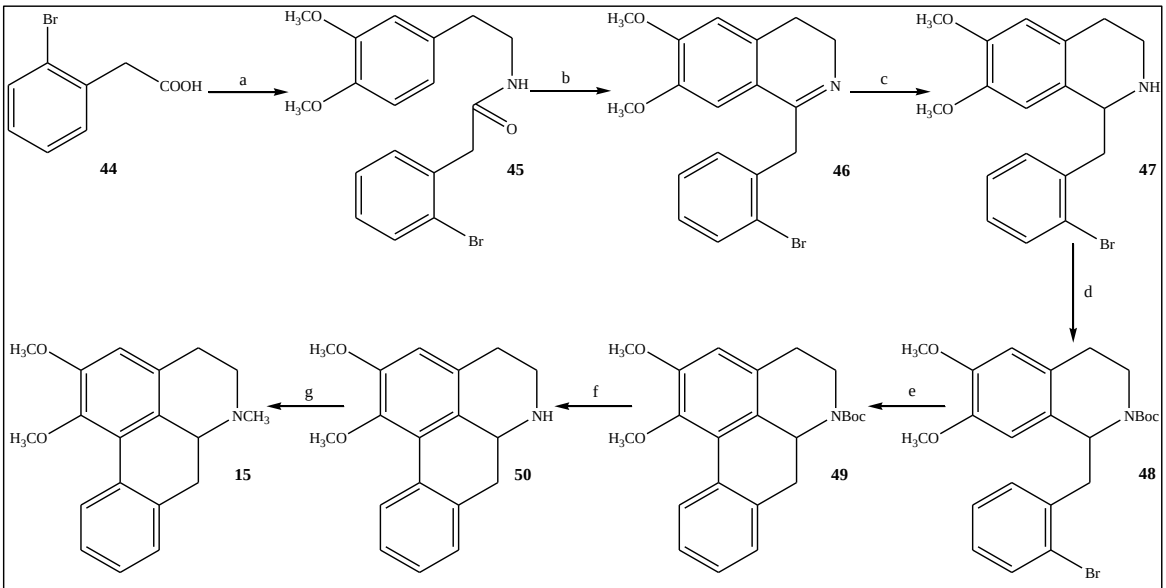

Reagents and conditions: (a) 3,4-(dimethoxy)phenylethyl amine, CDI, THF, **95%** (b) PCl_5, CH_2Cl_2, rt, 24 h (c) $NaBH_4$, MeOH, 0 ^{o}C, 24 h, (d) Boc anhydride,DMAP, *i*Pr_2EtN, CH_2Cl_2, 36 h, rt, **70%** over three steps (e) Pd(II)-acetate, K_2CO_3, Ligand, DMA, 130 ^{o}C, 24 h, **90%** (f) $ZnBr_2$, CH_2Cl_2, rt, **97%** (g) HCHO, CH_2Cl_2, $Na(OAc)_3BH$, rt, 24 h, **98%**.

Scheme 2.10 Synthesis of nantenine analog **15**

Analog **15** was obtained using the similar procedure that we used for the synthesis of nantenine analogs **6-12**. This analog was synthesized as shown in Scheme 2.10 above.

2.3.4 Synthesis of C-1 analogs

C-1 analogs **17-22** were synthesized using microwave assisted biaryl coupling as detailed by us elsewhere.[19] They were also evaluated for antagonism at 5-HT_{2A} receptor.[26] Information we obtained from SAR study of this group of nantenine analogs was implemented in molecular modeling study together with the other analogs; details of these experiments are provide in the next chapter.

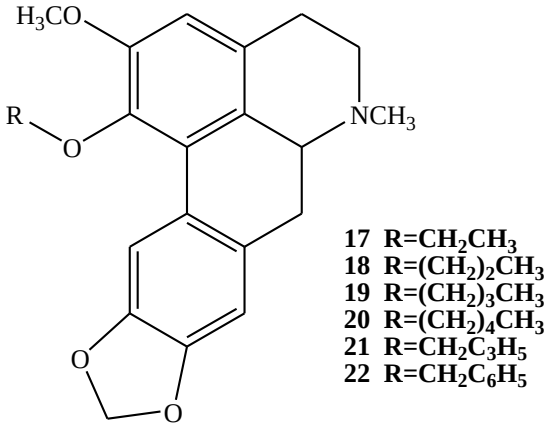

Figure 2.10 C-1 nantenine analogs

2.4 Biological Results

2.4.1 Binding Affinity of Nantenine at CNS Receptors

Nantenine was submitted to the PDSP (Psychoactive Drug Screening Program)[27] at the NIH for binding affinity at CNS receptors. Data available is provided in Table 2-1. The data indicates that nantenine has moderate affinity for 5-HT_{2A} receptor (K_i=832 nM), but also shows that it is a very potent and selective ligand for α_{1A} receptor (K_i=2 nM). Given the α_{1A} selectivity, these results also suggest that this receptor may be responsible for the observed anti-MDMA effects of nantenine. Another important finding is that opioid receptors (DOR, MOR, KOR), β-adrenergic receptors, or dopamine and norepinephrine transporters (DAT and NET) do not seem to be responsible for nantenine's anti MDMA effects given the low affinity at these receptors. Since, there is a lot of evidence that antagonism at 5-HT_{2A} receptor is also important for anti-MDMA effects, our study to improve affinity of nantenine for this receptor is important, because dual 5-HT_{2A}/α_1 antagonists may be a good strategy to treat the actions of MDMA.

Table 2-1. Affinity of Nantenine at CNS receptors - data form PDSP

Receptor	K_i (nM)	Receptor	K_i (nM)	Receptor	K_i (nM)	Receptor	K_i (nM)
5-HT_{1A}	N.A.	**α_{1A} AR**	2	**D1**	895	**DOR**	>10000
5-HT_{1B}	100	**α_{1B} AR**	1191	**D2**	858	**MOR**	>10000
5-HT_{1D}	49	**α_{1D} AR**	340	**D3**	309	**KOR**	7265
5-HT_{2A}	832	**α_{2A} AR**	1288	**D4**	262	**H1**	>10000
5-HT_{2B}	543	**α_{2B} AR**	252	**D5**	2397	**H2**	672
5-HT_{2C}	1069	**α_{2C} AR**	181	**DAT**	>10000	**H3**	>10000
5-HT_{5A}	2224	**β_1 AR**	8565	**SERT**	244	**H4**	>10000
5-HT_6	257	**β_2 AR**	>10000	**NET**	>10000	**Sigma 2**	>10000
5-HT_7	67	**β_3 AR**	>10000				

2.4.2 5-HT_{2A} Receptor Apparent Affinities of Nantenine Analogs

Apparent $5HT_{2A}$ receptor affinity (K_e) data were obtained for each of the target nantenine analogs using a FLIPR (Fluorescent Imaging Plate Reader)-based assay[28] and are presented in Table 2-2. K_e values give an indirect measure of compound affinity. K_e and K_i values usually display the same trend in rank-order within a series of compounds[29] and thus it is acceptable to use K_e (instead of K_i) values in evaluations of relative compound affinities.

The apparent affinities of *seco*-C-ring analogs **1-3** were more than 11-fold less than the affinity of the lead compound, suggesting together with the results for analogs **4** (K_e = 5180 nM) and **5** (K_e > 10000 nM) that the intact aporphine core is required for 5-HT_{2A} receptor affinity.

Removal of the methyl group from position N6 (ie analog **7)** also led to a noticeable decrease in affinity as compared to nantenine. Placing bulkier ethyl and propyl groups instead of a methyl group at the same position, (analog **8** and **9**, respectively**)**, gave qualitatively similar results as the nantenine analog **7**. Evaluation of analog **10**, a compound with a bulky benzyl group at position N6, showed that the receptor doesn't tolerate such a change at that position. Nantenine analogs **6**, **11** and **12** showed decreased affinity, likely because of the absence of a basic nitrogen atom in these compounds; it has been previously proposed that the nitrogen of nantenine is involved in an ionic bond with Asp155 of helix 3 in the 5-HT_{2A} receptor and that this interaction is important for binding of nantenine to the receptor.[2] The importance of methylenedioxy ring was tested with analogs **13-16**. According to these results, it seems that this moiety is important structural requirement for antagonism of nantenine at 5-HT_{2A} receptor.

Table 2-2. Apparent affinities of nantenine analogs

Compound	K_e value(nM)	Compound	K_e value(nM)
(±)-Nantenine	850 (±5.8)	Analog 11	N/A
Ketanserin	2	Analog 12	>10000
Analog 1	>10000	Analog 13	1200
Analog 2	>10000	Analog 14	>10000
Analog 3	>10000	Analog 15	>10000
Analog 4	5180	Analog 16	N/A
Analog 5	>10000	Analog 17	890 ± 430
Analog 6	>10000	Analog 18	297 ± 130
Analog 7	>10000	Analog 19	274 ± 80
Analog 8	>10000	Analog 20	171 ± 50
Analog 9	>10000	Analog 21	68 ± 8
Analog 10	>10000	Analog 22	4600

On the other hand, most C1 analogs showed enhanced affinity as compared to nantenine. Increasing the C1 alkyl chain length by one carbon (analog **17**) had little effect on 5-HT_{2A} antagonist activity. However, incremental additions of 2, 3 and 4 carbons gave a progressive increase in 5-HT_{2A} antagonist activity (analogs **18**, **19** and **20**). Replacement of the C1 methyl group of nantenine with a cyclopropylmethyl moiety (analog **21**) resulted in a 12-fold enhancement in activity as compared to nantenine.

Interestingly, the C1 benzyl analog was found to be a negative allosteric modulator (IC_{50} = 4600 nM).

Our biological results indicate that increasing the length of the C1 alkyl chain beyond two carbon atoms, results in an increase in 5-HT_{2A} antagonist activity in this series of aporphines. The C1 site may thus be a key position for further structural modifications to increase 5-HT_{2A} antagonist activity. Analog **21** was the most active compound identified and showed a 12-fold increase in activity as compared to nantenine. This compound is the most potent 5-HT_{2A} antagonist known with an aporphine skeleton. Our work has also identified a low activity negative allosteric modulator, analog **22**.

2.4.3 Behavioral Tests

Both nantenine enantiomers were evaluated in a food-reinforced operant assay in rats trained under a fixed-ratio 20 (FR20) schedule in the presence of an illuminated stimulus light. All experiments were conducted by our collaborator Dr. Fantegrossi. This behavior was maintained by delivery of one 94 mg food pellet. Behavioral sessions were run daily and consisted of 4 discrete components; each component was terminated after rats earned 20 pellets, or after 20 min—whichever happened first. Each component was separated by a 10 min timeout where stimulus lights were extinguished and lever presses had no programmed consequences. As a positive control, the 5-$HT_{2A/2C}$ antagonist ketanserin was also tested against the rate suppressant effects of MDMA. Importantly, ketanserin has previously been shown to block a range of behavioral and physiological effects of MDMA in mice,[30] rats,[31] rhesus monkeys[32] and humans[33] which guided our selection of this compound as a standard against which to compare the effects of the nantenine enantiomers.

Rats were injected with various dose combinations of ketanserin, (*R*)- or (*S*)-nantenine, and 3.0 mg/kg racemic MDMA. Responding during the first behavioral component following drug administration, normalized to baseline data collected in sessions where no injections were administered, is presented in Figure 2.12. At a dose of 3.0 mg/kg (IP), MDMA profoundly suppresses operant behavior in this first component in all subjects, although responding gradually recovered throughout the remainder of the session. Since this rate of behavioral recovery in subsequent components differed among rats, we present only response data from the first behavioral component as an index of the apparent antagonist effects of the nantenine enantiomers against MDMA-induced behavioral suppression. All pretreatments were administered 15 min prior to MDMA injection. Following two saline injections (separated by 15 min, open square), response rates were essentially unchanged from control. All rats responded at high rates and earned all 20 available food pellets.

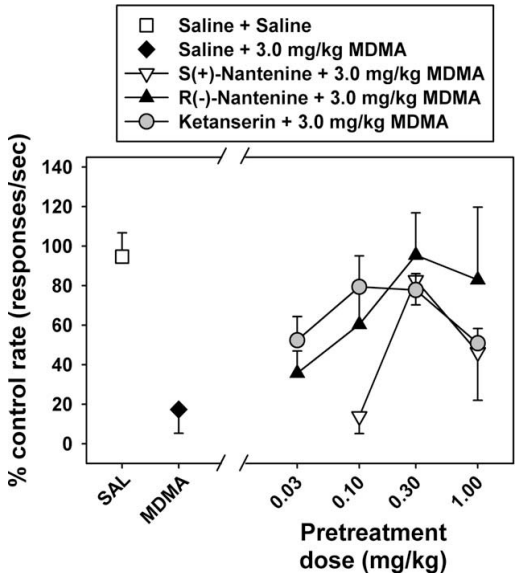

Figure 2.11 Rate suppressant assay with nantenine enantiomers and ketanserin

When 3.0 mg/kg MDMA was injected 15 min after an initial saline injection (filled diamond), response rates were reduced to approximately 20% of control levels,

and rats earned 2 or fewer food pellets. Injection of ketanserin 15 min before MDMA administration (filled circles) had biphasic effects on response rates. At a dose of 0.03 mg/kg ketanserin, MDMA continued to suppress operant behavior to approximately 50% of control levels. At higher doses (0.1 and 0.3 mg/kg), ketanserin blocked the rate suppressant effects of MDMA. At the highest ketanserin dose tested (1.0 mg/kg), ketanserin produced lethargy in all subjects during the pretreatment interval, and these effects likely explain the descending limb of the dose-effect function in Figure 2.12. In comparison, injection of (*S*)-nantenine 15 min before MDMA administration (open inverted triangles) also had biphasic effects. The lowest tested dose (0.1 mg/kg) did not alter the effects of MDMA on operant behavior. However, 0.3 mg/kg (*S*)-nantenine completely blocked MDMA-induced behavioral suppression, and only 1 rat failed to earn all available food pellets at this dose. Higher doses likely had direct effects of their own, and administration of 10.0 mg/kg (*S*)-nantenine appeared to have sedative effects during the pretreatment period, with most rats failing to emit even a single response at this dose (not shown). Like the other antagonists studied, administration of (*R*)-nantenine 15 min before MDMA injection (filled triangles) also had biphasic effects. The lowest dose tested (0.03 mg/kg) did not alter the effects of MDMA on operant behavior. At 0.1 mg/kg, (*R*)-nantenine partially blocked the rate suppressant effects of MDMA. The highest two doses tested (0.3 and 1.0 mg/kg) completely blocked the effects of MDMA on operant responding.

2.5 Discussion

In 2002, Indra *et al*. reported that nantenine is an antagonist at 5-HT_{2A} and α_1 receptors.[2,3,34] In experiments done by our collaborator, nantenine was shown to block and reverse MDMA-induced hyperthermia and also to antagonize a wide range of other MDMA-induced effects in mice.[1] Previous studies have shown that selective antagonists at 5-HT_{2A} and α_1 receptors block or reverse MDMA-induced effects in both, human and rodents.[1,33,35] Also, recently, risperidone, a dual 5-HT_{2A}/α_1-adrenoreceptor antagonist, was shown to attenuate MDMA-induced hyperthermia in rats.[36]

Based on the above, nantenine is a good starting point for synthesis of MDMA antagonists.

The central hypothesis of our project is that nantenine may be structurally modified to give more potent antagonists at the 5-HT_{2A} receptor. To test this hypothesis we synthesized various nantenine analogs and screened them in a FLIPR-based 5-HT_{2A} assay for antagonist activity.

Although a number of SAR studies have been performed with aporphines at other receptors, very few such studies have been done at 5-HT_{2A} receptor.[37,38]

In order to perform an SAR study, we needed to establish a high-yielding route to synthesize the lead molecule, nantenine. We needed significant quantities of nantenine for our biological assays in animals and for in vitro screening at various CNS receptors. Additionally, we anticipated that this route would be useful for synthesis of various nantenine analogs.

There are several commonly employed approaches for the synthesis of aporphines.[39-42] A popular route involves oxidative biaryl coupling of the intermediates

that are precursors of the aporphine skeleton. Metal-based oxidatizing agents (eg. $VOCl_3$, $Pb(OAc)_4$, RuO_2, Cr_2O_3, etc.) are usualy employed (Table 2-3). Some of these reagents are toxic, and the yields obtained are low. We decided to use PIFA- promoted oxidative biaryl coupling, since it has shown high yields in the formation of aporphines.[11] In our hands, however, only 10% of desired product was obtained using similar conditions as that reported in the literature for similar substrates.[5,8,43]

Table 2-3. Oxidative coupling of laudinosine (See Figure 2.2)
(Anakabe et al, *Synthesis*, **2004**, *7*, 1093)

Reagents	T (°C)	Yield (%)
Cr_2O_3/TFAA/TFA	reflux	-
$Ce(OH)_4$/TFAA/TFA/$BF_3{\cdot}OEt_2$	0 °C	60
$Ce(OH)_4$/TFAA/TFA/$BF_3{\cdot}OEt_2$	r.t.	10
RuO_2/ $BF_3{\cdot}OEt_2$/TFAA/TFA	-10 °C	60
Bu_3SnH/AlBN	reflux	-

A group in 2007 proposed two mechanistic postulates to rationalize how PIFA-mediated biaryl coupling might occur with oxygenated tetrahydroisoquinoline substrates.[13] According to this study the aporphine precursor will undergo either of these mechanisms depending on the methoxylation pattern on the aromatic ring and the nature of the substituents on the nitrogen. They concluded that alkoxy group in positions C3 and C9 will allow direct *p-p* coupling, affording aporphines in good yields. On the other hand, absence of methoxy groups at these positions led to low reaction yields, and they proposed that these precursors of aporphines might instead undergo bridgehead *p-p* coupling. In keeping with these observations, we noticed low yields for this reaction in synthesis of nantenine (10% comparing with their reported 36%), and our efforts to improve the yield of this step were unsuccessful. It would be interesting to use a

nantenine precursor with an additional alkoxy group at position C3 to see whether this would improve the yields of PIFA-mediated biaryl coupling. Another possible contributor to the low yield obtained in this reaction might be a stereoelectronic effect.[44] Sha *et al*. used Friedel-Crafts type cyclization to obtain alkaloid cephalotaxine (Figure 2.12). When they used a precursor that had two methoxy groups attached to aromatic moiety, the cyclization went smoothly, in a moderate yield (56%), but when a methylenedioxy ring was present on the phenyl ring under the same reaction conditions, no cyclized product was obtained. They attributed this dramatic difference in reactivity between these two starting compounds to a stereoelectronic effect.

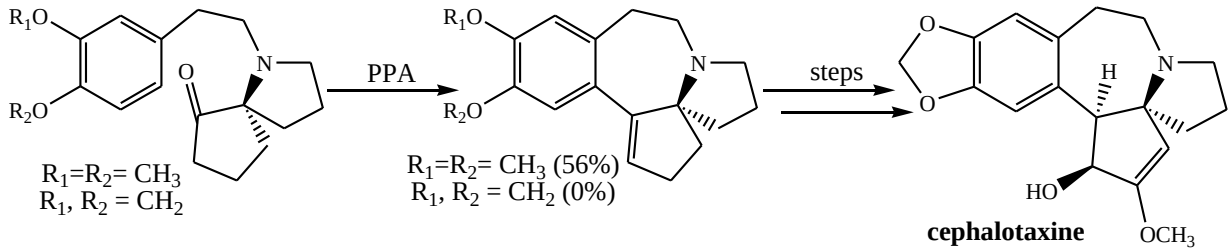

Figure 2.12 Fridel-Crafts cyclization approach toward cephalotaxine synthesis (Sha et al, *J. Org. Chem.*, **1991**, *56*, 2694)

In the compound that has two methoxy groups, the lone pairs of electrons of these groups could have a good orbital overlap with the π-system of the phenyl ring as a result of their free rotation. However, in compound with the rigid methylenedioxy substituent on the phenyl ring, this group does not allow a complete orbital overlap between oxygen lone pairs of electrons and the π-system of the phenyl group (Figure 2.13).

Due to this stereoelectronic effect, the phenyl ring of the dimethoxy substrate is of higher electron density and therefore more reactive toward an electrophilic reaction than that of the methylenedioxy substrate.[45]

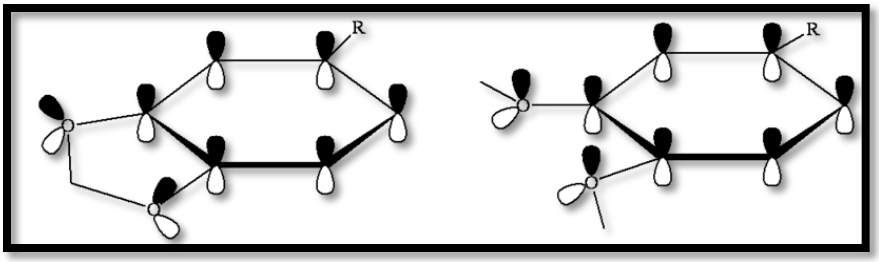

Figure 2.13 The orientation of lone pairs of electrons of oxygen atoms in two compounds that were used as starting materials for Friedel-Crafts cyclization by Sha *et al.*

Since nantenine precursor has a methylenedioxy moiety attached to one of the aromatic rings, it is possible that due to stereoelectronic effects, the methylenedioxy ring is a poor nucleophile, and this might be a reason why PIFA-mediated biaryl coupling in our reaction does not proceed smoothly.

In 2007, Fagnou et al, reported a synthesis of various aporphines using thermal Pd-catalyzed direct biaryl coupling conditions.[15] We decided to design a route for synthesis of nantenine using this approach. This route provided nantenine-cyclized precursor in a moderate yield (48%). Addition of pivalic acid, a known enhancer of biaryl coupling reactions,[18] did not result in any improvement in the overall yield. Microwave irradiation is being increasingly utilized in organic synthesis because it is a much more rapid procedure, operationally simpler and the product yields are comparable or in some cases superior to standard thermal conditions.[46,47] Microwave-assisted versions of various biaryl coupling methodologies such as Suzuki, Heck and Negishi reactions have been reported in the literature,[48-51] however only a few reports are available on the use of microwave irradiation in direct biaryl coupling procedures. In order to increase the yield of biaryl coupling step, we employed microwaves and reported the first rapid, high-yielding microwave-assisted biaryl coupling in the synthesis of aporphines.[19] This route

was amenable to the synthesis of nantenine as well as a library of nantenine analogs for our SAR study.

Screening of nantenine, for binding affinities at various CNS receptors, showed high selectivity for α_{1A} receptor (up to date this is the highest affinity aporphine alkaloid at this receptor) and moderate affinity for 5-HT_{2A} receptor.[52] This data may indicate that previously observed anti-MDMA effects of nantenine[1] may be due at least in part to antagonism at α_{1A}-adrenoreceptor. However, there is a lot of evidence in literature that antagonism at 5-HT_{2A} receptor is also beneficial for treatment of MDMA-caused intoxication.[35] Thus our study is an important foundation in the process of development of dual 5-HT_{2A}/α_{1A} receptor antagonists, as a good strategy for preparing new MDMA antagonists. Interestingly, in this assay, nantenine also showed good affinity for 5-HT_{1D}, 5-HT_6, 5-HT_7, D3, D4 and SERT. Therefore our study has opened up new areas to explore for the development of ligands which are potent and selective for these receptors. Furthemore, these findings also support a widely accepted property of aporphines- that the aporphine skeleton is a "privileged structure"- one that is receptor non-selective, but which may nevertheless be "tuned" to a particular receptor or a group of receptors.[53]

Previously it has been shown that the catecholic function of aporphines contributes to the high dopaminergic activity due to H-bonding with DA receptors.[37] While some aporphines bind with high affinity to D2 receptor,[38,54,55] nantenine showed higher affinity for D3 and D4 receptors. Future extensive SAR studies on natenine and screening of analogs for affinity at D2, D3 and D4 receptors should provide more information about which structural features of nantenine are responsible for this selectivity. One should be aware that these results we obtained from multi-receptor

screening of nantenine are only for affinity of nantenine for the various CNS receptors. In order to elucidate whether nantenine has agonist or antagonist activity at these receptors, further experiments are needed.

Previous SAR studies on aporphine alkaloids at dopamine D2 receptors have shown the importance of the chiral center that is present at carbon 6a, for example (*R*)-aporphines act as agonist, while (*S*)-aporphines have antagonistic activity at dopamine D2 receptor, both *in vitro* and *in vivo*.[37] However, resolution of nantenine into (*R*)- and (*S*)-enantiomers showed that both (*R*)- and (*S*)-nantenine can completely reverse the behavioral suppression induced by MDMA in mice in a dose-dependent manner.[52] In this experiment, mice treated with MDMA in a dose of 3.0 mg/kg showed suppressed food intake, compared to a group of control mice that were treated only with saline. Mice treated with 3.0 mg/kg MDMA and 0.3 mg/kg (*S*)- or (*R*)- nantenine have shown to have food intake same as control mice. These results suggest that both nantenine enantiomers in this dose act as MDMA antagonists. Further increases in dose of (*S*)- or (*R*)- nantenine to 1.0 mg/kg, resulted in suppression of food intake. The suppression of food intake at higher doses may be because of direct effect of nantenine or a metabolite on locomotor activity of mice at that dosage.

To screen our nantenine analogs at the 5-HT_{2A} receptor a FLIPR-based assay was used. Since it is known that 5-HT_{2A} receptors are linked to the Gq family of G-proteins and subsequent activation of phospholipase C, induction of phosphoinositide metabolism and an increase in intracellular calcium concentration,[56,57] this assay has been developed to quantify intracellular Ca^{2+} by use of calcium-sensitive dye. In the most common FLIPR protocols fluo-4 has been used as a calcium sensitive dye which increases its

quantum yield upon binding to calcium. Several reports have shown that there is a good correlation between agonist/antagonist affinities using a FLIPR assay and those reported in radioligand binding studies.[58,59] The major advantages for using a FLIPR assay is that this is a nonradioactive method, fully automated with several easily developed protocols so that both agonists and antagonists of the same receptor can be detected in a single screening assay.[28] Another advantage is that this assay allows for the simultaneous determination of affinity and activity (agonist or antagonist). Quantification of released calcium allows for the determination of the degree of activation of the receptor. Modifications of the Cheng-Prusoff equation are used to calculate the apparent affinity (K_e), again based on quantification of released calcium.

To elucidate whether our compounds were binding to 5-HT_{2A} receptor, we used CHO-K1 cells that overexpress gene for human 5-HT_{2A} receptor. The results obtained with this cell line, were compared with the results from wild-type cells.

In agonist mode, compounds were run in parallel with serotonin. After comparing the change in fluorescence we found that our compounds did not produce effects similar to that of serotonin. This indicated that they do not have agonistic activity. When searching for antagonistic activity both wild-type and mutant cells were preincubated with the test compound and basal (unstimulated) fluorescence intensity was recorded. The cells were then treated with serotonin and fluorescence measured. Basal fluorescence was subtracted from the fluorescence caused by the serotonin addition. These results were compared with fluorescence measured from the cells treated only with serotonin. Our experiments showed that the cells preincubated with our compounds had exhibited impaired increase in fluorescence. Since the effect was much more pronounced in mutant

cells, this confirmed that this reduced fluorescence (decreased calcium release) was due to binding of our compounds to the 5-HT_{2A} receptor. In the case of nantenine analogs **17-21** a parallel rightward shift of the serotonin dose-response curve with no alternation in maximal response was observed. This is indicative of competitive antagonism.[60] In the case of compound **22**, a rightward shift of the 5-HT dose-response curve was observed with a depression in the maximal response, suggesting negative allosteric modulation at the receptor by this compound.[60]

SAR explorations have revealed that the rigid structure of nantenine is important for antagonistic activity at 5-HT_{2A} receptor; increasing molecular flexibility was associated with a decrease in affinity for this receptor. Flexible analogs **1-3**, that were designed to test the role of ring C in the nantenine antagonism at 5-HT_{2A} receptor are new compounds belonging to the group of *seco*-C ring aporphines. These compounds showed an interesting NMR effect. Namely, we noticed that these analogs have two sets of ^{13}C signals. Since these analogs contain the biaryl bond of nantenine, but the ring C is absent, this will provide additional possible rotation around the biaryl bond. We believe that the duplication of NMR signals for these compounds is due to atropisomerism, a type of stereoisomerism that is observed in systems such as biaryls where there is free rotation about the single sp^2-sp^2 carbon-carbon bond.[61]

Analog **4**, the most flexible compound in our library of nantenine analogs, retained some, although diminished activity. A possible explanation could be that this compound binds to the receptor in a linear orientation (the lowest energy form), resembling the class II antagonists (spiperone, ketanserin, M100907, etc.). Since we know that 5-HT_{2A} receptor antagonist can be classified in two different classes, analog **4**

might be a good starting compound to use to make more potent 5-HT_{2A} receptor antagonists by designing compounds that retain the class II pharmacophoric features but which also contain a class I pharmacophore.

Our SAR study also suggested that the *N*-methyl group as well as the methylenedioxy ring play a significant role in nantenine's antagonism at 5-HT_{2A} receptor. We found that *nor*-methyl nantenine analog, analog **7** is inactive. Also the introduction of more bulky groups: ethyl, propyl and benzyl, in analogs **8**, **9** and **10**, respectively resulted in a dramatic reduction of activity towards the 5-HT_{2A} receptor. The data for analogs **7** and **8** are consistent with the data reported by Indra et al.[2] Analogs **6**, **11** and **12** were also inactive, suggesting that basic nitrogen is required for the activity at 5-HT_{2A} receptor. This data also supports mutagenesis data, which indicates that replacement of a conserved residue, Asp155 (located in TM3) with other amino acids leads to a loss of activity due to inability of the *N*-protonated ligand to form a hydrogen bond with the mutated residue.[62] Again, this may be a direct consequence of the decreased basicity of the nitrogen atom in these analogs which thereby precludes protonation and H-bonding. However, it is also possible that undesirable interactions with the *N*-substituents may be occuring in this area of the receptor. Alternatively, it is possible that these compounds bind in a completely different manner as compared to nantenine and other similar compounds. There are 5-HT_{2A} receptor antagonist reported which do not have basic nitrogen.[63]

Although our library of nantenine analogs that were designed to elucidate the role of methylenedioxy ring in nantenine antagonistic effect at 5-HT_{2A} receptor consisted of

only a few analogs, based on *in vitro* results so far we might conclude that this ring is important structural requirement for 5-HT_{2A} receptor antagonism.

On the other hand, our biological results showed that increasing the length of the C1 alkyl chain beyond two carbon atoms, resulted in an increase in 5-HT_{2A} antagonist activity in this series of aporphines.[26] The C1 site may thus be a key position for further structural modifications to increase 5-HT_{2A} antagonist activity. Further SAR studies at this position are expected to clarify the role of steric, lipophilicity and electronic effects in improving antagonism at the 5-HT_{2A} receptor. For example, it would be useful to explore and evaluate other C1 analogs, such as those shown in Figure 2.14 below in future.

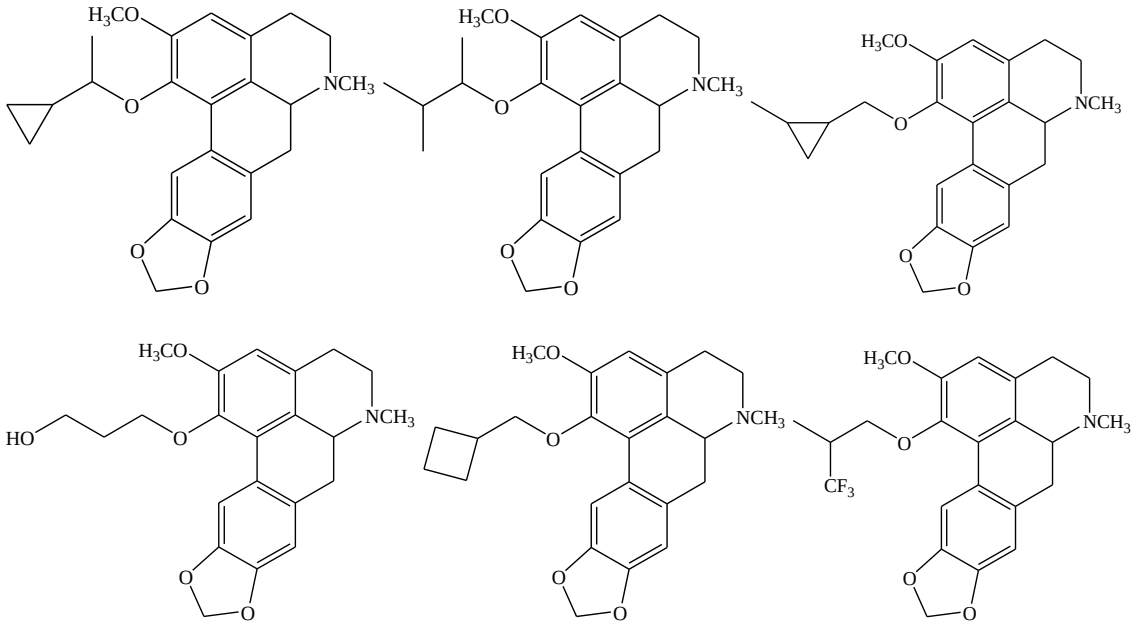

Figure 2.14 C1 nantenine analogs for follow-up SAR study

In vitro screening of C1 nantenine analogs at α_{1A}-adrenoreceptor to be conducted in future will show how these structural changes affect antagonism at this receptor. Furthermore, behavioral tests on C1 nantenine analogs will show the importance of

antagonism at both 5-HT_{2A} and α_{1A} receptors, and/or if a certain ratio in antagonizing these two receptors is desirable for maximal anti-MDMA effects. A similar antagonism ratio concept between, 5-HT_{2A} and D4 receptors (the so-called Meltzer ratio),[64] has been used for the development of new atypical antipsychotics.[65]

It is known that aporphines in general have low bioavailability and short duration of action.[37] Since the human body is almost 75% water, the solubility of a drug molecule in water affects several pharmacological and pharmacokinetic properties such as absorption, distribution, metabolism and elimination. On the other hand, a drug molecule needs to posses some lipophilic properties in order to pass the biological membranes, which consist of lipid bilayers. Still the blood-brain barrier (BBB) remains one of the greatest challenges in the development of new drugs for treatment of different CNS disorders. It has been shown that BBB does not have only the role in transport from and into the CNS, it appears that BBB also plays a role in progression of certain brain disorders, such as AD, Parkinson's disease, multiple sclerosis and stroke.[66-70] The drug optimization is therefore one of the most challenging steps in the process of the drug development. Lipinski et al[71] defined a set of five general rules that would govern drug-like properties that can be used in drug optimization. According to them, a good absorption and permeability is likely if:

- Molecular weight is ≤ 500
- ClogP is ≤ 5
- Hydrogen bond donors ≤ 5
- Hydrogen bond acceptors ≤ 10
- Number of rotatable bonds ≤ 10

This "rule of five" has been modified for the CNS drugs since penetrability of the BBB is an important additional property which should be taken in account. It has been suggested that drugs which should penetrate BBB should have: molecular weight < 450, ClogP < 3, hydrogen bond donors less than 4, and hydrogen bond acceptors less than 8.[72]

Nantenine has molecular weight of 345.43, calculated logP of 3.6 and by looking at its structure there are no hydrogen bond donors, and 5 possible hydrogen bond acceptors. Clearly, the ClogP has to be improved in order to use nantenine as a potential CNS drug. We calculated logP, using ChemDraw 11.0, for other C1 nantenine analogs, and they are presented in Table 2-4 below.

Table 2-4. ClogP values of nantenine and C1 nantenine analogs

Compound	K_e (nM)	CLogP
Nantenine	850 (±5.8)	3.60
17	890 (±430)	4.13
18	297 (±130)	4.66
19	274 (±80)	5.19
20	171 (±50)	5.72
21	68 (±8)	4.58
22	4600	5.37

Based on this table, different structural replacements at C1 resulted in improved antagonistic activity for 5-HT_{2A} receptor (K_e values), but did not enhance the ClogP of nantenine. Still the ClogP values are in the reasonable range for further development of these drugs as potential therapeutic candidates. Water solubility of new potential drug can be improved by making a salt of that compound. Other reported approach to increase both bioavailability and longer duration of action in aporphines is to introduce the fluorine in aromatic ring instead of hydrogen.[73] However, although heterocyclic replacement, functional group interchange, or more drastic changes such as addition of

substituents, would improve the bioavailability, one needs to be aware that these could also completely change the properties, affinities and increase the side effects of the drugs as well.[74,75]

2.6 Conclusion

PIFA-mediated oxidative biaryl coupling procedure for the synthesis of nantenine is low-yielding with a variety of conditions investigated. A new, facile and high-yielding procedure for synthesis of nantenine and aporphine derivatives using a microwave irradiation has been optimized.

Nantenine was found to have high affinity and selectivity for the α_{1A} adrenoceptor, while being only a moderate 5-HT_{2A} receptor antagonist. Both (*R*)- and (*S*)-nantenine completely blocked behavioral suppression induced by MDMA.

Our SAR study on nantenine at the 5-HT_{2A} receptor has shown that the intact aporphine core, *N*-methyl group and methylenedioxy ring are structurally important requirements for nantenine's antagonism at this receptor. A number of C1 nantenine analogs that are more potent antagonists at the 5-HT_{2A} receptor than the lead compound nantenine were identified. Among them, analog **21** is a compound with 12-fold increased activity at the 5-HT_{2A} receptor compared with nantenine, to date this is most potent 5-HT_{2A} antagonist known with an aporphine skeleton.

Our work has positively impacted the field of MDMA research by allowing us to identify novel 5-HT_{2A} receptor antagonists based on a nantenine scaffold. Such molecules will be useful to study and develop further as potential MDMA antagonists.

Although the development of 5-HT_{2A} receptor antagonists is useful for the field of MDMA, these antagonists will have collateral benefits since the 5-HT_{2A} antagonists are useful for treatment of a variety of disease/conditions.[76]

2.7 Experimental

General Methods and Instrumentation

Chemistry: High Resolution Electron Impact Mass Spectra (HREIMS) were obtained using an Agilent 6520 Q-TOF instrument. NMR data were collected on a Bruker 500 MHz machine with TMS as internal standard and $CDCl_3$ as solvent unless stated otherwise. Chemical shift (δ) values are reported in ppm and coupling constants in Hertz (Hz). Melting points were obtained on a Mel-Temp capillary electrothermal melting point apparatus. Reactions were monitored by TLC with Analtech Uniplate silica gel G/UV 254 precoated plates (0.2 mm). TLC plates were visualized by UV (254 nm) and by staining with phosphomolybdic acid reagent followed by heating. Flash column chromatography was performed with Silicagel 60 (EMD Chemicals, 230-400 mesh, 0.04-0.063 µm particle size). HPLC spectra were obtained on an Agilent 1200 system. Sample was dissolved in MeOH with sample concentration 1 mg/mL. Flow rate was 1 mL/min and injection volume was 30 µL. Methanol and acetonitrile were used as a mobile phase and detection wavelength was 285 nm. To determine enantiomeric excess Chiralcel®, 150x4.6 cm, column was used. To determine purity of all final compounds Zorbax® C18, 150x4.6 cm, column was used. All compounds tested *in vitro* and *in vivo* were at least 95% pure as determined by HPLC. Stereochemistry of (*R*)- and (*S*)- nantenine was

determined by CD spectroscopy (all samples were dissolved in 95% ethanol with sample concentration 0.2 mg/mL).[77]

FLIPR Calcium Mobilization Assay: Our collaborator Dr. Hernan Navarro has stably expressed the human 5-HT_{2A} receptor in CHO-K1 cells (ATCC). This clonal cell line was used to develop a robust FLIPR-based functional assay for receptor activation. The calcium 4 dye assays (Molecular Devices, Sunnyvale, CA) were run according to manufacturer's specifications. Briefly, wells of black clear bottom 96-well tissue culture-treated plates were seeded with 20,000 cells the afternoon before assay. The day of assay, the cells were incubated with the calcium indicator dye for 1 hour at 37 °C. For antagonist assay the test compound was preincubated with the cells during the last 15 min of the dye incubation. The plate was then placed into FlexStation pre-warmed to 37 °C. Basal or unstimulated fluorescence intensity was recorded for 13 seconds followed by the addition of the test compound (intrinsic activity) or 5-HT (antagonist and K_e assays). Fluorescence intensity was recorded for an additional 47 seconds. The effect of test compound was determined by subtracting the minimum from the maximum florescence recorded for each well during the 47-seconds recording period. Thus, each well served as its own control. All samples were run in duplicate. For the agonist screening assays, the compounds were added directly to the cells and their effect on basal fluorescence was recorded. For the antagonist screening assays, the cells were preincubated with the test compounds for 15 minutes at 37 °C before the FlexStation added 5-HT at its EC_{80} (~20 nM). Any compound that inhibits the effects of 5-HT by at least 50%, its apparent affinity (K_e) were determined (see below). On-plate controls for screening assays: It is important to monitor assay performance because cell responsiveness can change over

time. For this reason, a 6-point log-unit 5-HT curve, 1 mM ketanserin (selective for 5-HT_{2A} receptor), and 1 mM SB 206553 (selective for 5-$HT_{2B/2C}$ receptors) were run on each assay plate. If the EC_{50} value for 5-HT was more than two SD different from the historical average that assay plate had to be rerun. If a consistent shift in the 5-HT EC_{50} was observed, a new batch of 5-HT_{2A} –expressing cells were used. Antagonists had their apparent affinity or K_e values determined by running a 8-point half log 5-HT concentration response curve in the presence and absence of a single concentration of antagonist. The EC_{50} values were calculated for 5-HT (A) and 5-HT + test compound (A`), and these were used to calculate the test compound $K_e$ using the formula: $K_e$ = [L]/(DR-1), where [L] equals to concentration of test compound in the assay and DR equals the dose ratio or A`/A. The concentration of antagonist was chosen such that it caused at least a 2-fold increase (shift to right) in the 5-HT curve. If an antagonist was found to produce an insurmountable inhibition of 5-HT, it was assumed to be acting in a noncompetitive manner. In these cases, the compound had its IC_{50} determined by running a concentration response curve in presence of the 5-HT EC_{80}. Assay performance for compound characterization was monitored as described above for the screening assays. In the case of the K_e experiments, the 5-HT curve also served to monitor assay performance.

2-(benzo[*d*][1,3]dioxol-5-yl)-*N*-(3,4-dimethoxyphenethyl)acetamide (25). A solution of 3,4-(methylenedioxy) phenylacetic acid **23**, (7.45 g, 41.38 mmol) and 1,1'-carbonyldiimidazole (6.71 g, 41.38 mmol) in 100 mL of anhydrous THF was stirred at 0 °C for 1.5 h and then at room temperature for 1 h. The mixture was cooled again in an ice bath and stirred for 1 h. Then 3,4-dimethoxy-phenethylamine **24**, (4.58 mL, 27.58 mmol)

was added and the solution was stirred at 0 °C for 4 h, and at room temperature overnight under nitrogen atmosphere. The THF was evaporated under reduced pressure and the residue was dissolved in hot EtOAc (200 mL) and was washed with 1N HCl (75 mL), water (100 mL) and aqueous $NaHCO_3$ (75 mL). The organic layer was evaporated and the crude product was crystallized from EtOAc to give the amide **25** (8.71 g, 91%): **mp**: 92-93 °C; **^{1}H NMR** (500 MHz, $CDCl_3$): δ 6.75 (m, 2H), 6.61 (m, 4H), 5.96 (s,2H), 5.38 (bs, 1H), 3.86 (s, 3H), 3.84 (s, 3H), 3.46 (m, 2H), 3.44 (s, 2H), 2.69 (m, 2H); **^{13}C NMR** (125 MHz, $CDCl_3$): δ 170.9, 149.0, 148.0, 147.7, 146.9, 131.0, 128.3, 122.6, 120.6, 111.7, 111.2, 109.7, 108.6, 101.1, 55.9, 55.8, 43.5, 40.6, 35.0; **HRESIMS**: calcd. for $C_{19}H_{21}NO_5$ $[M+H]^+$ 344.1420; found 344.1509.

1-(benzo[*d*] [1, 3]dioxol-5-ylmethyl)-6, 7-dimethoxy-3, 4-dihydroisoquinoline (26). Phosphorus pentachloride (1.21 g, 5.82 mmol) was added during 30 min in three portions to a chilled (0 °C) solution of amide **25** (1.00 g, 2.91 mmol) in dry CH_2Cl_2 (15 mL) under argon and the mixture was stirred for 30 min. Then, the ice bath was removed and the mixture was stirred at room temperature for 24 h. The reaction mixture was then poured onto a saturated solution of aqueous $NaHCO_3$ (25 mL) and the contents of the flask were stirred for 1 h. The aqueous layer was extracted twice with CH_2Cl_2 (10 mL) and the combined organic extracts were washed with saturated solution of aqueous $NaHCO_3$ (50 mL), dried over Na_2SO_4, filtered and evaporated to give imine **26**. Since compound **26** is prone to air oxidation, it was used without further purification for the preparation of **27**.

1-(benzo[*d*] [1, 3] dioxol-5-ylmethyl)-6, 7-dimethoxy-1, 2, 3, 4-tetrahydroisoquinoline (27). Sodium borohydride (6.55 g, 173.15 mmol) was added portion wise to a stirred solution of crude **26** (3.50 g, 8.65 mmol) in MeOH (100 mL) and the mixture was stirred at 0 °C for 4 h. The reaction mixture was concentrated, and excess $NaBH_4$ was destroyed by adding water (100 mL) and glacial acetic acid (50 mL). The mixture was extracted with CH_2Cl_2 (3x35 mL), dried over Na_2SO_4 and concentrated to give crude yellow solid **27**. This compound was used for the next step without any further purification.

1-(benzo [*d*] [1,3] dioxol-5-ylmethyl)-6,7-dimethoxy-2-methyl-1, 2, 3, 4-tetrahydro-isoquinoline (28). Compound **27** (0.70 g, 2.13 mmol) and formaldehyde solution, 37% (4.35 mL, 4.27 mmol) were mixed in anhydrous CH_2Cl_2 (50 mL) and then treated with sodium triacetoxy-borohydride (2.25 g, 10.65 mmol). The mixture was allowed to stir at room temperature for 1.5 h. The reaction was quenched with 5% aq $NaHCO_3$ (25 mL), and extracted with EtOAc (2x25 mL), and dried over Na_2SO_4 and concentrated to dryness. The residue was purified through flash chromatography (silicagel, MeOH:CH_2Cl_2, 5:95) to obtain compound **28** (0.49 g, 68%) as a bright yellow oil: **^{1}H NMR** (500 MHz, $CDCl_3$): δ 6.71 (d, 1H, *J*=7.8 Hz), 6.64 (s, 1H), 6.55 (m, 2H), 6.11 (s, 1H), 5.91 (s, 2H), 3.84 (s, 3H), 3.66-3.65 (m, 1H), 3.62 (s, 3H), 3.17-3.08 (m, 2H), 2.83-2.72 (m, 3H), 2.60-2.57 (m, 1H), 2.51 (s, 3H); **^{13}C NMR** (125 MHz, $CDCl_3$): δ 147.3, 147.3, 146.4, 145.7, 133.8, 129.2, 125.9, 122.6, 111.1, 110.9, 110.1, 107.9, 100.7, 64.9, 55.7, 55.6, 46.8, 42.6, 41.0, 25.3; **HRESIMS**: calcd. for $C_{20}H_{23}NO_4$ $[M+H]^+$ 342.16271; found 342.17045.

Nantenine (51). A solution of PIFA (0.50 g, 1.16 mmol) in CH_2Cl_2 (15 mL) was added at -20 °C to a solution of **28** (0.32 g, 0.93 mmol) and $BF_3{\cdot}OEt_2$ (0.29 mL, 2.325 mmol) in CH_2Cl_2 (25 mL). The mixture was stirred for 60 min and then was quenched with MeOH (10 mL). The solvent was evaporated and the crude product was purified by flash chromatography (silicagel, MeOH:CH_2Cl_2, 1:99) to obtain nantenine (0.03g, 10%) as a bright yellow solid: **mp**: 122-123 °C; **^{1}H NMR** (500 MHz, $CDCl_3$): δ 7.93 (s, 1H), 6.75 (s, 1H), 6.59 (s, 1H), 5.97 (d, 2H, *J*=7.8 Hz), 3.87 (s, 3H), 3.65 (s, 3H), 3.14 (m, 1H), 3.04-2.96 (m, 3H), 2.52-2.45 (m, 6H); **^{13}C NMR** (125 MHz, $CDCl_3$): δ 151.9, 146.5, 146.3, 144.4, 130.8, 128.6, 127.3, 126.9, 125.5, 110.5, 108.8, 108.2, 100.8, 62.5, 60.2, 55.8, 53.2, 44.0, 35.1, 29.2; **HRESIMS**: calcd. for $C_{20}H_{21}NO_4$ $[M+H]^+$ 340.1543; found 340.1489.

2-(6-bromobenzo[*d*][1,3]dioxol-5-yl)acetic acid (29). To a solution of 3,4-(methylene-dioxy) phenylacetic acid **23** (4.96 g, 27.56 mmol) in glacial acetic acid (50 mL) was added a solution of Br_2 (1.55 mL, 30.04 mmol) at room temperature. The mixture was stirred overnight and the solvent evaporated. The residue was dissolved in toluene and the solvent evaporated. The residue was treated with toluene (50 mL), the mixture heated for 15 min, cooled to room temperature and the product filtered, to afford **29** (6.8 g, 95%), as a brown solid: **mp:** 182-184 °C; **^{1}H NMR** (500 MHz, $CDCl_3$): δ 7.05 (s, 1H), 6.81 (s, 1H), 6.00 (s, 2H), 3.77 (s, 2H); **^{13}C NMR** (125 MHz, $CDCl_3$): δ 174.9, 148.0, 146.9, 126.2, 115.5, 112.8, 111.0, 101.9, 40.8; **HRESIMS**: calcd. for $C_9H_7BrO_4$ $[M]^+$ 257.9528; found 257.9536.

2-(6-bromobenzo [*d*] [1,3] dioxol-5-yl)-N-(3,4-dimethoxyphenethyl) acetamide (30). A solution of **29** (5.00 g, 19.30 mmol) and 1,1'-carbonyldiimidazole (3.13 g, 19.30 mmol) in 75 mL of anhydrous THF was stirred at 0 °C for 1.5 h and at room temperature for 1 h. The mixture was cooled again in an ice bath and stirred for 1 h; then 3,4-dimethoxy-phenethylamine **24** (3.20 mL, 19.30 mmol) was added and the solution was stirred at 0 °C for 4 h and at room temperature overnight under nitrogen atmosphere. The THF was evaporated under reduced pressure and the residue was dissolved in EtOAc (150 mL) and was extracted with 1N HCl (50 mL), water (50 mL) and aqueous $NaHCO_3$ (75 mL). The organic layer was evaporated and the crude product was crystallized from EtOAc to give the amide **30** (7.20 g, 88%):**mp**: 165-168 °C; **^{1}H NMR** (500 MHz, $CDCl_3$): δ 6.98 (s, 1H), 6.75-6.73 (m, 2H), 6.64-6.61 (m, 2H), 5.98 (s, 2H), 5.41 (bs, 1H), 3.87-3.84 (m, 6H), 3.56 (s, 2H), 3.49-3.45 (m, 2H), 2.72-2.70 (m, 2H); **^{13}C NMR** (125 MHz, $CDCl_3$): δ 169.5, 149.0, 147.8, 147.7, 147.6, 131.0, 127.5, 120.6, 115.2, 112.8, 111.7, 111.2, 110.9, 101.9, 55.9, 55.8, 43.8, 40.6, 35.0; **HRESIMS**: $C_{19}H_{20}BrNO_5$ $[M]^+$ 421.0525; found 421.0498.

1-((6-bromobenzo[*d*][1,3]dioxol-5-yl)methyl)-6,7-dimethoxy-3,4-dihydroisoquinoline (31). Phosphorus pentachloride (3.45 g, 16.57 mmol) was added during 30 min in three portions to a chilled (0 °C) solution of amide **30** (3.5 g, 8.28 mmol) in 150 mL of dry CH_2Cl_2 under argon and the mixture was stirred for 30 min. Then, the ice bath was removed and the mixture was stirred at room temperature for 24 h. The reaction mixture was then poured onto a saturated solution of $NaHCO_3$ (75 mL) and the contents of the flask were stirred for 1 h. The aqueous layer was extracted twice with 30 mL CH_2Cl_2 and

the combined organic extracts were washed with saturated solution of $NaHCO_3$ (75 mL), dried over Na_2SO_4, filtered and evaporated to give **31**. Since imines are prone to air oxidation, compound **31** was used without further purification for the preparation of **32**. Small amount was purified using flash chromatography (silicagel, MeOH:CH_2Cl_2, 1:99) for the NMR purpose: **^{1}H NMR** (500 MHz, $CDCl_3$): δ 7.01 (s, 1H), 6.92 (s, 1H), 6.76 (s, 1H), 6.66 (s,1H), 5.90 (s, 2H), 4.08 (s, 2H), 3.88 (s, 3H), 3.82 (s, 3H), 3.73-3.70 (m, 2H), 2.68-2.65 (m, 2H); **^{13}C NMR** (125 MHz, $CDCl_3$): δ 165.2, 150.7, 147.6, 147.4, 147.1, 131.5, 130.6, 121.3, 114.4, 112.5, 110.2, 109.5, 109.0, 101.6, 56.2, 55.9, 47.3, 42.4, 25.7

1-((6-bromobenzo[*d*] [1,3] dioxol-5-yl) methyl)-6, 7-dimethoxy-1, 2, 3, 4-tetrahydro-isoquinoline (32). Sodium borohydride (6.55 g, 173.15 mmol) was added portion wise to a stirred solution of **31** (3.50 g, 8.65 mmol) in MeOH (100 mL) and the mixture was stirred at 0 °C for 4 h. The reaction mixture was concentrated, and excess $NaBH_4$ was destroyed by adding water (50 mL) and glacial acetic acid (50 mL). The mixture was extracted with CH_2Cl_2 (3x35 mL), dried over Na_2SO_4 and concentrated to give crude yellow solid **32**. This compound was used for next step without any further purification.

***tert*-butyl 1-((6-bromobenzo[*d*] [1,3] dioxol-5-yl)methyl)-6, 7-dimethoxy-3,4-dihydro-isoquinoline-2(1H)-carboxylate (33).** To a solution of the **32** (3.50 g, 8.61 mmol), diiso-propylethylamine (3.00 mL, 17.23 mmol) and 1-3 mg of 4-(dimethylamino)pyridine in anhydrous CH_2Cl_2 (50 mL) was added slowly di-tert-butyl dicarbonate (2.21 mL, 10.33 mmol) and the resulting mixture was stirred overnight at 23 °C. The reaction was then quenched by adding a solution of NH_4Cl (25 mL) and was extracted with CH_2Cl_2 (3x35mL). The crude reaction mixture was then purified by column chromatography

(silicagel, MeOH:CH_2Cl_2, 1:99), to obtain **34** (2,3 g, 65%) as white solid: **mp**: 144-147 °C; **^{1}H NMR** (500 MHz, $CDCl_3$): δ 7.05 (s, 1H), 6.81 (s, 1H), 6.64-6.59 (m, 3H), 5.97-5.88 (m, 2H), 4.39-4.37 (m, 1H), 3.88 (s, 6H), 3.23-3.18 (m, 2H), 2.91-2.86 (m, 3H), 1.18 (s, 9H); **^{13}C NMR** (125 MHz, $CDCl_3$): δ 154.3, 147.6, 147.2, 147.2, 147.2, 131.1, 128.7, 126.4, 115.2, 112.4, 111.4, 111.1, 109.3, 101.7, 79.5, 61.3, 55.8, 55.8, 53.8, 42.5, 36.1, 28.2, 28.1, 28.0; **HRESIMS**: $C_{24}H_{28}BrNO_6$ $[M+H]^+$ 506.1100; found 506.1173.

***tert*-butyl4,5,6a,7-tetrahydro-1,2-dimethoxy-9,11,-dioxa-6-azabenzo[*fg*]cyclopenta[*b*] anthracene-6-carboxylate (6).** K_2CO_3 (0.21 g, 1.48 mmol), 2-(diphenylphosphanyl)-2`-(dimethylamino)biphenyl (75.00 mg, 0.19 mmol), Pd(II)-acetate (22 mg, 0.09 mmol) and the **33** (250 mg, 0.49 mmol) are weighted to air and placed in a three-way round-bottomed flask with a magnetic stir bar. The flask is purged with argon (30 min). DMA (2 mL) is then added and the resulting mixture is heated to 130°C overnight. The reaction mixture is then concentrated and loaded onto a silicagel column for chromatography using hexane:EtOAc, 25:75. The analog **6** has been obtained as white crystals (92.00 mg, 43%): **mp**: 176-178 °C; **^{1}H NMR** (500 MHz, $CDCl_3$): δ 8.00 (s, 1H), 6.75 (s, 1H), 6.63 (s, 1H), 5.98 (s, 2H), 4.62 (bs, 1H), 4.40 (bs, 1H), 3.89 (s, 3H), 3.66 (s, 3H), 2.94-2.62 (m, 5H), 1.49 (s, 9H); **^{13}C NMR** (125 MHz, $CDCl_3$): δ 154.5, 151.9, 146.6, 146.5, 144.8, 131.5, 129.8, 127.6, 125.8, 125.1, 110.7, 108.9, 108.2, 100.9, 79.9, 60.0, 55.9, 51.7, 38.4, 35.4, 30.4, 28.5; **HRESIMS**: calcd. for $C_{24}H_{27}NO_6$ $[M+Na]^+$ 448.17384; found 448.17305.

Nornantenine (7). Aporphine **6** (0.50 g, 1.175 mmol) in dry, distilled CH_2Cl_2 (10 mL) is stirred magnetically with anhydrous $ZnBr_2$ (1.06 g, 4.70 mmol) under argon at room temperature for four hours. The reaction mixture was then quenched by adding a solution of saturated $NaHCO_3$ (50 mL) and was extracted with CH_2Cl_2 (2x25 mL), dried over Na_2SO_4 and concentrated to give crude **7** as yellow oil. We found this compound to be unstable; for long-term storage **7** was converted to its hydrochloride salt by treatment with 1N HCl in diethyl ether. Data for the hydrochloride salt follows: **^{1}H NMR** (500 MHz, DMSO-D_6): δ 7.77 (1H, s), 7.03 (1H, s), 6.89 (1H, s), 6.06 (2H, s), 4.20 (1H, d, *J*=14 Hz), 3.84 (3H, s), 3.60 (3H, s), 3.57 (1H, d, *J*=8 Hz), 3.34 (1H, bs), 3.22-3.15 (2H, m), 3.01 (1H, d, *J*=14 Hz), 2.91-2.80 (2H, m); **^{13}C NMR** (125 MHz, DMSO-D_6): δ 152.6, 146.5, 146.4, 144.4, 127.9, 126.6, 125.6, 124.3, 121.4, 111.3, 108.5, 107.9, 101.0, 59.7, 55.7, 51.6, 40.1, 32.8, 24.9; **HRESIMS**: calcd. for $C_{19}H_{19}NO_4$ [M^+] 325.1314; found 325.1313.

Nantenine (51). Aporphine **6** (0.30 g, 0.922 mmol) and formaldehyde solution, 37% (5.4 ml, 1.84 mmol) were mixed in anhydrous CH_2Cl_2 (20 mL) and then treated with sodium triacetoxy-borohydride (0.98 g, 4.61 mmol). The mixture was allowed to stir at room temperature overnight. The reaction was quenched with saturated $NaHCO_3$ (25 mL), and extracted with CH_2Cl_2 (2x25 mL), and dried over Na_2SO_4 and concentrated to dryness. The residue was purified through flash chromatography (silicagel, MeOH:CH_2Cl_2, 2:99) to obtain nantenine (0.29 g, 94%) as a bright yellow solid. Experimental data as previously reported.

Synthesis of nantenine analogs 1-3:

3-(benzo[*d*][1,3]dioxol-5-yl)-4,5-dimethoxybenzaldehyde (35). A mixture of $Pd(PPh_3)_4$ (2.35 g, 2.04 mmol) and commercially available 5-bromoveratraldehyde **34** (5.00 g, 20.40 mmol) in DME (250 mL) was stirred for 15 min at 20 °C under argon. 2M aqueous K_2CO_3 (71.5 mL, 142.8 mmol) was added to the mixture, followed by the 3,4-(methylenedioxy) boronic acid (6.77 g, 40.80 mmol) in DME. The mixture was refluxed for 18 h and then cooled at 20 °C. The reaction mixture was treated with water (100 mL) and EtOAc (100 mL). The organic extracts were washed with 1M NaOH (100 mL) and water (100 mL) and dried over Na_2SO_4, the solvent being evaporated to dryness to give compound **35**, which was purified by column chromatography (silicagel, hexane:EtOAc, 4:1).[20] Compound **35** (5.66 g, 96%) was obtained as pale yellow oil: **^{1}H NMR** (500 MHz, $CDCl_3$): δ 9.92 (s, 1H), 7.44 (d, 1H, *J*=2.0 Hz), 7.42 (d, 1H, *J*=2.0 Hz), 7.06 (d, 1H, *J*=1.7 Hz), 7.02 (dd, 1H, *J*=8.0, 1.7 Hz), 6.89 (d, 1H, *J*=8.0), 6.02 (s, 2H), 3.97 (s, 3H); 3.71 (s, 3H); **^{13}C NMR** (125 MHz, $CDCl_3$): δ 191.2, 153.7, 151.9, 147.5, 147.2, 135.7, 132.3, 130.8, 127.2, 122.7, 109.7, 109.3, 108.3, 101.2, 60.7, 56.1; **HRESISMS** calcd. for $C_{16}H_{14}O_5$ $[M]^+$ 286.0841; found 286.0841.

(E)-5-(2,3-dimethoxy-5-(2-nitrovinyl)phenyl)benzo[*d*][1,3]dioxole (36). A mixture of aldehyde **35** (5.31 g, 18.56 mmol), ammonium acetate (1.43 g, 18.56 mmol), nitromethane (4.98 mL, 92.82 mmol), and glacial acetic acid (50 mL) was refluxed for 4 h. After cooling to room temperature, the crystalline product was filtered and recrystallized from ethanol to afford **36**, as a yellow solid (5.15 g, 84%): **mp**: 124-127 °C; **^{1}H NMR** (500 MHz, $CDCl_3$): δ 7.97 (d, 1H, *J*=13.6 Hz), 7.55 (d, 1H, *J*=13.6 Hz),

7.14 (d, 1H, *J*=2.1 Hz), 7.02 (d, 1H, *J*=1.7 Hz), 7.01 (d, 1H, *J*=2.1 Hz), 6.96 (dd, 1H, *J*=8.0, 1.7 Hz), 6.88 (d, 1H, *J*=8.0 Hz), 6.02 (s, 2H), 3.95 (s, 3H); 3.68 (s, 3H); **^{13}C NMR** (125 MHz, $CDCl_3$): δ 153.0, 150.3, 147.8, 147.5, 139.2, 136.6, 136.6. 130.9, 125.9, 125.1, 122.9, 111.0, 109.9, 108.5, 101.4, 61.0, 56.3; **HRESIMS**: calcd. for $C_{17}H_{15}NO_6$ $[M+H]^+$ 330.0899; found 330.0971.

2-(3-(benzo[*d*][1,3]dioxol-5-yl)-4,5-dimethoxyphenyl)ethanamine (37). TMSCl (5.00 mL, 24.24 mmol) was added to a vigorously stirred suspension of $LiBH_4$ (0.35 g, 7.62 mmol) in anhyd. THF (15 mL) over a period of 2 min. After the gas evolution had ceased, the trimethylsilane was removed by purging the solution with argon for 15 min. Then, over a period of 5 min, a solution of **36** (1.00 g, 3.03 mmol) in anhyd. THF (15 mL) was added and the mixture was heated for 18 h at reflux. After cooling to room temperature, the mixture was quenched carefully at 0 °C with MeOH (25 mL). The solvent was removed with a rotatory evaporator, the resulting residue dissolved in 20% aq KOH (50 mL), and extracted with CH_2Cl_2 (3x50 mL). The combined extracts were dried over Na_2SO_4 and then concentrated under reduced pressure. The crude oily product **37** (1.36 g) was used for next step without further purification.

***N*-(3-(benzo[*d*][1,3]dioxol-5-yl)-4,5-dimethoxyphenethyl)formamide (38a).** The amine **37** (0.92 g, 3.10 mmol), ethyl formate (0.62 mL, 7.75 mmol) and triethylamine (0.86 mL, 6.20 mmol) were heated to reflux for 48 h. Removal of excess ethyl formate and triethylamine under reduced pressure gave dark-brown oil, that was purified by column chromatography (silicagel, MeOH:CH_2Cl_2, 1:99). Compound **38a** (0.92 g, 92%) was obtained as red-orange oil: **^{1}H NMR** (500 MHz, $CDCl_3$): δ 8.12 (s, 1H), 7.05 (s, 1H),

6.98 (d, 1H, *J*=8.0 Hz), 6.85 (d, 1H, *J*=8.0 Hz), 6.73 (br. s, 2H), 5.98 (s, 2H), 3.88 (s, 3H), 3.56 (m, 6H), 2.82 (t, 2H, *J*=6.9 Hz); **^{13}C NMR** (125 MHz, $CDCl_3$): δ 161.4, 153.1, 147.4, 146.8, 135.4, 134.4, 133.6, 131.9, 122.7, 122.6, 111.7, 109.9, 108.2, 101.2, 60.6, 56.1, 39.3, 35.5. **HRESIMS**: calcd. for $C_{18}H_{20}NO_5$ $[M+H]^+$ 330.1263; found 330.1333.

***N*-(3-(benzo[*d*][1,3]dioxol-5-yl)-4,5-dimethoxyphenethyl)acetamide (38b).** The amine **37** (0.32 g, 1.06 mmol), acetyl chloride (0.12 mL, 5.5 mmol) and triethylamine (0.45 mL, 10.00 mmol) were mixed with dichloromethane (10 mL) and stirred for 6 hours at 0 °C. The reaction was treated with saturated $NaHCO_3$, extracted with DCM (3×35 mL), dried over Na_2SO_4 and concentrated under reduced pressure to give a yellow oil, that was subsequently purified by column chromatography (MeOH:DCM, 1:99). Compound **38b** (0.33 g, 91.0%) was obtained as an orange-red oil: **^{1}H NMR** (500 MHz, $CDCl_3$): δ 8.12 (s, 1H), 7.06 (br. s, 1H), 6.98 (d, 1H, *J*=8.0 Hz), 6.86 (d, 1H, *J*=8.0 Hz), 6.73 (br. s, 1H), 5.98 (s, 2H), 5.71 (br. s, 1H), 3.88 (s, 3H), 3.58 (s, 3H), 3.51 (dd, 2H, *J*=13.2, 6.5 Hz), 2.78 (t, 2H, *J*=7.0 Hz), 1.95 (s, 3H); **^{13}C NMR** (125 MHz, $CDCl_3$): δ 170.1, 153.1, 147.4, 146.8, 145.0, 135.4, 134.7, 131.9, 122.6, 122.5, 111.7, 109.8, 108.1, 101.0, 60.5, 56.0, 40.7, 35.6, 23.4; **HRESIMS**: calcd. for $C_{19}H_{22}NO_5$ $[M+H]^+$ 344.1415; found 344.1488.

***N*-(3-(benzo[*d*] [1,3]dioxol-5-yl)-4, 5-dimethoxyphenethyl) propionamide (38c).** The amine **37** (0.85 g, 2.82 mmol), propionyl chloride (0.7 mL, 8.45 mmol) and triethylamine (1.25 mL, 8.45 mmol) were mixed with CH_2Cl_2 (20 mL) and stirred for 4 hours at 0 °C. The reaction was treated with saturated $NaHCO_3$ (25 mL), extracted with CH_2Cl_2 (3x35mL), dried over Na_2SO_4 and concentrated under reduced pressure to give red oil,

that was purified by column chromatography (silicagel, MeOH:CH_2Cl_2, 1:99). Compound **38c** (0.91 g, 90%) was obtained as red-orange oil: **^{1}H NMR** (500 MHz, $CDCl_3$): δ 7.08 (s, 1H), 6.99 (d, 1H, *J*=8.1 Hz), 6.88 (d, 1H, *J*=7.8 Hz), 6.73 (s, 2H), 6.02 (s, 2H), 5.63 (bs, 1H), 3.89 (s, 3H), 3.57 (s, 3H), 3.53 (q, 2H, *J*=6.4 Hz), 2.80 (t, 2H, *J*=6.8 Hz), 2.19 (q, 2H, *J*=7.5 Hz), 1.14 (t, 3H, *J*=7.5 Hz); **^{13}C NMR** (125 MHz, $CDCl_3$): δ 174.0, 153.1, 147.4, 146.9, 144.8, 135.4, 134.9, 131.9, 122.7, 122.6, 111.5, 109.9, 108.3, 101.2, 60.7, 56.0, 40.7, 35.7, 29.9, 10.1; **HRESIMS**: calcd. for $C_{20}H_{24}NO_5$ $[M+H]^+$ 358.1576; found 358.1618.

General procedure for the synthesis of imine 39a-c: To a stirred solution of the amides **38a-c** (0.46 g, 1.40 mmol) in acetonitrile (5 mL) was added $POCl_3$ (0.65 mL, 7.00 mmol) at room temperature, and the resulting mixture was heated at 50 °C for 12 h. The reaction mixture was concentrated, and the quaternary salt was dissolved in CH_2Cl_2 (25 mL). After cooling to 0 °C, the mixture was diluted with water (50 mL), made basic with 5% aqueous NH_4OH, and extracted with CH_2Cl_2 (2x25 mL). The organic solution was washed with water, dried with anhydrous Na_2SO_4 and concentrated to give:

a) **8-(benzo[*d*] [1,3]dioxol-5-yl)-6, 7-dimethoxy-3, 4-dihydroisoquinoline (39a)** as a yellow crude solid (0.48 g);

b) **8-(benzo[*d*] [1,3] dioxol-5-yl)-6, 7-dimethoxy-1-methyl-3, 4-dihydroisoquinoline (39b)** as a red crude solid (0.45 g);

c) **8-(benzo[*d*][1,3]dioxol-5-yl)-1-ethyl-6,7-dimethoxy-3,4-dihydroisoquinoline (39c)** as a yellow solid (0.41 g).

The crude imines were reduced immediately without further purification.

General procedure for the synthesis of amine 40a-c: Sodium borohydride (1.04g, 27.6 mmol) was added portionwise to a stirred solution of **39a-c** (0.43 g, 1.38 mmol) in MeOH (20 mL) and the mixture was stirred at 0 °C for 3 h. The reaction mixture was concentrated, and excess $NaBH_4$ was destroyed by adding water (50 mL) and glacial acetic acid (50 mL). The mixture was extracted with CH_2Cl_2 (3x25 ml), dried over Na_2SO_4 and concentrated to give:

a) **8-(benzo[*d*][1,3]dioxol-5-yl)-6,7-dimethoxy-1,2,3,4-tetrahydroisoquinoline (40a)** as a orange oily product.

b) **8-(benzo[*d*] [1,3] dioxol-5-yl)-6, 7-dimethoxy-1-methyl-1, 2, 3, 4-tetrahydroiso-quinoline (40b)** as a yellow oily product.

c) **8-(benzo[*d*] [1,3]dioxol-5-yl)-1-ethyl-6,7-dimethoxy-1,2,3,4-tetrahydroisoquinoline (40c)** as a yellow oily product.

These compounds were used for next step without any further purification.

General procedure for the synthesis of 1-3: Compound **40a-c** (0.40 g, 1.27 mmol) and formaldehyde solution, 37% (2.59 mL, 2.55 mmol) were mixed in anhydrous CH_2Cl_2 (10 mL) and then treated with sodium triacetoxy-borohydride (1.35 g, 6.38 mmol). The mixture was allowed to stir at room temperature for 24 h. The reaction was quenched with 5% aq $NaHCO_3$ (25 mL), and extracted with EtOAc (2x25 mL), and dried over Na_2SO_4 and concentrated to dryness. The residue was purified through flash chromatography (silicagel, MeOH:CH_2Cl_2, 2:98) to obtain:

a) **8-(benzo[*d*] [1,3]dioxol-5-yl)-6, 7-dimethoxy-2-methyl-1, 2, 3, 4-tetrahydroiso-quinoline (1).** (0.38g, 88%) as a bright yellow crystals: **mp**: 82-84 °C; **^{1}H NMR** (500

MHz, $CDCl_3$): δ 6.87 (d, 1H, *J*=7.9 Hz), 6.70-6.65 (m, 3H), 6.01 (d, 2H, *J*=8.4 Hz), 3.88 (s, 3H), 3.54 (s, 3H), 3.15 (br. s, 2H), 2.94 (br. s, 2H), 2.65 (br. s, 2H), 2.35 (s, 3H); **^{13}C NMR** (125 MHz, $CDCl_3$): δ 151.0, 147.3, 146.5, 144.8, 134.0, 129.8, 129.5, 125.8, 122.6, 111.6, 110.0, 108.2, 101.0, 60.8, 56.5, 55.8, 52.6, 46.3, 29.8; **HRESIMS**: calcd. for $C_{19}H_{21}NO_4$ $[M]^+$ 327.1478; found 327.1471.

b) **8-(benzo[*d*][1,3]dioxol-5-yl)-6, 7-dimethoxy-1,2-dimethyl-1, 2, 3, 4-tetrahydroiso-quinoline (2).** mixture of isomers (0.49g, 90%) as a bright yellow crystals: **mp**: 101-104 °C; **^{1}H NMR** (500 MHz, $CDCl_3$): δ 6.87-6.84 (m, 1H), 6.76-6.67 (m, 1H), 6.66-6.65 (m, 2H), 6.03-6.00 (m, 2H), 3.87 (s, 3H), 3.78-3.71 (m, 1H), 3.53-3.49 (m, 3H), 3.08-3,07 (m, 2H), 2.77-2.71 (m, 2H), 2.38-2.46 (m, 3H), 0.97-0.94 (m, 3H); **^{13}C NMR** (125 MHz, $CDCl_3$) (doubling of signals observed; average values for isomeric shifts reported): δ 151.0, 147.3, 146.5, 145.1, 134.6, 130.8, 129.9, 128.6, 123.3, 112.0, 110.6, 108.1, 101.0, 60.8, 55.7, 55.0, 44.1, 42.0, 26.3, 16.2; **HRESIMS**: calcd. for $C_{20}H_{23}NO_4$ $[M]^+$ 341.1627; found 341.1628.

c) **8-(benzo[*d*][1,3]dioxol-5-yl)-1-ethyl-6,7-dimethoxy-2-methyl-1,2,3,4-tetrahydroiso-quinoline (3).** (0.25g, 68%) as a yellow solid: **mp**: 111-113 °C; **^{1}H NMR** (500 MHz, $CDCl_3$): δ 6.89-6.84 (m, 1H), 6.76 (m, 1H), 6.64-6.60 (m, 2H), 6.03-6.00 (m, 2H), 3.88-3.84 (m, 3H), 3.54-3.50 (m, 3H), 3.41 (d, 1H, *J*=8.6 Hz), 3.31 (d, 1H, *J*=8.6 Hz), 3.23 (m, 1H), 2.94 (ddd, 1H, *J*=16.9, 10.5, 6.6 Hz), 2.76 (dd, 1H, *J*=10.6, 6.7 Hz), 2.57 (d, 1H, *J*=13.4), 2.45 (m, 3H), 1.31 (m, 2H), 0.64-0.59 (m, 3H); **^{13}C NMR** (125 MHz, $CDCl_3$): δ 150.7, 147.3, 146.5, 145.1, 135.2, 130.1, 124.8, 122.4, 111.9, 111.3, 109. 8, 107.9, 100.9,

61.7, 60.8, 55.6, 44.4, 42.4, 27.7, 23.8, 11.6 ; **HRESIMS**: calcd. for $C_{21}H_{25}NO_4$ $[M]^+$ 355.1784; found 355.1781.

Synthesis of nantenine analog 4:

2-(benzo[*d*][1,3]dioxol-5-yl)-*N*-(3,4-dimethoxyphenethyl)ethanamine (41). Amide **25** (2.50 g, 7.21 mmol) in anhydrous THF (75 mL) was reduced by BF_3-etherate (ca.47%, 1.5 mL, 7.00 mmol) and 1M BH_3-THF solution (20 mL, 20.00 mmol) carefully added dropwise, at room temperature and then, the mixture was refluxed for 2.5 h, under N_2 atmosphere. Excess reagent was destroyed with 5 N aq HCl solution (25 mL). The organic solvent was evaporated off and the aqueous solution was made basic with 15% aq NH_4OH (25 mL), and then extracted with EtOAc (3x35 mL). The combined organic phases were washed with brine (50 mL), dried over Na_2SO_4 and concentrated to dryness. Compound **27** (2.23 g, 88%) was obtained as pale yellow oil showing a single spot on tlc: **^{1}H NMR** (500 MHz, $CDCl_3$): δ 6.71 (s, 1H), 6.63 (s, 3H), 6.60 (s, 1H), 6.51 (s, 1H), 5.96 (s, 2H), 3.85 (s, 6H), 2.86 (m, 4H), 2.72 (m, 4H); **^{13}C NMR** (125 MHz, $CDCl_3$): δ 147.6, 147.4, 145.9, 133.6, 130.3, 129.1, 129.0, 128.2, 121.5, 120.5, 111.9, 111.4, 108.9, 108.5, 100.8, 55.9, 55.8, 51.1, 35.7 **HRESIMS**: calcd. for $C_{19}H_{23}NO_4$ $[M+H]^+$ 330.1627; found 330.1701.

2-(benzo[*d*] [1, 3]dioxol-5-yl)-*N*-(3, 4-dimethoxyphenethyl)-*N*-methylethanamine (4). Compound **41** (2.00 g, 6.07 mmol) and formaldehyde solution, 37% (12.37 mL, 12.14 mmol) were mixed in anhydrous CH_2Cl_2 (15 mL) and then treated with sodium triacetoxy-borohydride (6.41 g, 30.35 mmol). The mixture was allowed to stir at room

temperature for 1.5 h. The reaction was quenched with 5% aq sodium bicarbonate (25 mL), and extracted with EtOAc (2x25 mL), and dried over Na_2SO_4 and concentrated to dryness. The residue was purified through flash chromatography (silicagel, MeOH:CH_2Cl_2, 5:95) to obtain analog **4** (1.80 g, 85%) as a bright yellow oil: **^{1}H NMR** (500 MHz, $CDCl_3$): δ 6.82-6.65 (m, 6H), 5.91 (s, 2H), 3.89 (s, 3H), 3.87 (s, 3H), 2.78-2.64 (m, 8H), 2.39 (s, 3H); **^{13}C NMR** (125 MHz, $CDCl_3$): δ 148.8, 147.5, 147.3, 145.7, 134.2, 133.1, 121.4, 120.5, 112.0, 111.3, 109.1, 108.2, 100.8, 59.7, 59.7, 55.9, 55.8, 42.2, 33.6, 33.5; **HRESIMS**: calcd. for $C_{20}H_{25}NO_4$ $[M+H]^+$ 343.17386; found 343.18660.

Synthesis of nantenine analog 5:

1-(benzo [*d*] [1,3] dioxol-5-ylmethyl)-6, 7-dimethoxy-2-methyl-1, 2, 3, 4-tetrahydro-isoquinoline (5). Compound **27** (0.70 g, 2.13 mmol) and formaldehyde solution, 37% (4.35 mL, 4.27 mmol) were mixed in anhydrous CH_2Cl_2 (50 mL) and then treated with sodium triacetoxy-borohydride (2.25 g, 10.65 mmol). The mixture was allowed to stir at room temperature for 1.5 h. The reaction was quenched with 5% aq $NaHCO_3$ (25 mL), and extracted with EtOAc (2x25 mL), and dried over Na_2SO_4 and concentrated to dryness. The residue was purified through flash chromatography (silicagel, MeOH:CH_2Cl_2, 5:95) to obtain analog **5** (0.49 g, 68%) as a bright yellow oil: **^{1}H NMR** (500 MHz, $CDCl_3$):): δ 6.71 (d, 1H, *J*=7.8 Hz), 6.64 (s, 1H), 6.55 (m, 2H), 6.11 (s, 1H), 5.91 (s, 2H), 3.84 (s, 3H), 3.66-3.65 (m, 1H), 3.62 (s, 3H), 3.17-3.08 (m, 2H), 2.83-2.72 (m, 3H), 2.60-2.57 (m, 1H), 2.51 (s, 3H); **^{13}C NMR** (125 MHz, $CDCl_3$): δ 147.3, 147.3, 146.4, 145.7, 133.8, 129.2, 125.9, 122.6, 111.1, 110.9, 110.1, 107.9, 100.7, 64.9, 55.7,

55.6, 46.8, 42.6, 41.0, 25.3; **HRESIMS**: calcd. for $C_{20}H_{23}NO_4$ $[M+H]^+$ 342.16271; found 342.17045.

Synthesis of nantenine analogs 8-12:

Ethylnornantenine (8). Analog **7** (0.1 g, 0.307 mmol) and acetaldehyde solution (0.7 mL, 1.23 mmol) were mixed in anhydrous CH_2Cl_2 (10 mL) and then treated with sodium triacetoxy-borohydride (0.32 g, 1.53 mmol). The mixture was allowed to stir at room temperature overnight. The reaction was quenched with saturated $NaHCO_3$ (20 mL), and extracted with CH_2Cl_2 (2x25 mL), and dried over Na_2SO_4 and concentrated to dryness. The residue was purified through flash chromatography (silicagel, MeOH:CH_2Cl_2, 1:99) to obtain **8** (0.08 g, 72%) as a bright red solid: **mp**: 122-124 °C; **^{1}H NMR** (500 MHz, $CDCl_3$): δ 7.92 (1H, s), 6.75 (1H, s), 6.59 (1H, s), 5.97 (2H, dd, *J*=7.7, 1.3 Hz), 3.87 (3H, s), 3.64 (3H, s), 3.24 (1H, m), 3.11 (3H, m), 2.97 (1H, dd, *J*=13.8, 3.8 Hz), 2.68 (1H, m), 2.51 (3H, m), 1.14 (3H, t, *J*=7.1, 7.1, 7.1 Hz); **^{13}C NMR** (125 MHz, $CDCl_3$): δ 151.8, 146.4, 146.3, 144.4, 131.0, 129.0, 127.9, 127.1, 125.6, 110.6, 108.9, 108.2, 100.8, 60.2, 59.2, 55.8, 48.3, 47.8, 35.0, 29.3, 10.8; **HRESIMS**: calcd. for $C_{21}H_{24}NO_4$ $[M+H^+]$ 354.1627; found 354.1650.

Propylnornantenine (9). Analog **7** (0.10 g, 0.307 mmol) and propionyl aldehyde solution, (0.035g, 0.614 mmol) were mixed in anhydrous CH_2Cl_2 (20 mL) and then treated with sodium triacetoxy-borohydride (0.195 g, 0.922 mmol). The mixture was stirred at rt overnight. The reaction was than quenched with saturated aq $NaHCO_3$ (20mL), and extracted with CH_2Cl_2 (3x20 mL), and dried over Na_2SO_4 and concentrated to dryness. The residue was purified through flash chromatography (silicagel,

MeOH:CH_2Cl_2, 1:99) to obtain analog **9** (0.096 g, 85%) as a bright yellow solid: **^{1}H NMR** (500 MHz, $CDCl_3$): δ 7.92 (s, 1H), 6.76 (s, 1H), 6.59 (s, 1H), 5.98 (m, 2H), 3.87 (s, 3H), 3.64 (s, 3H), 3.23-3.04 (m, 3H), 2.99-2.87 (m, 2H), 2.70-2.65 (m, 1H), 2.54-2.39 (m, 3H), 1.64-1.57 (m, 2H), 1.26 (s, 1H), 0.98 (m, 3H); **^{13}C NMR** (125 MHz, $CDCl_3$): δ 151.9, 146.6, 146.4, 144.5, 131.2, 129.2, 128.2, 127.3, 125.7, 110.7, 109.0, 108.4, 101.0, 60.3, 60.0, 56.5, 56.0, 49.3, 35.3, 29.5, 19.7, 12.29; **HRESIMS**: calcd. for $C_{22}H_{25}NO_4$ $[M+H]^+$ 368.1784; found 368.1801.

Benzylnornantenine (10). Analog **7** (0.10 g, 0.276 mmol) and benzaldehyde (0.05 mL, 0.414 mmol) were mixed in anhydrous CH_2Cl_2 (10 mL) and then treated with sodium triacetoxy-borohydride (0.18 g, 0.829 mmol). The mixture was allowed to stir at room temperature overnight. The reaction was quenched with saturated $NaHCO_3$ (25 mL), and extracted with CH_2Cl_2 (2x25 mL), and dried over Na_2SO_4 and concentrated to dryness. The residue was purified through flash chromatography (silicagel, hexane:EtOAc, 1:4) to obtain analog **10** (0.09 g, 81%) as a white solid: **mp**: 145-147 °C; **^{1}H NMR** (500 MHz, $CDCl_3$): δ 7.93 (s, 1H), 7.42-7.27 (m, 5H), 6.76 (s, 1H), 6.59 (s, 1H), 5.98 (m, 2H), 4.33 (d, 1H, *J*=13.7), 3.88 (s, 3H), 3.66 (s, 3H), 3.33 (bs, 2H), 3.12-3.01 (m, 3H), 2.63-2.57 (m, 2H), 2.37 (bs, 1H); **^{13}C NMR** (125 MHz, $CDCl_3$): δ 151.9, 146.5, 146.3, 144.4, 128.9, 128.5, 128.3, 127.6, 127.2, 126.9, 125.6, 110.6, 108.9, 108.2, 100.8, 60.3, 60.2, 58.6, 55.8, 48.9, 35.4, 29.2; **HRESIMS**: calcd. for $C_{26}H_{25}NO_4$ $[M]^+$ 415.1784; found 415.1782.

***N*-acetylnornantenine (11).** Analog **7** (0.10 g, 0.307 mmol) and acetyl chloride (0.03 mL, 0.46 mmol) were mixed in anhydrous CH_2Cl_2 (20 mL) and then treated with triethylamine (0.13 mL, 0.921 mmol). The mixture was allowed to stir at 0 °C for 3h under argon. The reaction was quenched with saturated $NaHCO_3$ (20 mL), and extracted with CH_2Cl_2 (3x20 mL), and dried over Na_2SO_4 and concentrated to dryness. The residue was recrystallized in EtOAc to obtain **11** (0.07 g, 67%) as a white solid: **mp**: 190-192 °C; **^{1}H NMR** (500 MHz, $CDCl_3$): δ 8.01 (1H, m), 6.77 (1H, s), 6.64 (1H, s), 5.99 (2H, m), 5.05 (1H, dd, *J*=13.9, 3.7), 3.91 (3H, m), 3.67 (3H, m), 3.29 (1H, m), 2.93 (2H, m), 2.72 (3H, m), 2.23 (3H, m); **^{13}C NMR** (125 MHz, $CDCl_3$): δ 169.1, 151.9, 146.6, 145.1, 131.1, 130.5, 128.7, 125.8, 124.9, 110.9, 110.5, 108.9, 108.2, 101.1, 60.0, 55.9, 50.4, 41.9, 30.7, 29.8, 21.6; **HRESIMS**: calcd. for $C_{21}H_{22}NO_5$ [M+H$^+$] 368.3951; found 368.3988.

***N*-mesylnornantenine (12).** Analog **7** (0.10 g, 0.307 mmol) and methanesulfonyl chloride (0.05 mL, 0.614 mmol) were mixed in anhydrous CH_2Cl_2 (20 mL) and then treated with triethylamine (0.13 mL, 0.921 mmol). The mixture was allowed to stir at 0 °C overnight. The reaction was quenched with saturated $NaHCO_3$ (25 mL), and extracted with CH_2Cl_2 (2x25 mL), and dried over Na_2SO_4 and concentrated to dryness. The residue was recrystallized in diethyl ether to obtain **12** (0.07 g, 58%) as a white solid: **mp**: 197-199 °C; **^{1}H NMR** (500 MHz, $CDCl_3$): δ 7.98 (1H, s), 6.77 (1H, s), 6.64 (1H, s), 5.99 (2H, d, *J*=6.8 Hz), 3.90 (3H, s), 3.66 (3H, s), 3.25 (1H, m), 2.92 (6H, m), 1.39 (3H, t, *J*=7.2, 7.2, 7.2 Hz); **^{13}C NMR** (125 MHz, $CDCl_3$): δ 152.4, 146.8, 146.7, 145.2, 130.8,

128.5, 128.0, 124.8, 124.5, 110.8, 108.9, 108.8, 101.0, 60.06, 55.9, 53.0, 46.1, 40.4, 39.6, 37.4; **HRESIMS**: calcd. for $C_{20}H_{22}NO_6S$ $[M+H^+]$ 404.1090; found 404.1160.

Synthesis of nantenine analogs 13, 14 and 16:

Glaucine (13). To a solution of (+)-boldine (**42**, 4.50 g, 13.76 mmol) and trimethylphenylammonium chloride (8.26 g, 48.17 mmol) in dry DMF (25 mL) was added potassium *t*-butoxide (5.69 g, 48.17 mmol) and the suspension was refluxed under N_2 for 48 h. After removal of the organic solvent, the residue was dissolved in chloroform (75 mL) and washed with 5% NaOH solution (50 mL x 2) followed by water (3x50 mL). The organic layer was dried over anhydrous Na_2SO_4 and evaporated under reduced pressure. The residue was purified by flash chromatography (silicagel, MeOH:chloroform, 5:95) to afford analog **13** (3.25 g, 72%); **m.p.** 112-114°C; $\mathbf{[\alpha]_D^{25}}$ +122 (c 1, MeOH); **^{1}H NMR** (500 MHz, $CDCl_3$): 8.06 (s, 1H), 6.75 (s, 1H), 6.58 (s, 1H), 3.91 (s, 3H), 3.88 (s, 3H), 3.86 (s, 3H), 3.64 (s, 3H), 3.07-2.97 (m, 4H), 2.53 (s, 3H), 2.70-2.48 (m, 3H). **^{13}C NMR** (125 MHz, $CDCl_3$): δ 151.9, 147.9, 147.4, 144.2, 129.2, 128.8, 127.0, 126.8, 124.4, 111.4, 110.7, 110.3, 62.5, 60.1, 56.03, 55.9, 55.7, 53.3, 44.0, 34.4, 29.2. **HRESIMS**: calcd. for $C_{21}H_{25}NO_4$ $[M+H]^+$ 356.1784; found 356.1790.

Lirioferine (14). The solution of analog **13** (1.50 g, 4.22 mmol) in glacial acetic acid (50 mL) was bubbled with gaseous hydrogen bromide to saturation and the mixture was refluxed for 1 h. The reaction residue (1.65 g) obtained after removal of acetic acid under reduced pressure was mixed with water-acetone (1:2, 100 mL) and barium carbonate (200 mg) and the resultant suspension was heated under reflux for 30 min. The reaction

mixture was cooled, concentrated to remove organic solvent and the suspension was extracted with chloroform (3x25 mL). The combined chloroform layer was dried over sodium sulfate and evaporated to give a residue (0.85 g) which was chromatographed over a silica gel column (40 g) eluted with MeOH in chloroform (0-5%) to give analog **14** (0.20 g, 15%); **m.p.** 170-173°C; **$[\alpha]_D^{25}$** +128 (c=0.61, $CHCl_3$); **^{1}H NMR** (500 MHz, $CDCl_3$): 8.07 (s, 1H), 6.80 (s, 1H), 6.59 (s, 1H), 3.93 (s, 6H), 3.89 (s, 3H), 3.18-3.04 (m, 4H), 2.57 (s, 3H), 2.69-2.53 (m, 3H). **^{13}C NMR** (125 MHz, $CDCl_3$): δ 147.7, 147.2, 145.8, 140.66, 129.04, 128.51, 125.30, 123.93, 119.45, 111.09, 111.00, 108.80, 62.62, 56.18, 56.01, 55.94, 53.30, 43.90, 34.52, 28.89. **HRESIMS**: calcd. for $C_{20}H_{23}NO_4$ $[M+H]^+$ 342.1627; found 342.1777.

1,2,9,10-tetrahydroxyaporphine (43). Boldine **42** (0.25 g, 0.76 mmol) was dissolved in CH_2Cl_2 (10 mL) under argon atmosphere and 10 mL of 1M BBr_3 in CH_2Cl_2 was added at 0 °C, followed by stirring at room temperature for 4 h. The reaction then was quenched with MeOH (25 mL) and evaporated to dryness. The residue was dissolved in MeOH (25 mL), refluxed for 1 h, and evaporated again. The resulting material was dissolved in small amount of MeOH and added to diethyl ether. After filtration, white solids were collected to give **43** (0.21 g, 72%), as hydrobromide salt: **^{1}H NMR** (500 MHz, MeOD): δ 8.02 (s, 1H), 6.77 (s, 1H), 6.59 (s, 1H), 4.18 (bs, 1H), 3.73 (bs, 1H), 3.49 (bs, 1H), 3.16 (bs, 3H), 2.95 (m, 1H), 2.76 (m, 1H); **^{13}C NMR** (125 MHz, MeOD): δ 146.0, 144.3, 143.8, 141.8, 136.2, 124.2, 124.2, 123.8, 120.5, 116.6, 115.4, 114. 4, 111.6, 63.3, 52.8, 40.5, 31.2, 25.3, 11.2

Neolitsine (16). Finely ground NaOH (52.00 mg, 1.3 mmol), was added to a solution of **43** (0.10 g, 0.26 mmol) in 10 mL of dry DMSO at ambient temperature under N_2. Stirring was continued for 1 h. Methylene dibromide (0.10 mL, 1.04 mmol) was added, and the mixture was heated at 80 °C for 24 hours. After cooling, the solution was poured onto ice water and extracted with EtOAc (25 mL). Drying over Na_2SO_4 and evaporation of the organic solvent under reduced pressure gave analog **16** as oil. The title compound was isolated by flash chromatography (silicagel, MeOH:CH_2Cl_2, 1:99). Recrystallization of the product from AcOEt afforded **16** (45 mg, 52%) as yellow crystals: **mp**: 187-190 °C; **^{1}H NMR** (500 MHz, $CDCl_3$): δ 7.64 (s, 1H), 6.78 (s, 1H), 6.55 (s, 1H), 6.09 (d, 1H, *J*=1.5 Hz), 6.00-5.95 (m, 3H), 3.16-3.05 (m, 4H), 2.65-2.54 (m, 2H), 2.51 (s, 3H); **^{13}C NMR (125 MHz**, $CDCl_3$): δ 146.6, 146.5, 146.5, 141.8, 129.8, 126.5, 126.5, 124.6, 116.6, 108.6, 107.4, 106.8, 101.0, 100.6, 62.2, 53.5, 44.0, 34.7, 29.2. **HRESIMS**: calcd. for $C_{19}H_{17}NO_4$ $[M+H]^+$ 324.1158; found 324.225.

Synthesis of nantenine analog 15:

2-(2-bromophenyl)-*N*-(3,4-dimethoxyphenethyl)acetamide (45). A solution of **44** (11.86 g, 55.17 mmol) and 1,1'-carbonyldiimidazole (8.95 g, 55.17 mmol) in 175 mL of anhydrous THF was stirred at 0 °C for 1.5 h and at room temperature for 1 h. The mixture was cooled again in an ice bath and stirred for 1 h; then 3,4-dimethoxy-phenethylamine **24** (9.16 mL, 55.17 mmol) was added and the solution was stirred at 0 °C for 4 h and at room temperature overnight under nitrogen atmosphere. The THF was evaporated under reduced pressure and the residue was dissolved in EtOAc (250 mL) and was washed with 1N HCl (75 mL), water (75 mL), and aqueous $NaHCO_3$ (100 mL). The

organic layer was evaporated and the crude product was crystallized from EtOAc to give the amide **45** (19.05 g, 91%): **mp**: 127-129 °C; **^{1}H NMR** (500 MHz, $CDCl_3$): δ 7.56 (s, 1H), 7.16 (s, 1H), 6.73 (s, 1H), 6.62 (s, 2H), 5.43 (s, 1H), 3.85 (m, 7H), 3.67 (s, 2H), 3.48 (s, 2H), 2.71 (m, 2H). **^{13}C NMR** (125 MHz, $CDCl_3$): δ 169.4, 148.9, 147.5, 134.7, 133.1, 131.6, 131.0, 129.1, 127.9, 124.9, 120.5, 111.6, 111.2, 55.9, 55.8, 44.1, 40.8, 35.0; **HRESIMS**: calcd. for $C_{18}H_{20}BrNO_3$ $[M]^+$ 377.0627; found: 377.1316.

1-(2-bromobenzyl)-6,7-dimethoxy-3,4-dihydroisoquinoline (46). Phosphorus pentachloride (2.47 g, 11.89 mmol) was added during 30 min in three portions to a chilled (0 °C) solution of amide **45** (3.0 g, 7.93 mmol) in 50 mL of dry CH_2Cl_2 under argon and the mixture was stirred for 30 min. Then, the ice bath was removed and the mixture was stirred at room temperature for 24 h. The reaction mixture was then poured onto a saturated solution of $NaHCO_3$ and the contents of the flask were stirred for 1 h. The aqueous layer was extracted twice with 30 mL CH_2Cl_2 and the combined organic extracts were washed with saturated solution of $NaHCO_3$ (50 mL), dried over Na_2SO_4, filtered and evaporated to give **46**. Since imines are prone to air oxidation, compound **46** was used without further purification for the preparation of **47**.

1-(2-bromobenzyl)-6,7-dimethoxy-1,2,3,4-tetrahydroisoquinoline (47). Sodium borohydride (4.19 g, 111.00 mmol) was added portion-wise to a stirred solution of **46** (2.00 g, 5.55 mmol) in MeOH (50 mL) and the mixture was stirred at 0 °C for 4 h. The reaction mixture was concentrated, and excess $NaBH_4$ was destroyed by adding water (50 mL) and glacial acetic acid (50 mL). The mixture was extracted with CH_2Cl_2 (3x35 mL), dried

over Na_2SO_4 and concentrated to give crude yellow solid **47**. This compound was used for next step without any further purification.

***tert*-butyl 1-(2-bromobenzyl)-6, 7-dimethoxy-3, 4-dihydroisoquinoline-2 (1*H*)-carboxylate (48).** To a solution of the **47** (2.00 g, 4.32 mmol), diisopropylethylamine (1.5 mL, 8.65 mmol) and 1-3 mg of 4-(dimethylamino)pyridine in anhydrous CH_2Cl_2 (15 mL)was added slowly di-tert-butyl dicarbonate (1.11 mL, 5.20 mmol) and the resulting mixture was stirred overnight at room temperature. The reaction was then quenched by adding a solution of NH_4Cl (25 mL) and was extracted with CH_2Cl_2 (3x35 mL). The crude reaction mixture was then purified by column chromatography (silicagel, MeOH:CH_2Cl_2, 1:99), to obtain **48** (1.79 g, 89%) as white solid: **mp**: 108-110 °C; **^{1}H NMR** (500 MHz, $CDCl_3$): δ 7.59 (m, 1H), 7.18 (m, 3H), 6.82 (m, 1H), 6.62 (s, 1H), 4.39 (m, 1H), 3.87 (m, 7H), 3.71 (m, 1H), 3.28 (m, 2H), 3.00 (m, 1H), 2.92 (s, 1H), 2.68 (s, 1H), 1.21 (s, 9H). **^{13}C NMR** (125 MHz, $CDCl_3$): δ 154.3, 147.8, 147.4, 138.2, 132.5, 131.9, 128.9, 128.3, 127.5, 126.5, 125.3, 111.4, 109.7, 79.5, 55.9, 53.7, 42.7, 41.9, 38.8, 36.2, 28.3, 28.2, 27.9; **HRESIMS**: calcd. for $C_{23}H_{28}BrNO_4$ $[M+Na]^+$ 484.1099; found: 484.1006.

***tert*-butyl-4,5,6a,7-tetrahydro-1,2-dimethoxydibenzo [*de,g*] quinoline-6-carboxylate (49).** K_2CO_3 (0.67 g, 4.90 mmol), 2-(diphenylphophanyl)-2`-(dimethyl-amino)biphenyl (93.45 mg, 0.25 mmol), Pd(II)-acetate (27.5 mg, 0.12 mmol) and the **48** (1.13 g, 2.45 mmol) are weighted to air and placed in a three-way round-bottomed flask with a magnetic stir bar. The flask is purged with argon (30 min). DMA (4 mL) is then added and the resulting mixture is heated to 130 °C overnight. The reaction mixture is then

concentrated and loaded onto a silicagel column for chromatography using hexane:EtOAc, 25:75. The compound **49** has been obtained as white crystals (0.53 g, 56.7%): **mp**: 149-151 °C; **^{1}H NMR** (500 MHz, $CDCl_3$): δ 8.46 (d, 1H, *J*=7.8 Hz), 7.35-7.25 (m, 3H), 6.70 (s, 1H), 4.69 (d, 1H, *J*=12 Hz), 4.45 (m, 1H), 3.93 (m, 3H), 3.69 (m, 3H), 3.00-2.83 (m, 5H), 2.68 (d, 1H, *J*=14.7), 1.50 (m, 9H); **^{13}C NMR** (125 MHz, $CDCl_3$): δ 154.7, 152.0, 145.6, 137.0, 131.7, 130.0, 129.8, 128.4, 128.1, 127.7, 127.6, 126.9, 126.5, 111.4, 79.8, 60.0, 55.9, 51.6, 31.6, 30.4, 28.5, 22.6, 14.1; **HRESIMS**: calcd. for $C_{23}H_{27}NO_4$ $[M]^+$ 381.1943; found: 381.3421.

Nornuciferine (50). Compound **49** (0.14 g, 0.35 mmol), in dry CH_2Cl_2 (10 mL) is stirred magnetically with ahydrous $ZnBr_2$ (0.40 g, 1.77 mmol) under argon at room temperature for 12 h. The reaction mixture is filtered over Celite and the filtrate is stripped off of its solvent to get **50** as hydrobromide. After free-basing with aqueous saturated K_2CO_3 solution (25 mL), amine **50** has been extracted with CH_2Cl_2 (2x25 mL), dried over Na_2SO_4 and concentrated to get **50** (0.90 g, 89%), as yellow crystals: **mp**: 144-146 °C; **^{1}H NMR** (500 MHz, $CDCl_3$): δ 8.43 (d, 1H, *J*=8.1 Hz), 7.35-7.24 (m, 3H), 6.68 (s, 1H), 3.92 (s, 3H), 3.85 (dd, 1H, *J*=13.7, 4.4), 3.70 (s, 3H), 3.37-3.39 (m, 1H), 3.06-3.01 (m, 2H), 2.87-2.83 (m, 1H), 2.77-2.71 (m, 2H), 1.72 (bs, 1H); **^{13}C NMR** (125 MHz, $CDCl_3$): δ 152.0, 145.0, 136.3, 132.2, 129.2, 129.1, 128.4, 127.8, 127.3, 127.0, 126.5, 111.7, 60.3, 55.9, 53.6, 43.3, 37.7, 29.3

Nuciferine (15). Compound **50** (0.10 g, 0.35 mmol) and formaldehyde solution, 37% (0.78 mL, 0.71 mmol) were mixed in anhydrous CH_2Cl_2 (10 mL) and then treated with

sodium triacetoxy-borohydride (0.38 g, 1.77 mmol). The mixture was allowed to stir at room temperature for 24 h. The reaction was quenched with 5% aq $NaHCO_3$ (25 mL), and extracted with EtOAc (2x25 mL), and dried over Na_2SO_4 and concentrated to dryness. The residue was purified through flash chromatography (silicagel, MeOH:CH_2Cl_2, 1:99) to obtain analog **15** (0.60 g, 57%) as a bright yellow oil: **^{1}H NMR** (500 MHz, $CDCl_3$): δ 8.36 (d, 1H, *J*=8.1), 7.32-7.21 (m, 3H), 6.63 (s, 1H), 3.88 (s, 3H), 3.65 (s, 3H), 3.16-3.02 (m, 4H), 2.70-2.48 (m, 6H); **^{13}C NMR** (125 MHz, $CDCl_3$): δ 151.9, 145.1, 136.5, 132.1, 128.7, 128.3, 128.0, 127.8, 127.3, 127.0, 126.9, 111.2, 62.3, 60.2, 55.8, 53.3, 44.0, 35.1, 29.2; **HRESIMS**: calcd. for $C_{19}H_{21}NO_2$ $[M+H]^+$ 296.1572; found 296.1610.

2.8 Appendix

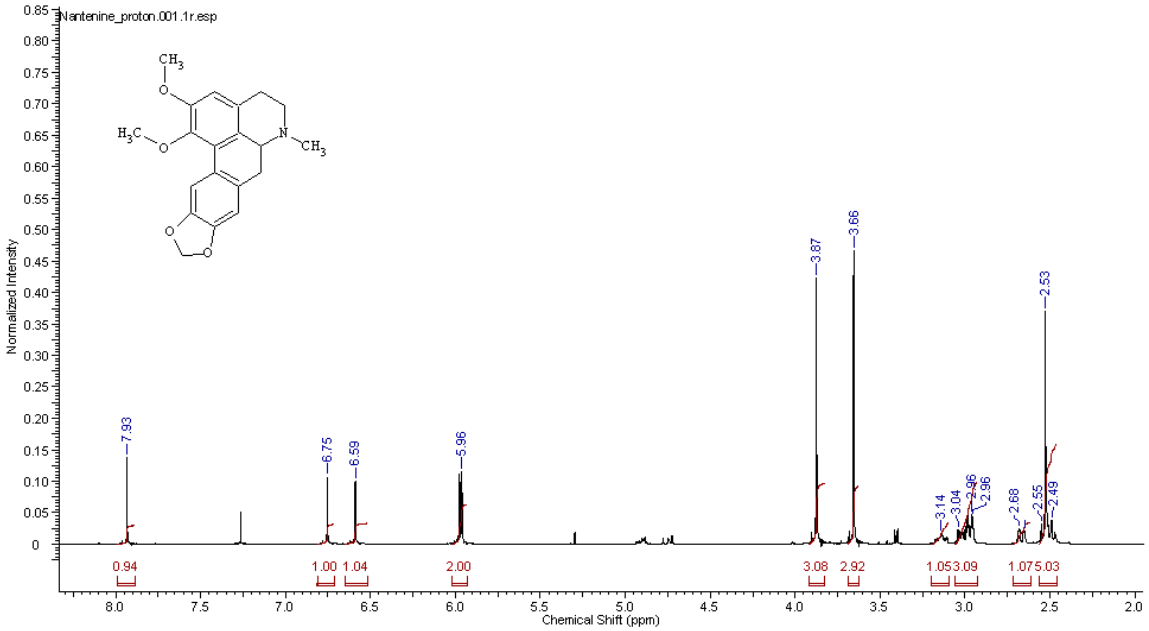

Figure 2.15 ^{1}H NMR (500 MHz, $CDCl_3$) of **Nantenine**.

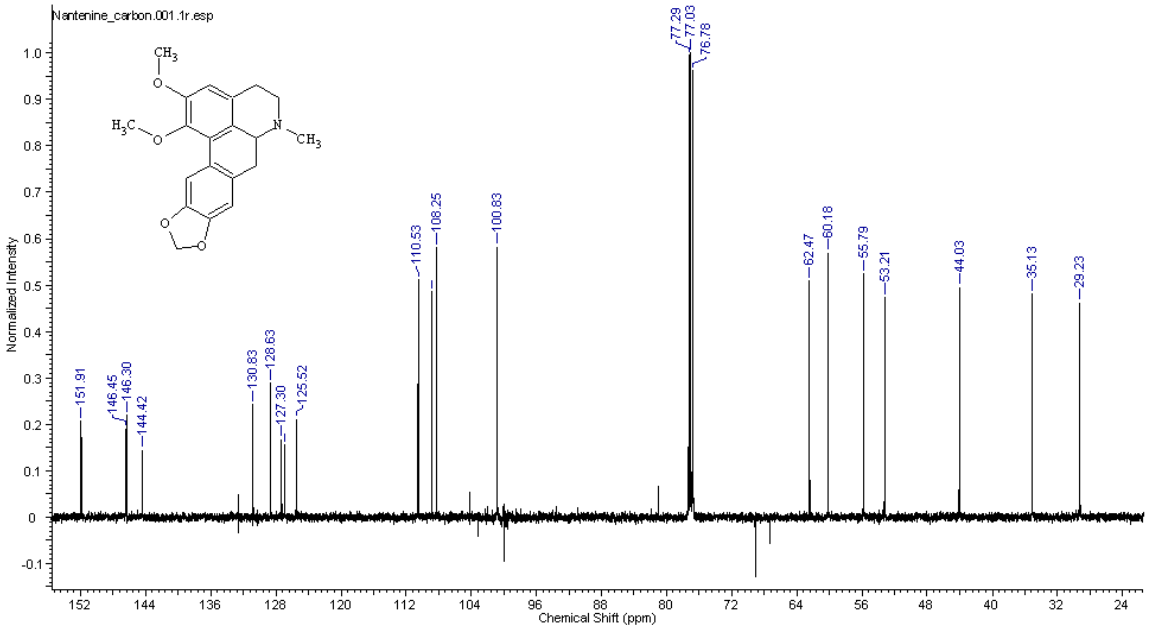

Figure 2.16 ^{13}C NMR (125 MHz, $CDCl_3$) of **Nantenine**.

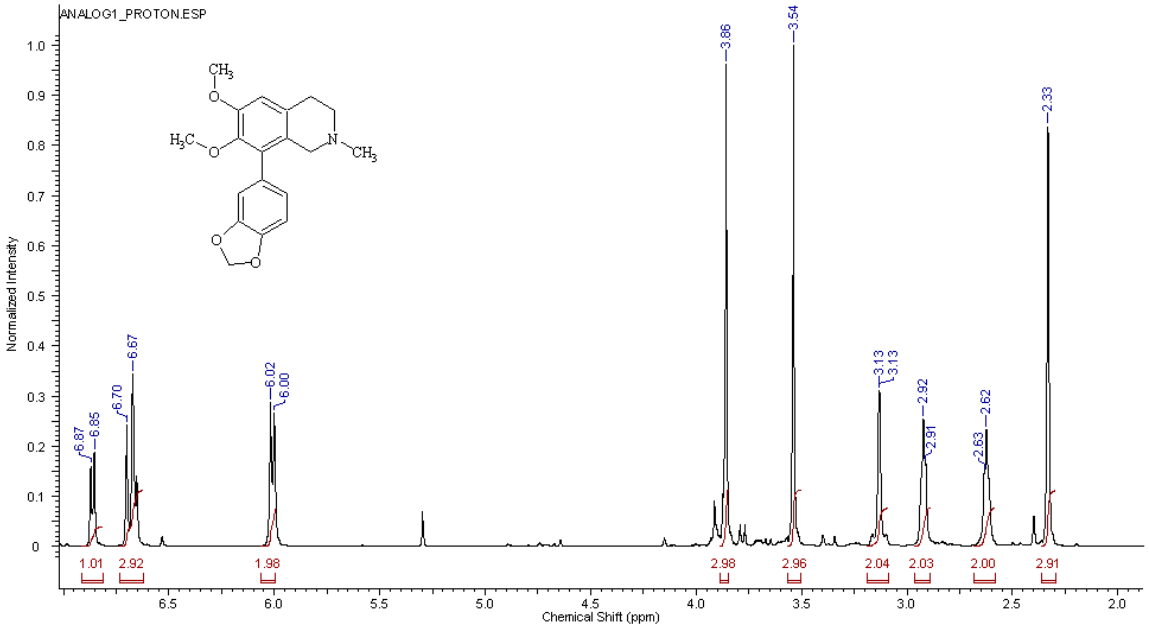

Figure 2.17 ^{1}H NMR (500 MHz, $CDCl_3$) of 8-(benzo[*d*][1,3]dioxol-5-yl)-6,7-dimethoxy -2-methyl-1,2,3,4-tetrahydroisoquinoline (**1)**.

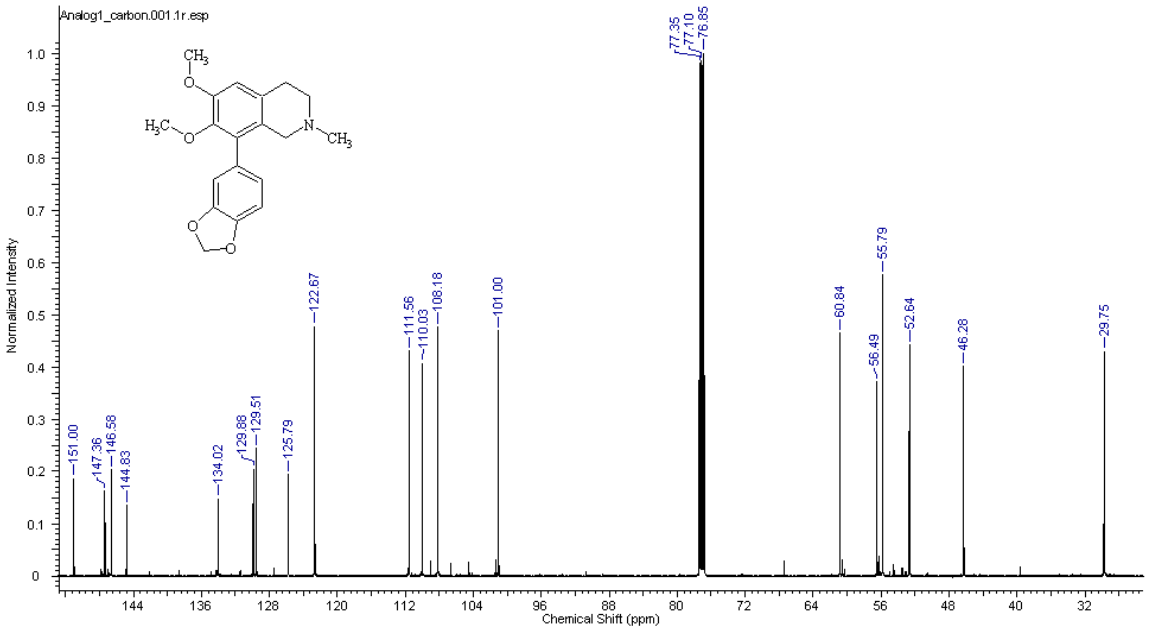

Figure 2.18 ^{13}C NMR (500 MHz, $CDCl_3$) of 8-(benzo[*d*][1,3]dioxol-5-yl)-6,7-dimethoxy-2-methyl-1,2,3,4-tetrahydroisoquinoline (**1)**.

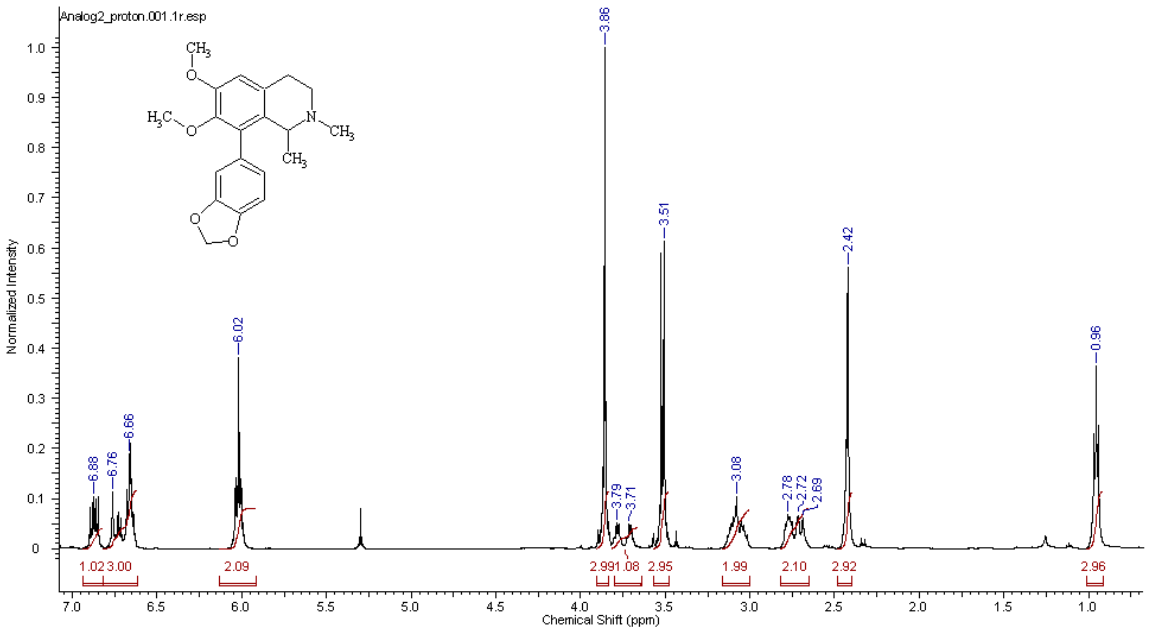

Figure 2.19 ^{1}H NMR (500 MHz, $CDCl_3$) of 8-(benzo[*d*][1,3]dioxol-5-yl)-6,7-dimethoxy -1,2-dimethyl-1, 2, 3, 4-tetrahydroisoquinoline (**2)**.

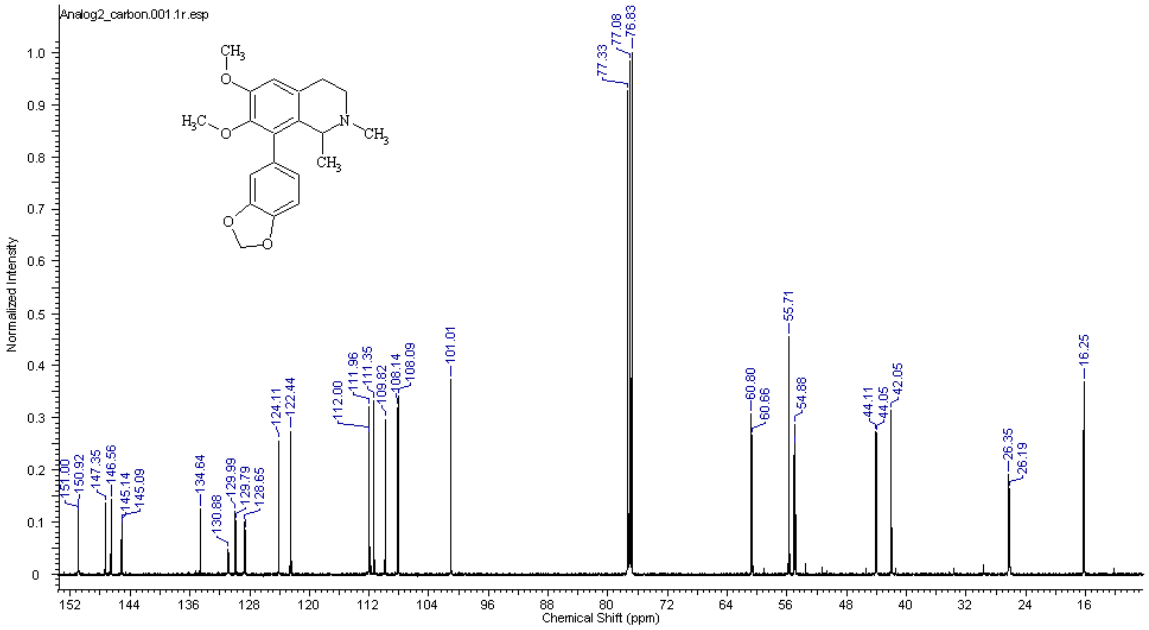

Figure 2.20 ^{13}C NMR (125 MHz, $CDCl_3$) of 8-(benzo[*d*][1,3]dioxol-5-yl)-6,7-dimethoxy-1,2-dimethyl-1, 2, 3, 4-tetrahydroisoquinoline (**2)**.

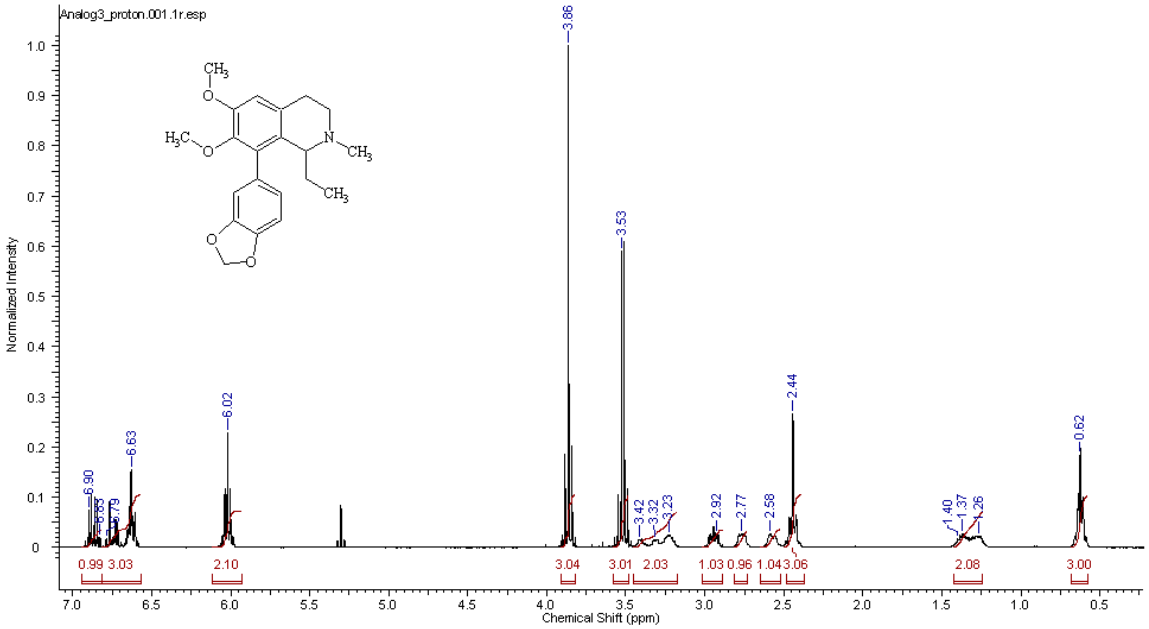

Figure 2.21 ^{1}H NMR (500 MHz, $CDCl_3$) of 8-(benzo[*d*][1,3]dioxol-5-yl)-1-ethyl-6,7-dimethoxy-2-methyl-1,2,3,4-tetrahydroisoquinoline (**3)**.

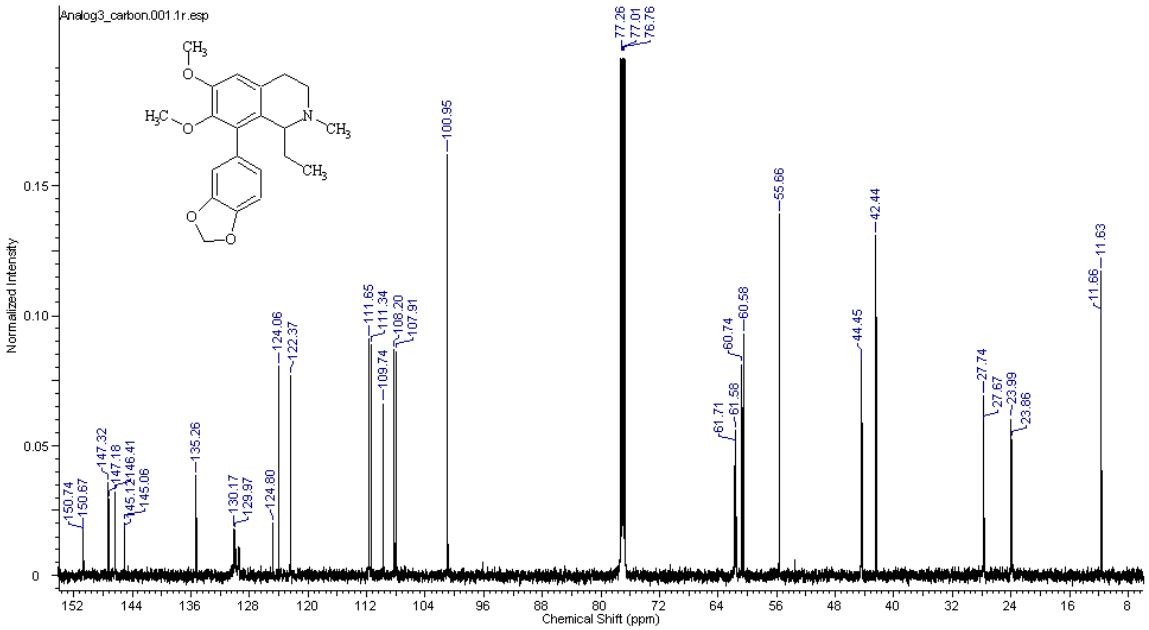

Figure 2.22 ^{13}C NMR (125 MHz, $CDCl_3$) of 8-(benzo[*d*][1,3]dioxol-5-yl)-1-ethyl-6,7-dimethoxy-2-methyl-1,2,3,4-tetrahydroisoquinoline (**3)**.

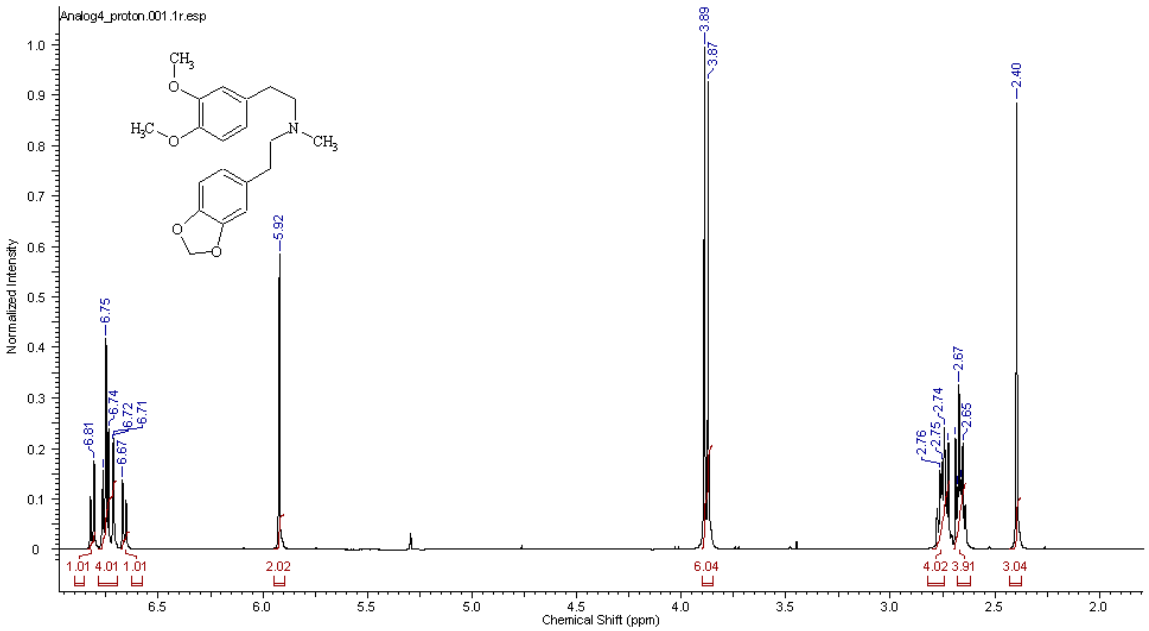

Figure 2.23 ^{1}H NMR (500 MHz, $CDCl_3$) of 2-(benzo[*d*][1,3]dioxol-5-yl)-*N*-(3,4-dimethoxyphenethyl)-*N*-methylethanamine (**4)**.

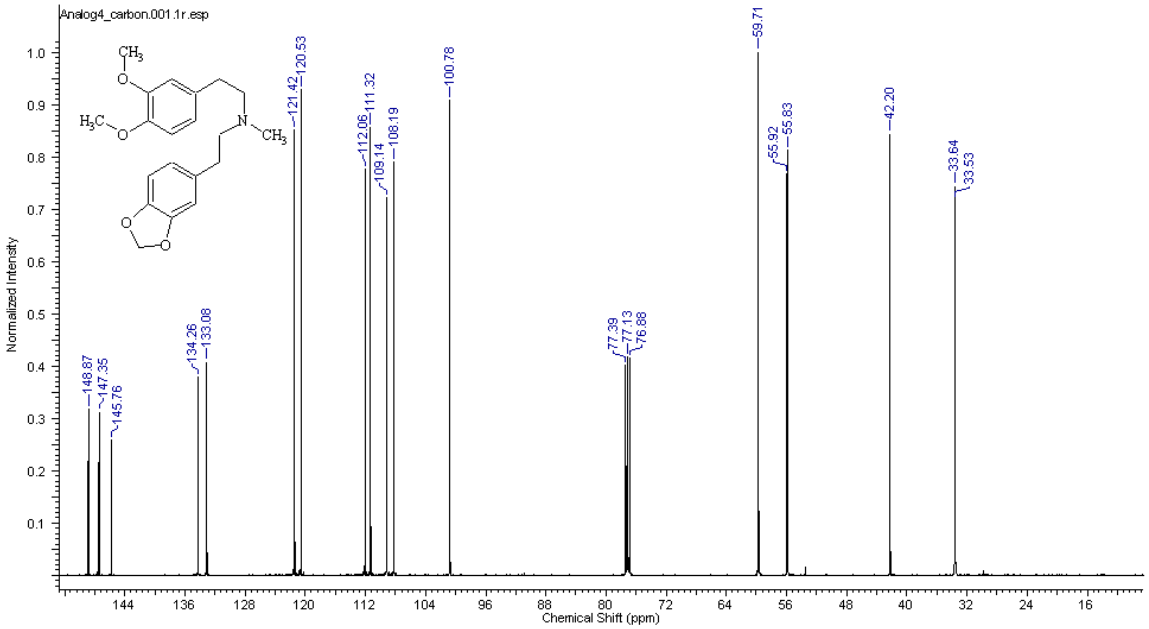

Figure 2.24 ^{13}C NMR (125 MHz, $CDCl_3$) of 2-(benzo[*d*][1,3]dioxol-5-yl)-*N*-(3,4-dimethoxyphenethyl)-*N*-methylethanamine (**4)**.

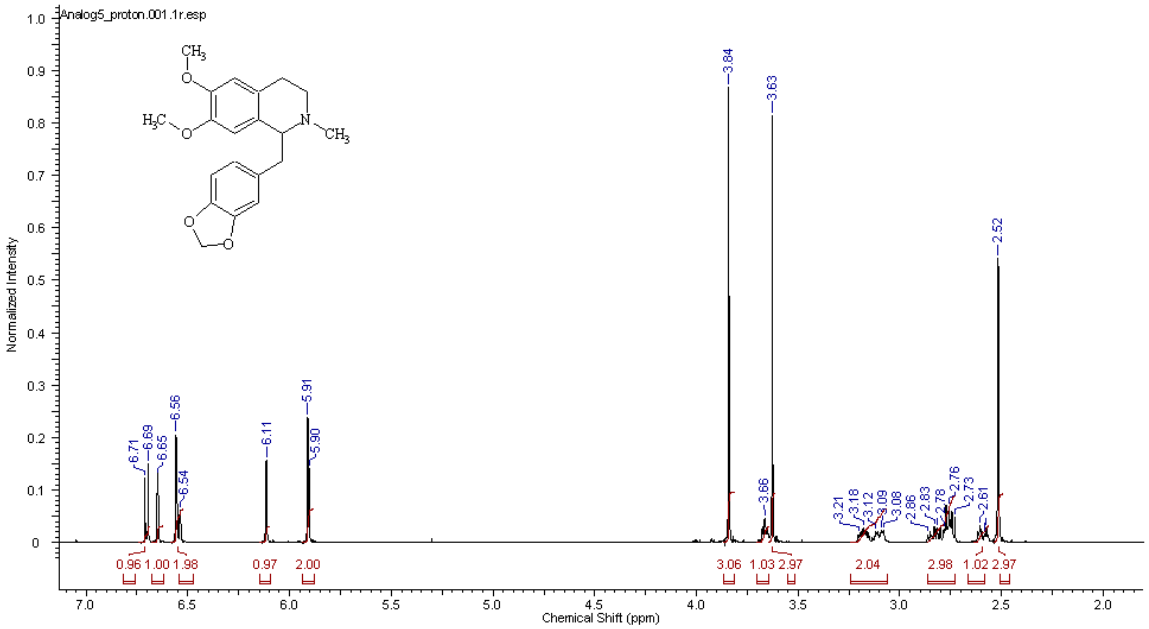

Figure 2.25 ^{1}H NMR (500 MHz, $CDCl_3$) of 1-(benzo [*d*][1,3]dioxol-5-ylmethyl)-6,7-dimethoxy-2-methyl-1,2,3,4-tetrahydroisoquinoline (**5)**.

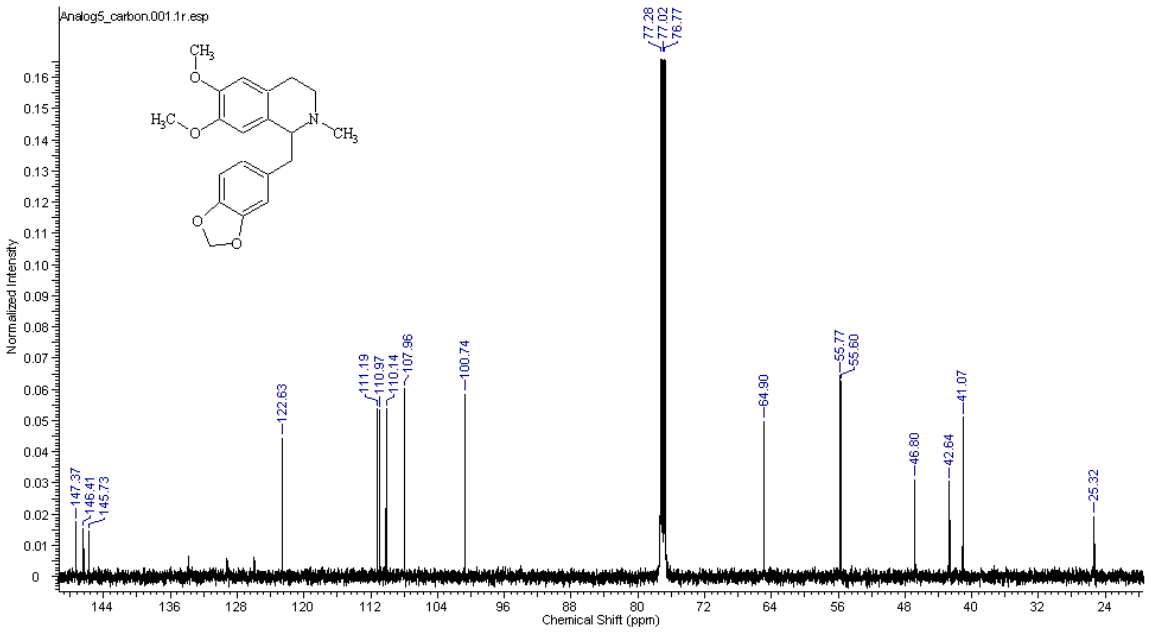

Figure 2.26 ^{13}C NMR (125 MHz, $CDCl_3$) of 1-(benzo [*d*][1,3]dioxol-5-ylmethyl)-6,7-dimethoxy-2-methyl-1,2,3,4-tetrahydroisoquinoline (**5)**.

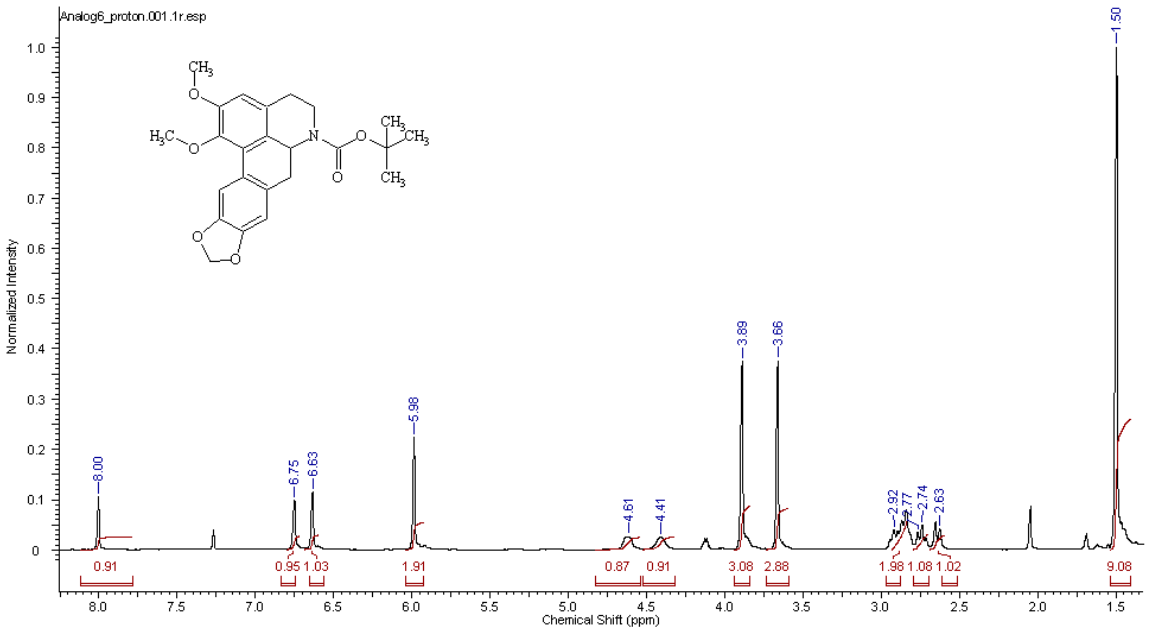

Figure 2.27 ^{1}H NMR (500 MHz, $CDCl_3$) of *tert*-butyl4,5,6a,7-tetrahydro-1,2-dimethoxy-9,11,-dioxa-6-azabenzo[*fg*]cyclopenta[*b*]anthracene-6-carboxylate (**6**).

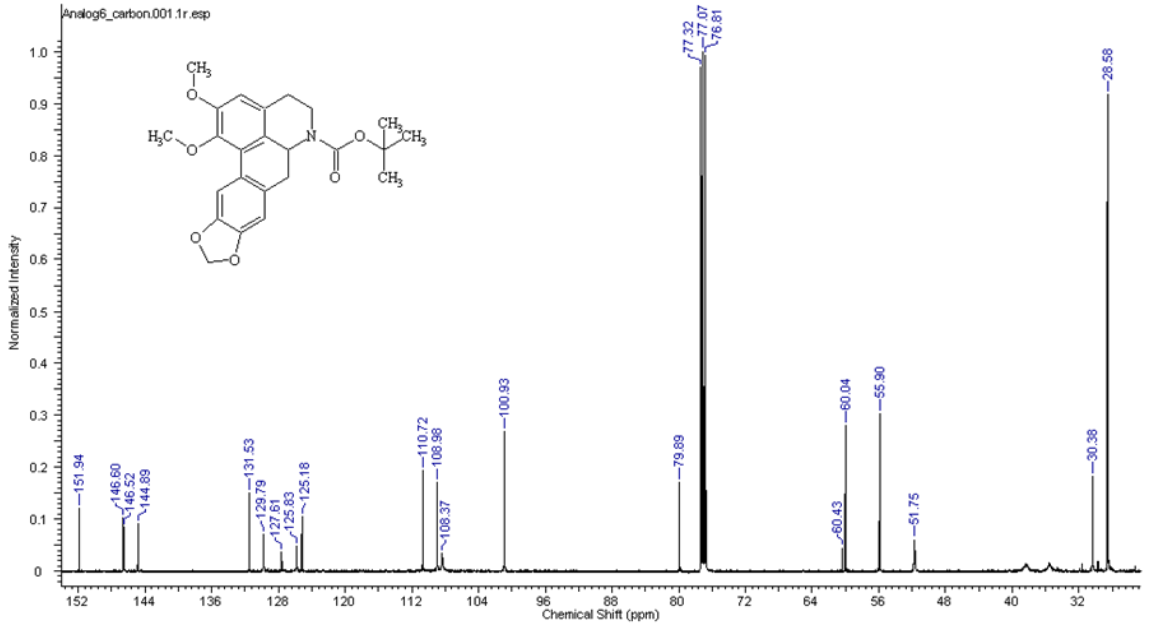

Figure 2.28 ^{13}C NMR (125 MHz, $CDCl_3$) of *tert*-butyl4,5,6a,7-tetrahydro-1,2-dimethoxy-9,11,-dioxa-6-azabenzo[*fg*]cyclopenta[*b*]anthracene-6-carboxylate (**6**).

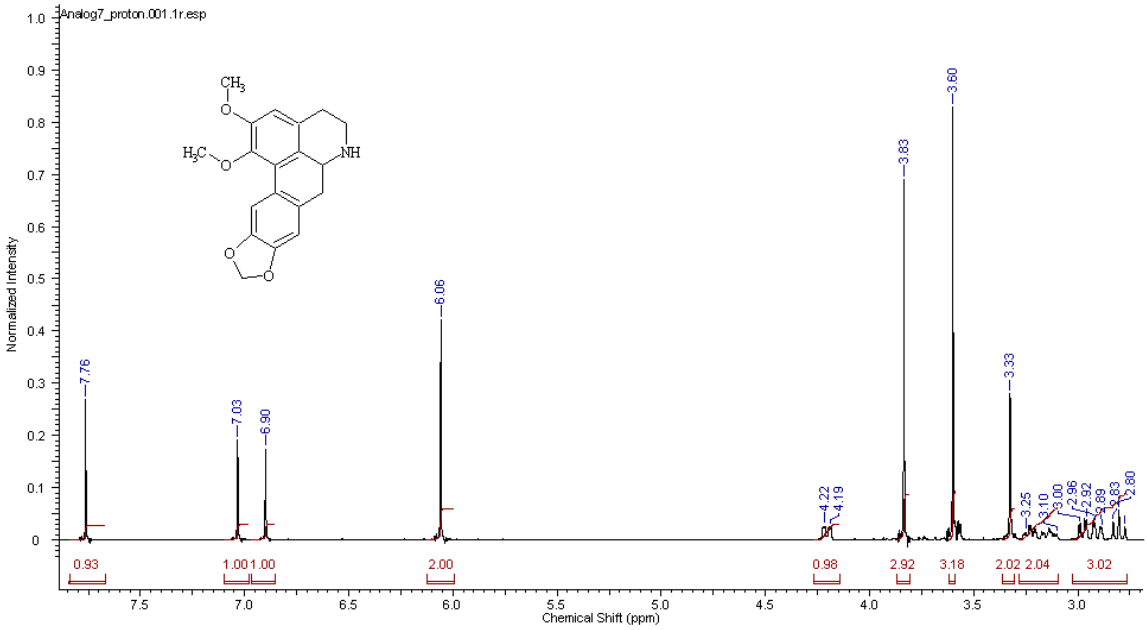

Figure 2.29 ^{1}H NMR (500 MHz, DMSO-D_6) of Nornantenine (**7**).

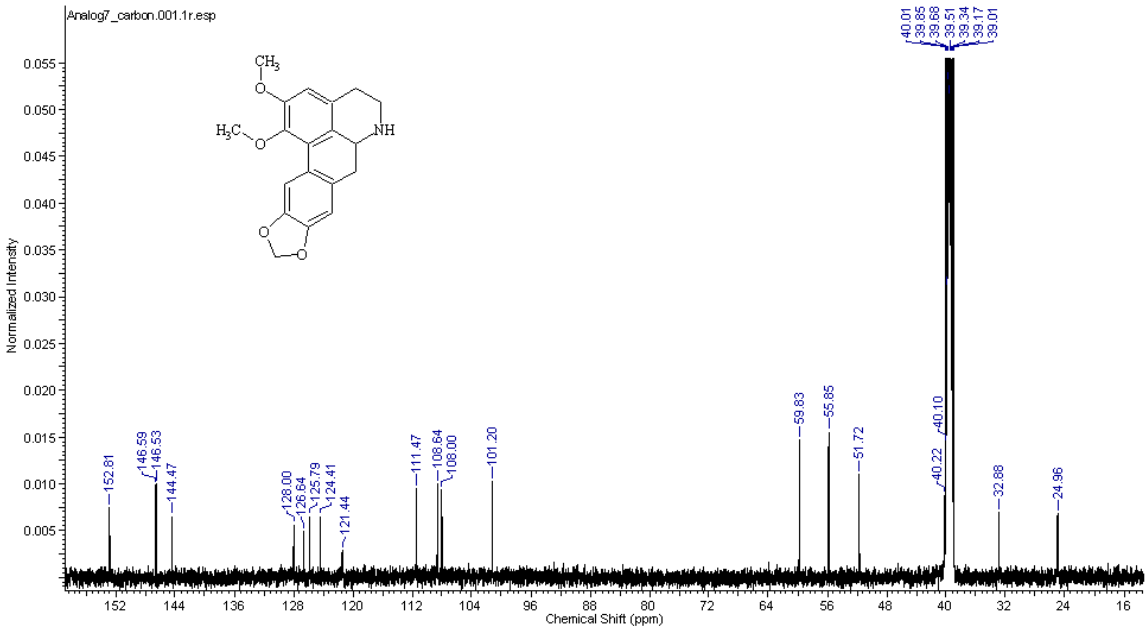

Figure 2.30 ^{13}C NMR (125 MHz, DMSO-D_6) of Nornantenine (**7**).

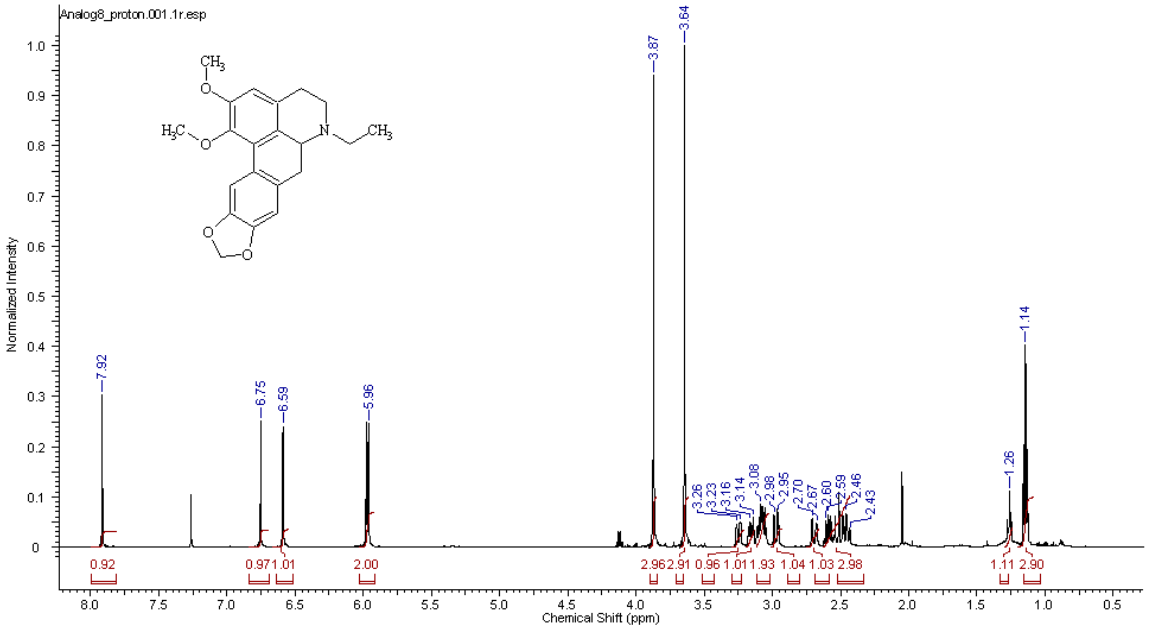

Figure 2.31 ^{1}H NMR (500 MHz, $CDCl_3$) of Ethylnornantenine (**8**).

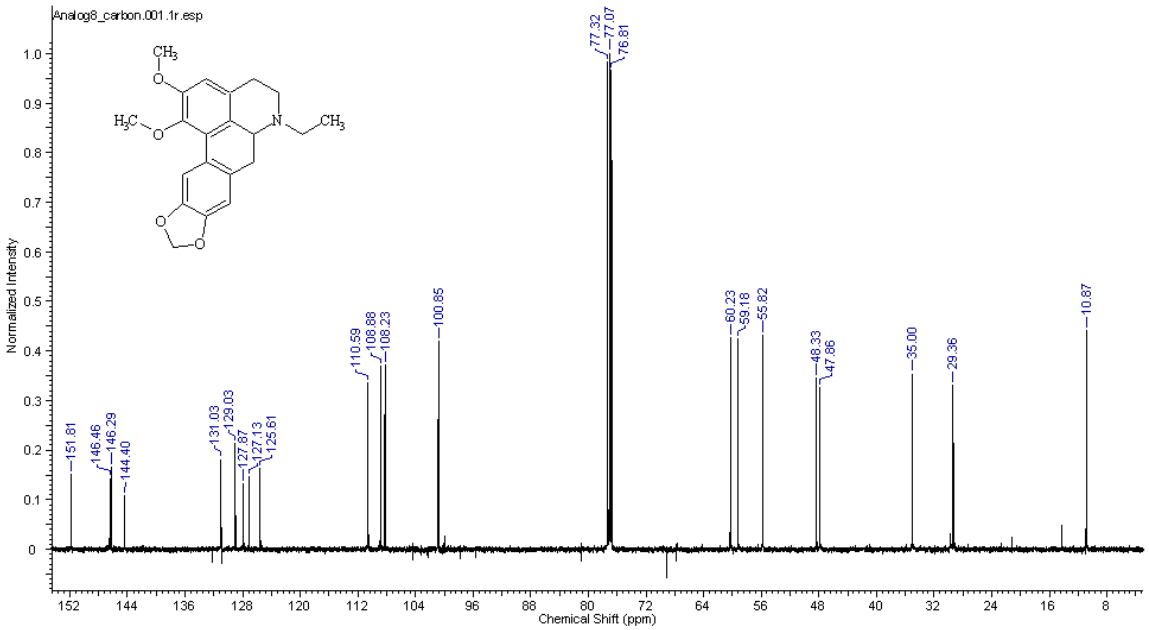

Figure 2.32 ^{13}C NMR (125 MHz, $CDCl_3$) of Ethylnornantenine (**8**).

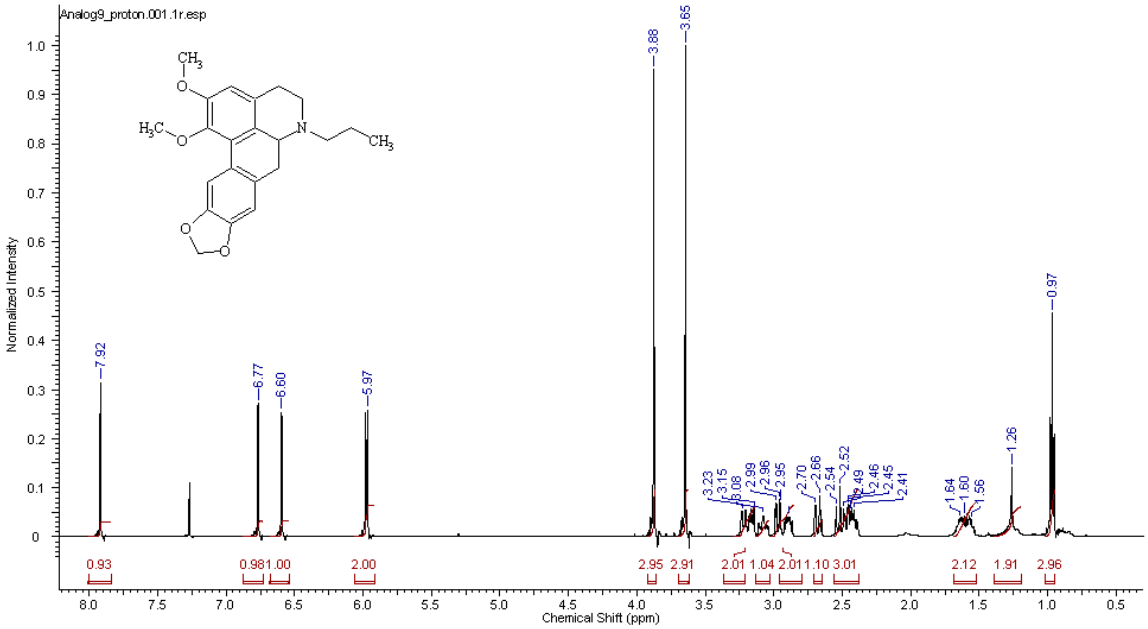

Figure 2.33 ^{1}H NMR (500 MHz, $CDCl_3$) of Propylnornantenine (**9**).

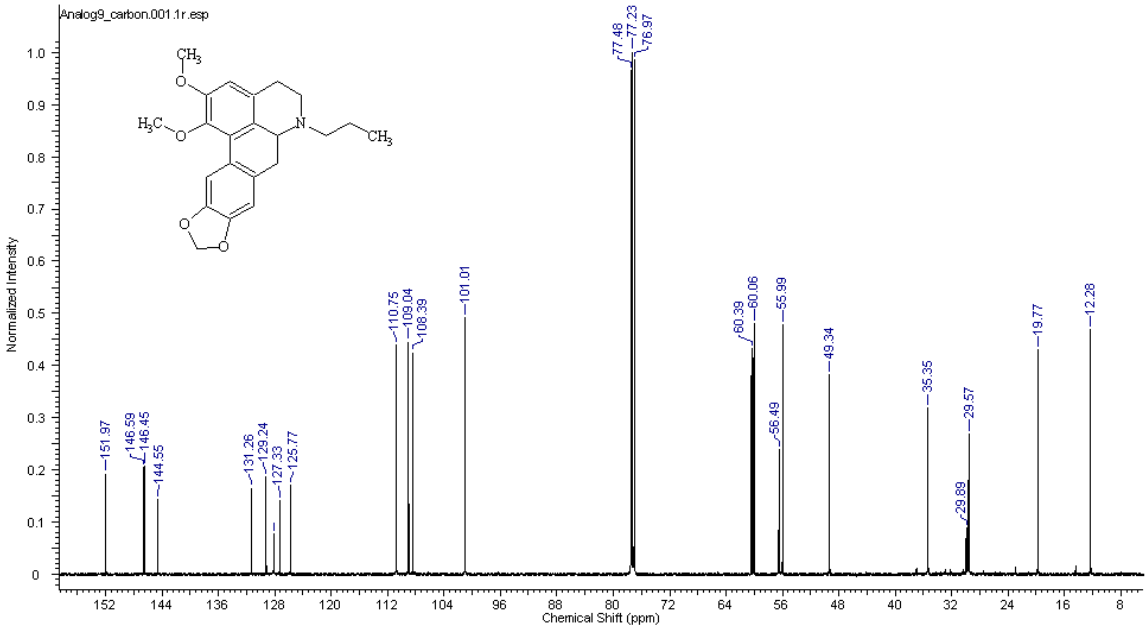

Figure 2.34 ^{13}C NMR (125 MHz, $CDCl_3$) of Propylnornantenine (**9**).

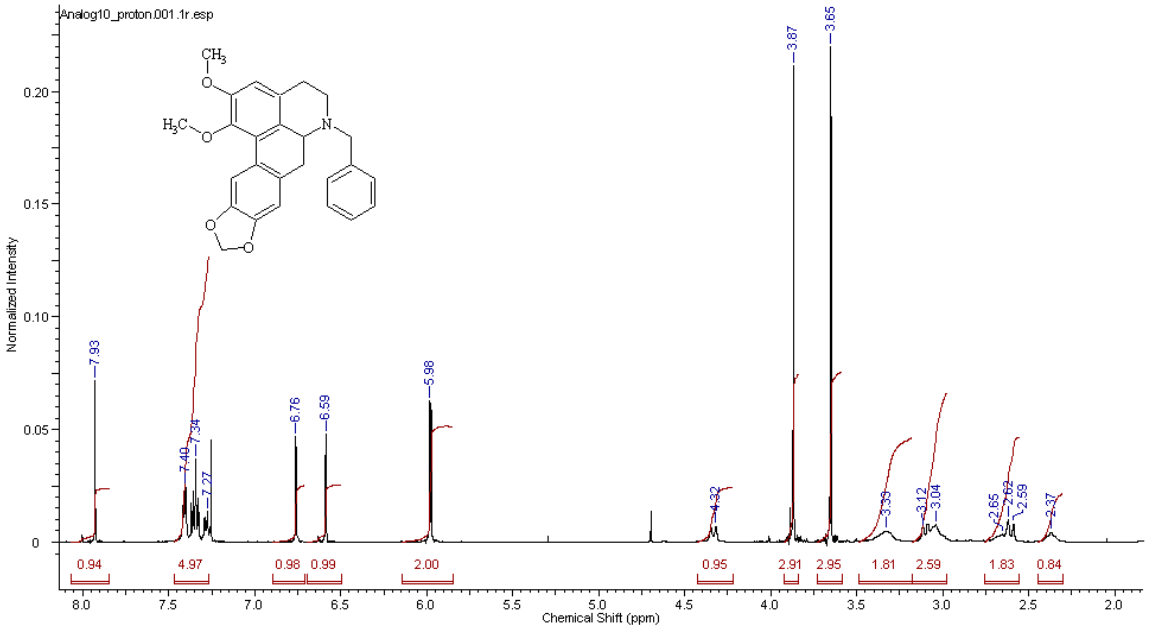

Figure 2.35 ^{1}H NMR (500 MHz, $CDCl_3$) of Benzylnornantenine (**10**).

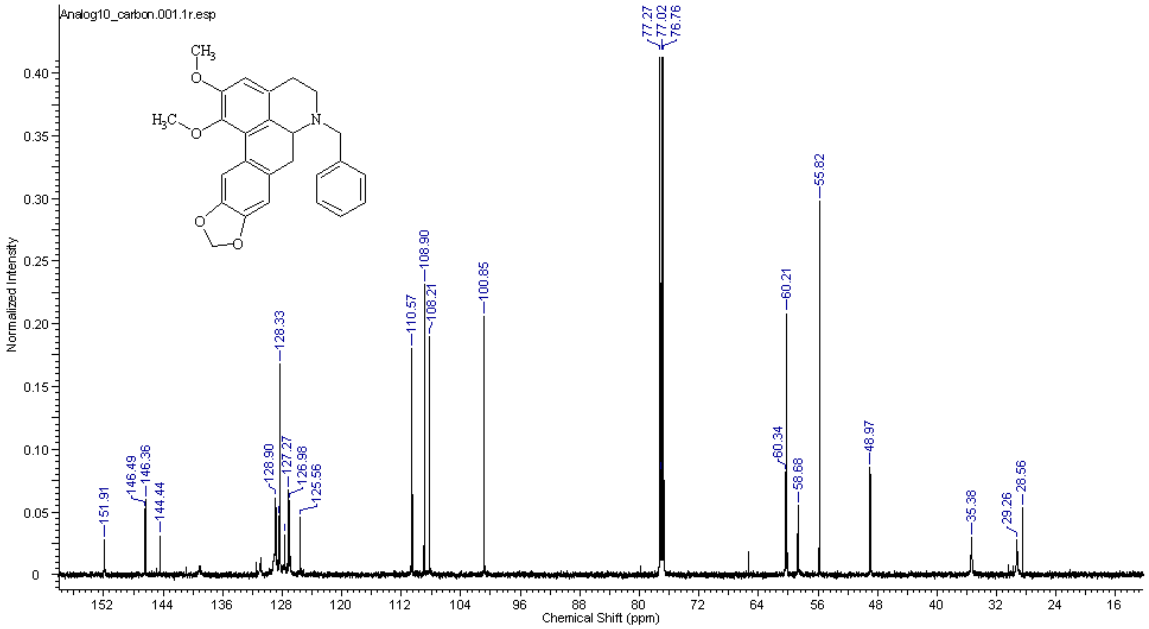

Figure 2.36 ^{13}C NMR (125 MHz, $CDCl_3$) of Benzylnornantenine (**10**).

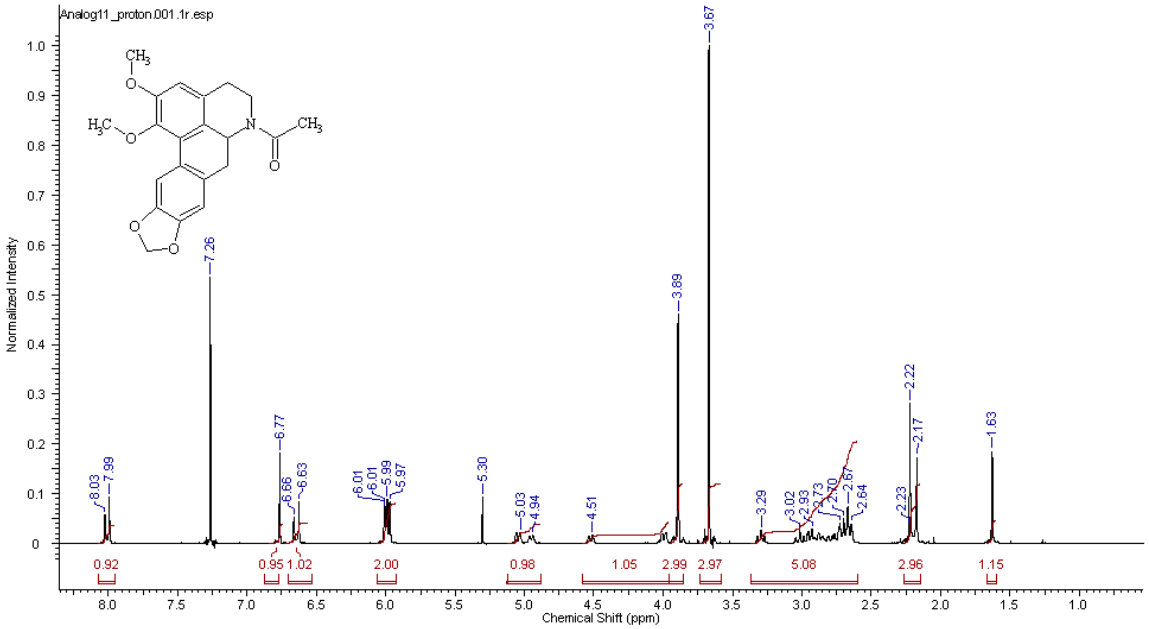

Figure 2.37 ^{1}H NMR (500 MHz, $CDCl_3$) of *N*-Acetylnornantenine (**11**).

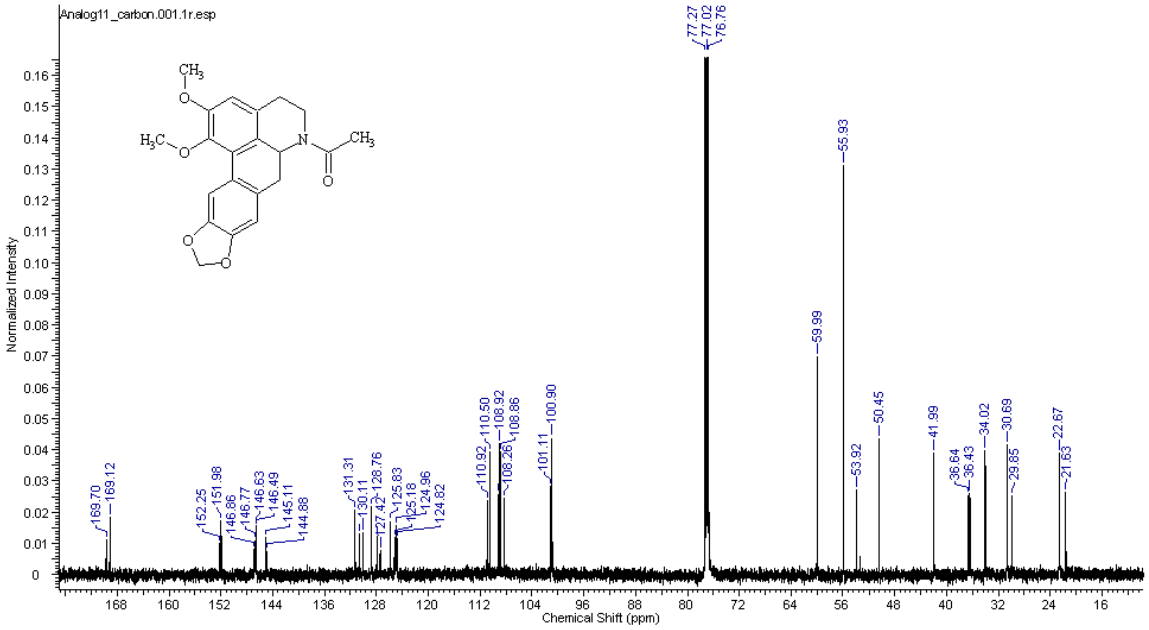

Figure 2.38 ^{13}C NMR (125 MHz, $CDCl_3$) of *N*-Acetylnornantenine (**11**).

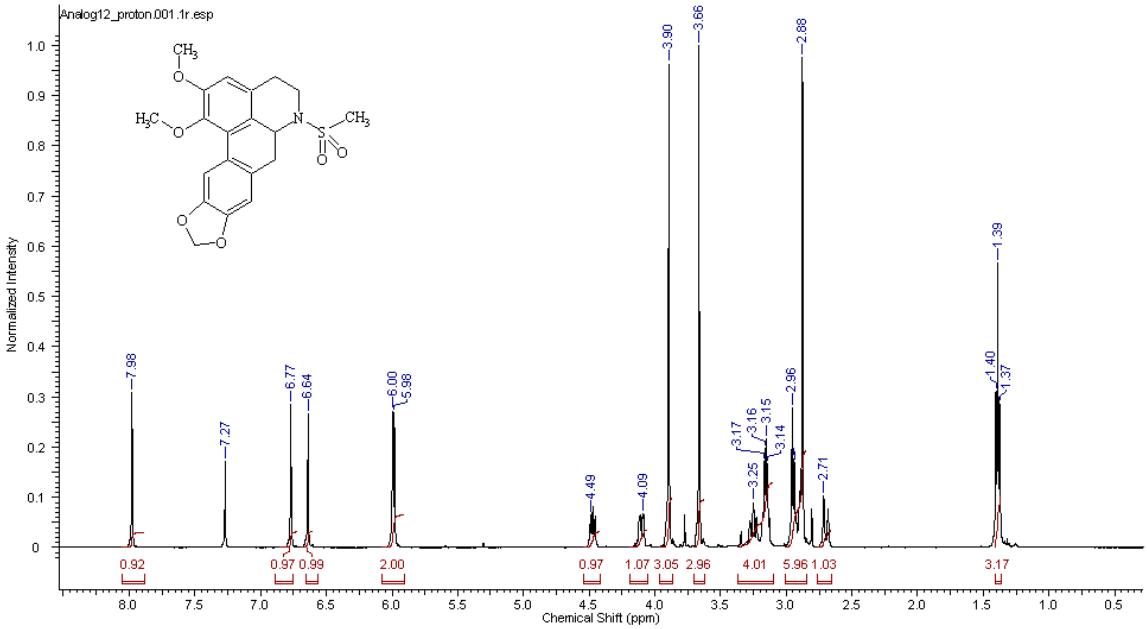

Figure 2.39 ^{1}H NMR (500 MHz, $CDCl_3$) of *N*-Mesylnornantenine (**12)**.

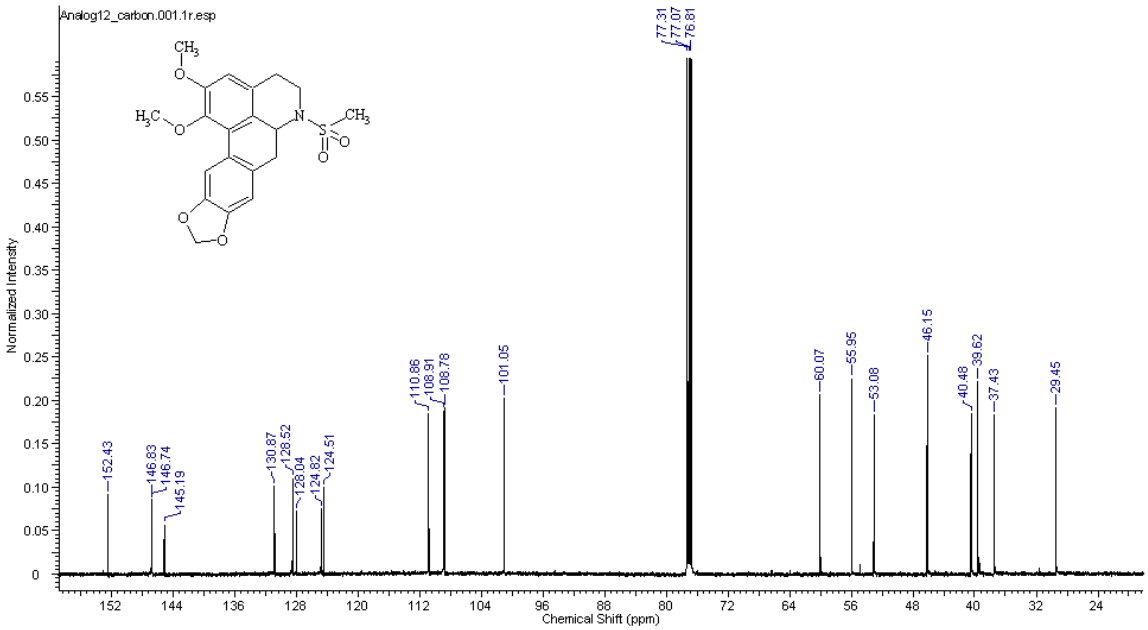

Figure 2.40 ^{13}C NMR (125 MHz, $CDCl_3$) of *N*-Mesylnornantenine (**12)**.

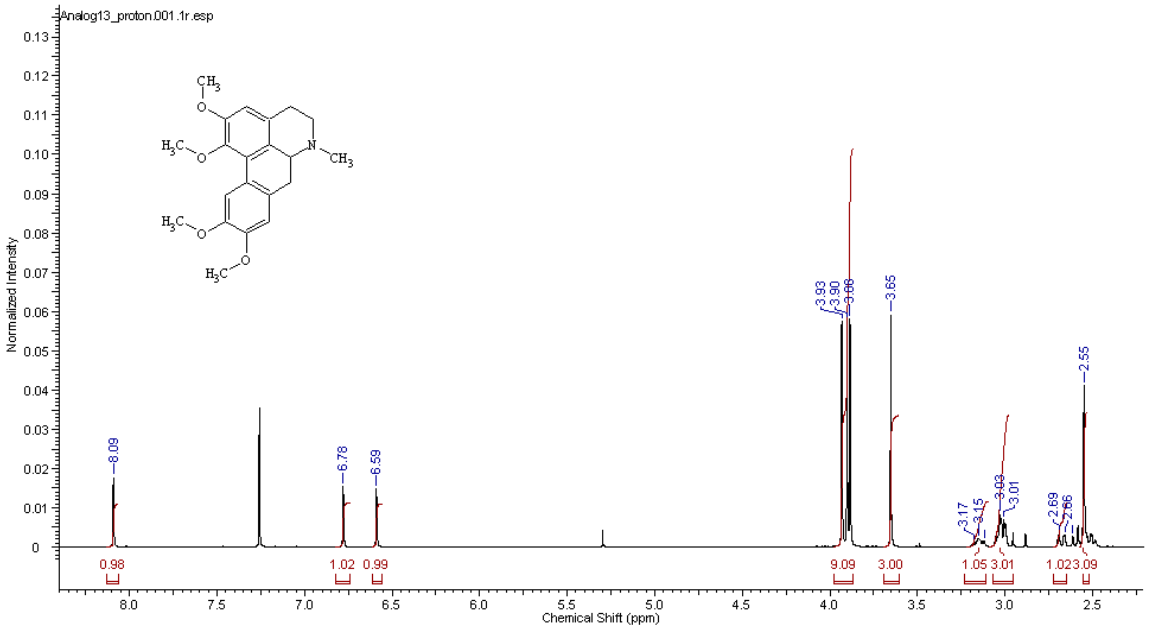

Figure 2.41 ^{1}H NMR (500 MHz, $CDCl_3$) of Glaucine (**13**).

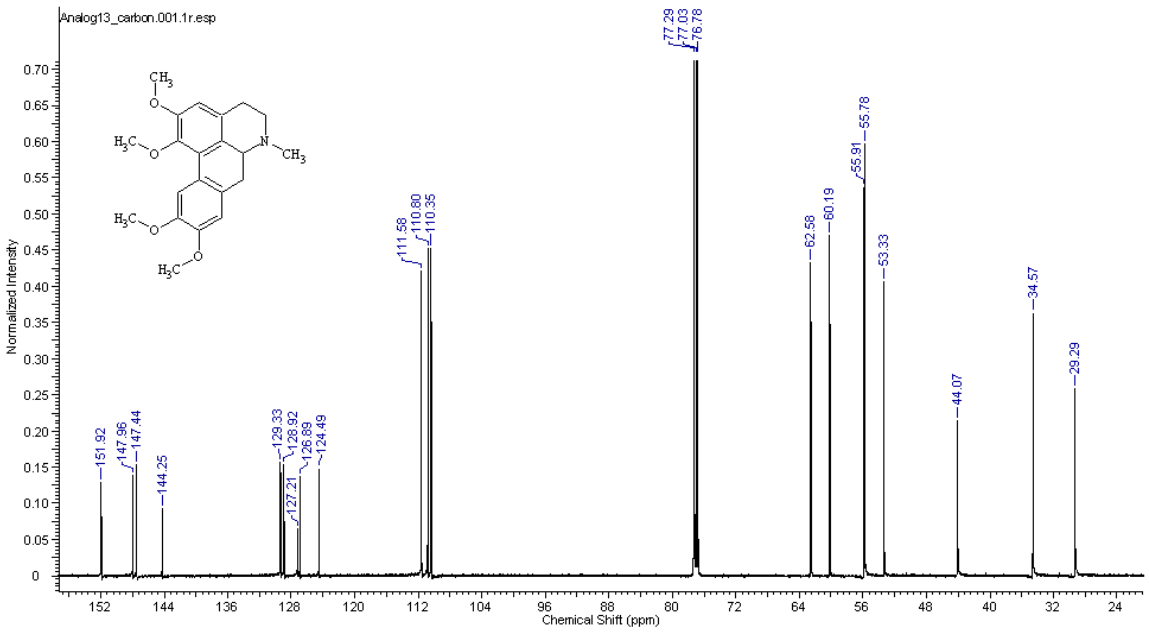

Figure 2.42 ^{13}C NMR (125 MHz, $CDCl_3$) of Glaucine (**13**).

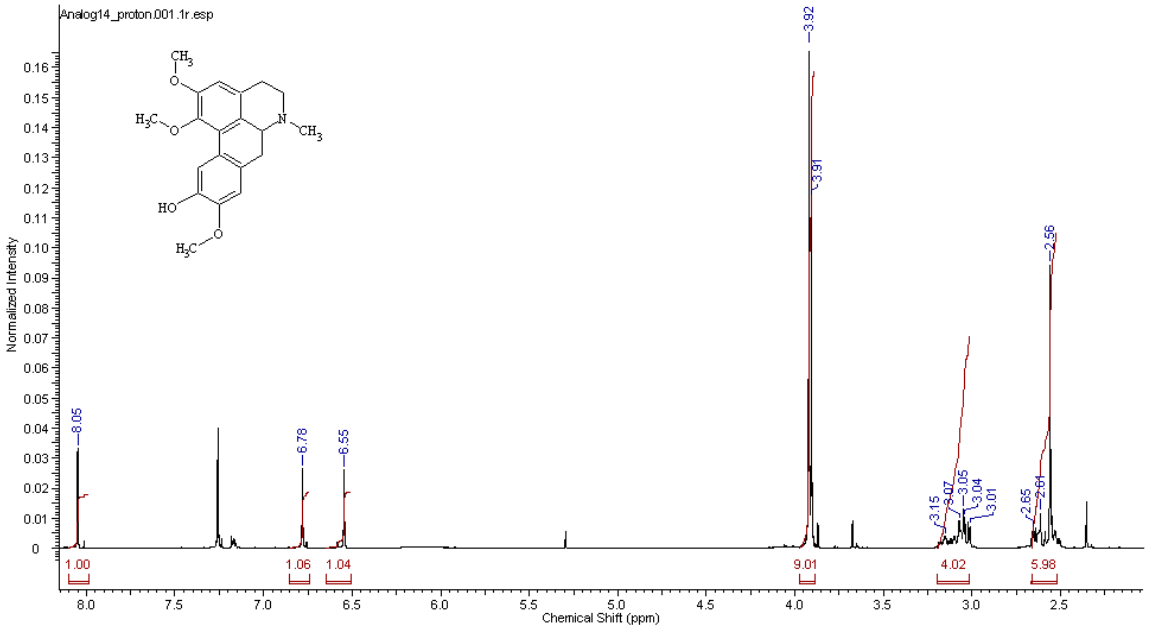

Figure 2.43 ^{1}H NMR (500 MHz, $CDCl_3$) of Lirioferine (**14**).

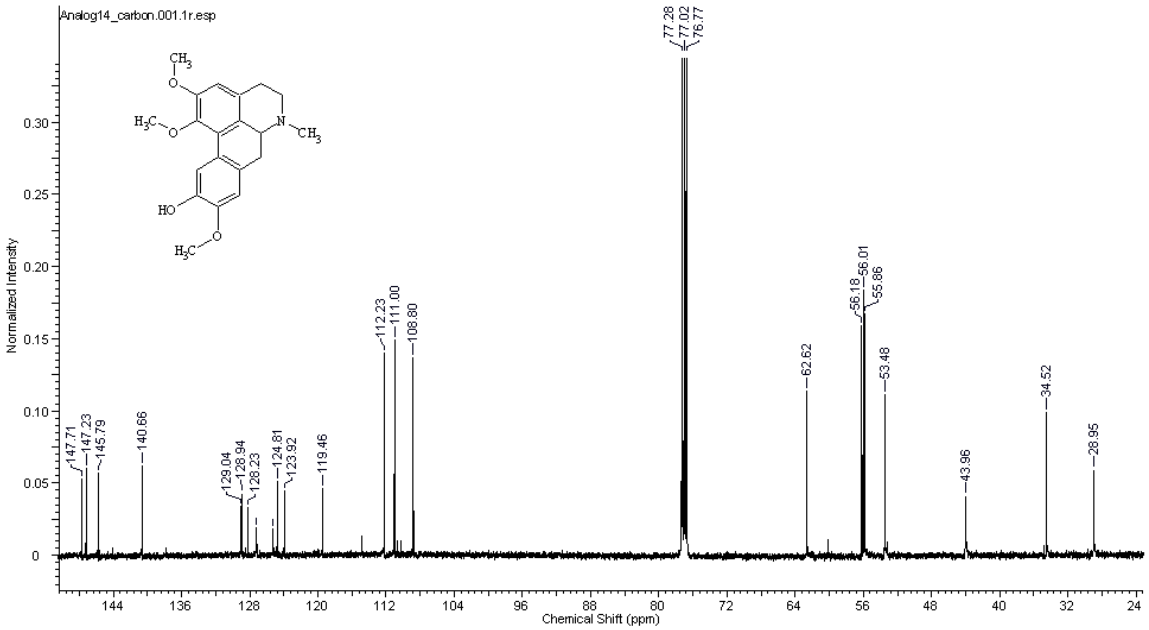

Figure 2.44 ^{13}C NMR (125 MHz, $CDCl_3$) of Lirioferine (**14**).

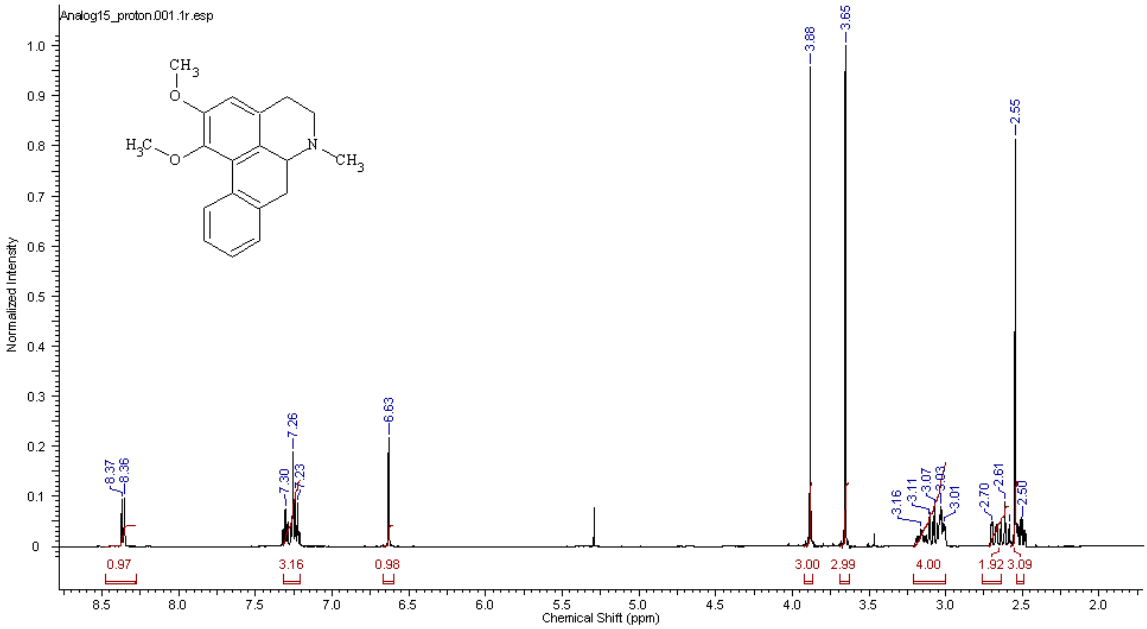

Figure 2.45 ^{1}H NMR (500 MHz, $CDCl_3$) of Nuciferine (**15**).

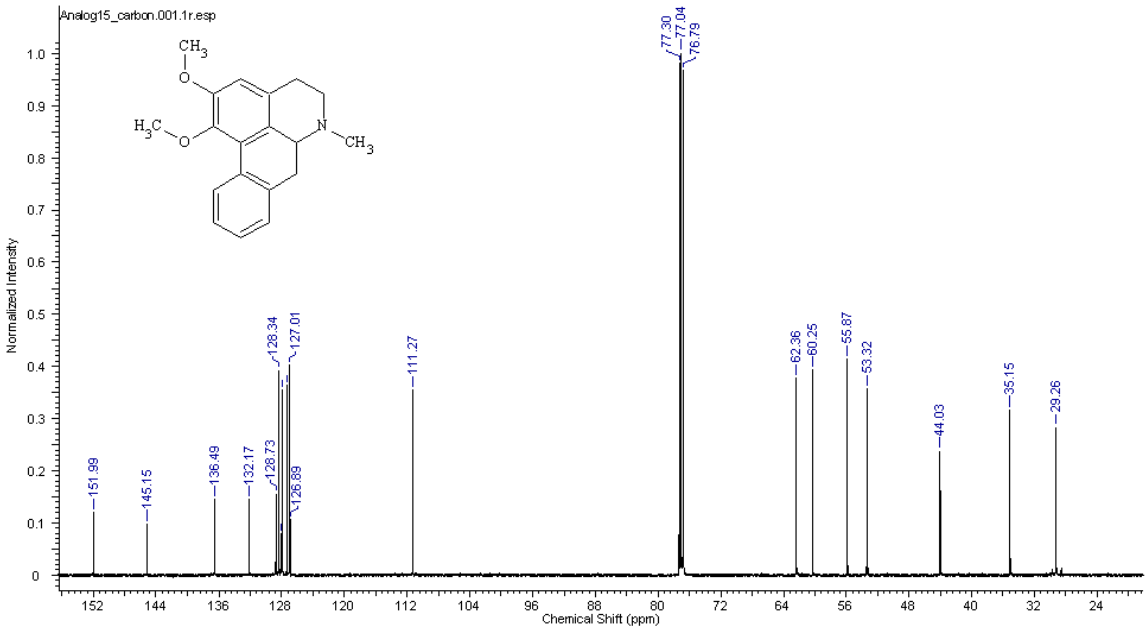

Figure 2.46 ^{13}C NMR (125 MHz, $CDCl_3$) of Nuciferine (**15**).

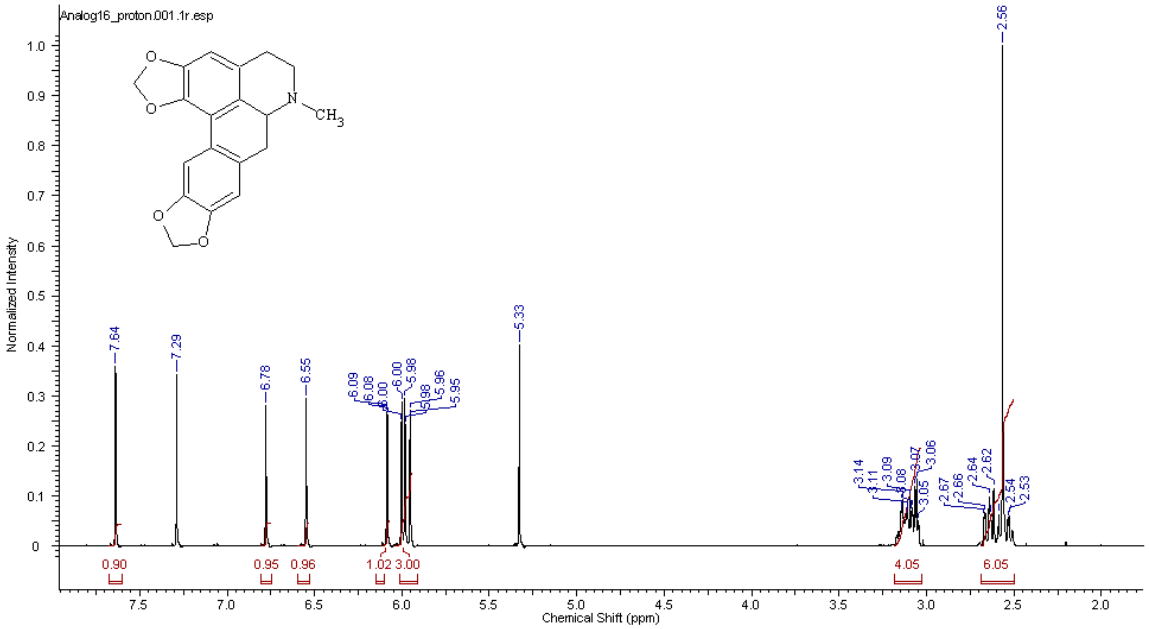

Figure 2.47 ^{1}H NMR (500 MHz, $CDCl_3$) of Neolitsine (**16**).

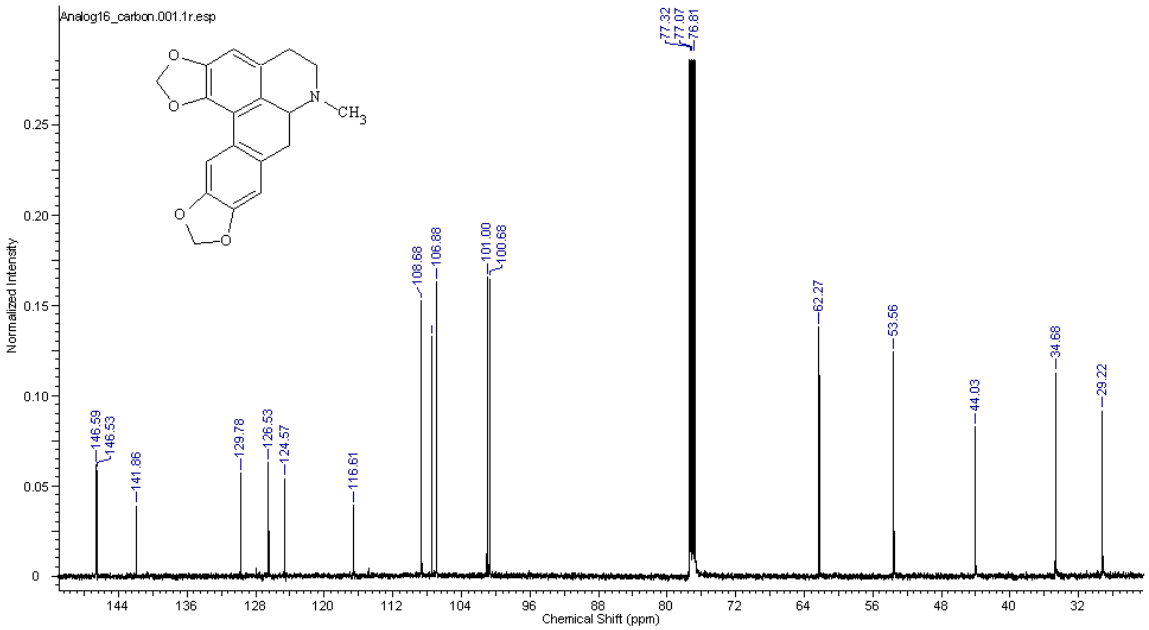

Figure 2.48 ^{13}C NMR (125 MHz, $CDCl_3$) of Neolitsine (**16**).

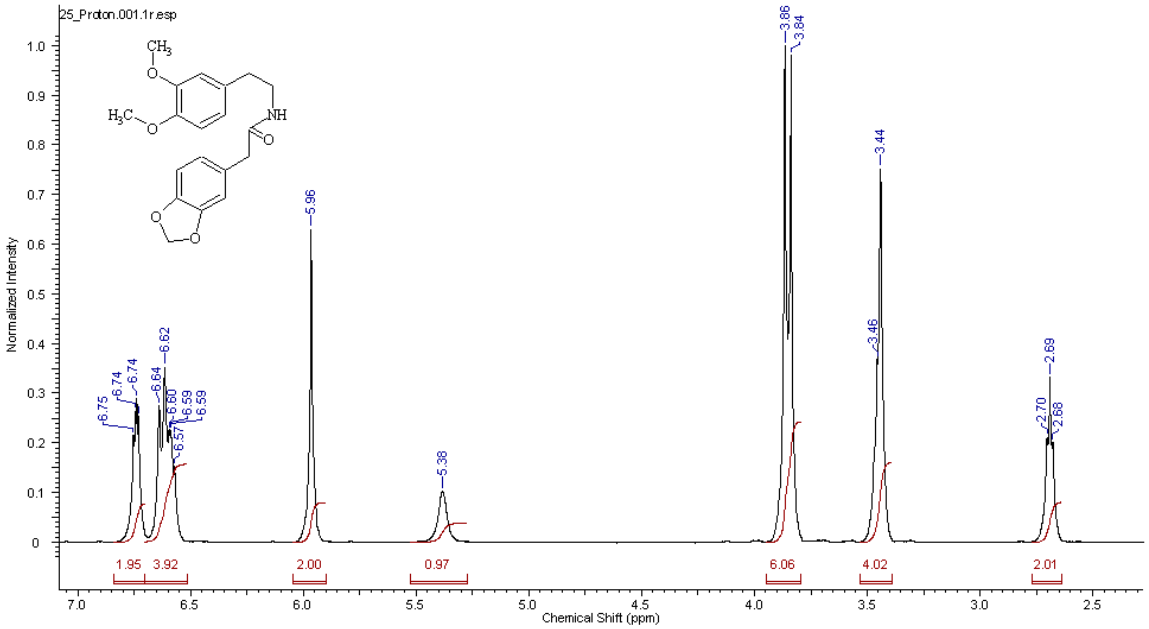

Figure 2.49 ^{1}H NMR (500 MHz, $CDCl_3$) of 2-(benzo[*d*][1,3]dioxol-5-yl)-*N*-(3,4-dimethoxyphenethyl)acetamide (**25)**.

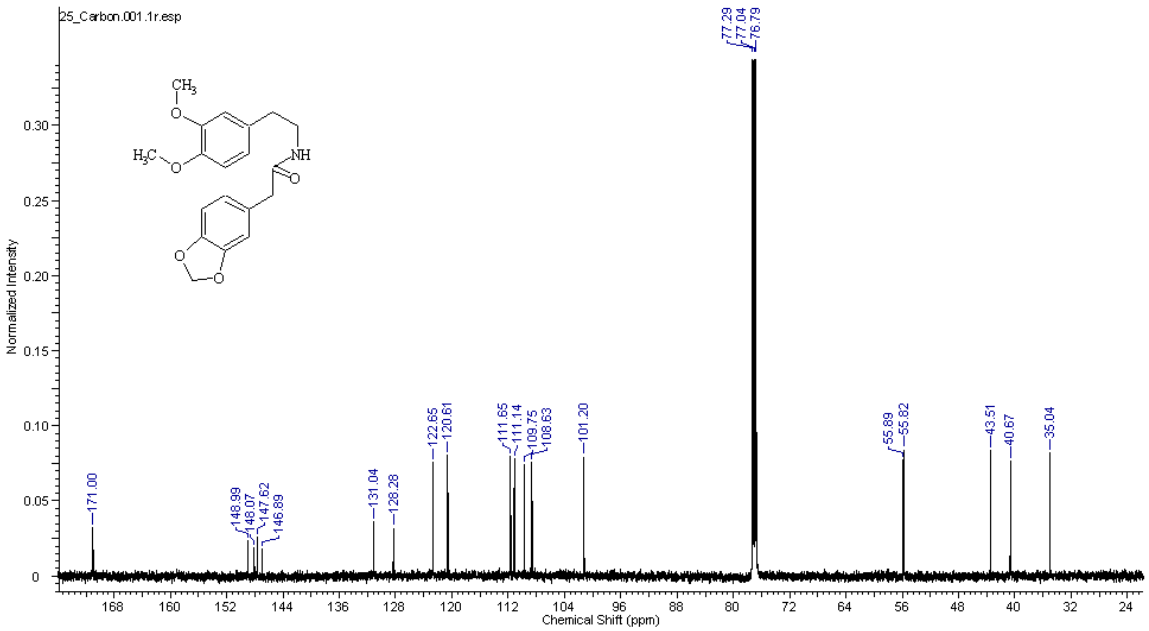

Figure 2.50 ^{13}C NMR (125 MHz, $CDCl_3$) of 2-(benzo[*d*][1,3]dioxol-5-yl)-*N*-(3,4-dimethoxyphenethyl)acetamide **(25)**.

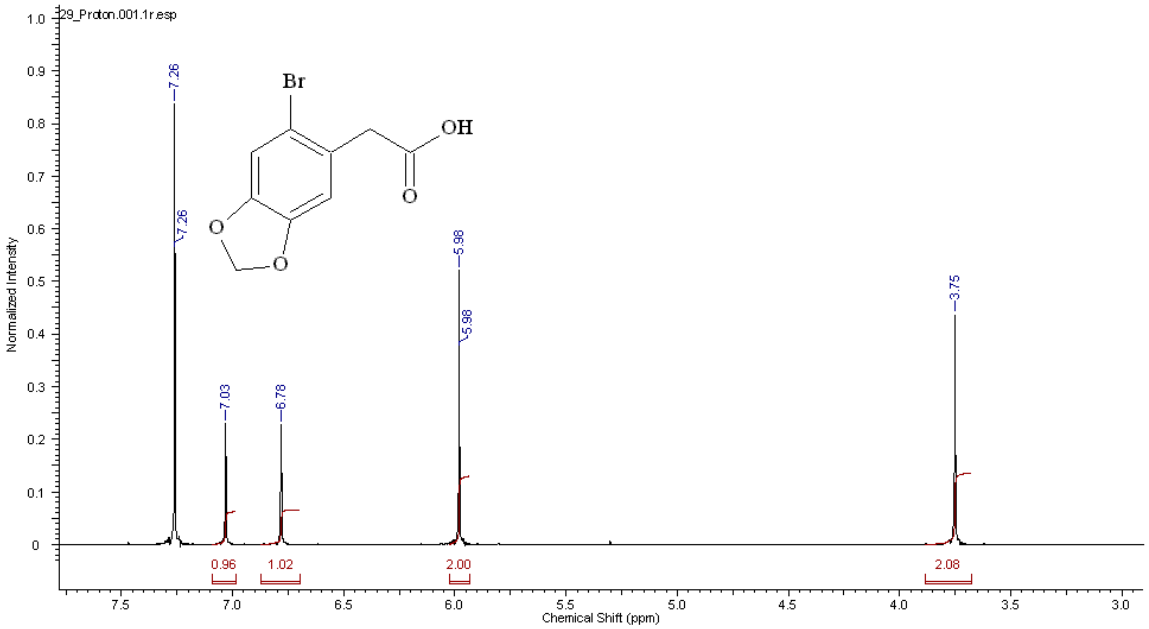

Figure 2.51 ^{1}H NMR (500 MHz, $CDCl_3$) of 2-(6-bromobenzo[*d*][1,3]dioxol-5-yl)acetic acid (**29**).

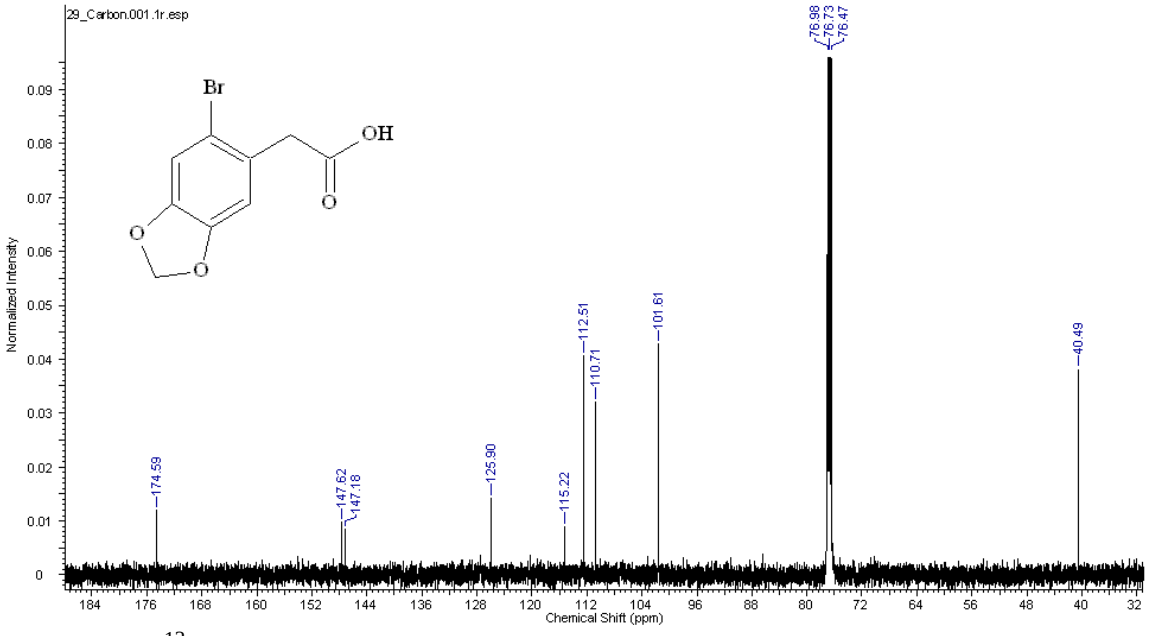

Figure 2.52 ^{13}C NMR (500 MHz, $CDCl_3$) of 2-(6-bromobenzo[*d*][1,3]dioxol-5-yl)acetic acid (**29**).

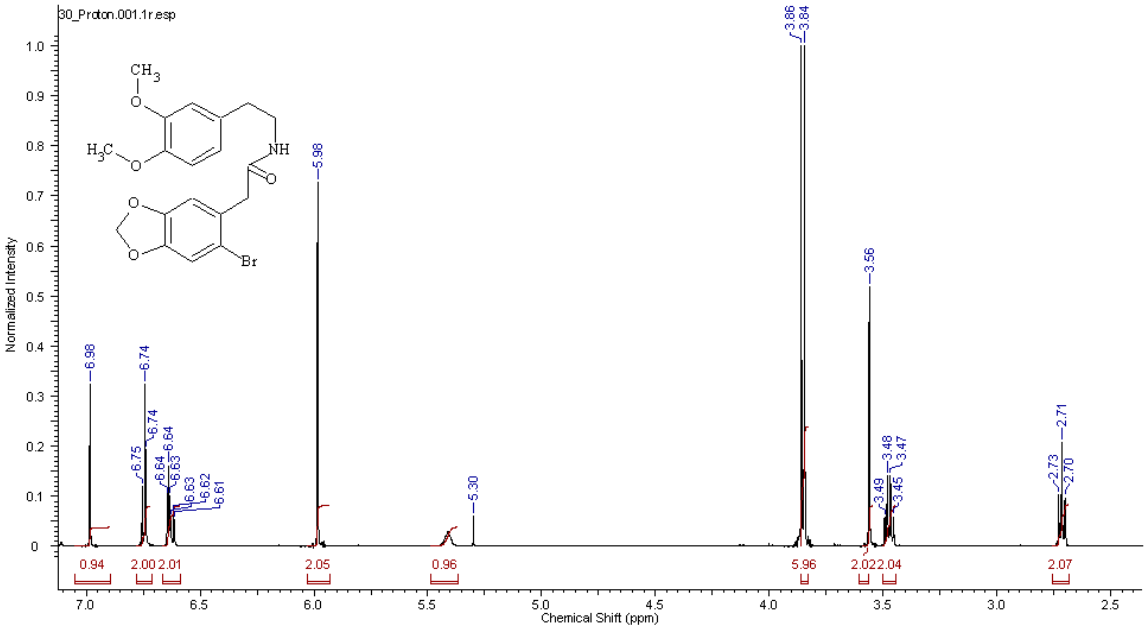

Figure 2.53 ^{1}H NMR (500 MHz, $CDCl_3$) of 2-(6-bromobenzo [*d*][1,3]dioxol-5-yl)-*N*-(3,4-dimethoxyphenethyl)acetamide (**30**).

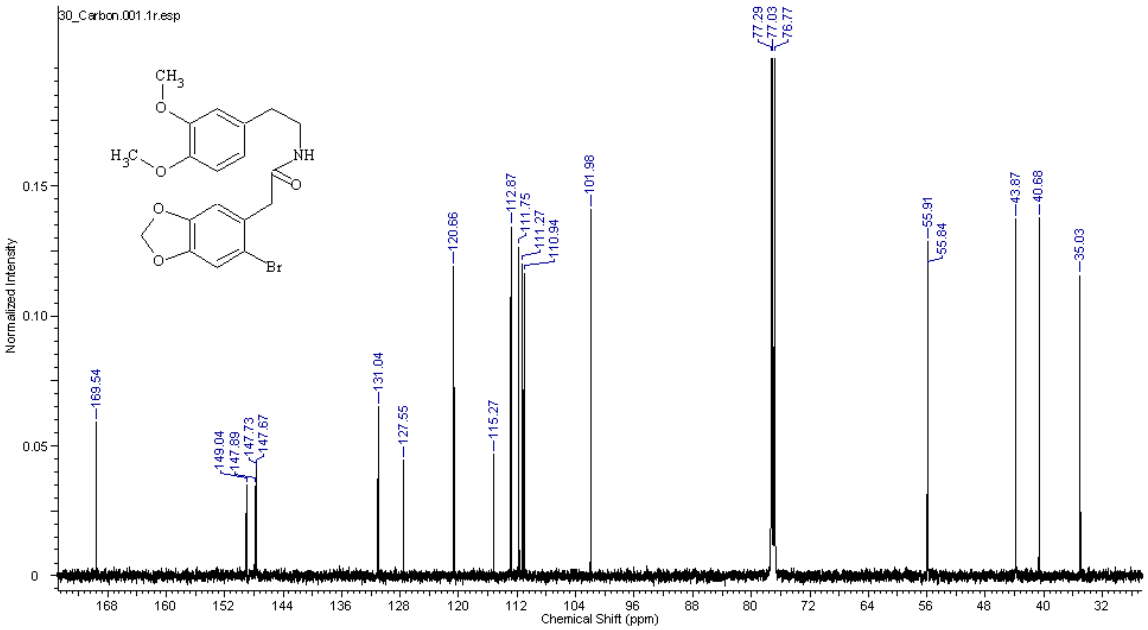

Figure 2.54 ^{13}C NMR (125 MHz, $CDCl_3$) of 2-(6-bromobenzo [*d*][1,3]dioxol-5-yl)-*N*-(3,4-dimethoxyphenethyl)acetamide (**30**).

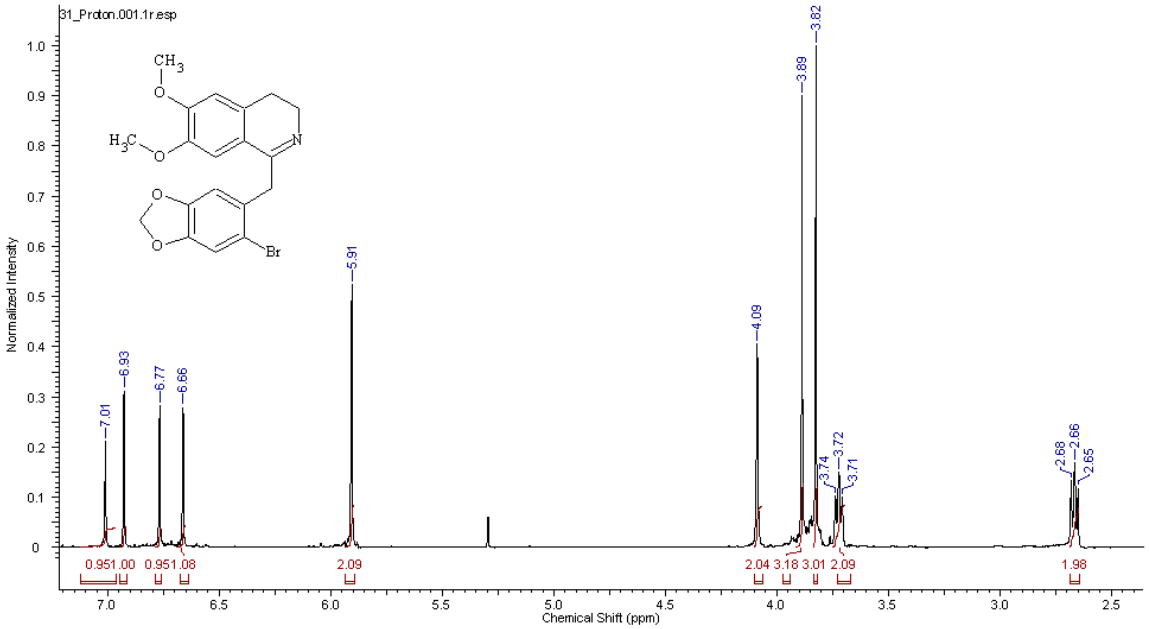

Figure 2.55 ^{1}H NMR (500 MHz, $CDCl_3$) of 1-((6-bromobenzo[*d*][1,3]dioxol-5-yl)methyl)-6,7-dimethoxy-3,4-dihydroisoquinoline (**31)**.

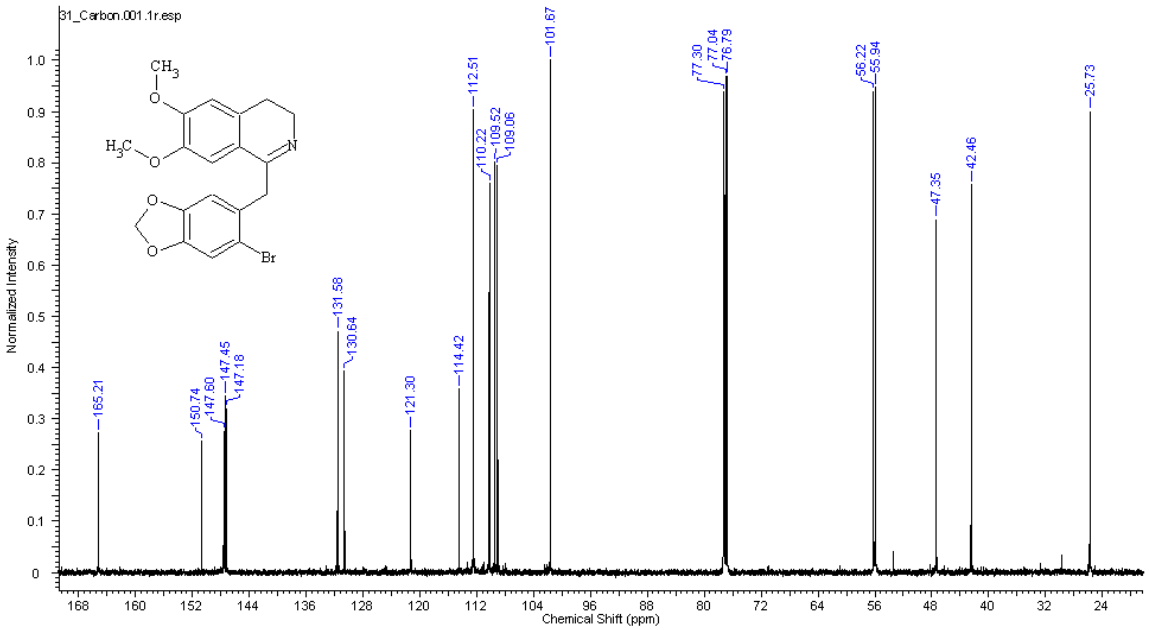

Figure 2.56 ^{13}C NMR (125 MHz, $CDCl_3$) of 1-((6-bromobenzo[*d*][1,3]dioxol-5-yl)methyl)-6,7-dimethoxy-3,4-dihydroisoquinoline (**31)**.

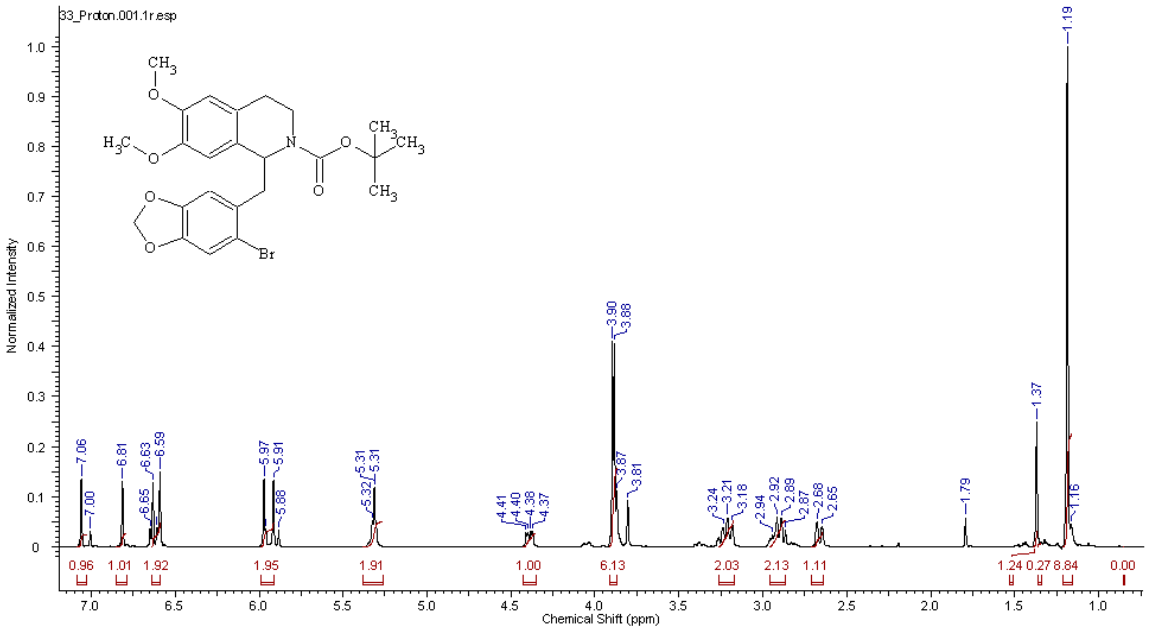

Figure 2.57 ^{1}H NMR (500 MHz, $CDCl_3$) of *tert*-butyl1-((6-bromobenzo[*d*][1,3]dioxol-5-yl)methyl)-6,7-dimethoxy-3,4-dihydro-isoquinoline-2(1*H*)-carboxylate **(33)**.

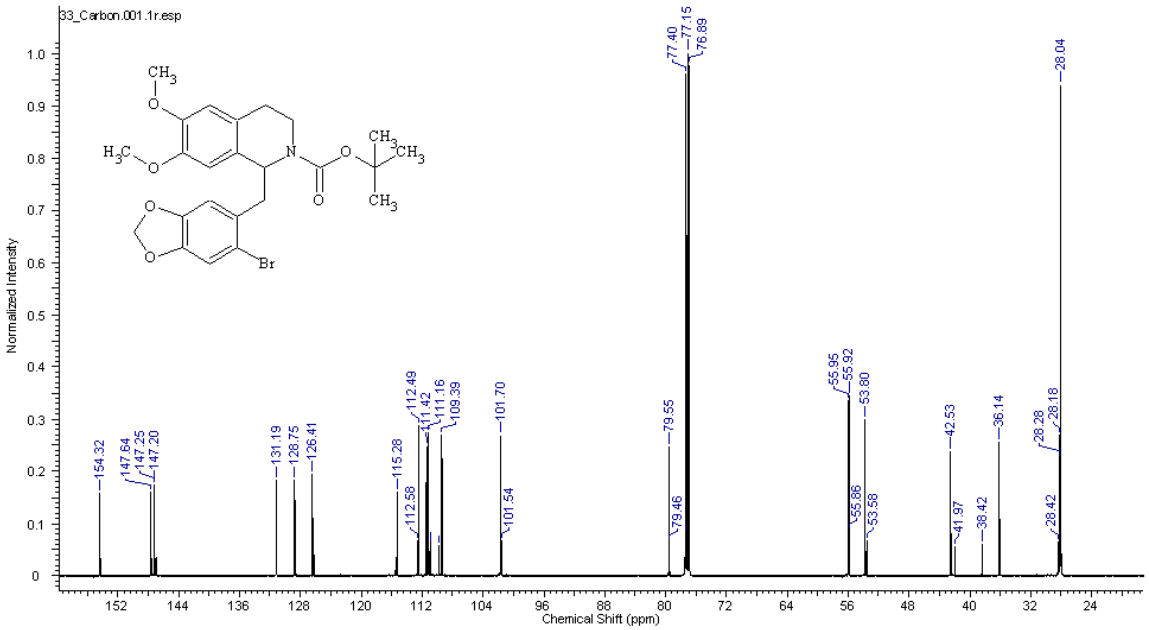

Figure 2.58 ^{13}C NMR (125 MHz, $CDCl_3$) of *tert*-butyl1-((6-bromobenzo[*d*][1,3]dioxol-5-yl)methyl)-6,7-dimethoxy-3,4-dihydro-isoquinoline-2(1*H*)-carboxylate **(33)**.

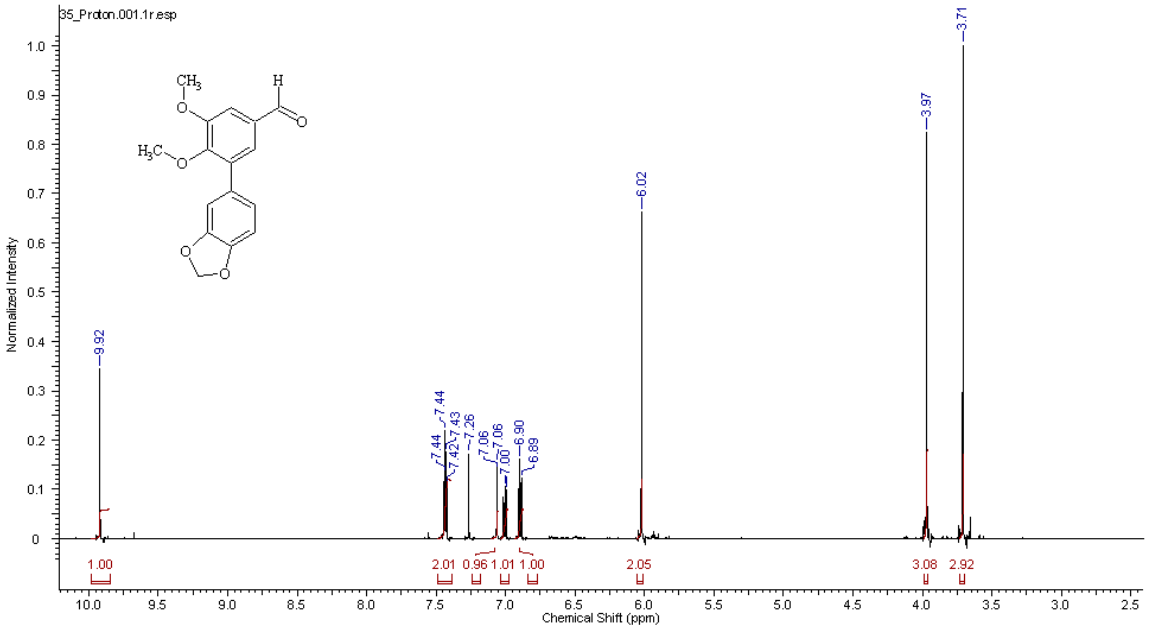

Figure 2.59 ^{1}H NMR (500 MHz, $CDCl_3$) of 3-(benzo[*d*][1,3]dioxol-5-yl)-4,5-dimethoxybenzaldehyde **(35)**.

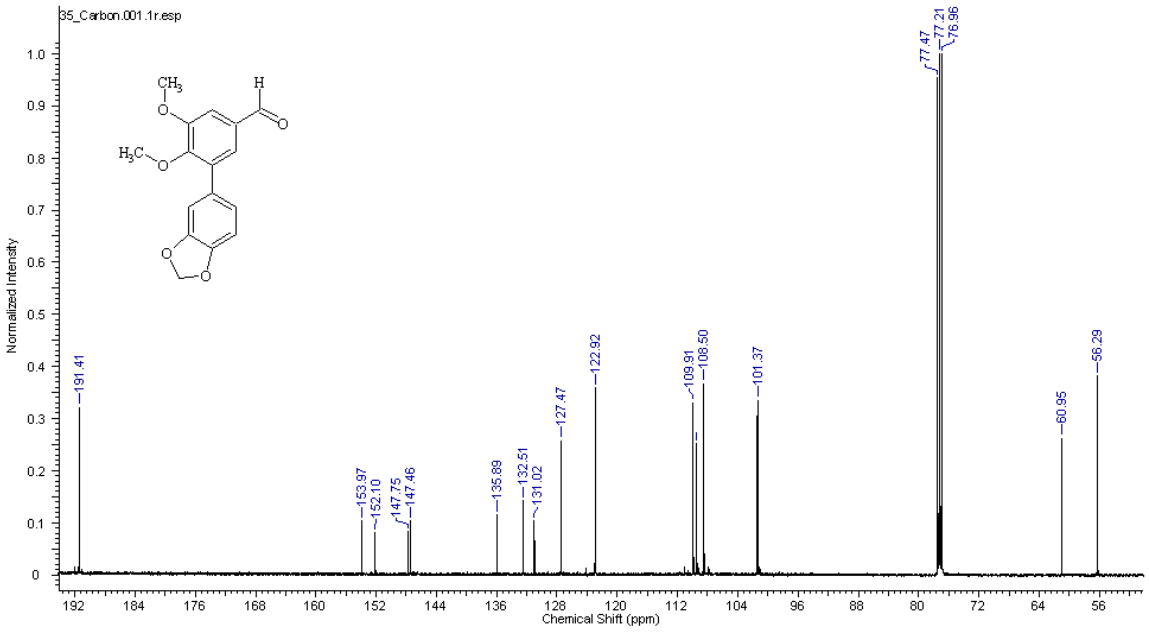

Figure 2.60 ^{13}C NMR (125 MHz, $CDCl_3$) of 3-(benzo[*d*][1,3]dioxol-5-yl)-4,5-dimethoxybenzaldehyde **(35)**.

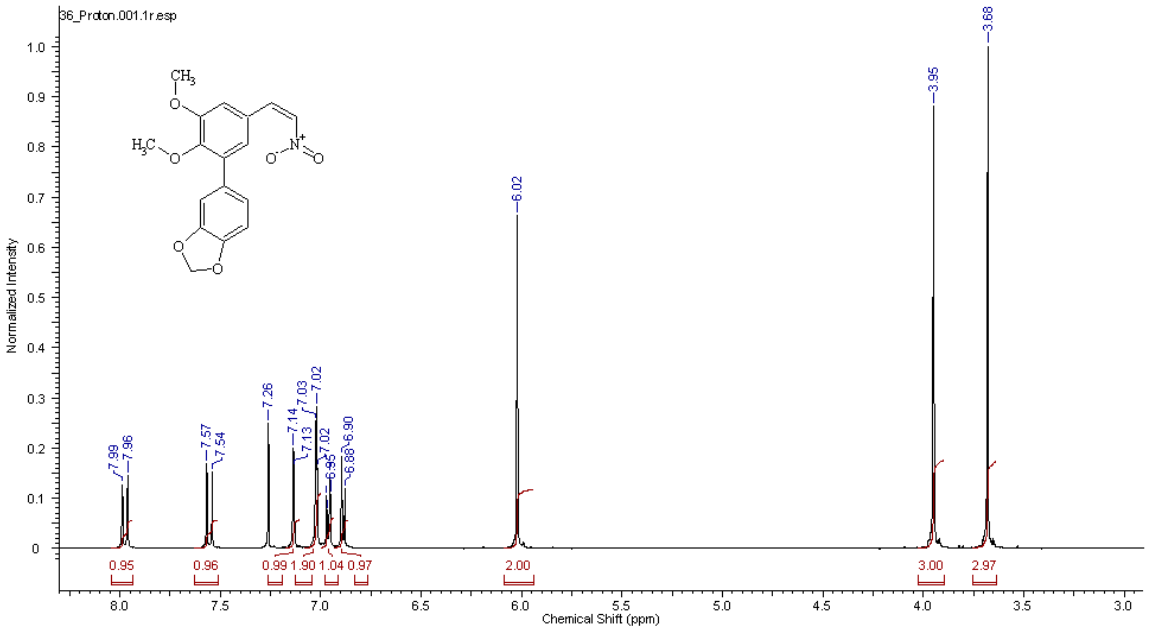

Figure 2.61 ^{1}H NMR (500 MHz, $CDCl_3$) of (E)-5-(2,3-dimethoxy-5-(2-nitrovinyl) phenyl)benzo[*d*][1,3]dioxole **(36)**.

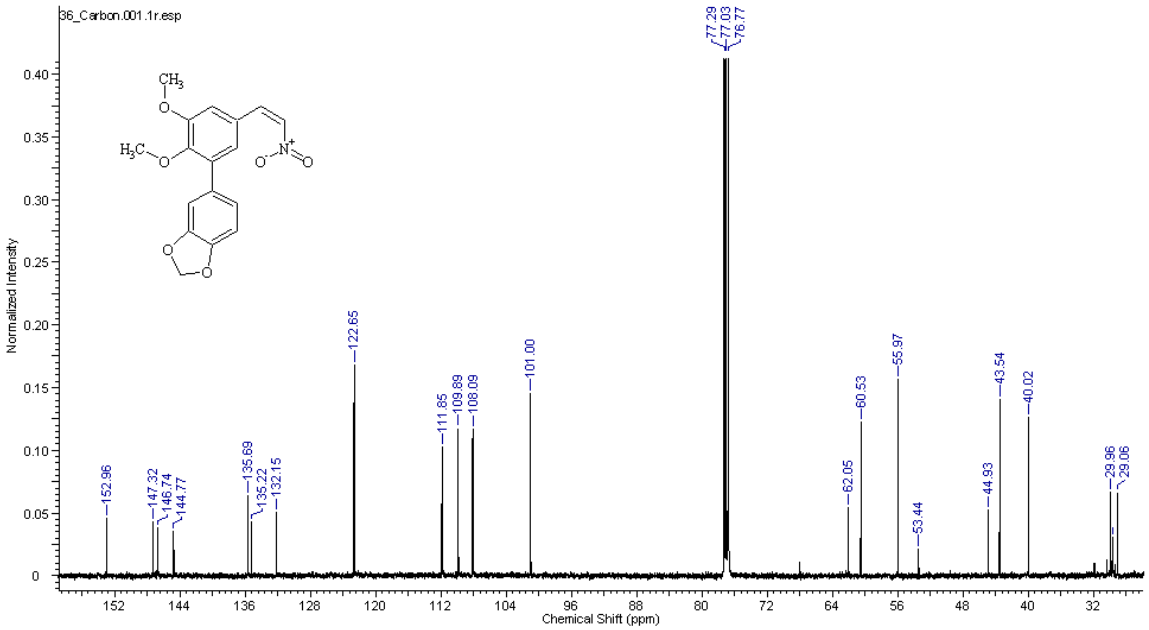

Figure 2.62 ^{13}C NMR (125 MHz, $CDCl_3$) of (E)-5-(2,3-dimethoxy-5-(2-nitrovinyl) phenyl)benzo[*d*][1,3] **(36)**.

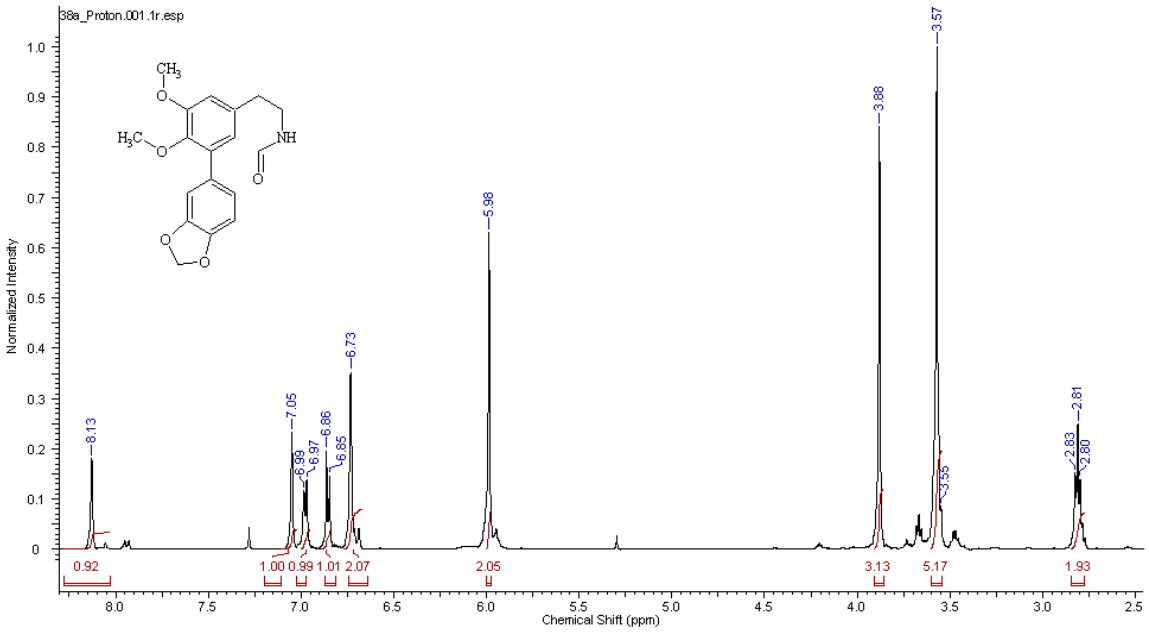

Figure 2.63 ^{1}H NMR (500 MHz, DMSO-D$_6$) of *N*-(3-(benzo[*d*][1,3]dioxol-5-yl)-4,5-dimethoxyphenethyl)formamide **(38a)**.

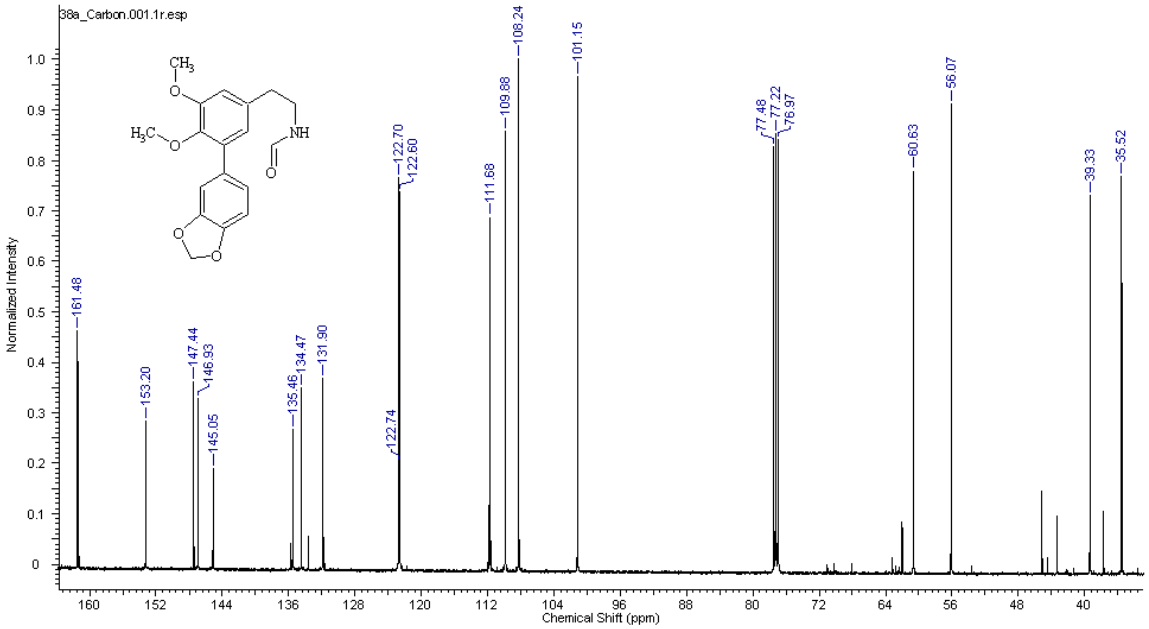

Figure 2.64 ^{13}C NMR (125 MHz, DMSO-D$_6$) of *N*-(3-(benzo[*d*][1,3]dioxol-5-yl)-4,5-dimethoxyphenethyl)formamide **(38a)**.

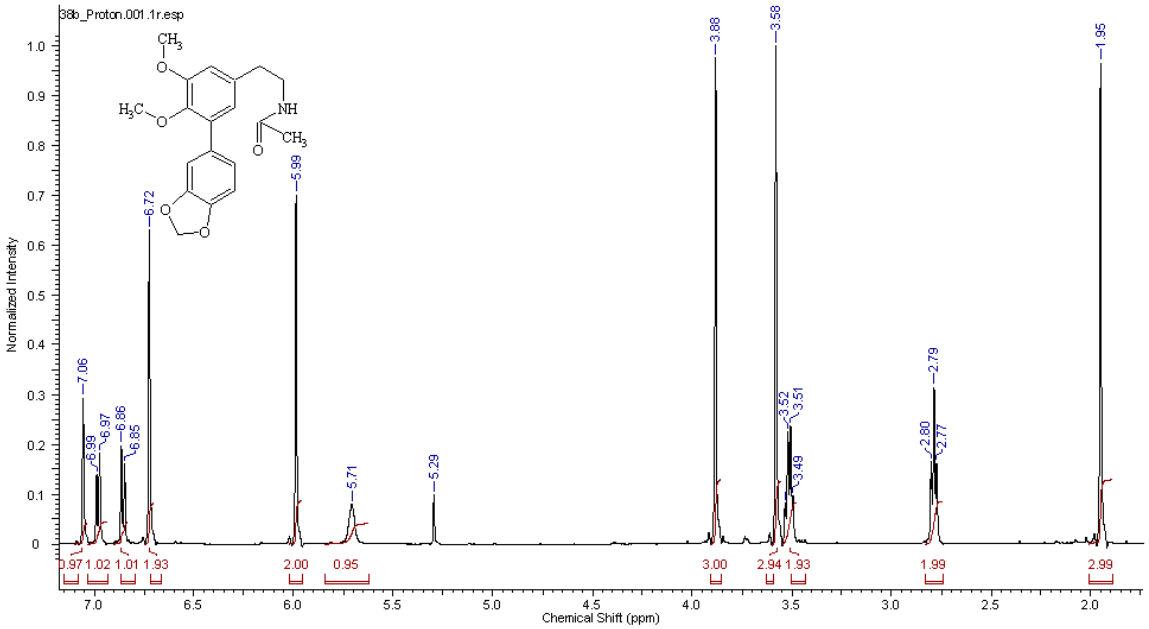

Figure 2.65 ^{1}H NMR (500 MHz, $CDCl_3$) of *N*-(3-(benzo[*d*][1,3]dioxol-5-yl)-4,5-dimethoxyphenethyl)acetamide **(38b)**.

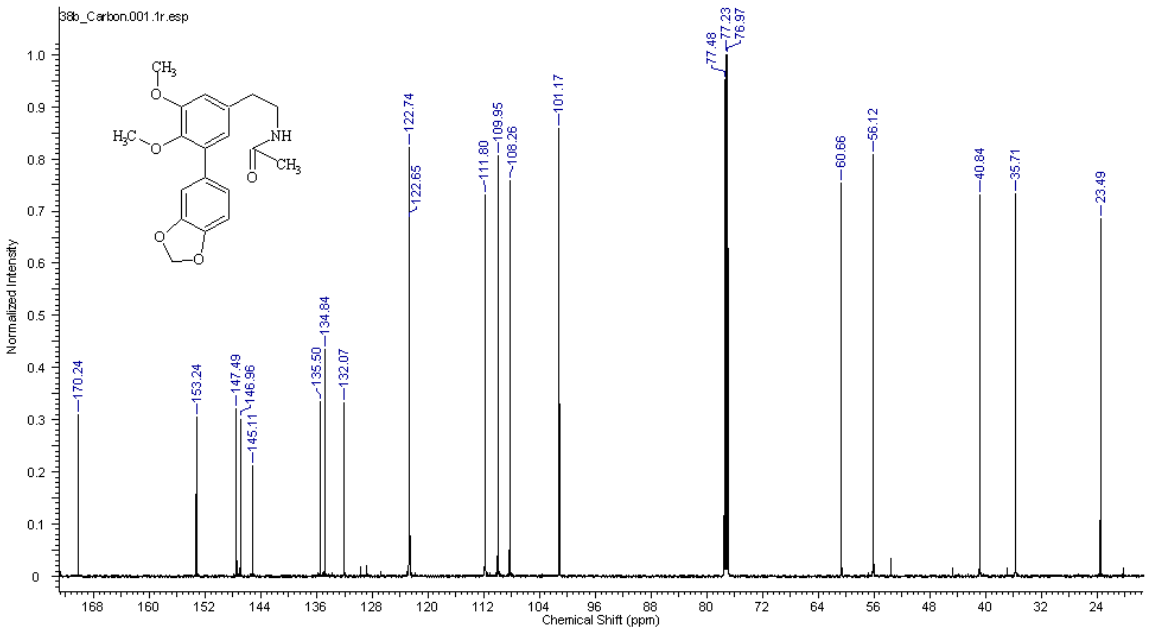

Figure 2.66 ^{13}C NMR (125 MHz, $CDCl_3$) of *N*-(3-(benzo[*d*][1,3]dioxol-5-yl)-4,5-dimethoxyphenethyl)acetamide **(38b)**.

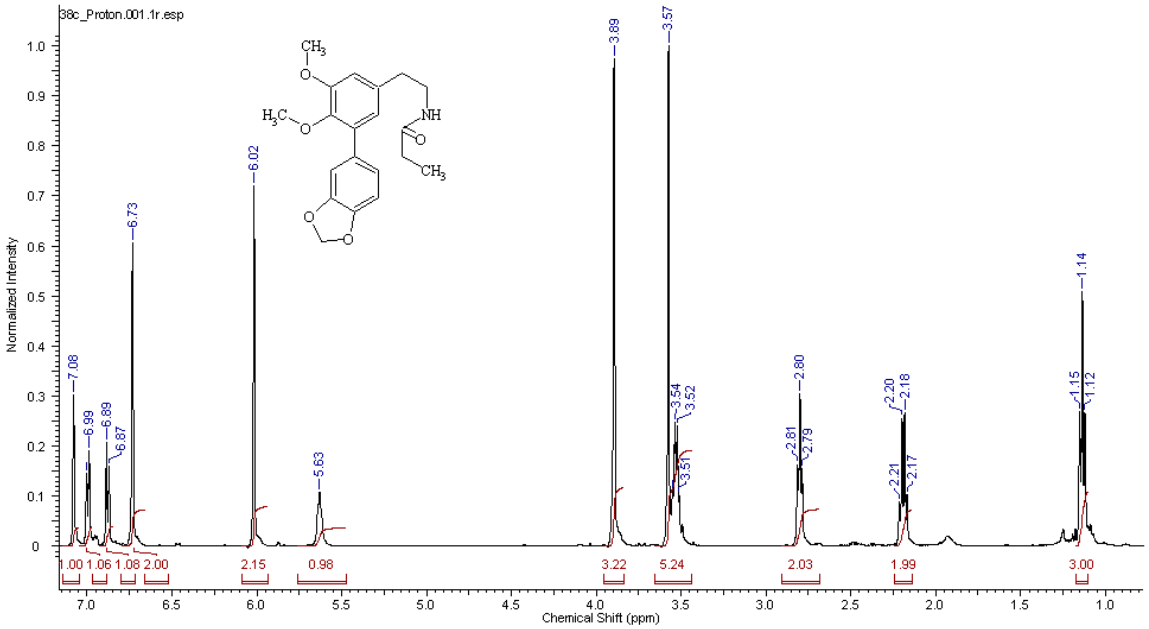

Figure 2.67 ^{1}H NMR (500 MHz, $CDCl_3$) of *N*-(3-(benzo[*d*] [1,3]dioxol-5-yl)-4, 5-dimethoxyphenethyl) propionamide **(38c).**

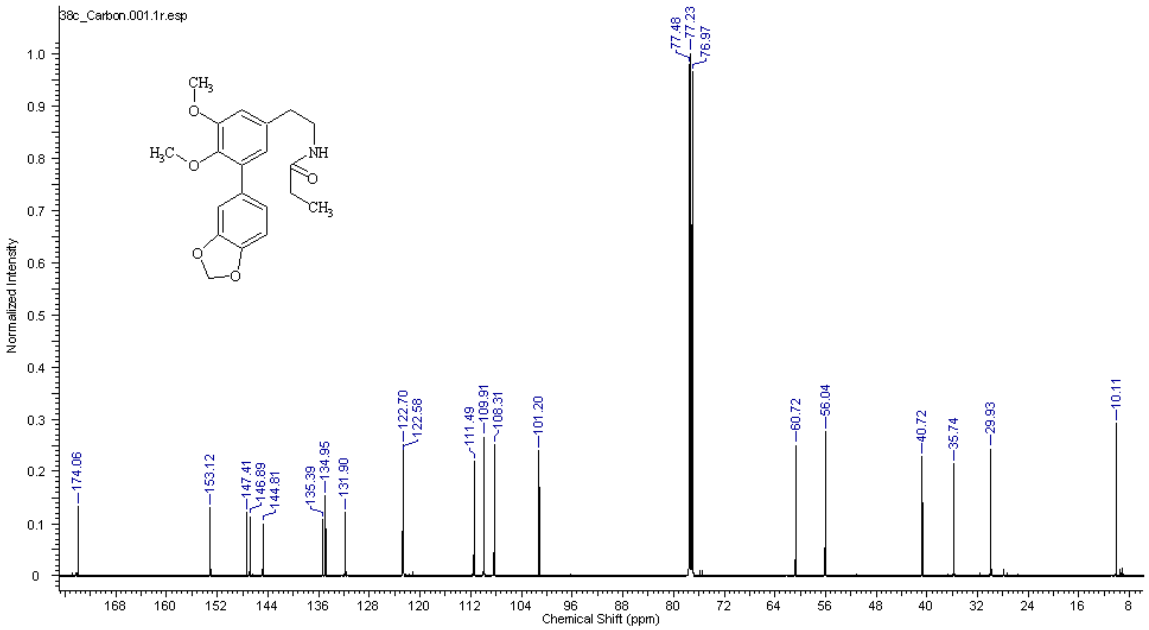

Figure 2.68 ^{13}C NMR (125 MHz, $CDCl_3$) of *N*-(3-(benzo[*d*] [1,3]dioxol-5-yl)-4, 5-dimethoxyphenethyl) propionamide **(38c).**

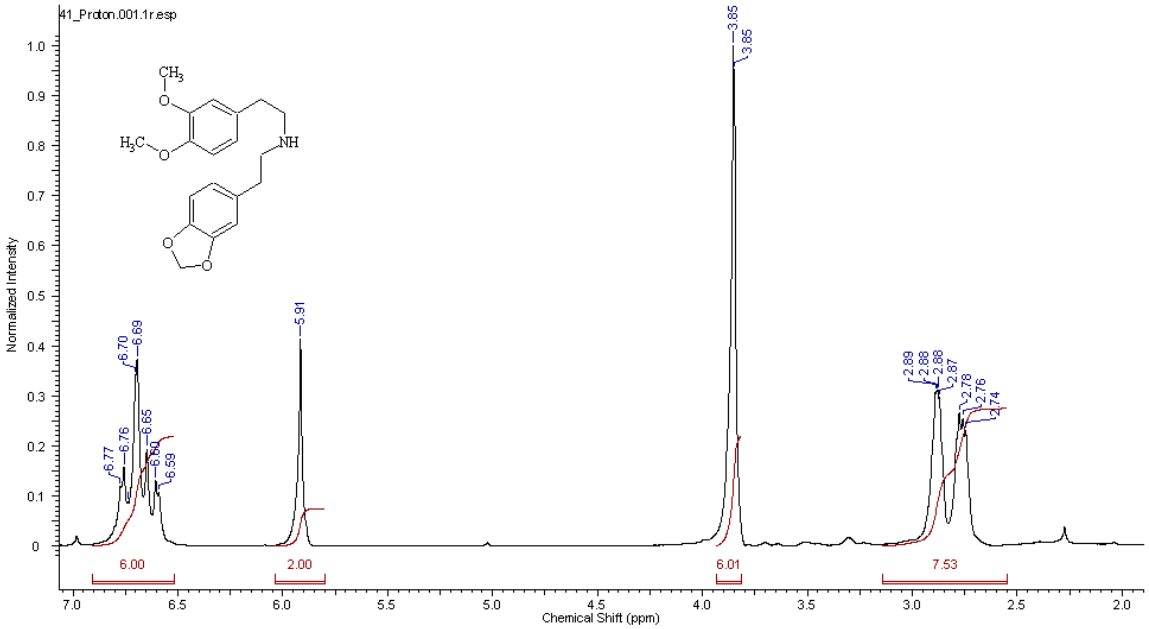

Figure 2.69 ^{1}H NMR (500 MHz, $CDCl_3$) of 2-(benzo[*d*][1,3]dioxol-5-yl)-*N*-(3,4-dimethoxyphenethyl)ethanamine **(41).**

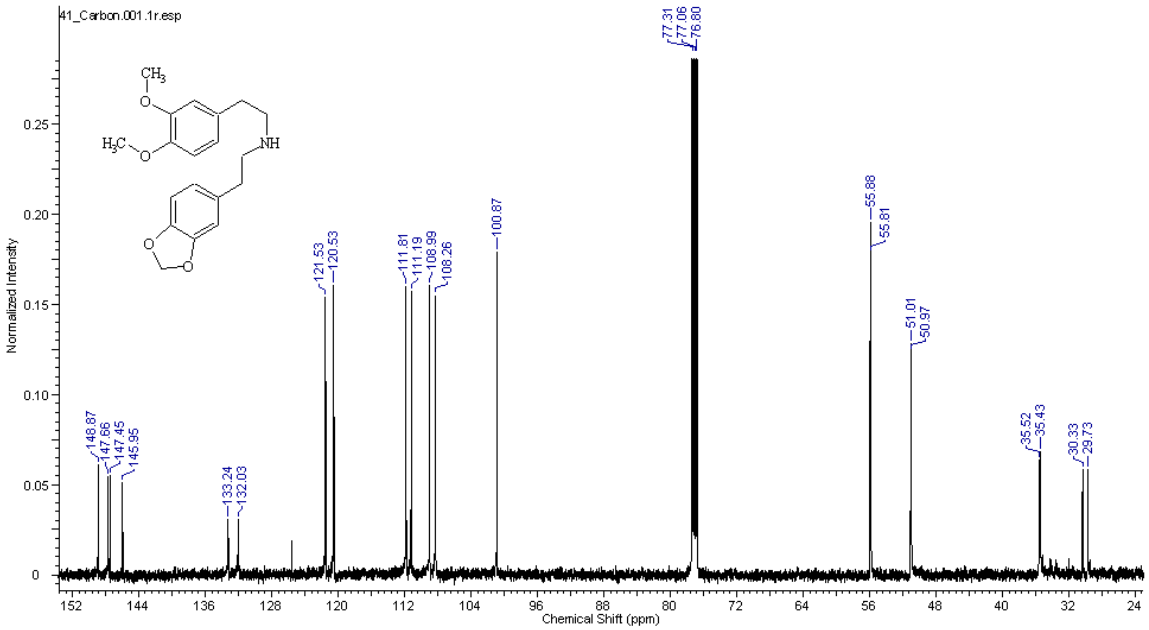

Figure 2.70 ^{13}C NMR (125 MHz, $CDCl_3$) of 2-(benzo[*d*][1,3]dioxol-5-yl)-*N*-(3,4-dimethoxyphenethyl)ethanamine **(41).**

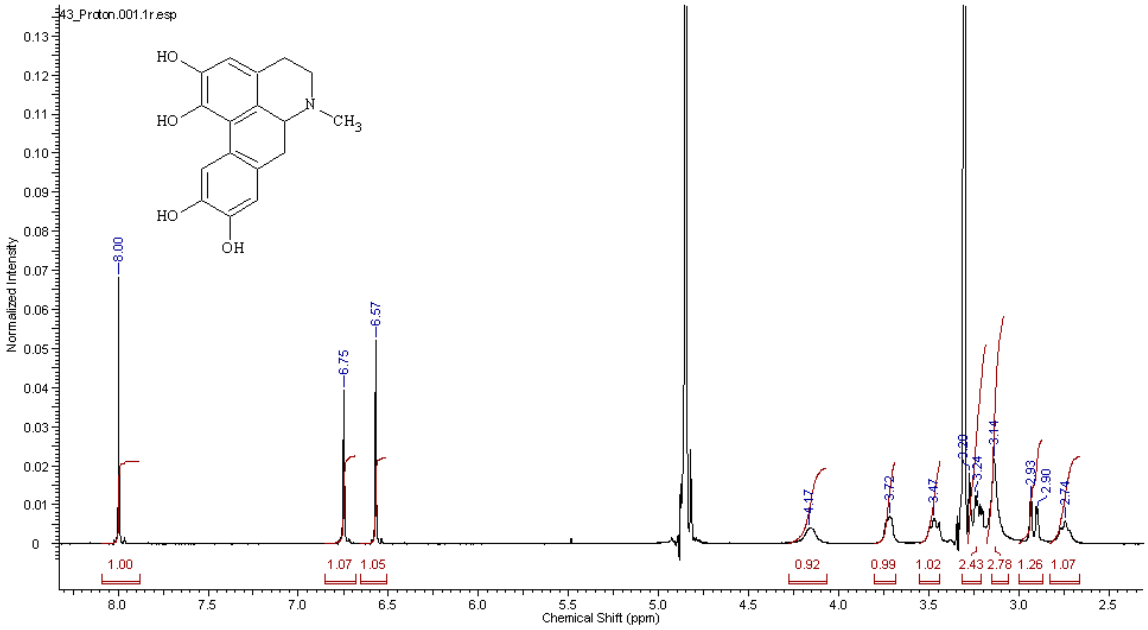

Figure 2.71 ^{1}H NMR (500 MHz, MeOD) of 1,2,9,10-tetrahydroxyaporphine **(43).**

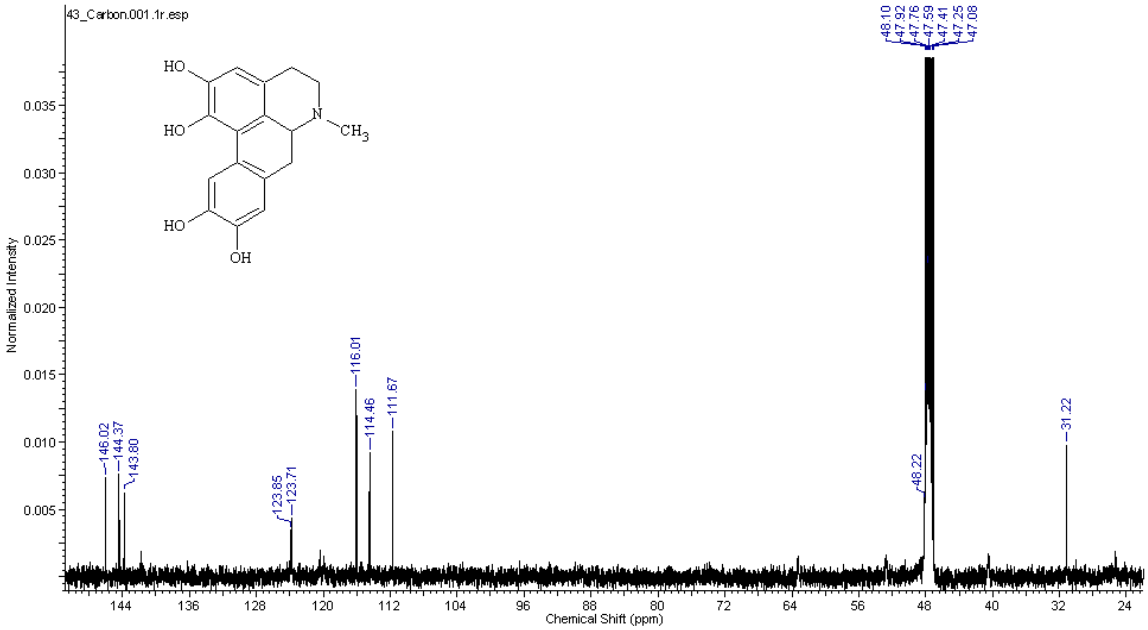

Figure 2.72 ^{13}C NMR (125 MHz, MeOD) of 1,2,9,10-tetrahydroxyaporphine **(43)**.

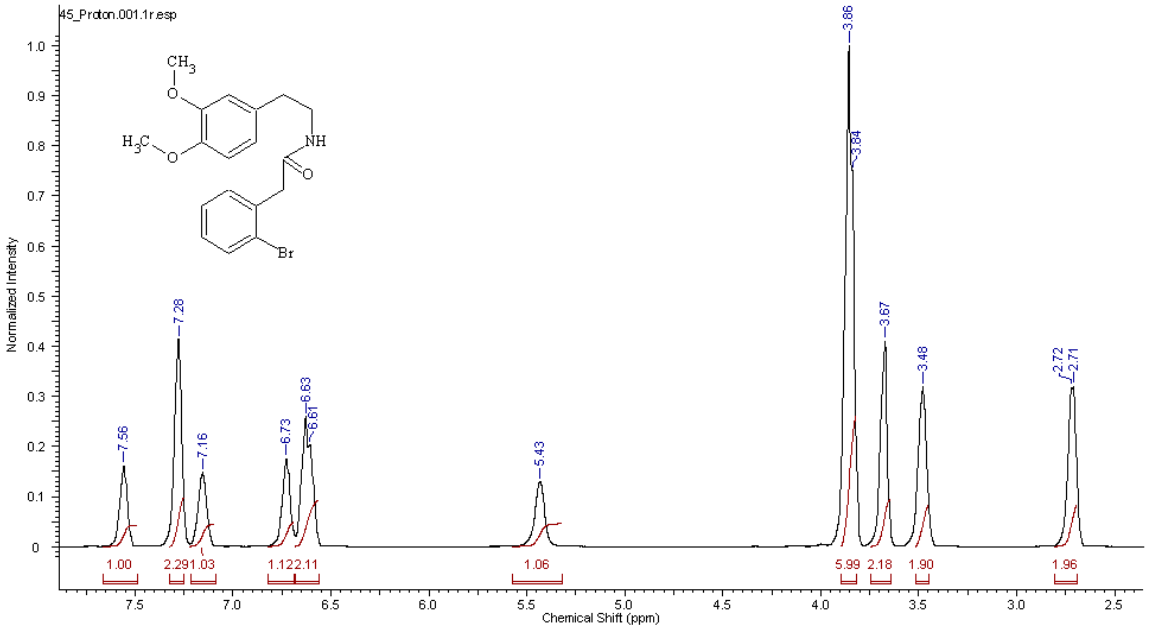

Figure 2.73 ^{1}H NMR (500 MHz, $CDCl_3$) of 2-(2-bromophenyl)-*N*-(3,4-dimethoxy phenethyl)acetamide **(45)**.

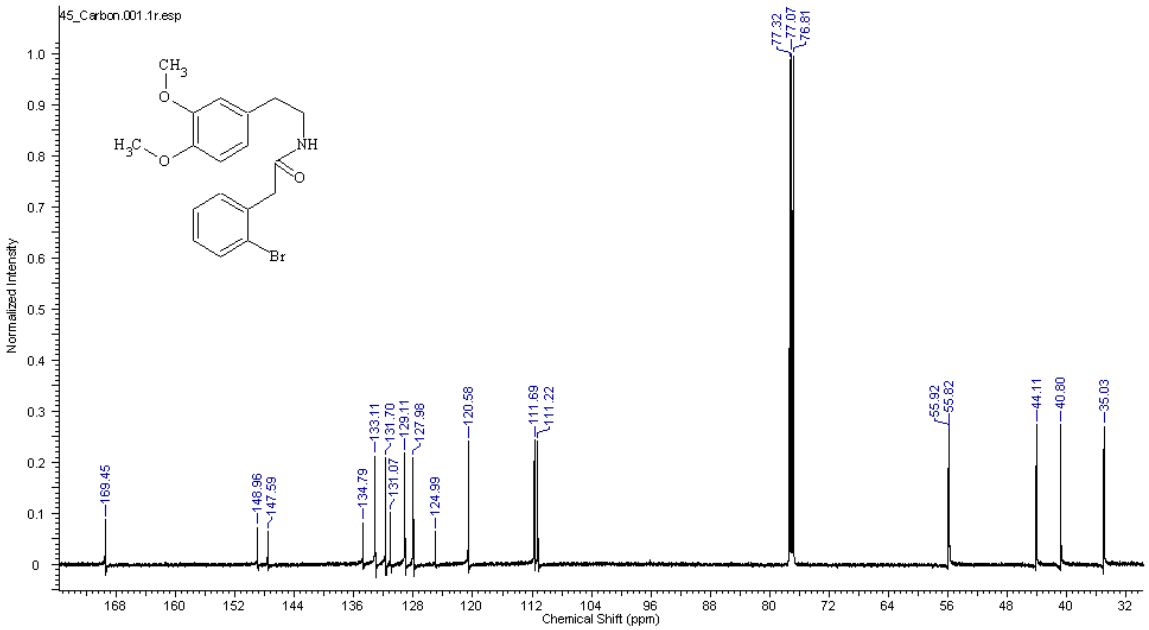

Figure 2.74 ^{13}C NMR (125 MHz, $CDCl_3$) of 2-(2-bromophenyl)-*N*-(3,4-dimethoxy phenethyl)acetamide **(45)**.

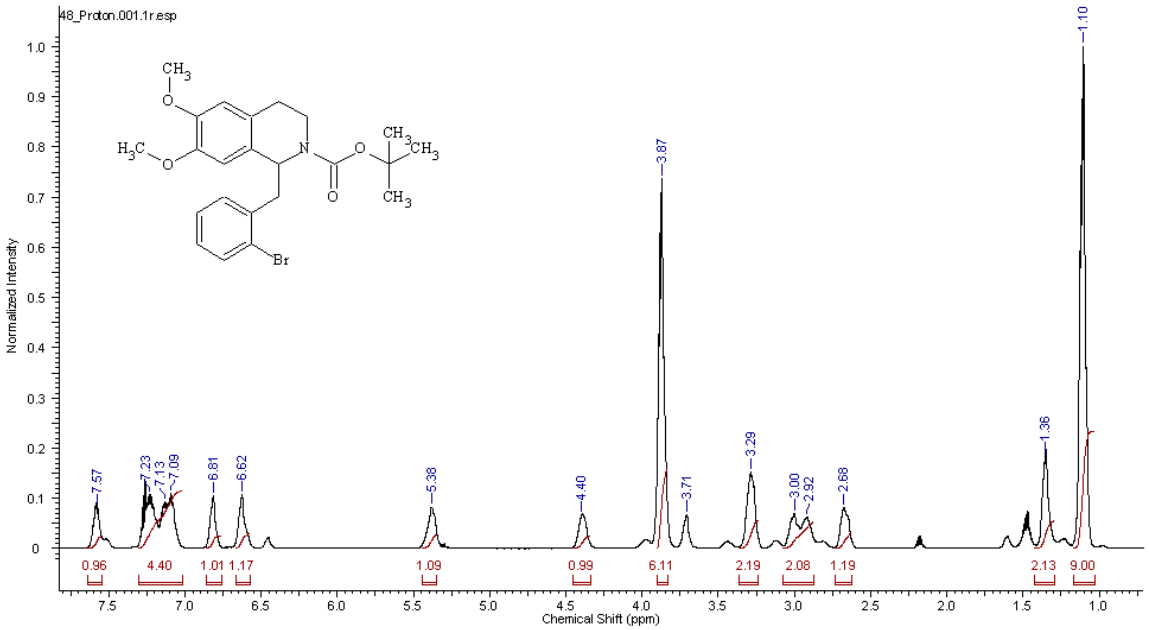

Figure 2.75 ^{1}H NMR (500 MHz, $CDCl_3$) of *tert*-butyl 1-(2-bromobenzyl)-6, 7-dimethoxy-3, 4-dihydroisoquinoline-2 (1*H*)-carbo-xylate **(48)**.

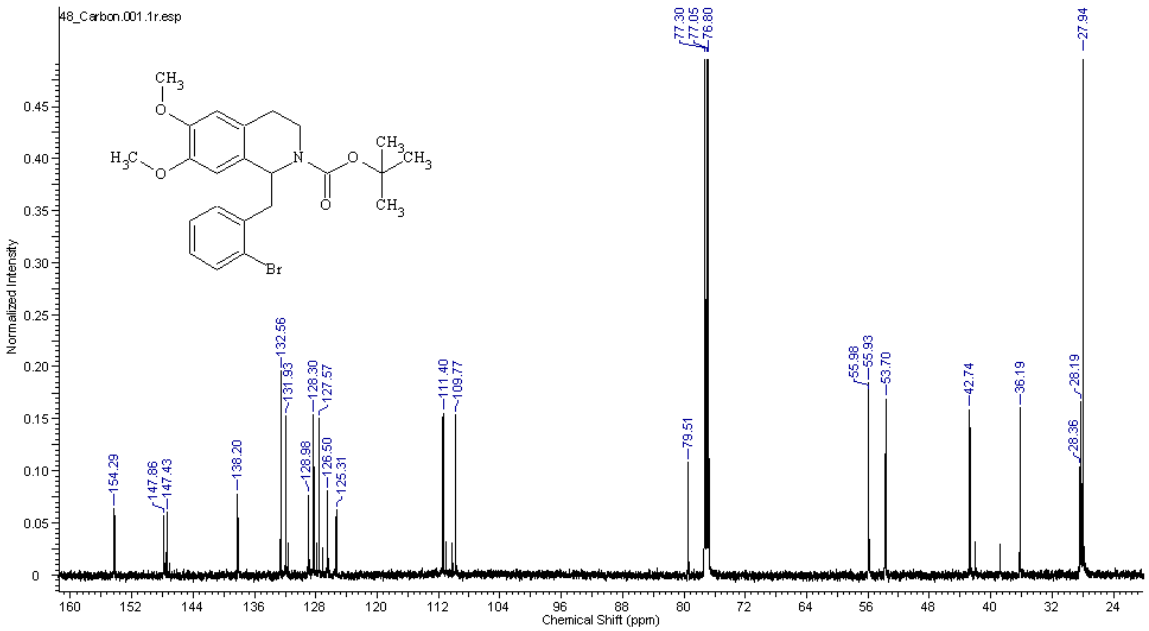

Figure 2.76 ^{13}C NMR (125 MHz, $CDCl_3$) of *tert*-butyl 1-(2-bromobenzyl)-6, 7-dimethoxy-3, 4-dihydroisoquinoline-2 (1*H*)-carbo-xylate **(48)**.

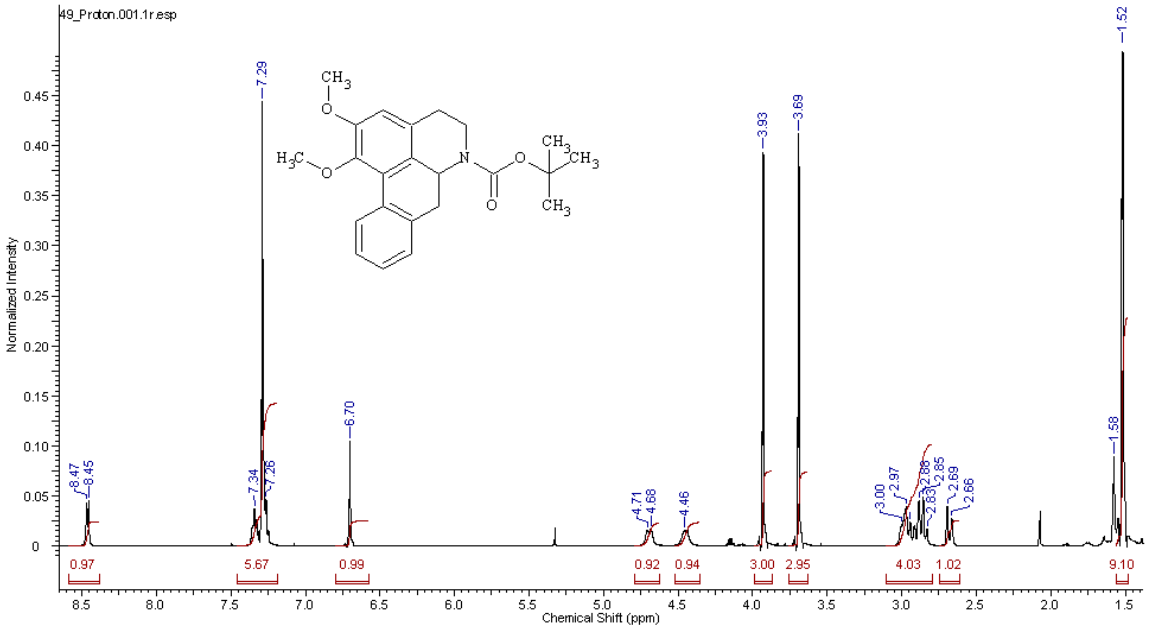

Figure 2.77 ^{1}H NMR (500 MHz, $CDCl_3$) of *tert*-butyl-4,5,6a,7-tetrahydro-1,2-dimethoxydibenzo [*de*,*g*] quinoline-6-carboxylate **(49)**.

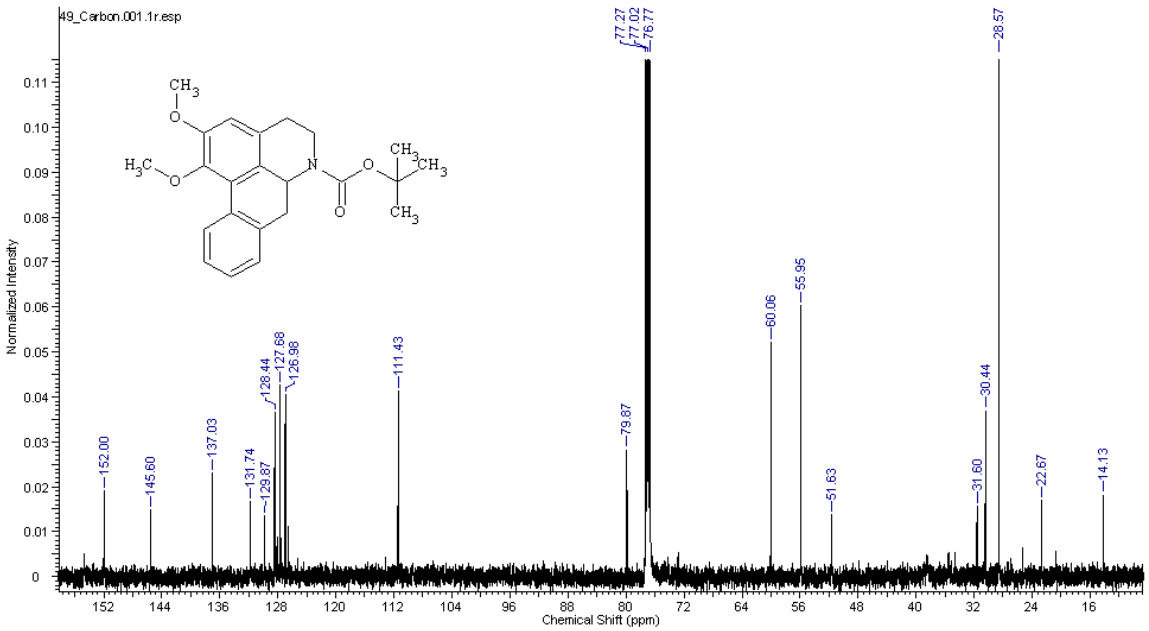

Figure 2.78 ^{13}C NMR (125 MHz, $CDCl_3$) of *tert*-butyl-4,5,6a,7-tetrahydro-1,2-dimethoxydibenzo [*de*,*g*] quinoline-6-carboxylate **(49)**.

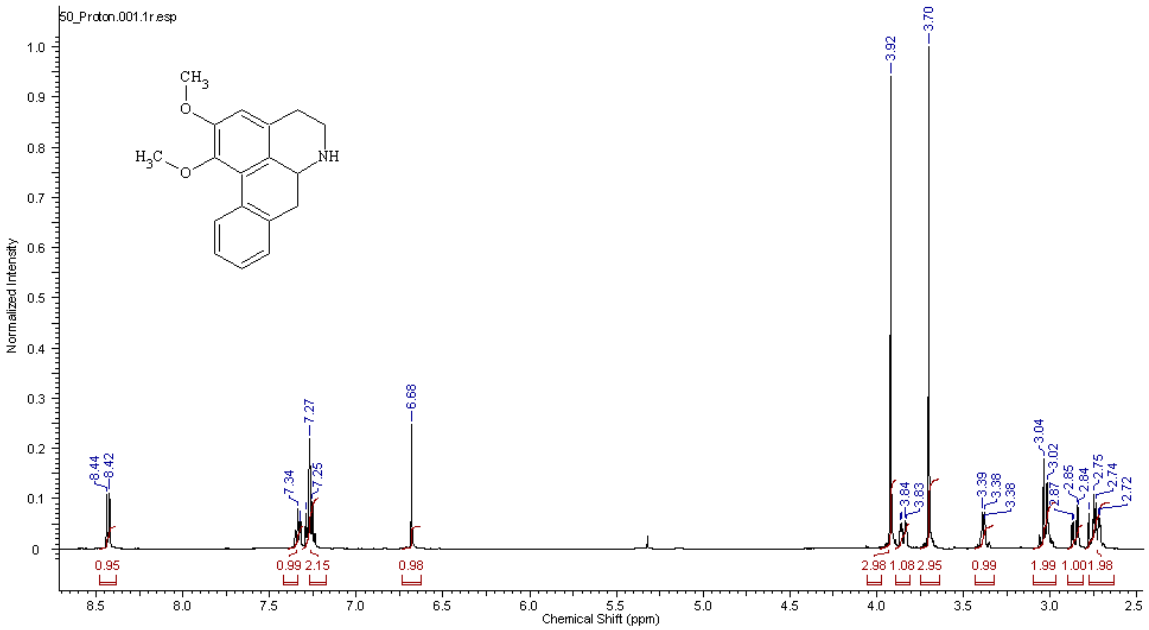

Figure 2.79 ^{1}H NMR (500 MHz, $CDCl_3$) of Nornuciferine **(50)**.

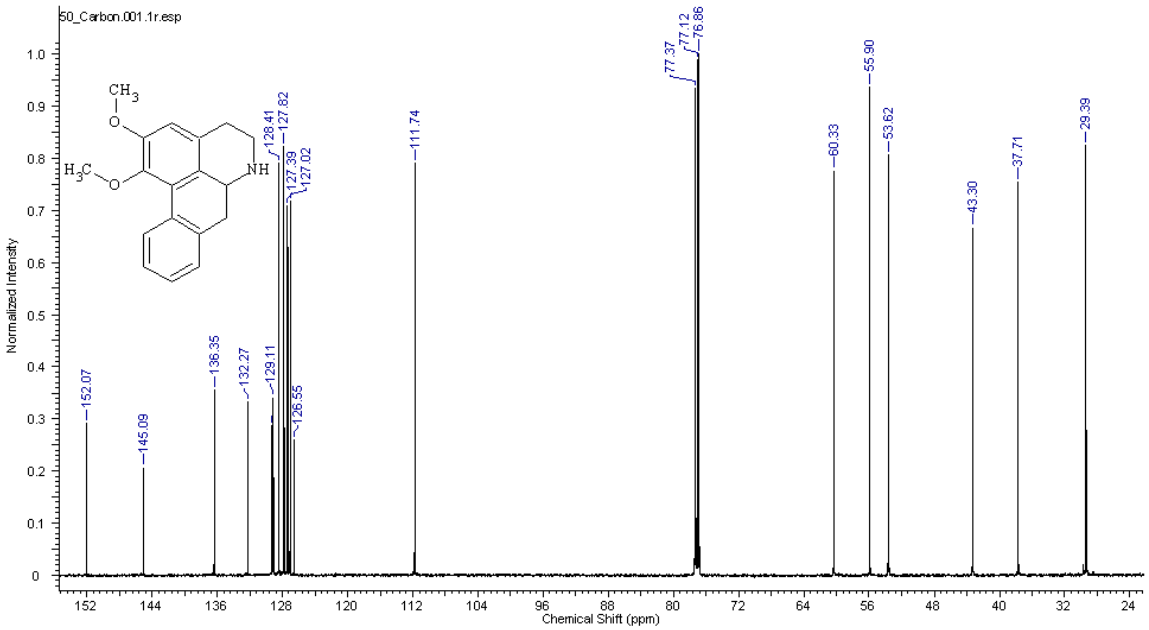

Figure 2.80 ^{13}C NMR (125 MHz, $CDCl_3$) of Nornuciferine **(50)**.

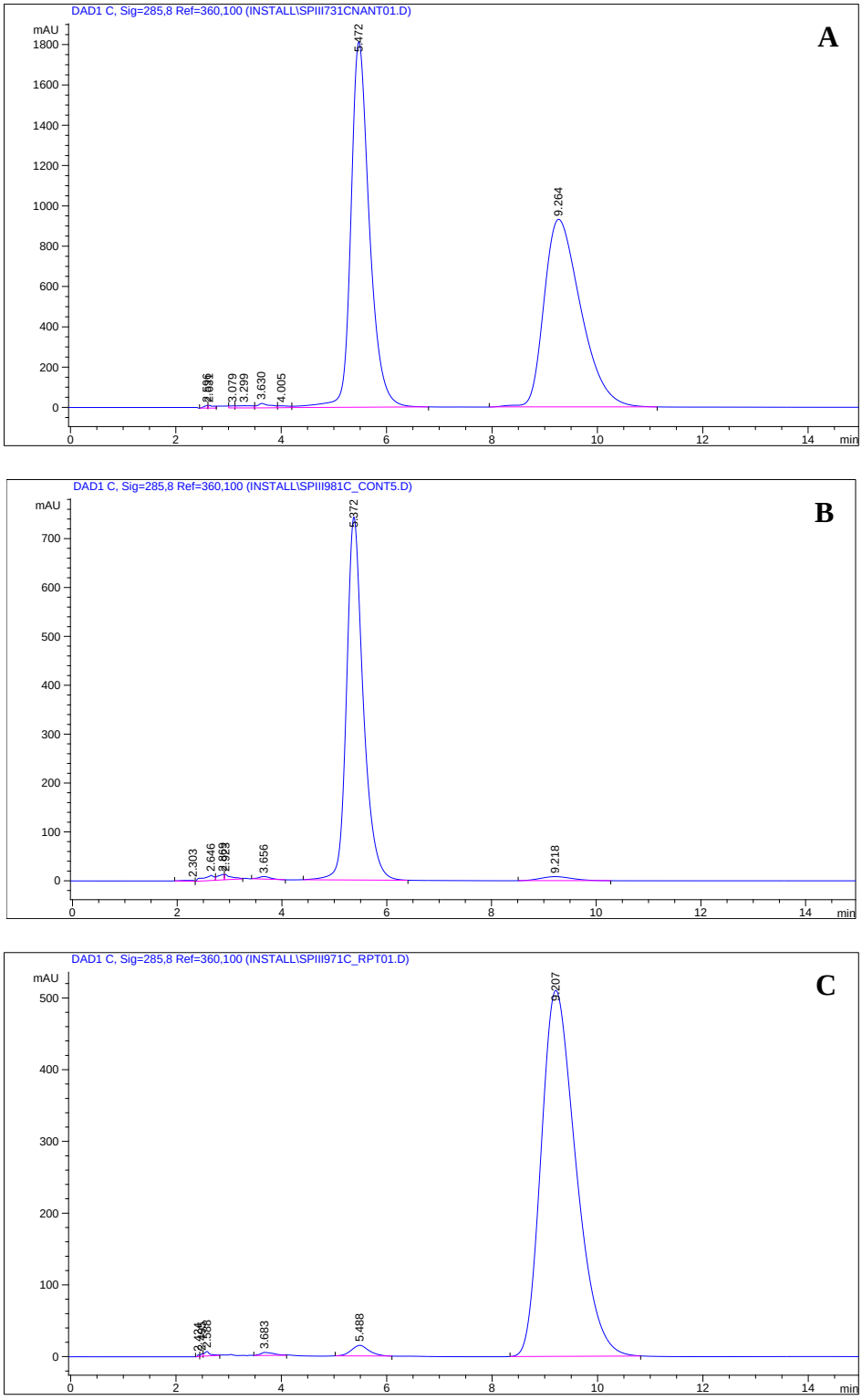

Figure 2.81 HPLC traces of a) racemic nantenine;
b) *R*-nantenine; and c) *S*-nantenine

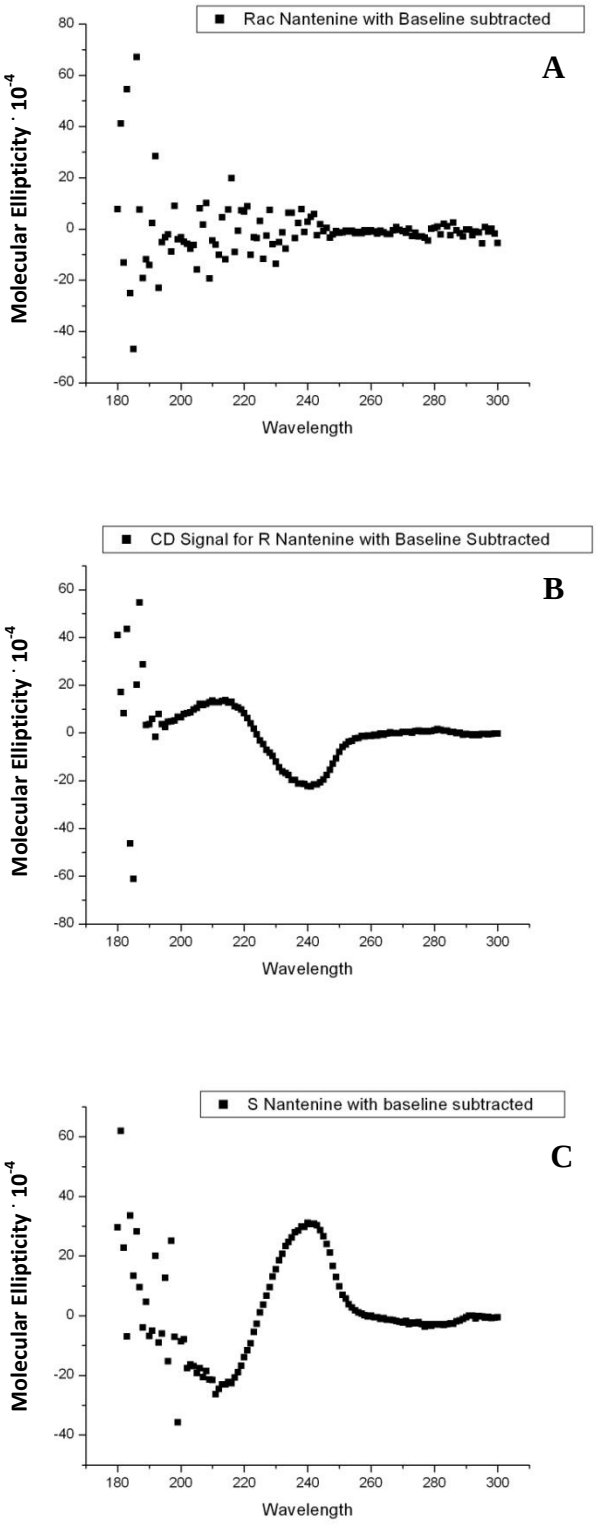

Figure 2.82 CD traces of a) racemic nantenine;
b) *R*-nantenine; and c) *S*-nantenine

2.9 References

(1) Fantegrossi, W. E.; Kiessel, C. L.; Leach, P. T.; Van Martin, C.; Karabenick, R. L.; Chen, X.; Ohizumi, Y.; Ullrich, T.; Rice, K. C.; Woods, J. H. *Psychopharmacology* **2004**, *173*, 270.

(2) Indra, B.; Matsunaga, K.; Hoshino, O.; Suzuki, M.; Ogasawara, H.; Ishiguro, M.; Ohizumi, Y. *Canadian journal of physiology and pharmacology* **2002**, *80*, 198.

(3) Indra, B.; Matsunaga, K.; Hoshino, O.; Suzuki, M.; Ogasawara, H.; Ohizumi, Y. *European journal of pharmacology* **2002**, *437*, 173.

(4) Kupchan, S. M.; Liepa, A. J. *Journal of the American Chemical Society* **1973**, *95*, 4062.

(5) Hoshino, O.; Suzuki, M.; Ogasawara, H. *Heterocycles* **2000**, *52*, 751.

(6) Hara, H.; Komoriya, S.; Miyashita, T.; Hoshino, O. *Tetrahedron: Asymmetry* **1995**, *6*, 1683.

(7) Landais, Y.; Robin, J. P. *Tetrahedron* **1992**, *48*, 7185.

(8) Gottlieb, L.; Meyers, A. I. *J. Org. Chem* **1990**, *55*, 5659.

(9) Kita, Y.; Arisawa, M.; Gyoten, M.; Nakajima, M.; Hamada, R.; Toma, H.; Takada, T. *J Org Chem* **1998**, *63*, 6625.

(10) Herrero, M. T.; Tellitu, I.; Dominguez, E.; Hernandez, S.; Moreno, I.; SanMartin, R. *Tetrahedron* **2002**, *58*, 8581.

(11) Anakabe, E. *Synthesis* **2004**, *7*, 1093.

(12) Moreno, I.; Tellitu, I.; Etayo, J.; SanMartin, R.; Dominguez, E. *Tetrahedron* **2001**, *57* 5403.

(13) Pingaew, R.; Ruchirawat, S. *Synlett* **2007**, *15*, 2363.

(14) Zalan, Z.; Martinek, T.; Lazar, L.; Fulop, F. *Tetrahedron* **2003**, *59*, 9117.

(15) Lafrance, M.; Gorelsky, S. I.; Fagnou, K. *Journal of the American Chemical Society* **2007**, *129*, 14570.

(16) Campeau, L. C.; Parisien, M.; Leblanc, M.; Fagnou, K. *Journal of the American Chemical Society* **2004**, *126*, 9186.

(17) Garcia-Cuadrado, D.; de Mendoza, P.; Braga, A. A.; Maseras, F.; Echavarren, A. M. *Journal of the American Chemical Society* **2007**, *129*, 6880.

(18) Lafrance, M.; Lapointe, D.; Fagnou, K. *Tetrahedron* **2008**, *64*, 6015.

(19) Chaudhary, S.; Pecic, S.; Legendre, O.; Harding, W. W. *Tetrahedron Lett* **2009**, *50*, 2437.

(20) Moreno-Manas, M. R., A.; Suau, R. *Tetrahedron* **2004**, *60*, 5725.

(21) Ahmed F. Abdel-Magid; Kenneth G. Carson; Bruce D. Harris; Cynyhia A. Maryanoff; Shah, R. D. *J. Org. Chem.* **1996**, *61*, 3849.

(22) Bermejo, A.; Andreu, I.; Suvire, F.; Leonce, S.; Caignard, D. H.; Renard, P.; Pierre, A.; Enriz, R. D.; Cortes, D.; Cabedo, N. *Journal of medicinal chemistry* **2002**, *45*, 5058.

(23) Chambers, J. J.; Nichols, D. E. *Journal of computer-aided molecular design* **2002**, *16*, 511.

(24) Julie A. McCarron, V. W. P. *Journal of Labelled Compounds and Radiopharmaceuticals* **2003**, *46*, 1127.

(25) Rao, N. S. K. L., Shoei-Sheng *Journal of the Chinese Chemical Society* **2000**, *47*, 1227.

(26) Chaudhary, S.; Pecic, S.; Legendre, O.; Navarro, H. A.; Harding, W. W. *Bioorg Med Chem Lett* **2009**, *19*, 2530.

(27) http://www.pdsp.med.unc.edu/.

(28) Leifert, W. R. *G Protein Coupled Receptors in Drug Discovery*; Humana Press: New York, 2009; Vol. 552.

(29) Schmidhammer, H.; Jennewein, H. K.; Krassnig, R.; Traynor, J. R.; Patel, D.; Bell, K.; Froschauer, G.; Mattersberger, K.; Jachs-Ewinger, C.; Jura, P.; et al. *J Med Chem* **1995**, *38*, 3071.

(30) Fantegrossi, W. E.; Godlewski, T.; Karabenick, R. L.; Stephens, J. M.; Ullrich, T.; Rice, K. C.; Woods, J. H. *Psychopharmacology* **2003**, *166*, 202.

(31) Nash, J. F. *Life sciences* **1990**, *47*, 2401.

(32) Fantegrossi, W. E.; Ullrich, T.; Rice, K. C.; Woods, J. H.; Winger, G. *Psychopharmacology* **2002**, *161*, 356.

(33) Liechti, M. E.; Saur, M. R.; Gamma, A.; Hell, D.; Vollenweider, F. X. *Neuropsychopharmacology* **2000**, *23*, 396.

(34) Indra, B.; Tadano, T.; Nakagawasai, O.; Arai, Y.; Yasuhara, H.; Ohizumi, Y.; Kisara, K. *Life sciences* **2002**, *70*, 2647.

(35) Blessing, W. W.; Seaman, B.; Pedersen, N. P.; Ootsuka, Y. *J Neurosci* **2003**, *23*, 6385.

(36) Shioda, K.; Nisijima, K.; Yoshino, T.; Kuboshima, K.; Iwamura, T.; Yui, K.; Kato, S. *Neurotoxicology* **2008**, *29*, 1030.

(37) Zhang, A.; Zhang, Y.; Branfman, A. R.; Baldessarini, R. J.; Neumeyer, J. L. *J Med Chem* **2007**, *50*, 171.

(38) Cannon, J. G.; Flaherty, P. T.; Ozkutlu, U.; Long, J. P. *J Med Chem* **1995**, *38*, 1841.

(39) Yasuda, M.; Yamashita, T.; Kojima, R.; Shima, K. *Heterocycles* **1996**, *43*.

(40) Yasuda, M.; Hamasuna, S.; Yamano, K.; Kubo, J.; Shima, K. *Heterocycles* **1992**, *34*, 965.

(41) Suau, R.; Lopez-Romero, J. M.; Rico, R. *Tetrahedron Lett* **1996**, *37*, 9357.

(42) Ramana, M. M. V.; Prashant, V. P. *Tetrahedron Lett* **1996**, *37*, 1671.

(43) Kupchan, S. M.; Liepa, A. J.; Kameswaran, V.; Bryan, R. F. *Journal of the American Chemical Society* **1973**, *95*, 6861.

(44) Deslongchamps, P. *Stereoelctronic Effect in Organic Chemistry*; Pergamon Press: Oxford, 1983.

(45) Sha, C. K.; Young, J. J.; Yeh, C. P.; Chang, S. C.; Wang, S. L. *Journal of Organic Chemistry* **1991**, *56*, 2694.

(46) Mavandadi, F.; Pilotti, A. *Drug Discov Today* **2006**, *11*, 165.

(47) Kappe, C. O.; Dallinger, D. *Nat Rev Drug Discov* **2006**, *5*, 51.

(48) Lindh, J.; Enquist, P. A.; Pilotti, A.; Nilsson, P.; Larhed, M. *J Org Chem* **2007**, *72*, 7957.

(49) Arvela, R. K.; Leadbeater, N. E. *J Org Chem* **2005**, *70*, 1786.

(50) Datta, G. K.; Vallin, K. S.; Larhed, M. *Mol Divers* **2003**, *7*, 107.

(51) Walla, P.; Kappe, C. O. *Chem Commun (Camb)* **2004**, 564.

(52) Legendre, O.; Pecic, S.; Chaudhary, S.; Zimmerman, S. M.; Fantegrossi, W. E.; Harding, W. W. *Bioorg Med Chem Lett* **2010**, *20*, 628.

(53) Liu, Z.; Chen, X.; Yu, L.; Zhen, X.; Zhang, A. *Bioorg Med Chem* **2008**, *16*, 6675.

(54) Cannon, J. G.; Mohan, P.; Bojarski, J.; Long, J. P.; Bhatnagar, R. K.; Leonard, P. A.; Flynn, J. R.; Chatterjee, T. K. *J Med Chem* **1988**, *31*, 313.

(55) Neumeyer, J. L. *Synthesis and Structure-Activity Relationships of Aporphines as Dopamine Receptor Agonists and Antagonists*; Springer-Verlag: Berlin, 1985.

(56) Martin, G. R.; Humphrey, P. P. *Neuropharmacology* **1994**, *33*, 261.

(57) Porter, R. H.; Benwell, K. R.; Lamb, H.; Malcolm, C. S.; Allen, N. H.; Revell, D. F.; Adams, D. R.; Sheardown, M. J. *Br J Pharmacol* **1999**, *128*, 13.

(58) Newton, R. A.; Phipps, S. L.; Flanigan, T. P.; Newberry, N. R.; Carey, J. E.; Kumar, C.; McDonald, B.; Chen, C.; Elliott, J. M. *J Neurochem* **1996**, *67*, 2521.

(59) Jerman, J. C.; Brough, S. J.; Gager, T.; Wood, M.; Coldwell, M. C.; Smart, D.; Middlemiss, D. N. *European journal of pharmacology* **2001**, *414*, 23.

(60) Kenakin, T. *ACS Chem Biol* **2009**.

(61) Lloyd-Williams, F.; Giralt, E. *Chem Soc Rev* **2001**, *30*, 145.

(62) Runyon, S. P.; Mosier, P. D.; Roth, B. L.; Glennon, R. A.; Westkaemper, R. B. *J Med Chem* **2008**, *51*, 6808.

(63) Aranda, R.; Villalba, K.; Ravina, E.; Masaguer, C. F.; Brea, J.; Areias, F.; Dominguez, E.; Selent, J.; Lopez, L.; Sanz, F.; Pastor, M.; Loza, M. I. *J Med Chem* **2008**, *51*, 6085.

(64) Meltzer, H. Y.; Matsubara, S.; Lee, J. C. *Psychopharmacol Bull* **1989**, *25*, 390.

(65) Roth, B. L.; Tandra, S.; Burgess, L. H.; Sibley, D. R.; Meltzer, H. Y. *Psychopharmacology* **1995**, *120*, 365.

(66) Wisniewski, H. M.; Vorbrodt, A. W.; Wegiel, J. *Annals of the New York Academy of Sciences* **1997**, *826*, 161.

(67) Thomas, T.; Bryant, M.; Clark, L.; Garces, A.; Rhodin, J. *Microvasc Res* **2001**, *61*, 28.

(68) Rhodin, J. A.; Thomas, T. *Microcirculation* **2001**, *8*, 207.

(69) Chodobski, A.; Szmydynger-Chodobska, J. *Microsc Res Tech* **2001**, *52*, 65.

(70) Petty, M. A.; Lo, E. H. *Prog Neurobiol* **2002**, *68*, 311.

(71) Lipinski, C. A.; Lombardo, F.; Dominy, B. W.; Feeney, P. J. *Adv Drug Deliv Rev* **2001**, *46*, 3.

(72) Reichel, A. *Curr Drug Metab* **2006**, *7*, 183.

(73) Zhang, A.; Csutoras, C.; Zong, R.; Neumeyer, J. L. *Organic letters* **2005**, *7*, 3239.

(74) Csutoras, C.; Zhang, A.; Zhang, K.; Kula, N. S.; Baldessarini, R. J.; Neumeyer, J. L. *Bioorg Med Chem* **2004**, *12*, 3553.

(75) Bhal, S. K.; Kassam, K.; Peirson, I. G.; Pearl, G. M. *Mol Pharm* **2007**, *4*, 556.

(76) Lemke, T. W., David *Foye`s Principles of Medicinal Chemistry*; Sixth ed., 2008.

(77) Ringdahl, B.; Chan, R. P. K.; Craig, C.; Cava, M. P.; Shamma, M. *J. Nat. Prod.* **1981**, *44*, 80.

CHAPTER 3: Molecular Docking Analysis of Nantenine and Nantenine Analogs at the Human 5-HT_{2A} Receptor

3.1 Introduction

At present there are thirteen distinct serotonin G-protein-coupled receptors that are divided into six families, based on pharmacology, amino acid sequences, gene organization and second messenger coupling pathways.[1,2] The serotonin 5-HT_{2A} receptors are of significant clinical interest because of their potential involvement in cardiovascular function and in certain mental disorders.[3] Agonists at this receptor may be used for treatment of sleep disorders and arousal.[4] The utility of antagonists in the treatment of depression and certain psychotic conditions has already been well explored.[5,6] The investigation of 5-HT_{2A} antagonists as potential drug-abuse therapeutics is topical in the recent literature.[7,8]

As part of our research to develop novel 5-HT_{2A} antagonists as potential MDMA antagonists, we prepared a series of analogs based on nantenine (described in detail in previous chapter) to investigate the structural features required for its affinity and activity at the 5-HT_{2A} receptor.[9] The analogs were designed to investigate the role of molecular rigidity, N-substitution, methylenedioxy ring and substitution at the C1 position on 5-HT_{2A} affinity. This study resulted in the identification of C1 analogs with up to 12-fold increase in 5-HT_{2A} apparent affinity (K_e) as compared to nantenine.[9]

In order to understand the possible binding modes of nantenine and nantenine analogs at the human 5-HT_{2A} receptor (to complement future drug design efforts), we have conducted a docking study with our library of compounds. Since the crystal structure of the 5-HT_{2A} receptor has not been solved, our approach necessitated the use of a homology model for this receptor. Although other homology models for the 5-HT_{2A} receptor have been previously described[3,10,11] we decided to build and evaluate a number of homology models using various *in silico* tools in order to determine which model was best in line with our *in vitro* data. Four homology models were built based on bovine rhodopsin (PDB code 1U19) and human β2-adrenoceptor (PDB code: 2RH1) templates using two programs for molecular modeling - Modeller and ICM Pro. To determine the extent to which our *in vitro* results correlated with each homology model, we then performed docking/scoring experiments, using three docking programs: ICM Pro, Glide and Gold.

Homology modeling has become a common technique in the last couple years, and this procedure usually consists of four sequential steps[12]:

i) template recognition,

ii) alignment of the target sequence and template structure(s),

iii) model building, and

iv) model verification

Docking studies usually follow homology modeling as separate experiments. Scheme 3.1 summarizes the approach we have taken in this study.

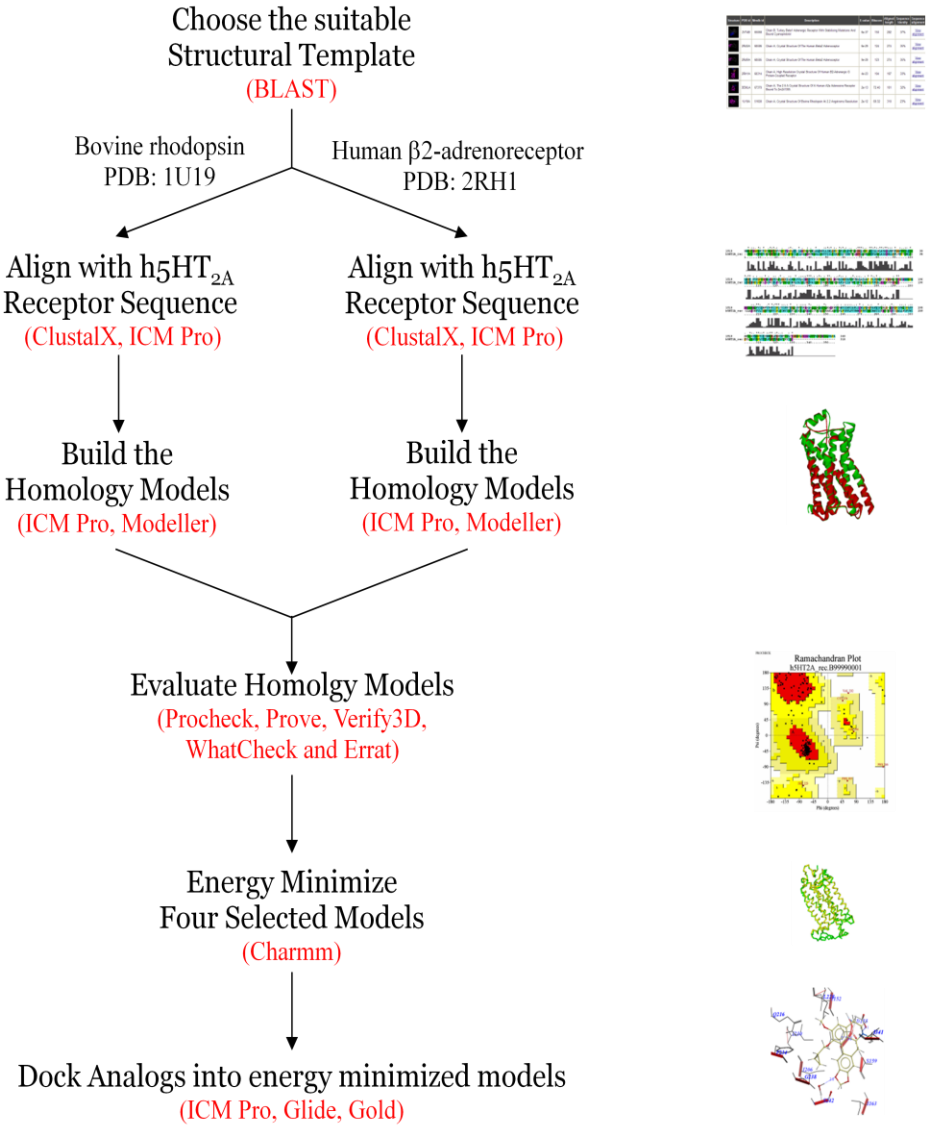

Scheme 3.1 Overview of procedures for building a homology model and docking experiments

3.2 Results

3.2.1 Identification of suitable template

The main challenge in homology modeling is to find a suitable template. Since the crystal structure of the 5-HT_{2A} receptor is still not solved, and till now the direct determination, by X-ray crystallography of the atomic structure of any member of serotonin receptors family has not yet been accomplished, the only way to achieve our objective is to use a similar GPCR structure as a template to build the homology model.

The first step of any homology modeling method begins with the selection of a suitable structural template from the Protein Data Base (http://www.pdb.org).[13] We searched for templates using BLAST[14] (Basic Local Alignment Search Tool), - see Experimental. Currently there are five available crystal structures of Family A GPCRs: turkey β1-adrenergic receptor (PDB code: 2VT4),[15] human adenosine A2A receptor (PDB code: 3EML),[16] human β2-adrenergic receptor (PDB code: 2RH1)[17], bovine rhodopsin (PDB code: 1U19)[18] and squid rhodopsin (PDB code: 2Z73).[19] It is important not to assume that adrenergic receptor structures are better templates than rhodopsin structures for modeling GPCRs. Sequence alignment must be used as a guide to which sections of each structure are appropriate templates for the query sequence.[12] This is especially important in loop regions that exhibit the greatest variability in both sequence and structure. In a recent report, it is suggested (*The Venn Diagram*)[20] that different homology models for GPCRs could be built using either template that are shown at circle intersections, while the specific sequences that would be better modeled using one specific template are shown within circles (Figure 3.1). Sequences with identity difference greater than 10% between available targets are placed into template exclusive

areas in the diagram. It is suggested in this diagram that, to build the homology model of the serotonin 5-HT_{2A} receptor, the most appropriate structural templates are either the crystal structure of the human β2-adrenergic receptor or turkey β1-adrenergic receptor.

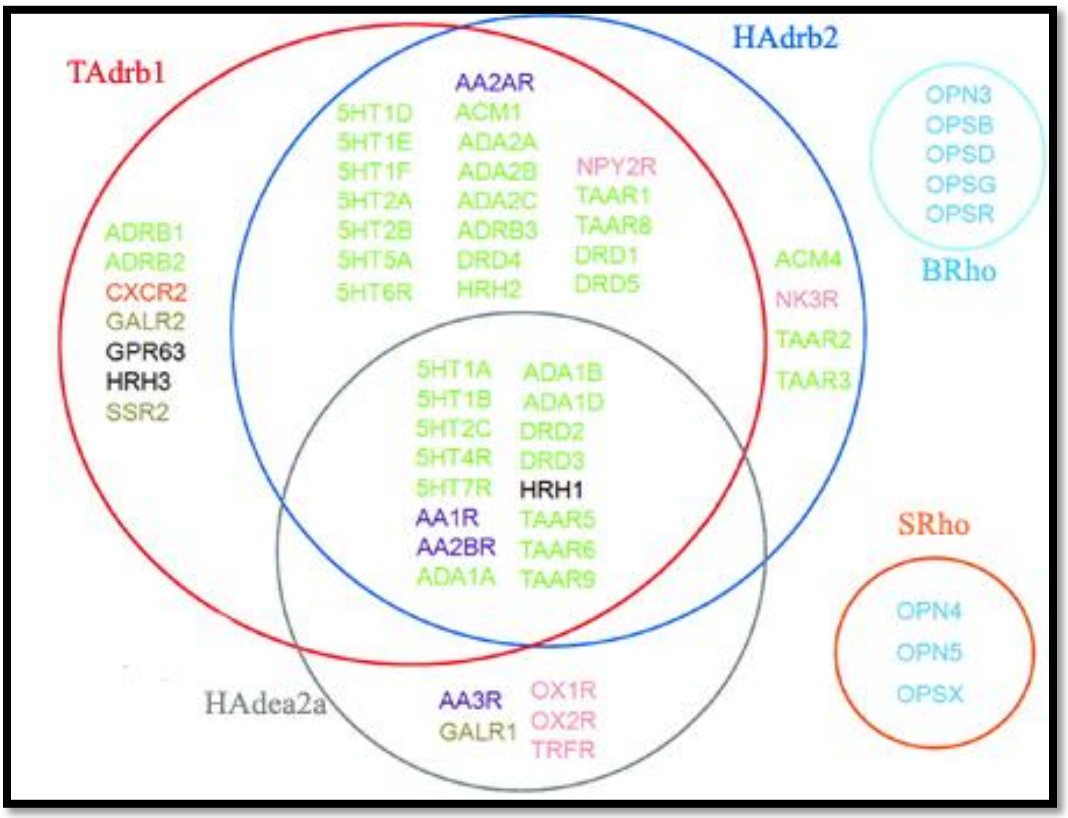

Figure 3.1 The Venn Diagram
(Mobarec et al, *J Med Chem*, **2009**, *52*, 5207-5216)

Template selection: As a template for building the 5-HT_{2A} receptor homology model we selected two different available GPCR crystal structures (See Table 3-1 in Appendix). The first one is bovine rhodopsin (PDB code: 1U19) since it has been shown in many previous reports[3,11,21,22] that this structure is a reliable template for 5-HT_{2A} receptor homology models and also because its crystal structure is solved at high resolution (2.20 Å). Generally, values below 2.2 Å are normally regarded as very good for docking, yielding good results for most typical applications.[23] We also selected the human β2-adrenergic receptor (PDB code: 2RH1) as a second template, because this is to

date the highest-solved resolution (2.40 Å) of any GPCR neurotransmitter receptor and represents the most suitable template for building the homology model of the 5-HT_{2A} receptor.[20] We omitted the other BLASTP hits because of their low resolution. These two templates are chosen for several specific reasons. First of all, there are several disadvantages of using only bovine rhodopsin as a template; for example, it shares a low sequence similarity to 5-HT_{2A} receptor (less than 20%) and it is a retinal-binding protein, functionally completely different from 5-HT_{2A} receptor, which is a typical representative of the neurotransmitter GPCRs. On the other hand, high-resolution of its crystal structure and the specific arrangement of the seven transmembrane helices stabilized by a series of intramolecular interactions make bovine rhodopsin a very good structural template for generating molecular models of the 5-HT_{2A} receptor. Since very recently, there were no experimental structures available for any neurotransmitter GPCRs. A high resolution (2.4 Å) of human β-2 adrenergic receptor (PDB code 2RH1) has been reported in 2008. It has better sequence similarity with the 5-HT_{2A} receptor (almost 30%) and it is definitely functionally closer to the family of serotonin receptors, since it also belongs to the neurotransmitter GPCRs. Disadvantages are that this crystal structure has been solved at lower resolution than the one at bovine rhodopsin, and there is only one 5-HT_{2A} receptor homology model built using this structure as a template.[10] Also only one group (Indra et al) has tried to explain a binding mode of (±)-nantenine at the 5-HT_{2A} receptor.[24] However, this study described a homology model of a rat 5-HT_{2A} receptor. Since our *in vitro* data was based on human rather than rat 5-HT_{2A} receptor data, we decided to construct homology models based on the human 5-HT_{2A} receptor. The Indra model proposes that Asp155, a residue in transmembrane helix 3 that is strongly conserved

across the family of serotonin receptors, forms a strong ionic bond with *N*6 of nantenine. The oxygen atom of the C1 methoxy group interacts with Asn343, a residue from transmembrane helix 6, also strongly conserved in many GPCRs. It is hypothesized that this interaction may be directly involved in 5-HT_{2A} receptor antagonism.[24]

To improve the quality of GPCR models, Mobarec *et al.*[20] tested the possibility of using multiple templates for homology modeling. Their analysis suggested that the use of multiple templates can provide similar or slightly improved models of the TM region of GPCRs when compared to receptor models obtained using single templates. Also, the models that were built using multiple alignment, showed lower predictive accuracy when they were used for docking experiments, than the models that were built using single templates showed. These results are possible if we consider that for docking purposes the correct orientation of side chains within the binding pocket are more important than the global measure of the properties of the complete structure.

3.2.2 Sequence alignments

Despite recent advances in methods used to generate homology models, a difficult aspect is the initial alignment between the target sequence and template structure. A common method to align the target and the template is by using sequence alignment software. Alignments of target sequence to the template structures were made using the ClustalX[25] alignment tool and the ICM Pro sequence alignment program,[26] both using their default parameters.

The sequence alignment of the human 5-HT_{2A} receptor using ClustalX shows good sequence identity with the bovine rhodopsin template (19.5%) with more than 45%

sequence similarity (See Figure 3.2 in Appendix). The same human 5-HT_{2A} receptor sequence has, compared with bovine rhodopsin sequence, higher sequence identity with the human β2-adrenergic receptor template (almost 28%) with more than 48% sequence similarity (See Figure 3.3 in Appendix). Although the ICM Pro alignment program is based on a different algorithm and method (it uses ZEGA algorithm with zero gap and penalties)[27] than ClustalX, the sequence of the human 5-HT_{2A} receptor nevertheless showed 19% sequence identity with the bovine rhodopsin template which is almost the same as we determined using ClustalX (See Figure 3.4 in Appendix). Also comparable results, (30% identity), were obtained when we used the ICM Pro alignment program for β2-adrenergic receptor template and 5-HT_{2A} receptor sequence, (See Figure 3.5 in Appendix).

I	II	III	IV	V	VI	VII
-	-	-	-	-	-	-
-	-	:29 I/V (94)	-	-	-	:29 R/K (79)
-	-	-	-	-	-	:28 F/Y (77)
-	-	-	-	-	: 0 K/R (75)	-
-	-	:26 Y (79)	-	-	-	-
-	-	:25 R (99)	-	:25 I/V (72)	-	-
-	-	:24 D/E (94)	-	== =-= ===	-	-
== =-= ===	== =-= ===	== =-= ===	-	-	-	== =-= ===
-	-	:22 S/A (87)	== =-= ===	:22 Y (91)	== =-= ===	-
:21 V (76)	-	:21 I (60)	-	-	-	:21 Y (95)
-	-	-	-	-	-	-
-	-	-	-	-	-	-
:18 N (99)	: 9 N/S (88)	:18 L (74)	-	:18 I/M (79)	-	:18 P (98)
:17 G (69)	:10 L (96)	-	-	-	-	:17 N/D (99)
-	:11 A (86)	-	:11 W (96)	-	-	-
-	-	-	-	-	:12 F (82)	-
-	:13 A/S (85)	:14 S (77)	-	:14 P (85)	-	:14 S/C (76)
-	:14 D (94)	-	:14 S/A (79)	-	-	:13 N/S (80)
-	-	-	-	-	:15 C (71)	-
-	-	-	-	:11 F (70)	:16 W (85)	-
-	-	-	-	-	-	-
-	-	-	-	-	:18 P (100)	-
-	-	-	-	-	-	-
-	-	-	:20 P (68)	-	-	-
-	-	-	-	-	-	== =-= ===
-	-	-	== =-= ===	== =-= ===	-	-
== =-= ===	== =-= ===	== =-= ===	-	-	== =-= ===	-

Figure 3.6 Conserved residues of GPCRs
(Baldwin et al, *J Mol Biol*, **1997**, *273*, 144-164)

Since the secondary structure elements are well-conserved among these sequences, the alignments were then manually refined to ensure a perfect alignment of the highly conserved residues of the GPCR superfamily, according to Baldwin *et al* (Figure 3.6).[28] In Figure 3.6 the standard numbers are denoted by helix number I to VII, followed by :position number. Figures in parentheses are the percentages of the 199 unique sequences that have this residue. Residues at the top of the columns are at the intracellular side of the membrane. == =-= === indicates the approximate boundary of the lipid bilayer core for each segment. Most of the conserved residues lie in the core of the lipid bilayer.

3.2.3 Homology modeling of a human 5-HT_{2A} receptor

Once we obtained a suitable template and generated alignments between the target and the template structures, we started creating a model of the 5-HT_{2A} receptor using spatial restraints. Spatial restraints can be obtained from a number of sources that include homology-derived restraints and molecular mechanics-based or statistically derived preferences for bonded and non-bonded interactions.[12] An example of a program that uses this style of homology modeling is Modeller.[29] In addition to the satisfaction of spatial restrains, other successfully used method to generate homology models is the concept of positional tethers. Tethering and other proprietary methods are available in ICM Pro[26] that contain integrated bioinformatics, modeling and visualization software. 3D-Model building was performed with the modeling suite, Discovery Studio 2.0, which uses Modeller for building protein structures. Twenty models were built for each of the templates using the homology module of Discovery Studio and one model for each

template was built by ICM Pro 3.6 model building software. The conserved disulfide bond between residues, C148 at the beginning of TM3 and C228 in the middle of extracellular loop 2, a feature common to many GPCR receptors, was also created and was kept during building homology models in both programs.

3.2.4 Model evaluation

Evaluation methods check whether a model satisfies standard steric and geometric criteria. Each of the tools used in the construction of a model (e.g. template selection, alignment, model building, and refinement) has its own internal measures of quality. In order to evaluate and select the best homology model for the purpose of our study we used several different programs for evaluation that are available via the server of the UCLA-DOE Institute for Genomics and Proteomics. This Institute offers a service called *Structural Analysis and Verification Server* (SAVES)[30] that encompass five verification tools for the model evaluation: Procheck,[31] What_check,[30] Errat,[32] Verify_3D[33] and Prove.[34]

Each homology model was first evaluated using the program Procheck. The aim of Procheck is to assess how normal, or how unusual, the geometry of the residues in a given protein structure is, as compared with stereochemical parameters derived from well-refined, high resolution structures. The results of Procheck evaluation for all the homology models are shown in Table 3-2 (*see Appendix*). Ramachandran plot, which is a plot of the φ-ψ torsion angles for all residues in the structure, is one of the important parameters in Procheck for assessment of structures. Ramachandran plots for final selected homology models are shown separately, for BRho_Modeller in Figure 3.7, for

HAdrb2_Modeller in Figure 3.8, for BRho_ICM in Figure 3.9 and for HAdrb2_ICM in Figure 3.10 (*See Appendix*). A simple measure of quality that can be used from the plot is the percentage of residues in core region, and allowed regions should be very high (>90% residues). Another important factor in structural assessment is Goodness factor or G-Factor which shows the quality of dihedral, covalent and overall bond angles. These scores should be above -0.5 for a reliable model.

The results obtained from Errat are shown in Table 3-3 (*see Appendix*). This program counts the number of nonbonded interactions between atoms (CC, CN, CO, NN, NO, and OO) within a cutoff distance of 3.5Å. It gives an overall quality factor for each protein structure which is expressed as the percentage of protein for which the calculated error value falls below 95% rejection limit. Good structures produce these values above 90%. Accepted range is above 50%. The template structure of bovine rhodopsin, 1U19, has Errat value of 85.294, while the template structure of human β2-adrenoreceptor, 2RH1, has Errat value of 97.08.

In Table 3-4 in Appendix are shown the Prove results for homology models that are built based on bovine rhodopsin and human β2-adrenoceptor templates. The stereochemical criterion implemented in this method is regularity or irregularity of atom volume. It provides an average volume Z-score of all the atoms. Z-score is calculated as the difference between the volume of the atom and the mean atomic volume for the corresponding atom type, divided by the standard deviation of the appropriate distribution.

Atoms in test proteins are scored using a Z-score standard deviation (Zstd), which is how many standard deviations their volume is from the mean (Zsm) for that atom type.

A structural Z-score RMS (Zrms) is calculated using the square root of these scores. High scores have been found to be associated with uncertainty in the structure. Structures with poor resolution generally have a Zrms greater than 1.2, while for well resolved structures, the Zrms is around 1.0.

Verify3D evaluates the sequences that are most compatible with the environments of the residues in the 3D structure. The environments are described by: the area of the residue buried in the protein and inaccessible to solvent, the fraction of sidechain area that is covered by polar atoms (O and N), and the local secondary structure. Verify3D works best on proteins with at least 100 residues. Verify3D measures a compatibility score to each residue of a full-atom protein structure, in other words, the compatibility of a model with its sequence. Verify3D results shown in Table 3-5 represent the Verify3D average data score of all the models generated in comparison with template. The score which matches the template and has value > 0.2 for all or most of the residues indicates a reliable model. Negative or less than 0.2 scores are indicative of potential problems. Figure 3.11 in Appendix shows Verify3D plots of all homology models built based on a bovine rhodopsin and the template (1U19), while Figure 3.12 (*See Appendix*) shows the Verify3D resulting plots but for the homology models built based on a human β2-adrenoreceptor and the 2RH1 template. In Figures 3.13 and 3.14 (*See Apppendix*) are shown the Verify3D curves of the best selected models built by Modeller, BRho_Modeller and HAdrb2_Modeller, respectively, compared with their appropriate templates. Figure 3.15 in Appendix shows the Verify3D plots of model BRho_ICM, while the Figure 3.16 represents the plot of the final HAdrb2 built by the ICM. We

selected the models which showed average scores close to thetemplate and in which maximum scores are above 0.2.

What_check program is derived from a subset of protein verification tools from the WHATIF program. It does extensive checking of many sterochemical parameters of the residues in the model and it gives an overall summary of the quality of the structure as compared with current reliable structures. This summary is most useful for biologists seeking a good structure to use for modeling calculations. The first part of the Tables 3-6 and 3-7 (*see Appendix*) shows a number of constraint-independent quality indicators. All structure Z-scores, like, second generation packing quality, Ramachandran plot appearance, chi-1/chi-2 rotamer normality, backbone conformation, and RMS Z-scores, should be positive numbers. The second part of these tables mostly gives an impression of how well the model conforms to common refinement constraint values and these numbers should be close to 1.0. The program evaluates: bond lengths, bond angles, omega angle restraints, side chain planarity, improper dihedral distribution and inside/outside distribution.

Finally, of course, the best discriminator between good and bad models is human evaluation and should be employed at each stage of the modeling process. We evaluated each model using the above methods and selected the final model for each template (see Experimental for details), which fits best in criteria of selection of each method. From twenty 5-HT_{2A} receptor homology models, which were built by Modeller based on bovine rhodopsin template (1U19), we selected one homology model (hereinafter called BRho_Modeller). A selected model, out of twenty homology models built by Modeller, based on human β2-adrenoreceptor template (2RH1), was named HAdrb2_Modeller.

Using ICM Pro software, two homology models, one for each template, were built, and both showed good evaluation scores; hence we decided to also use these for the purpose of docking experiments. We named them according to the origin of their templates, bovine rhodopsin and human β2-adrenoreceptor - BRho_ICM and HAdrb2_ICM, respectively.

3.2.5 Energy minimization and RMSD values

All selected homology models share a close homology with the template as indicated by their RMSD value of their backbone atoms with respect to the template. The four selected homology models were relaxed with 500 steps of steepest descent energy minimization using Charmm and using the Discovery Studio 2.0, we calculated the RMSD values for the each homology model and their appropriate template structure. The structural superposition of Cα trace of 5-HT_{2A} receptor homology models with respect to templates, gave us the RMSD values: 1.53 for BRho_Modeller, 2.69 for HAdrb2_Modeller, 3.73 for the BRho_ICM and 2.40 for the HAdrb2_ICM (See Figure 3.17 and Figure 3.18 in Appendix). The RMSD values close to 1.0 for two models and close to 3 for the other two selected models indicate the reliable and reasonable conformation for homology modeling. The resulting, energy minimized homology models were then saved and used as input for next step- docking experiments.

3.2.6 Docking

There are many commercially available docking software, each using a different combination of the searching methods and algorithms, and scoring functions (Figure

3.19).[23] We used three programs for docking experiments and compared the docking scores with our *in vitro* results. We selected ICM Pro docking algorithm, Glide and Gold method for the purpose of docking of our analogs. Each compound that was used for the docking experiment was prepared, converted to a 3D structure and energy minimized using Chem3D Ultra or LigPrep (described in detail in Experimental section). The results from our docking study are summarized in Table 3-8 in Appendix. After we performed the docking using different programs and obtained the docking scores, each structure was visually inspected to be assured that the molecules were actually docked into the expected binding site and that interactions with key residues of the active site were maintained. All final receptor-analog complexes, obtained from three different programs, were saved as PDB files and visualized in Discovery Studio 2.0. H-bonds, hydrophobic interactions and distances for each 3D structure were calculated and plotted by LigPlot[35] v 4.4.2., a program for schematic 2D diagrams of ligand and receptor plots.

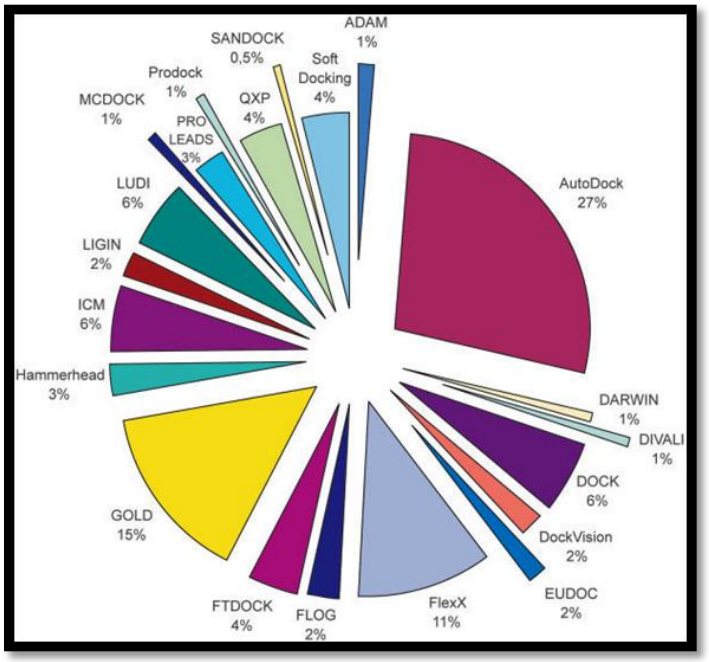

Figure 3.19 Available docking software
(Sousa et al, *Proteins*, **2006**, *65*, 15-26)

As shown in Table 3-8, the best agreement between the *in vitro* experimental findings and the docking scores are obtained by using a homology model that was built by MODELLER based on a bovine rhodopsin template (BRho_Modeller) and using the program GOLD for the docking purposes. In that regard, analogs which had low apparent affinity (K_e > 10,000) were predicted not to bind with the BRho_Modeller/GOLD combination whereas analogs with moderate to good apparent affinity (50 < K_e< 6000) gave reasonable and measurable GOLD scores. However, the rank order of GOLD scores did not correlate with the K_e values obtained possibly because the individual compounds have different binding modes.

Binding modes of nantenine as well as C1 analogs were further examined in order to begin to understand the trend in apparent affinity values observed in this series of compounds. Figure 3.20 shows 3D and 2D representations (generated with ICM Pro and LigPlot respectively) of important interactions of nantenine and the analogs in the 5-HT_{2A} receptor. We observed that C1 analogs **17-22** are binding in the 5-HT_{2A} receptor pocket differently than nantenine, while still maintaining a similar orientation among them. Figure 3.20 shows that nantenine makes an H-bond between the protonated N6 atom and Asp155, as well as a second key interaction between the oxygen atom of the C1 methoxy group and Asn343 located in TM6. This is in agreement with previous study done by Indra *et al.* although we used a different protein source (human vs. rat 5-HT_{2A} receptor) and methods for homology modeling and docking experiments.

Visual inspection of the binding mode of the C1 analogs with highest affinity - **20** (K_e = 171 nM) and **21** (K_e = 68 nM), revealed a different orientation of these molecules in the receptor as compared to nantenine (See in Appendix: Figure 3.21 and Figure 3.22,

respectively). In both these compounds there is a protonated N6/Asp155 H-bond and a H-bond between Ser242 and one of the oxygen atoms located in methylenedioxy ring. The H-bonding interaction between the C1 oxygen atom and Asn343 which is present in nantenine is absent in these binding poses. In addition to these strong stabilizing forces, the higher affinity of these compounds might be also accounted for by strong hydrophobic interactions that are formed between the spatially close residues Phe234 and Gly238 and the C1 alkyl groups in **20** and **21** respectively. Like **20** and **21**, compounds **18** and **19** (Figure 3.23 and Figure 3.24 respectively in Appendix), also form H-bonds with Asp155 and Ser242, but their C1 side chains do not make important hydrophobic interactions with neighboring residues. Absence of this hydrophobic interaction probably accounts for the 4.5-fold lower *in vitro* affinity of these two nantenine analogs (K_e = 297 nM for **18** and K_e = 274 nM for **19**), as compared to the most potent analog from this series, compound **21**. Compound **22**, which had the lowest affinity among C1 congeners (K_e = 4600 nM), showed only one H-bonding interaction (via protonated N6 and Asp155), and also hydrophobic interactions between its aromatic ring in the C1 side chain and Phe234 and Gly238 residues (Figure 3.25).

Taken together, the results above suggest that the binding orientation among C1 analogs may be different, but that both H-bond and hydrophobic interactions are important for achieving high affinity to the receptor in this series.

3.3 Discussion

Using two different programs, Modeller and ICM Pro, we generated 42 conformationally distinct homology models of the 5-HT_{2A} receptor based on two

templates, bovine rhodopsine and β1 adrenoreceptor. Five verification tools were applied in the process of selecting the homology models that were best in line with the geometric and steric criteria. The final four homology models that we selected were then used to compare results of *in vitro* data (5-HT_{2A} apparent affinity of nantenine analogs) with the docking scores obtained for the analogs with each homology model. These verification tools provided only information about the overall structural quality of the homology models, and based on RMSD values, all four models satisfy these criteria. Therefore, it is important to validate these models for docking experiments in this initial receptor model selection phase. It has been reported that a number of structurally similar compounds bind in completely different orientations to the same receptor binding pocket.[36] In order to select the best model we used receptor binding characteristic of the docked solutions for the compounds from previous ligand SAR and mutation data that are available. We used three automated docking programs Gold, Glide and ICM Pro to separately dock to each of these four selected models two known 5-HT_{2A} receptor antagonists, ketanserin (since a lot of mutagenesis data[3,37,38] are available for this compound), and nantenine (both SAR and molecular modeling studies[24] were reported). We then used a combination of docking scores and information from mutagenesis data to select the most valid homology model and docking software that we can use for the docking of other nantenine analogs. Mutation of the conserved residue Asp155 to a residue other than aspartate leads to complete or near loss of affinity for ketanserin.[37] Also a mutation of Phe340 to any other amino acid has no significant effect in ketanserin's binding affinity, which is consistent with the previously reported binding mode of ketanserin, because this residue is located in TM6 and does not interact with ketanserin.[39] Findings from an SAR study on

nantenine done by Indra et al,[24] show that replacement of methyl group at *N*6 with a hydrogen atom or an ethyl group, will decrease the affinity to the receptors, and that the replacement of the methoxy moiety at C1 with a hydroxyl group will cause a marked decrease in affinity. According to this group, substitution of both, a methoxy moiety at C1 with a hydroxyl group and a methyl group at *N*6 with a hydrogen atom will cause a complete loss of affinity to the 5-HT_{2A} receptor. Their molecular modeling study showed that two hydrogen bonds are important in stabilizing nantenine in the binding cleft of the 5-HT_{2A} receptor, and they proposed that the disturbance of the preferable electronic interactions at these two position: Asp155 and/or Asn343 may lead to the reduction of the binding activity of the nantenine derivatives.

Using this information from literature, mutagenesis binding data for ketanserin and SAR/molecular modeling studies for nantenine, we inspected binding modes of both these compounds in all four final selected homology models and compared docking scores obtained from three different docking software that were used. Additionally, to provide more accurate validation for our final models we also docked all nantenine analogs in the final four homology models, using all three docking software. Our results indicated that the homology model built from bovine rhodopsin template, generated with Modeller software package and evaluated by the Gold docking algorithm showed reasonable solutions for ketanserin and nantenine that were consistent with both mutagenesis data and previously reported SAR/molecular modeling studies. This model also gave docking scores which best correlated with our *in vitro* data. We also wanted to compare our homology model with other 5-HT_{2A} receptor models that are published. The model of 5-HT_{2A} by Chambers and Nichols was also constructed using bovine rhodopsin

as a template.[11] The major difference between these two models is the presence of a network of polar interaction "ionic lock" that is present between residues Arg135 (in TM3) and Glu247 (in TM6) in bovine rhodopsin, which bridges these two transmembrane helices, stabilizing the inactive-state conformation. It is also mentioned in this report from 2002 that the same interaction is believed to be preserved in all class A GPCRs. The crystal structures of other GPCRs have revealed that these polar interactions are broken in all the ligand-activated GPCR crystal structures, human β2-adrenoreceptor, turkey β1-andrenoreceptor and human adenosine A2A. We used this information, and our model retains the lack of network of this polar interaction.

In 2005, Evers and Klabunde generated the protein models by applying ligand-supported homology modeling using also bovine rhodopsin as a template.[40] They claimed that the comparison of the different methods in retrieving known antagonists from the virtual libraries shows that the ligand-based screening techniques outperform the molecular docking approach when sufficient ligand information is used for the generation of models. However, they agreed that their study cannot provide an exhaustive comparison of all currently available virtual screening methods. Still we think that their approach is not optimal for docking purposes due to the low sequence similarity and the distant homology to bovine rhodopsin template. It would be much better to see a similar kind of virtual screening study on a 5-HT_{2A} receptor model built using a better template such as adrenergic receptors.

Since 3D-coordinates and the information on model quality through any of the verification tools (Procheck, Verify_3D, Errat, etc) were not available for the model

constructed either by Chambers and Nichols or by Evers and Klabunde, we are unable to perform detailed structure comparisons of our model with theirs.

Recently, in 2009, was published a 5-HT_{2A} receptor homology model based on a human β-2 adrenoreceptor by Bruno et al.[41] Using this GPCR as a template was considered a more suitable template than the bovine rhodopsin template since sequence identity of human 5-HT_{2A} receptor with human β-2 adrenoreceptor is much better (around 30%), than with the bovine rhodopsin template (below 20%), and also both β2 and 5-HT_{2A} receptors belong to amine GPCR, which is a sub-group of class A GPCR. Also Mobarec et al. proposed that generating 5-HT_{2A} receptor homology model based on this template will produce better homology model.[42] We decided to use this template also as our second template. Comparing the alignment constructed by us with the alignment constructed by Bruno et al. was consistent, as well as the disulphide bridge between C148 on TM3 and C227 on ECL2. Since Procheck results for their model were included, we compared them with our Procheck results, and our results shows that fewer residues of our model fall outside the allowed region of Ramachandran plot. However, the docking results we obtained using this model were not in the agreement either with mutagenesis data for ketanserin, or with *in vitro* data for nantenine analogs. We believe this is due to lower resolution that β2-adrenoreceptor template is solved, and since the X-ray structure of this GPCR is solved with an artificial intracellular loop 3 (ICL3). Bruno and co-workers omitted this loop in their modeling, while we generated 10 different homology models using Modeller where we tried to derive the best possible homology model for our docking studies. Ramachandran plot (see Appendix) showed that only a few residues

from this loop (residue range: 265-317) are in generously allowed and disallowed regions.

However, although our model is better in some ways than the previously published models, and there is the advantage that the programs we used for homology building and evaluation are freely available, still the major drawback is the validation of the model that was done only by relatively small library of compounds that mostly share structural similarities. One way to improve the validity of the model is to virtually screen a library of different analogs, synthesize them, and evaluate them in a 5-HT_{2A} receptor assay for affinity and to correlate these results.

A group in 2007 generated a 5-HT_{2A} model using a similar methodology to the one that we described and obtained a binding mode for ketanserin in completely different orientation, still remaining consistency with all mutagenesis data,[43] suggesting valid alternate docked solutions for ketanserin. Once the X-ray structure of ketanserin bound to 5-HT_{2A} receptor is solved we will be able to completely understand the binding modes of this compound. Until then, a reasonable and rational approach is that of a combination of SAR study with molecular modeling of a number of different ligands (not only based on a nantenine scaffold), in order to further validate our model and to provide broader applications. To begin to test our model, we docked three known 5-HT_{2A} receptor antagonists (mianserin, ketanserin and risperidone). The docking scores we obtained could not be correlated with their reported K_i values,[44] probably because of the different orientations that these compounds bind to the receptor.

Our results indicate that the homology model based on a bovine rhodopsin template built by Modeller, showed correlation with the data we obtained from *in vitro*

biological screening at 5-HT_{2A} receptor. Visual inspection of the binding pose of the lead compound nantenine shows all the important interactions that are proposed for nantenine binding in 5-HT_{2A} receptor cleft as proposed by Indra et al. in 2002.[24] It is perhaps not surprising that our results are similar to Indra's, given the high degree of similarity between rat and human 5-HT_{2A} receptors (98%).[21]

Two important hydrogen bonds, one between the protonated nitrogen of nantenine and Asp 155 (located in TM3), and the second one between the oxygen atom of the C1 methoxy group and Asn343 (located in TM6), suggested that nantenine bind in Site 1, according to proposed possible binding sites for 5-HT_{2A} ligands (see Figure 1.6 in Chapter 1).

Furthermore, molecular docking studies also show that C1 nantenine analogs **17-22** bind in a different manner than nantenine, but in a similar orientation among them (Figure 3.26). Visual inspection of the final poses of these compounds, revealed as key interactions two H-bonds - one between Asp155 and protonated nitrogen of the analog, and the other between Ser242 (located in TM 5) and an oxygen atom in the methylenedioxy ring of the nantenine analogs. Hydrophobic interactions between the alkyl group at C1 and the residues Phe234 and Gly238 (both residues located in TM5) seems to be crucial for the enhanced affinity of this series at the 5-HT_{2A} receptor. The docking of C1 compounds suggests that these nantenine analogs also bind in proposed Site 1, but more shifted towards TM5, where their long C1 hydrophobic chain can fit probably much better. Further experimental studies are required to confirm the importance of these residues in the affinity of the analogs.

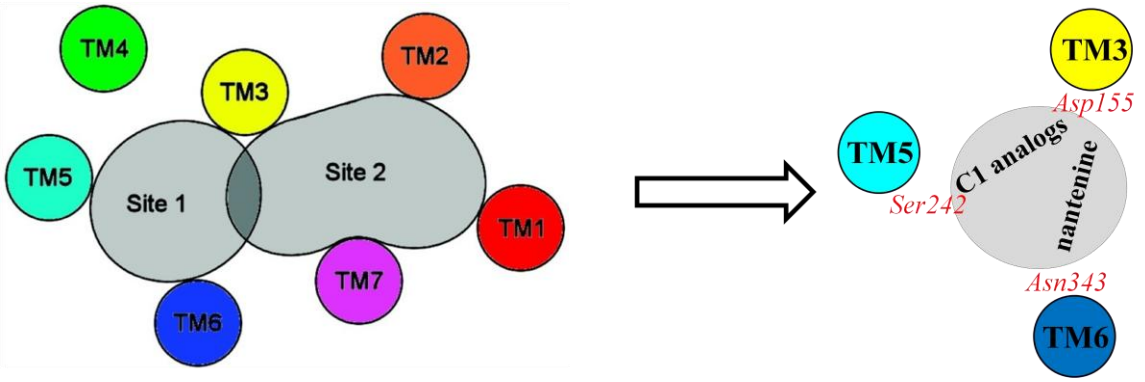

Figure 3.26 Proposed binding orientation of nantenine and C1 nantenine analogs

Our findings presented here will be useful in the future design of high affinity 5-HT_{2A} ligands based on the nantenine aporphine core structure.

For future extrapolations of this work, one can do a virtual screening of various C1 nantenine analogs (Figure 3.27), using Gold software and a selected homology model.

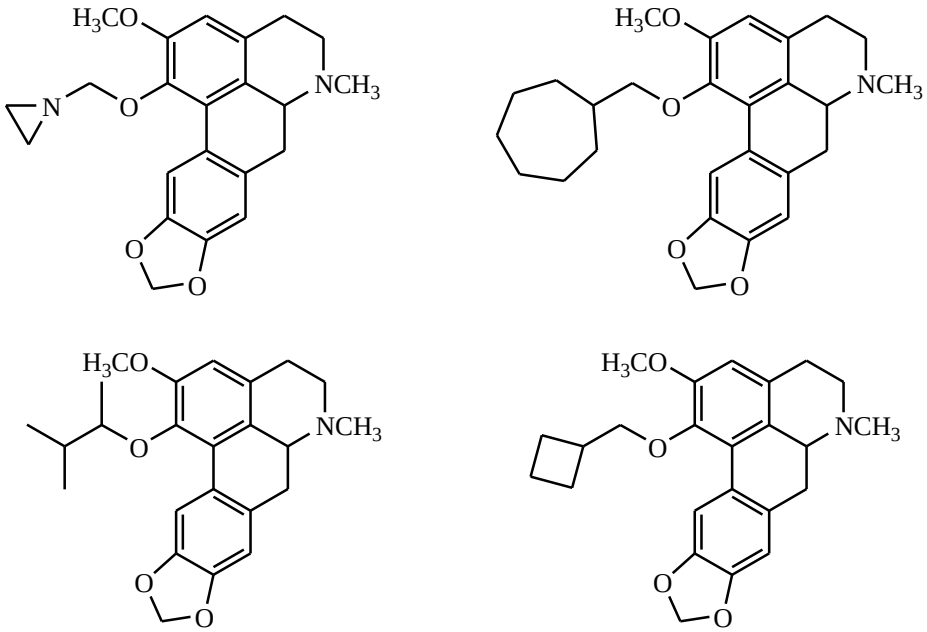

Figure 3.27 Some of the C1 nantenine analogs for future virtual screening study

Once compounds that bind in the same orientation as C1 nantenine analogs previously shown are identified, these compounds could be then synthesized and evaluated *in vitro*. This would allow for testing and refinement of homology model. As a

broader goal it will allow us to identify key pharmacophoric elements for this group of 5-HT_{2A} receptor antagonists.

3.4 Experimental

1) Sequence Alignment, Disulfide Bond Assignment, Model Building, Evaluation/ Selection of the best Model and Energy Minimization

Amino acid sequence of human 5-HT_{2A} receptor was retrieved from NCBI protein database.[45] Program BLASTP[14] was used to search for a suitable template from the protein structure database (PDB) for homology modeling. Sequence alignment was carried out with the ClustalX[46] software (using the Gonnet series matrix with the "gap open" and "gap elongation" penalties of 10 and 0.2 respectively) and ICM Pro 3.6[26] (based on ZEGA sequence alignment[27] - Needleman and Wunsch algorithm with zero gap and penalties). The alignment was then manually refined to ensure a perfect alignment of the highly conserved residues of GPCR superfamily, according to Baldwin et al.[28] The conserved disulfide bond between residue C148 at the beginning of TM3 and the cysteine C228 in the middle of extracellular loop 2 (a feature common to many GPCR receptors) was also created and was kept as a constraint in the geometric optimization. To make the homology models we used programs Modeller[29] by employing Discovery Studio 2.0 of Accelrys Inc and ICM Pro 3.6. Between several crystal structures available in PDB, as a template we selected bovine rhodopsin (PDB code 1U19) since in many previous reports it has been used as a good template for 5-HT_{2A} receptor and also because its crystal structure is solved at high resolution 2.20 Å. We also selected β2-adrenergic receptor (PDB code 2RH1) as a template, because this is up to date the highest solved

resolution (2.40 Å) of any GPCR neurotransmitter receptor. Twenty models were built for each of the template using Modeller and one model for each template using program ICM Pro 3.6. All homology models were evaluated using several different model evaluation tools such as Procheck, Verify3D, Errat, What_check and Prove from SAVES metaserver. After we evaluated each model using above methods we selected the final models, one from each template, which fits best by criteria of selection in each method. The best docking solution was energy minimized with the CHARMM as implemented in Discovery Studio 2.0 of Accerlys Inc., by applying 500 cycles of Smart Minimizer Algorithm, followed by gradient minimization until RMS gradient was lower than 0.01 kcal/molÅ. The models were renumbered, according to their original sequence. The four selected homology models were than superimposed with their templates using the protocol in Discovery Studio 2.0: structure superimposing by sequence alignment, and we determined the RMSD value for each model.

2) Preparing the Analogs and Receptors, Grid Generation and Docking Experiments

Nantenine and all analogs were drawn as 2D structure with ChemDraw Ultra version 9.0, with a formal positive charge centered on the nitrogen, and than energy minimized through Chem3D Ultra version 9.0/MOPAC, Job Type: Minimum RMS Gradient of 0.010 kcal/mol and RMS distance of 0.1 Å, and saved as MDL MolFiles (*.mol) for purpose of docking with ICM Pro, or as SYBYL2 files (*.mol2) for the purpose of docking with Glide and Gold software. Before docking with the Glide and Gold each analog was prepared using the LigPrep, an application that is available through Maestro 7.5 (a Linux graphical interface for Schrödinger06). After employing the energy minimization through MacroModel application, each 3D structure was saved as SD file

(*.sdf), and combined into one analogs library SD file, to be used for docking experiments. ICM docking: first the binding site of homology receptors was identified. The binding site was reviewed and adjusted: ICM made a box around the ligand binding site based on the information entered in the receptor setup section. The position of the box encompassed the residues expected to be involved in ligand binding. Then the receptor maps were made: Energy maps of the environment within the docking box were constructed. Flexibility of the receptor residues was set to 4.0. Interactive docking was used to dock nantenine and the other analogs. The thoroughness level was set to the maximum value of 10. ICM scores were obtained after this procedure. Glide docking: each homology receptor was prepared by Protein Preparation mode of Glide, and then the receptor grid was generated by specifying Asp155 as a central residue and selecting Extra Precision docking within 20 Å of it. After this step the G-scores were determined and the docking poses of each analog were visually inspected using Glide Pose Viewer. Gold docking: as input file for Gold docking both homology models were used as a PDB file. In Gold Wizard setup hydrogens were added, and the binding site was defined as the residues that are falling within 15 Å of Asp155. We chose Gold Score as fitness function. After docking was finished we inspected visually each top-scoring receptor-analog complex. High-scoring complexes that did not meet hydrogen bond Asp155-NH_3^+ requirement were discarded.

3) *Visualization of Selected Docking Posses*

All final receptor-analog complexes, obtained from three different programs, were saved as PDB files and visualized using 3D Window of Discovery Studio 2.0. Hydrogen bonds, hydrophobic interactions and distances for each 3D structure were calculated and

plotted by LigPlot v4.4.2., a program for schematic 2D diagrams of ligand and receptor plots. Hydrogen bonds are indicated by dashed lines between the atoms involved, while hydrophobic contacts are represented by an arc with spokes radiating towards the ligand atoms they contact.

3.5 Appendix

Table 3-1. Percentage sequence identity and expectation value of GPCR proteins with respect to human 5-HT_{2A} receptor obtained from BLAST. Sequence identity refers to the percentage of matches of the same amino acid residues between two aligned sequences. The lower the E-value, the more significant the score.

PDB ID	Description	Identity(%)	E-Value
2VT4_B	Chain B, Turkey Beta1-Adrenergic Receptor with Stabilizing Mutations	37	6e-37
2R4S_A	Chain A, Crystal Structure of the Human Beta2 Adrenoreceptor	35	6e-29
2R4R_A	Chain A, Crystal Structure of the Human Beta2 Adrenoreceptor	35	9e-29
2RH1_A	Chain A, High Resolution Crystal Structure of Human Beta2-Adrenergic GPCR	33	4e-23
3EML_A	Chain A, 2.6 Å Crystal Structure of a Human A2a Adenosine Receptor	32	2e-13
1U19_A	Chain A, Crystal Structure Of Bovine Rhodopsin at 2.2 Å Resolution	23	2e-12

Table 3-2. Ramachandran plot values and G-factors for all 5-HT_{2A} receptor homology models and their templates. Ramachandran plot qualities show the percentage of residues present in the core, allowed (AL), generally allowed (GA) and disallowed (DA) region of the plot. Greater percentage of residues in core region is indicator of good structure. Goodness factors show the quality of dihedral (DH), covalent (CV) and overall (OA) bond/angle distances; scores above -0.5 indicates a reliable model.

	Ramachandran Plot				**G-Factors**			**Ramachendran Plot**				**G-Factors**		
DS	**Core**	**AL**	**GA**	**DA**	**DH**	**CV**	**OA**	**Core**	**AL**	**GA**	**DA**	**DH**	**CV**	**OA**
	BRho Template							HAdrb2 Template						
M1	87.8	10.2	1.7	0.3	-0.05	-0.32	-0.15	89.3	6.9	2.4	1.4	0.03	-0.35	-0.11
M2	89.1	8.5	1.4	1	0.05	-0.33	-0.09	90	7.2	1.4	1.4	0	-0.82	-0.31
M3	88.8	8.8	1.7	0.7	0.07	-0.24	-0.05	89.7	7.2	2.8	0.3	0	-0.69	-0.26
M4	90.8	6.8	2	0.3	0.02	-0.25	-0.08	88.6	7.2	2.4	1.7	0	-0.61	-0.23
M5	87.1	11.2	1	0.7	0.03	-0.22	-0.06	88.3	8.3	2.8	0.7	-0.10	-1.05	-0.45
M6	88.1	8.8	3.1	0	-0.06	-0.38	-0.18	91.4	5.5	2.4	0.7	0.04	-0.31	-0.09
M7	88.4	8.8	2.4	0.3	0.04	-0.22	-0.06	91	5.5	2.4	1	0.03	-0.34	-0.11
M8	86.7	10.2	1.7	1.4	-0.06	-0.31	-0.15	89.3	7.2	1.4	2.1	0.05	-0.32	-0.09
M9	90.1	7.5	1	1.4	0.05	-0.24	-0.06	89	6.9	2.8	1.4	0.04	-0.3	-0.09
M10	90.5	7.1	2	0.3	0.05	-0.22	-0.05	90.7	6.6	1.4	1.4	0.03	-0.29	-0.09
M11	85.7	9.9	3.1	1.4	-0.13	-0.50	-0.26	86.6	7.9	3.4	2.1	-0.04	-1.01	-0.39
M12	87.4	9.2	2	1.4	-0.02	-0.65	-0.24	86.9	6.9	3.4	2.8	-0.08	-1.53	-0.62
M13	86.1	9.9	2.7	1.4	-0.02	-0.40	-0.18	86.9	7.9	4.1	1	-0.09	-1.18	-0.49
M14	87.5	9.5	2.4	2.4	-0.04	-0.42	-0.18	86.2	7.9	3.1	2.8	-0.05	-0.88	-0.35
M15	84	11.9	2.4	1.7	-0.02	-0.41	-0.16	87.2	9	2.4	1.4	-0.14	-1.12	-0.5
M16	86.1	10.5	2.7	0.7	-0.10	-0.57	-0.27	88.6	6.6	2.1	2.8	-0.06	-1.10	-0.44
M17	86.7	8.8	3.4	1	-0.05	-0.69	-0.29	87.9	6.9	3.4	1.7	-0.05	-0.78	-0.31
M18	84.4	10.9	3.1	1.7	-0.11	-0.44	-0.23	87.9	6.6	2.4	3.1	-0.02	-0.97	-0.37
M19	86.1	9.2	3.4	1.4	0	-0.46	-0.17	83.8	9	6.2	1	-0.08	-0.97	-0.4
M20	86.4	8.5	4.1	1	-0.03	-0.54	-0.22	87.6	7.2	2.1	3.1	-0.05	-1.07	-0.42
ICM	85	12.4	2.1	0.4	0.01	-0.24	-0.15	94.3	5.2	0.5	0	0.02	-0.05	-0.05
1U19	79.9	15.5	4	0.7	0.02	0.39	0.16							
2RH1								94.2	5.4	0.4	0	0.21	0.43	0.28

Table 3-3. Overall Quality Factor given by ERRAT. This is expressed as the percentage of protein for which the calculated error value falls below the 95% rejection limit. Good structures produce values above 90 and accepted range is above 50. The template structures 1U19 and 2RH1 have ERRAT values of 85.294 and 97.08 respectively.

OQF in % for 5-HT$_{2A}$ receptor homology models							
BRho Template				**HAdrb2 Template**			
M1	60	**M11**	58.71	**M1**	72.759	**M11**	71.575
M2	64.194	**M12**	66.774	**M2**	68.243	**M12**	70.169
M3	68.71	**M13**	67.419	**M3**	75.258	**M13**	75.945
M4	69.677	**M14**	71.613	**M4**	68.687	**M14**	76.431
M5	66.452	**M15**	69.677	**M5**	62.626	**M15**	70.946
M6	53.548	**M16**	57.742	**M6**	75.958	**M16**	74.216
M7	67.097	**M17**	70	**M7**	80	**M17**	88.772
M8	70.323	**M18**	70.645	**M8**	78.351	**M18**	75.258
M9	62.258	**M19**	60.645	**M9**	81.053	**M19**	80.282
M10	65.484	**M20**	66.129	**M10**	72.542	**M20**	66.441
ICM	N.A.	**1U19**	85.294	**ICM**	N.A.	**2RH1**	97.08

Table 3-4. Evaluation of 5-HT_{2A} recepotor homology models using PROVE. Atoms in test receptors are scored using a Z-score standard deviation (Zstd), which is how many standard deviations their volume is from the mean (Zsm) for that atom type . A structural Z-score RMS (Zrms) is calculated using the square root of these scores. High scores have been found to be associated with uncertainty in the structure. Structures with poor resolution generally have a Zrms greater than 1.2, while for well resolved structures, the Zrms is around 1.0.

		M1	**M2**	**M3**	**M4**	**M5**	**M6**	**M7**	**M8**	**M9**	**M10**	**ICM**
BRho Template	Zsm	0.352	1.348	0.369	2.192	1.266	0.304	1.335	1.405	0.431	1.369	-0.645
	Z-std	30.676	43.206	30.114	51.525	42.362	30.272	43.124	43.491	30.107	42.865	2.175
	Zrms	30.663	43.207	30.102	51.548	42.362	30.259	43.125	43.493	30.096	42.868	2.268
		M11	**M12**	**M13**	**M14**	**M15**	**M16**	**M17**	**M18**	**M19**	**M20**	**1U19**
	Zsm	1.451	66.774	67.419	71.613	69.677	57.742	70	70.645	60.645	66.129	0.612
	Z-std	44.075	0.549	0.468	0.553	0.522	0.444	0.579	0.515	0.496	0.482	26.888
	Zrms	44.078	30.402	30.288	30.497	30.108	30.833	31.279	30.917	30.241	29.821	26.885

		M1	**M2**	**M3**	**M4**	**M5**	**M6**	**M7**	**M8**	**M9**	**M10**	**ICM**
HArdb2 Template	Zsm	0.513	-0.42	-0.36	0.522	-0.47	-0.463	-0.421	0.624	-0.306	-0.476	0.728
	Z-std	30.503	1.703	1.673	30.804	1.675	1.735	1.701	30.944	1.675	1.66	31.73
	Zrms	30.493	1.753	1.71	30.793	1.739	1.795	1.752	30.936	1.702	1.726	31.722
		M11	**M12**	**M13**	**M14**	**M15**	**M16**	**M17**	**M18**	**M19**	**M20**	**2RH1**
	Zsm	0.618	0.459	0.67	0.712	0.693	-0.354	-0.225	0.615	-0.257	0.376	0.147
	Z-std	30.718	30.533	31.276	31.507	31.212	1.747	1.687	31.744	1.69	30.664	1.191
	Zrms	30.709	30.522	31.268	31.499	31.204	1.782	1.701	31.734	1.708	30.652	1.199

Table 3-5. Percentage of residues that exhibit a score of > 0.2. Verify3D average data score of all the models generated in comparison with template. The score which matches the template and has value > 0.2 for all or most of the residues indicates a reliable model. Negative or less than 0.2 scores are indicative of potential problems.

Verify3D % of residues that exhibit a score above 0.2							
BRho Template				**HAdrb2 Template**			
M1	32.6	**M11**	35.1	**M1**	43.49	**M11**	37.14
M2	35.11	**M12**	38.56	**M2**	56.83	**M12**	36.51
M3	38.24	**M13**	39.18	**M3**	49.52	**M13**	48.25
M4	39.5	**M14**	40.1	**M4**	52.7	**M14**	50.48
M5	40.75	**M15**	45.77	**M5**	48.89	**M15**	38.41
M6	33.9	**M16**	37.3	**M6**	50.79	**M16**	45.71
M7	37.3	**M17**	34.48	**M7**	50.16	**M17**	50.16
M8	33.54	**M18**	32.92	**M8**	47.62	**M18**	29.52
M9	32.9	**M19**	35.1	**M9**	53.97	**M19**	52.7
M10	35.74	**M20**	40.44	**M10**	52.38	**M20**	42.54
ICM	35.27	**1U19**	75.1	**ICM**	45.60	**2RH1**	72.79

Table 3-6. What_check results for the 5-HT_{2A} receptor homology models based on bovine rhodopsin template (1U19). Structure Z-scores: Second generation packing quality, Ramachandran plot appearance, chi-1/chi-2 rotamer normality, Backbone conformation, and RMS Z-scores, should be positive numbers. Bond lengths, Bond angles, Omega angle restraints, Side chain planarity, Improper dihedral distribution and Inside/Outside distribution should be close to 1.0.

BRho Template

	M1	**M2**	**M3**	**M4**	**M5**	**M6**	**M7**	**M8**	**M9**	**M10**	**ICM**
packing quality	-2.124	-1.714	-1.719	-1.737	-1.782	-2.155	-1.831	-2.136	-1.721	-1.883	-2.541
Ramach. plot	0.937	0.91	0.908	0.79	0.97	0.619	0.865	0.56	0.891	1.046	-4.287
chi-1/chi-2	-2.254	-1.593	-1.112	-2.248	-1.757	-2.835	-1.862	-2.666	-1.547	-2.023	-3.224
Backbone conf.	-8.31	-7.931	-7.669	-8.008	-7.118	-8.539	-7.572	-8.295	-7.728	-8.024	-9.501
Bond lengths	0.947	0.934	0.929	0.927	0.926	1.289	0.932	0.942	0.935	0.924	1.102
Bond angles	1.324	1.309	1.269	1.293	1.264	1.369	1.29	1.337	1.275	1.285	1.071
Ω angle rest.	0.727	0.746	0.725	0.751	1.321	0.823	0.639	0.784	0.692	0.661	0.825
Side chain planarity	0.362	0.362	0.344	0.349	0.281	0.345	0.323	0.28	0.335	0.353	0.142
Iddistrib.	1.017	0.959	1.302	1.299	0.948	0.936	1.316	1.322	1.297	1.296	1.578
I/O distrib.	1.32	1.341	0.866	0.94	0.722	0.955	0.906	0.892	0.917	0.88	1.289
	M11	**M12**	**M13**	**M14**	**M15**	**M16**	**M17**	**M18**	**M19**	**M20**	**1U19**
packing quality	-2.356	-1.754	-1.671	-1.838	-1.775	-2.211	-1.991	-2.191	-1.698	-1.869	-0.506
Ramach. plot	0.631	0.656	0.501	0.572	0.664	0.209	0.584	0.205	0.34	0.615	-4.392
chi-1/chi-2	-2.477	-1.9	-1.176	-2.084	-2.029	-2.967	-2.047	-2.629	-1.611	-2.419	-2.384
Backbone conf.	-8.533	-7.652	-8.675	-7.699	-8.572	-9.033	-9.17	-9.873	-7.809	-9.368	-7.197
Bond lengths	0.949	0.959	0.968	0.939	0.934	0.96	1.064	0.953	1.285	0.971	0.541
Bond angles	1.424	1.486	1.285	1.3	1.36	1.433	1.421	1.41	1.401	1.474	0.718
Ω angle rest.	0.801	1.01	0.882	0.954	0.744	0.897	0.921	0.95	0.825	0.962	0.284
Side chain planarity	0.336	0.697	0.509	0.527	1.314	1.288	0.344	1.322	0.593	0.496	0.295
Iddistrib.	1.31	1.315	0.975	1.224	1.001	1.161	3.466	0.999	1.124	1.3	1.212
I/O distrib.	1.316	1.194	1.368	1.362	0.508	0.44	1.312	0.604	0.965	1.218	0.484

Table 3-7. What_check results for the 5-HT_{2A} receptor homology models based on human β2-adrenoreceptor template (2RH1). Structure Z-scores: Second generation packing quality, Ramachandran plot appearance, chi-1/chi-2 rotamer normality, Backbone conformation, and RMS Z-scores, should be positive numbers. Bond lengths, Bond angles, Omega angle restraints, Side chain planarity, Improper dihedral distribution and Inside/Outside distribution should be close to 1.0.

HAdrb2 Template		**M1**	**M2**	**M3**	**M4**	**M5**	**M6**	**M7**	**M8**	**M9**	**M10**	**ICM**
	packing quality	-1.601	-1.929	-1.785	-1.681	N/A	-1.775	-1.711	-1.509	-1.751	-1.618	-0.958
	Ramach. plot	1.065	1.174	1.042	1.121	N/A	1.518	1.582	1.113	0.923	1.929	-2.047
	chi-1/chi-2	-1.424	-1.768	-1.864	-1.53	N/A	-1.968	-2.061	-1.26	-1.484	-1.562	-1.954
	Backbone conf.	-11.024	-11.769	-11.844	-9.188	N/A	-12.027	-9.085	-10.353	-9.494	-9.759	-6.908
	Bond lengths	0.924	1.084	1.045	0.992	N/A	0.929	0.931	0.922	0.925	0.921	1.13
	Bond angles	1.336	1.441	1.449	1.374	N/A	1.325	1.356	1.333	1.338	1.325	0.986
	Ω angle rest.	0.911	1.264	0.866	0.872	N/A	0.757	0.824	0.81	0.804	0.839	0.813
	Side chain planarity	0.345	0.294	0.298	0.439	N/A	0.42	0.359	0.341	0.279	0.397	0.054
	Iddistrib.	0.873	1.004	1.07	0.925	N/A	0.872	0.921	0.893	0.918	0.897	2.784
	I/O distrib.	1.282	1.251	1.269	1.246	N/A	1.261	1.245	1.259	1.245	1.25	1.235
		M11	**M12**	**M13**	**M14**	**M15**	**M16**	**M17**	**M18**	**M19**	**M20**	**1U19**
	packing quality	-1.762	-1.86	-1.815	-1.903	-2.07	-1.908	-1.785	-1.61	-1.697	-1.76	0.747
	Ramach. plot	0.477	0.747	0.683	0.84	0.585	1.15	1.033	0.871	0.298	1.694	-0.694
	chi-1/chi-2	-1.407	-1.78	-1.958	-1.673	-2.63	-2.291	-2.46	-1.447	-1.795	-1.961	0.369
	Backbone conf.	-11.15	-14.04	-12.07	-11.72	-12.2	-13.95	-10.78	-11.51	-11.00	-10.42	-3.196
	Bond lengths	1.144	1.177	2.035	1.079	1.114	1.139	0.975	1.077	1.02	1.671	0.577
	Bond angles	1.517	1.617	1.593	1.549	1.555	1.508	1.5	1.491	1.546	1.584	0.667
	Ω angle rest.	1.136	1.546	1.107	0.934	1.31	1.058	0.87	1.14	1.016	1.048	0.635
	Side chain planarity	0.467	0.429	0.464	0.405	0.375	0.451	0.41	0.393	0.362	0.999	0.064
	Iddistrib.	1.096	1.241	1.785	1.149	1.26	3.434	1.139	1.23	3.571	1.253	0.371
	I/O distrib.	1.281	1.261	1.29	1.25	1.268	1.283	1.261	1.271	1.259	1.258	1.219

Table 3-8. Results of docking experiments with ICM Pro, GLIDE and GOLD

		HAdrb2 ICM	BRho ICM	HAdrb2 Modeller	BRho Modeller	HAdrb2 Modeller	BRho Modeller
Compound	K_e, nM	ICM score	ICM score	GLIDE score	GLIDE score	GOLD score	GOLD score
Ketanserin	32	-75.82	-72.28	-11.43	-4.30	27.34	30.63
± **Nantenine**	850 ± 6	-54.93	N/A	-11.23	-8.03	27.19	23.42
1	>10000	-48.30	N/A	-12.03	-8.50	29.72	N/A
2	>10000	-50.94	N/A	N/A	-8.47	N/A	N/A
3	>10000	-50.40	N/A	N/A	-8.47	N/A	N/A
4	5180	-54.32	-47.69	-13.53	-8.76	31.44	20.81
5	>10000	N/A[a]	N/A	-10	-9.05	N/A	N/A
6	>10000	-51.64	N/A	-13.81	-8.31	30.84	N/A
7	>10000	N/A	N/A	-13.48	-8.22	33.83	N/A
8	>10000	-58.87	N/A	N/A	N/A	N/A	N/A
9	>10000	N/A	N/A	N/A	N/A	N/A	N/A
10	>10000	-65.45	-48.69	-9.53	N/A	34.16	N/A
11	>10000	-54.29	-50.98	N/A	-8.48	N/A	N/A
12	>10000	-63.71	N/A	N/A	-6.88	N/A	N/A
13	1200	-62.14	N/A	-10.1	-8.03	34.77	N/A
14	N/A	-53.27	N/A	-10.58	-8.31	31.66	21.61
15	>10000	-49.56	-49.55	-11.13	-8.03	N/A	N/A
16	N/A	-60.73	-50.71	-12.04	-8.3	32.63	22.71
17	890 ± 430	-55.14	N/A	-11.45	-8.30	30.19	24.22
18	297 ± 130	-65.37	-51.87	-8.94	-9.09	31.78	22.98
19	274 ± 80	-68.37	-54.23	-11.20	-5.01	32.53	29.10
20	171 ± 50	-70.39	N/A	-12.06	-5.05	33.17	30.52
21	68 ± 8	-64.75	N/A	-12.21	-8.03	33.30	29.06
22	4600	-69.79	N/A	-13.44	-11.67	35.64	29.48

[a]N/A - out of the binding pocket or no key Asp155-NH_3^+ interaction

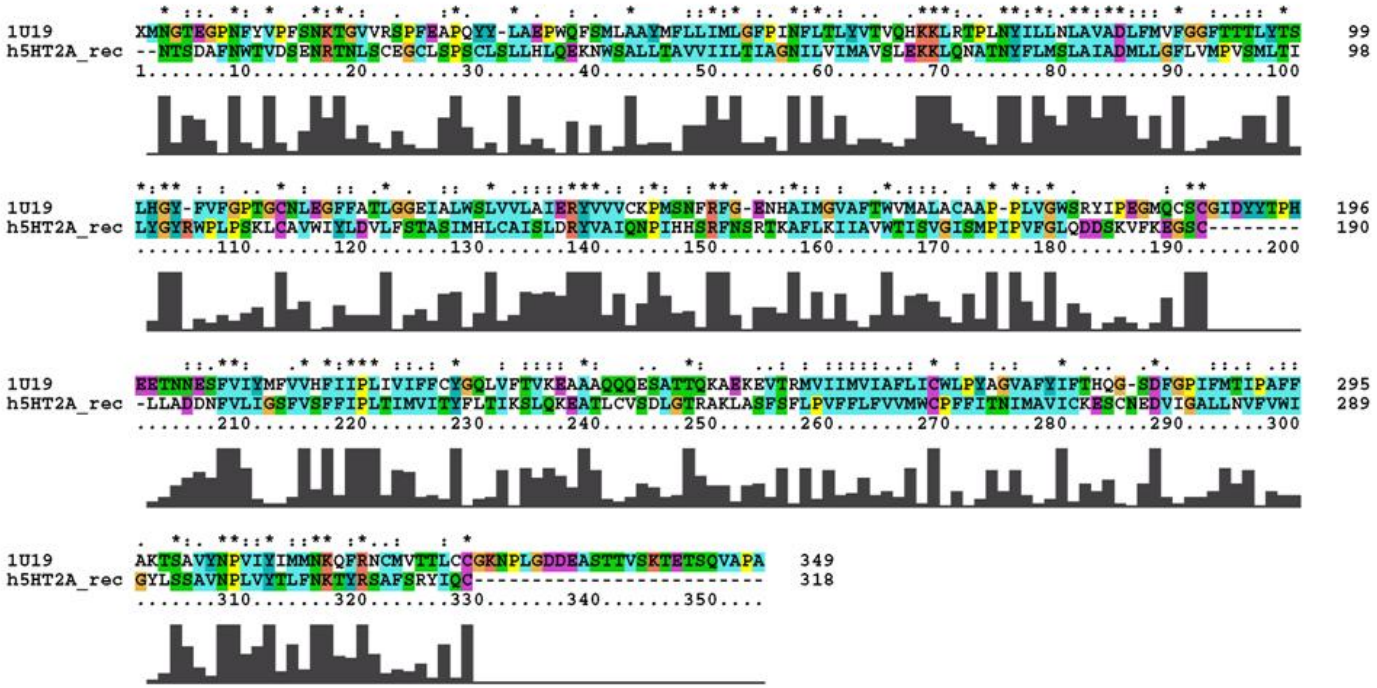

Figure 3.2 ClustalX sequence alignment of human 5-HT_{2A} receptor sequence with the bovine rhodopsine template (PDB: 1U19)

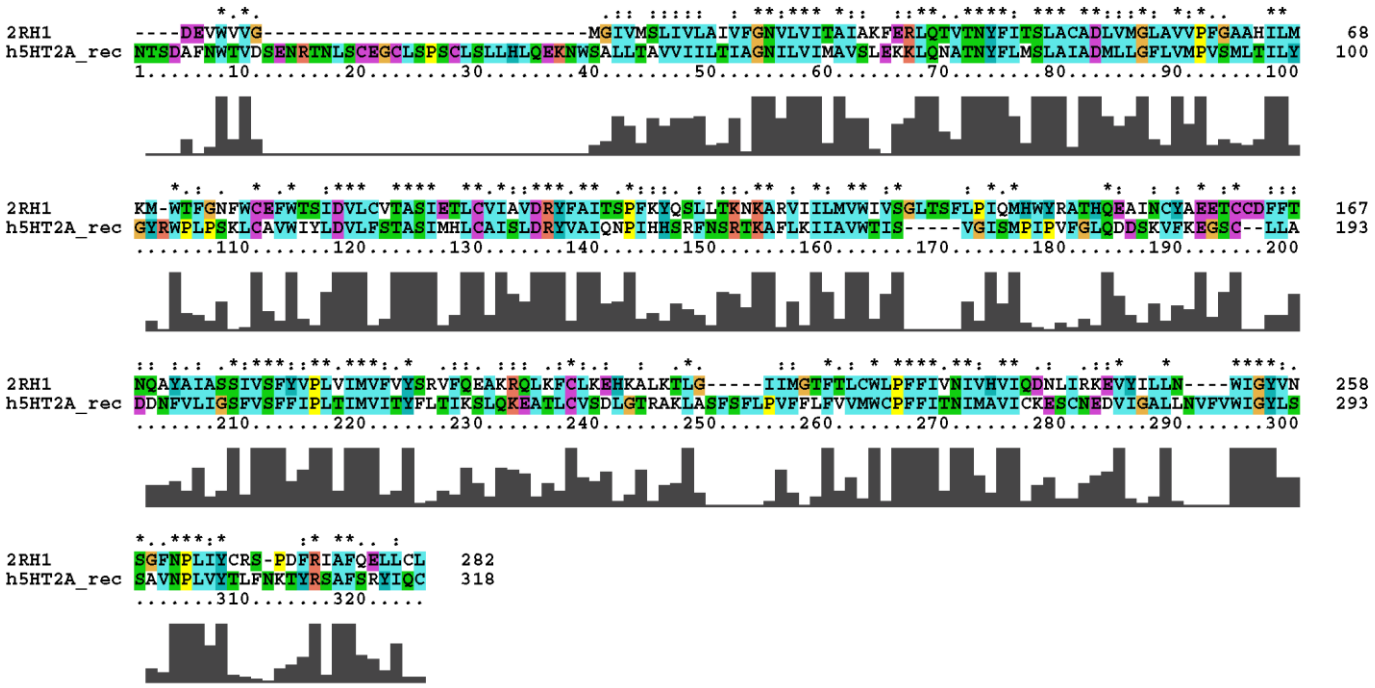

Figure 3.3 ClustalX sequence alignment of human 5-HT_{2A} receptor sequence with the human β2- adrenoreceptor template (PDB: 2RH1)

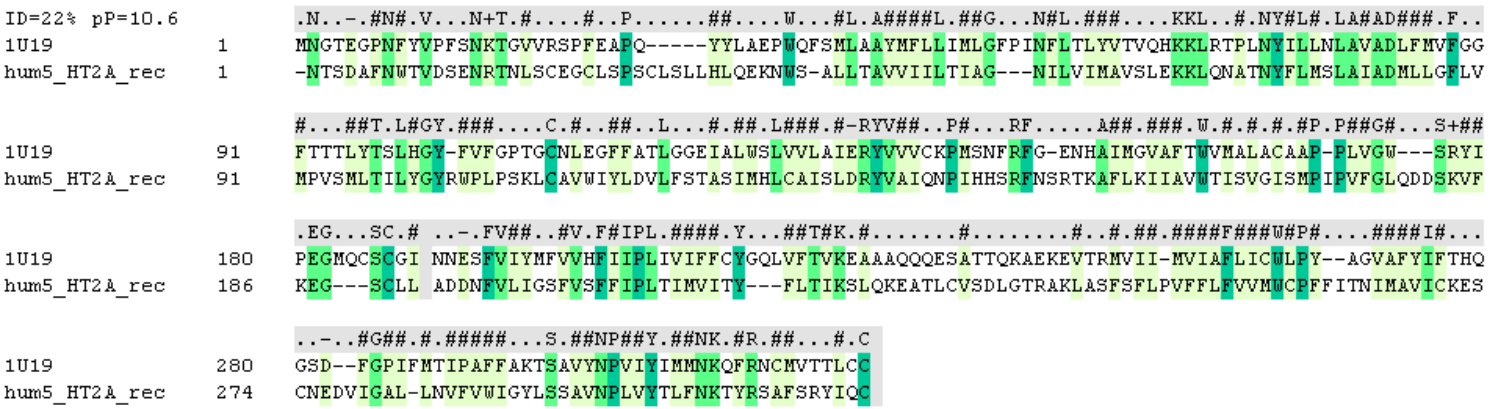

Figure 3.4 ICM Pro sequence alignment of human 5-HT_{2A} receptor sequence with the bovine rhodopsine template (PDB: 1U19)

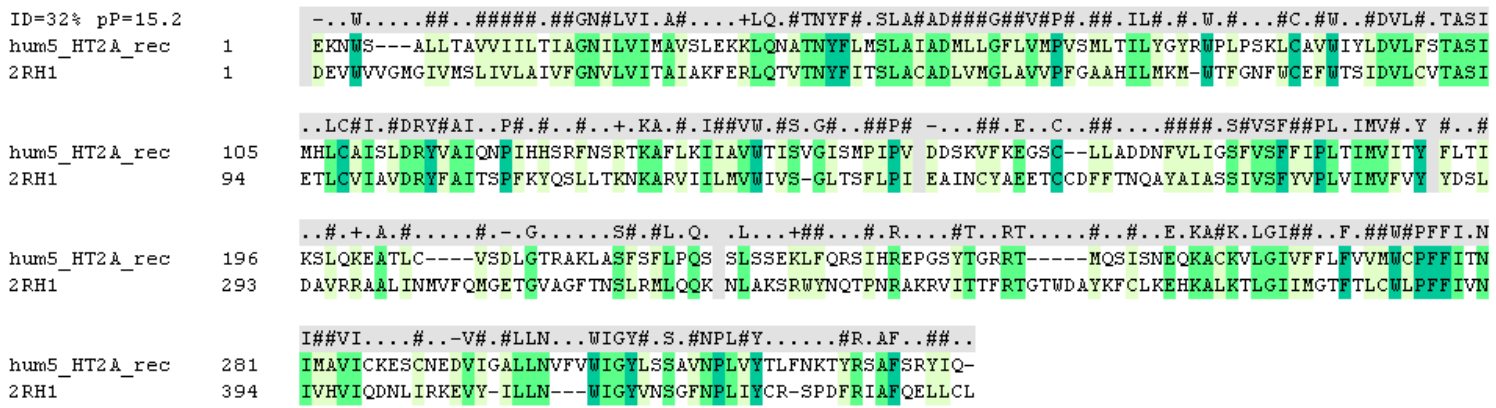

Figure 3.5 ICM Pro sequence alignment of human 5-HT_{2A} receptor sequence with the human β2- adrenoreceptor template (PDB: 2RH1)

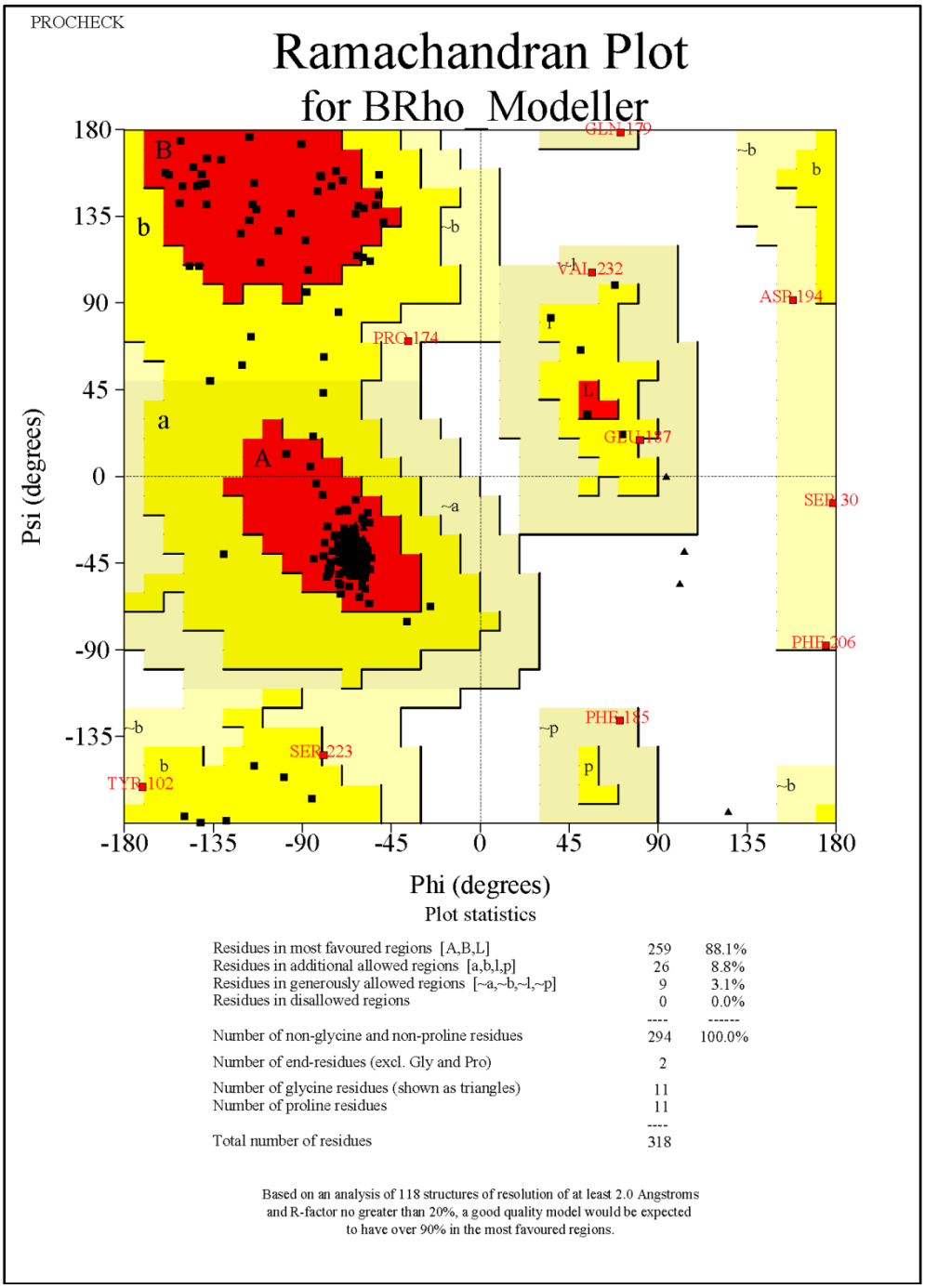

Figure 3.7. Ramachandran plot for BRho_Modeller: a final, selected homology model built by MODELLER based on bovine rhodopsine template (PDB: 1U19)

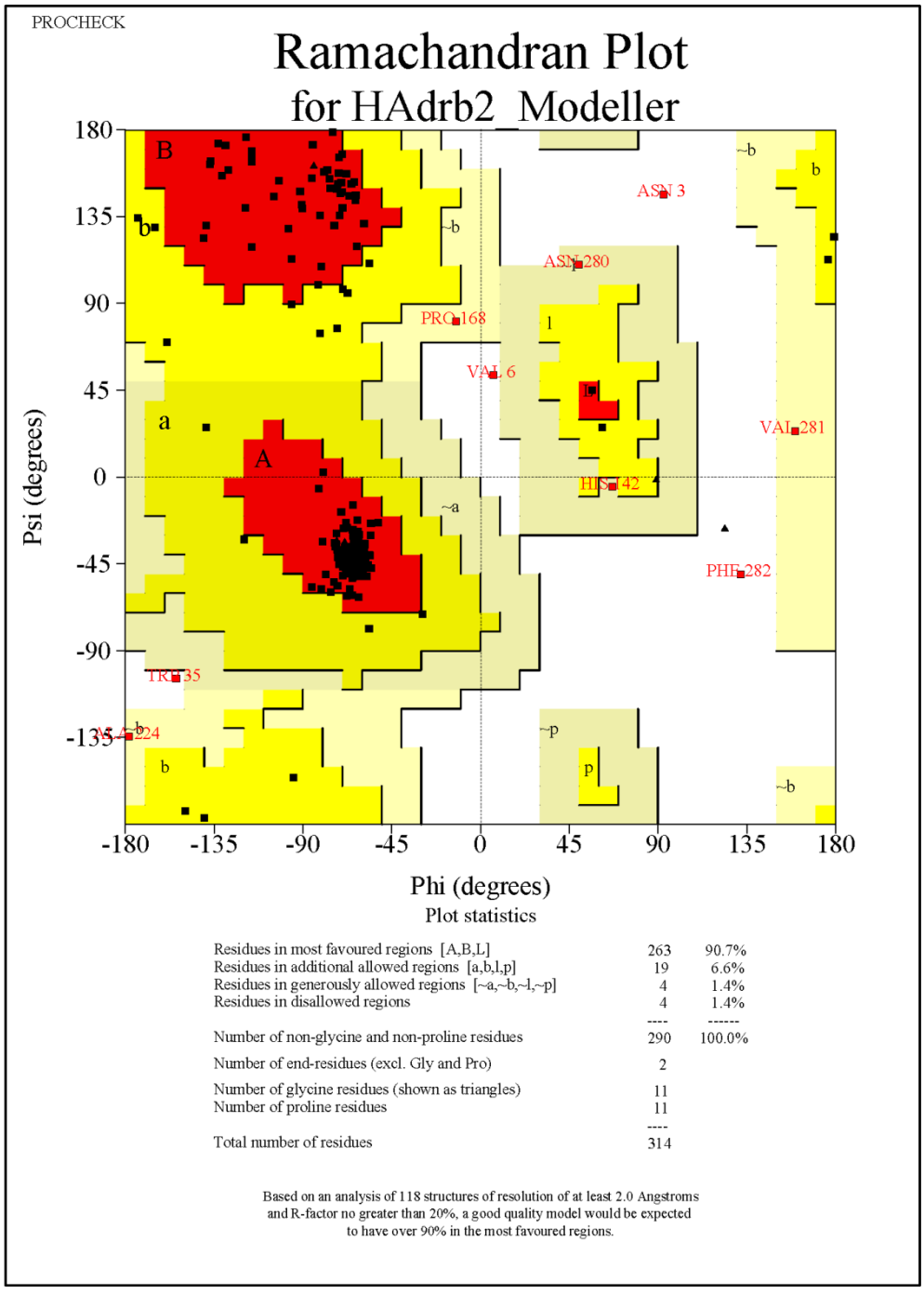

Figure 3.8. Ramachandran plot for HAdrb2_Modeller: a final, selected homology model built by MODELLER based on human β2- adrenoreceptor template (PDB: 2RH1)

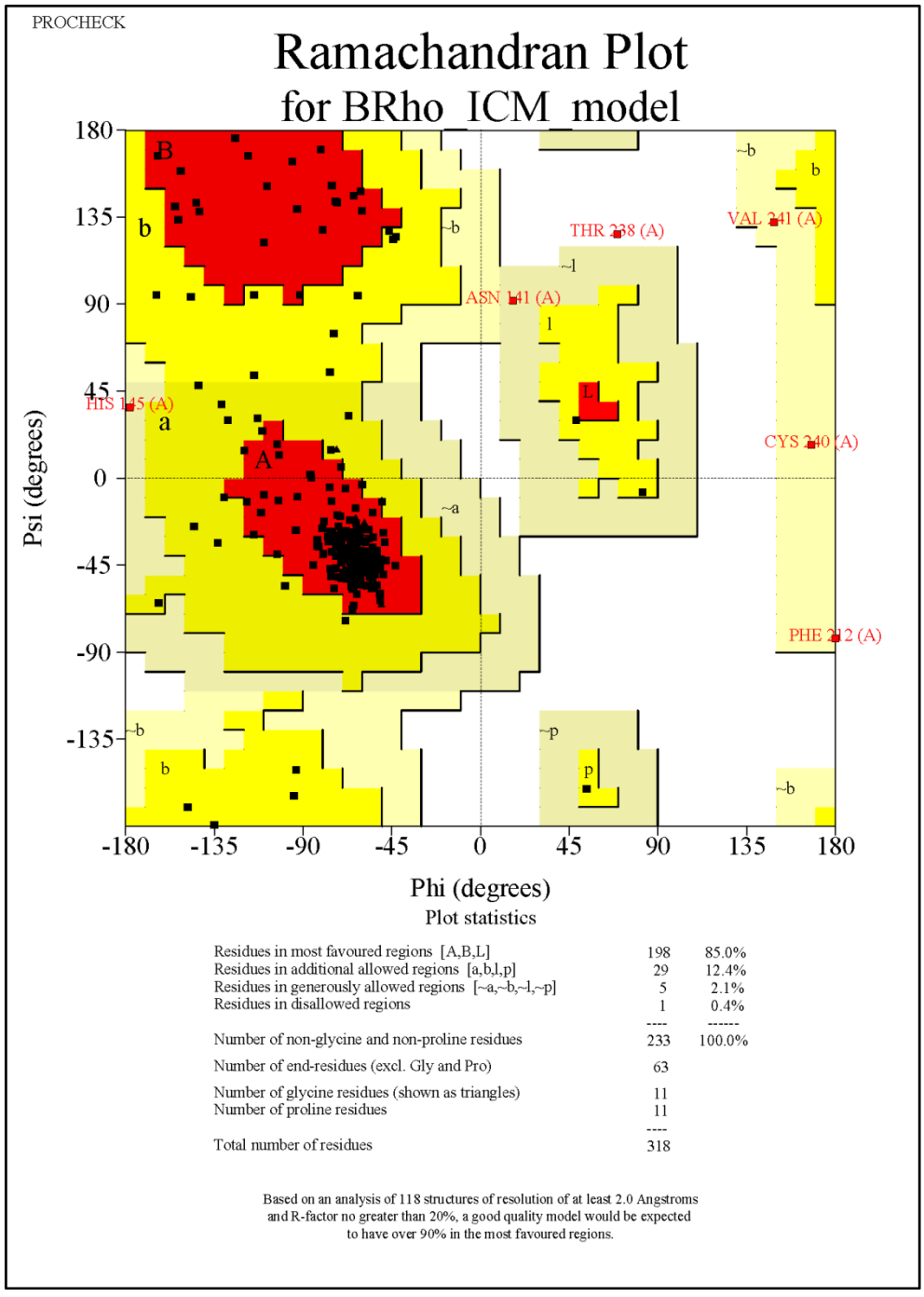

Figure 3.9. Ramachandran plot for BRho_ICM: a final, selected homology model built by ICM Pro based on bovine rhodopsine template (PDB: 1U19)

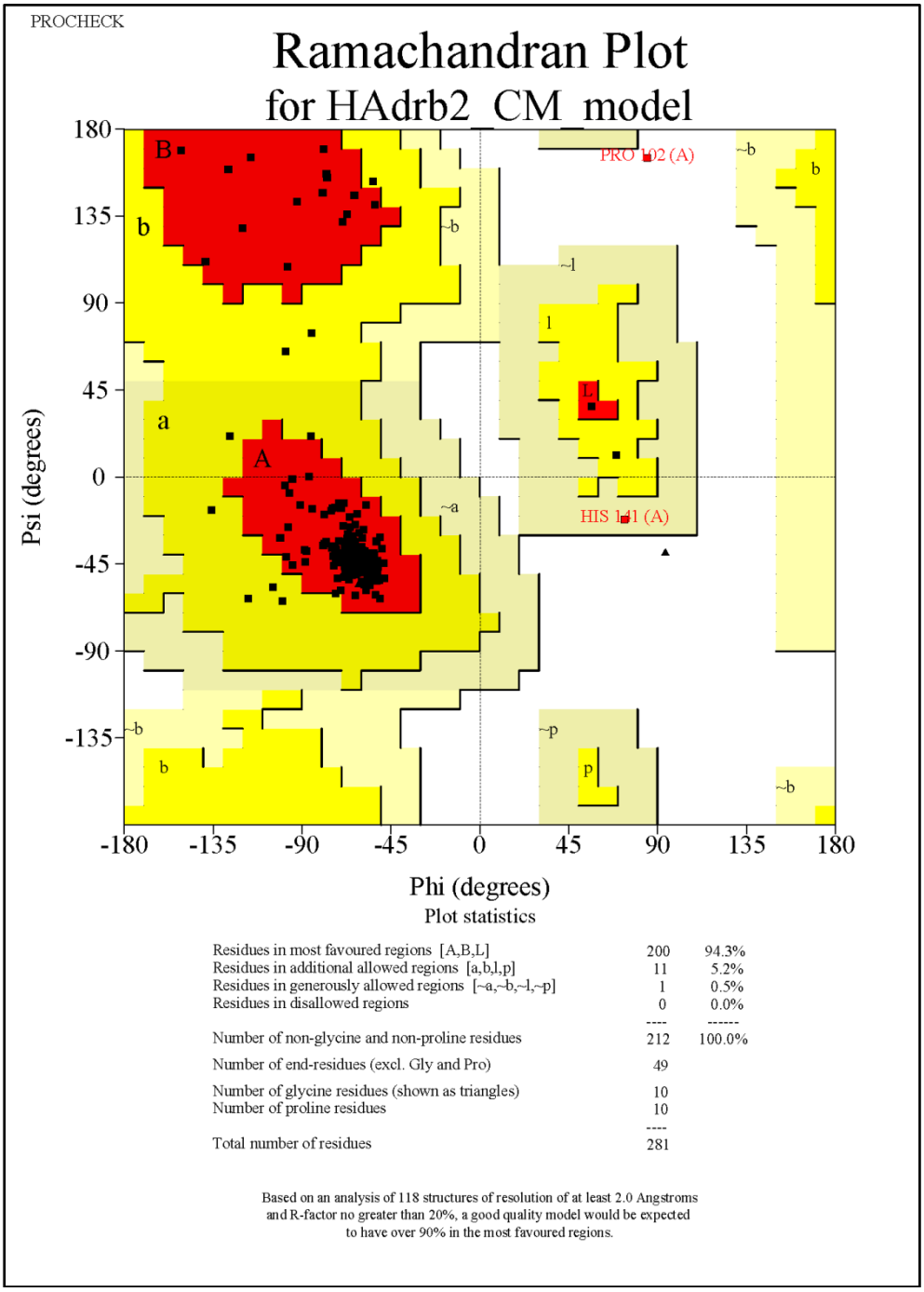

Figure 3.10. Ramachandran plot for HAdrb2_ICM: a final, selected homology model built by ICM Pro based on human β2- adrenoreceptor template (PDB: 2RH1)

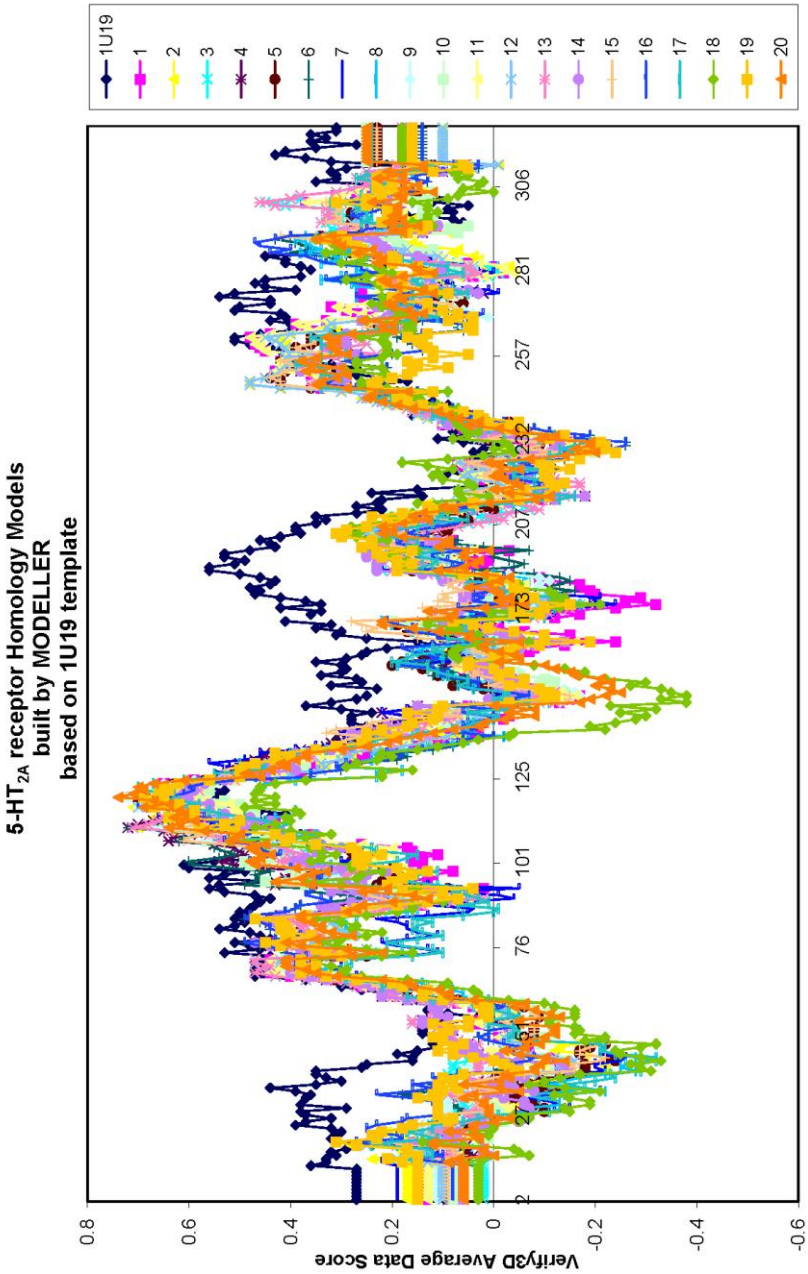

Figure 3.11. Verify3D plots of all homology models built based on a bovine rhodopsin template compared with a plot of the template 1U19 (blue color)

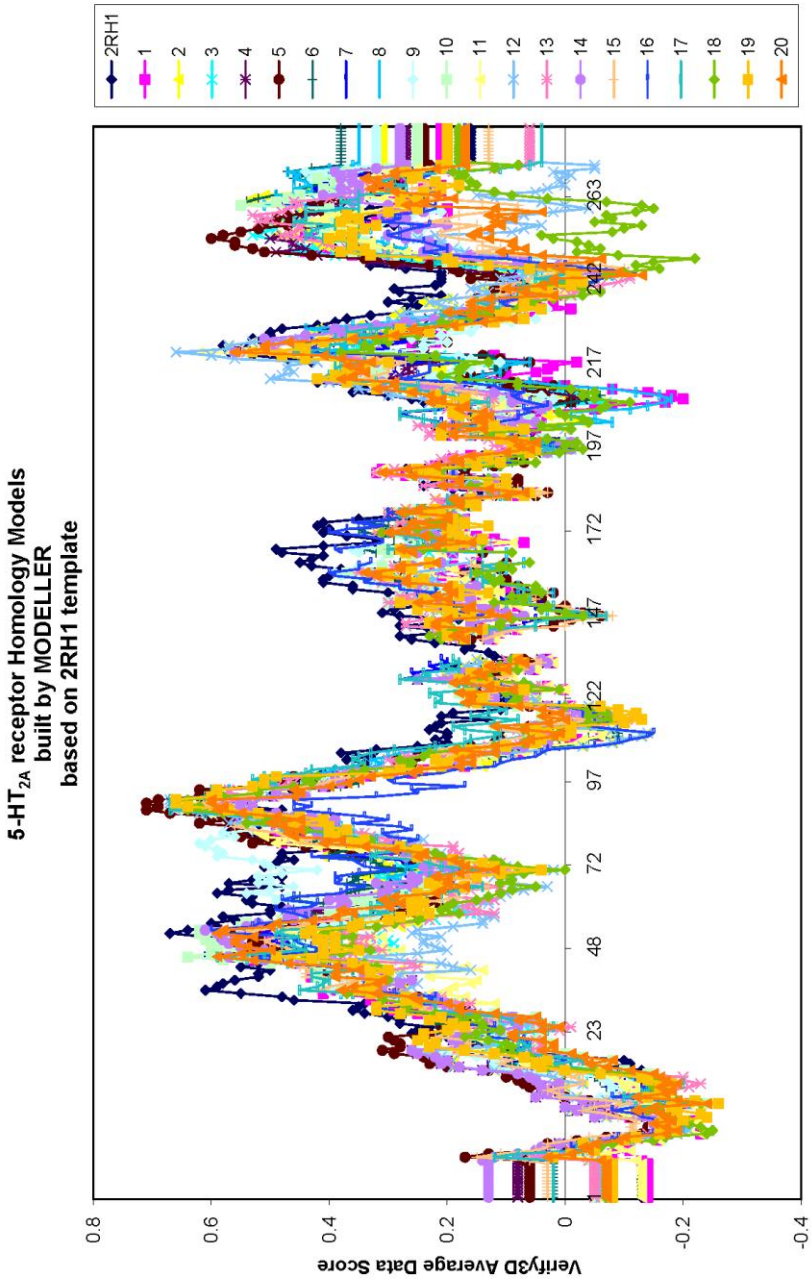

Figure 3.12. Verify3D plots of all homology models built based on a human β2- adrenoreceptor template compared with a plot of the template 2RH1 (blue color)

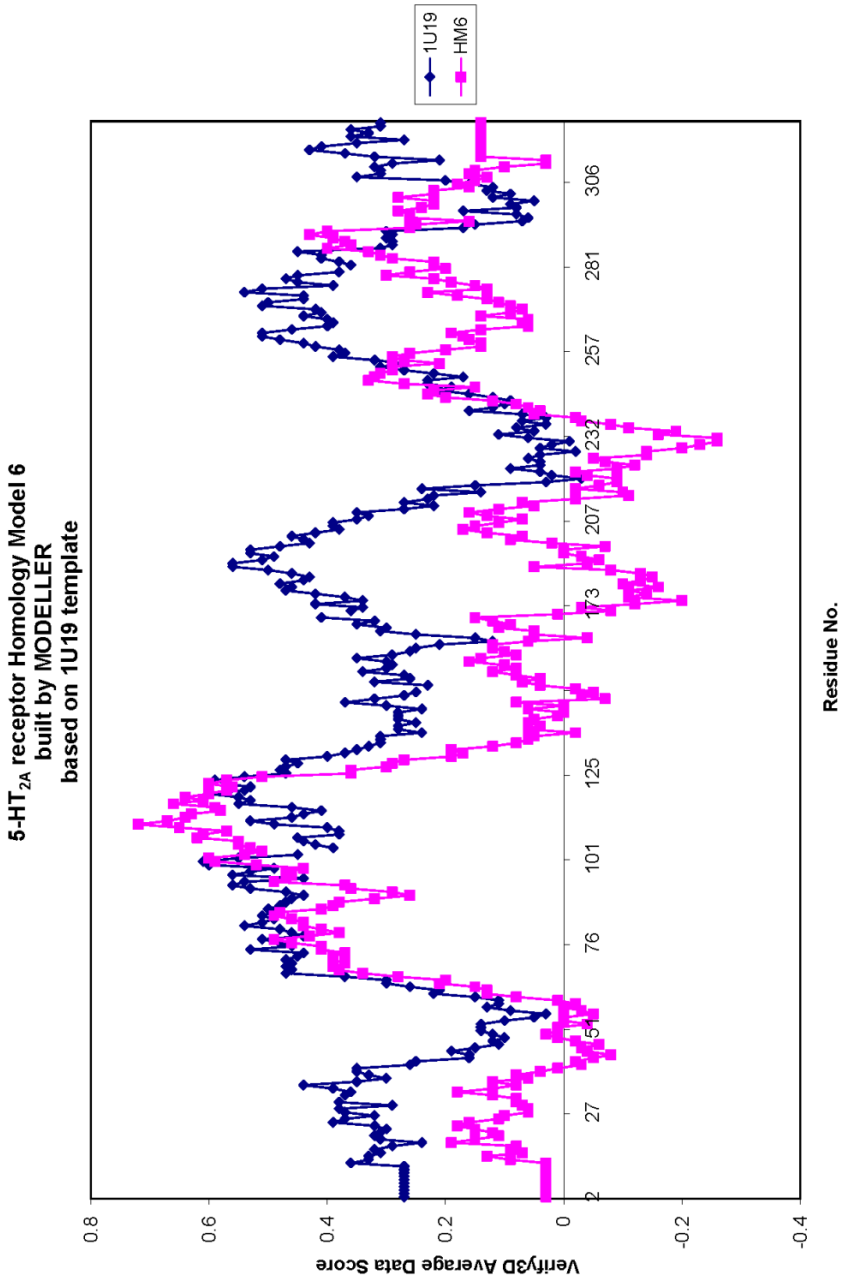

Figure 3.13. Verify3D plots of selected final model BRho_Modeller (red) and bovine rhodopsin template 1U19 (blue)

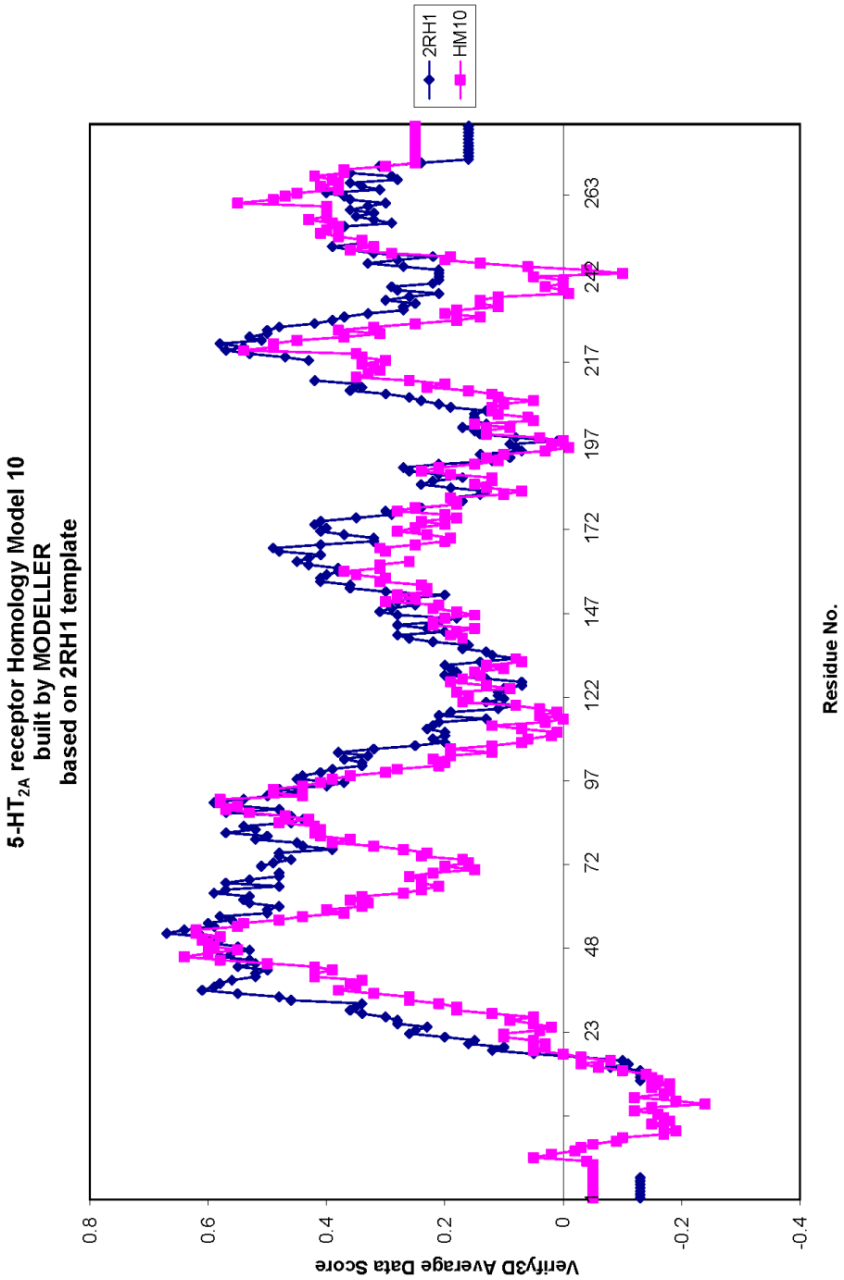

Figure 3.14. Verify3D plots of selected final model HAdrb2_Modeller (red) and human β2-adrenoreceptor template 2RH1 (blue)

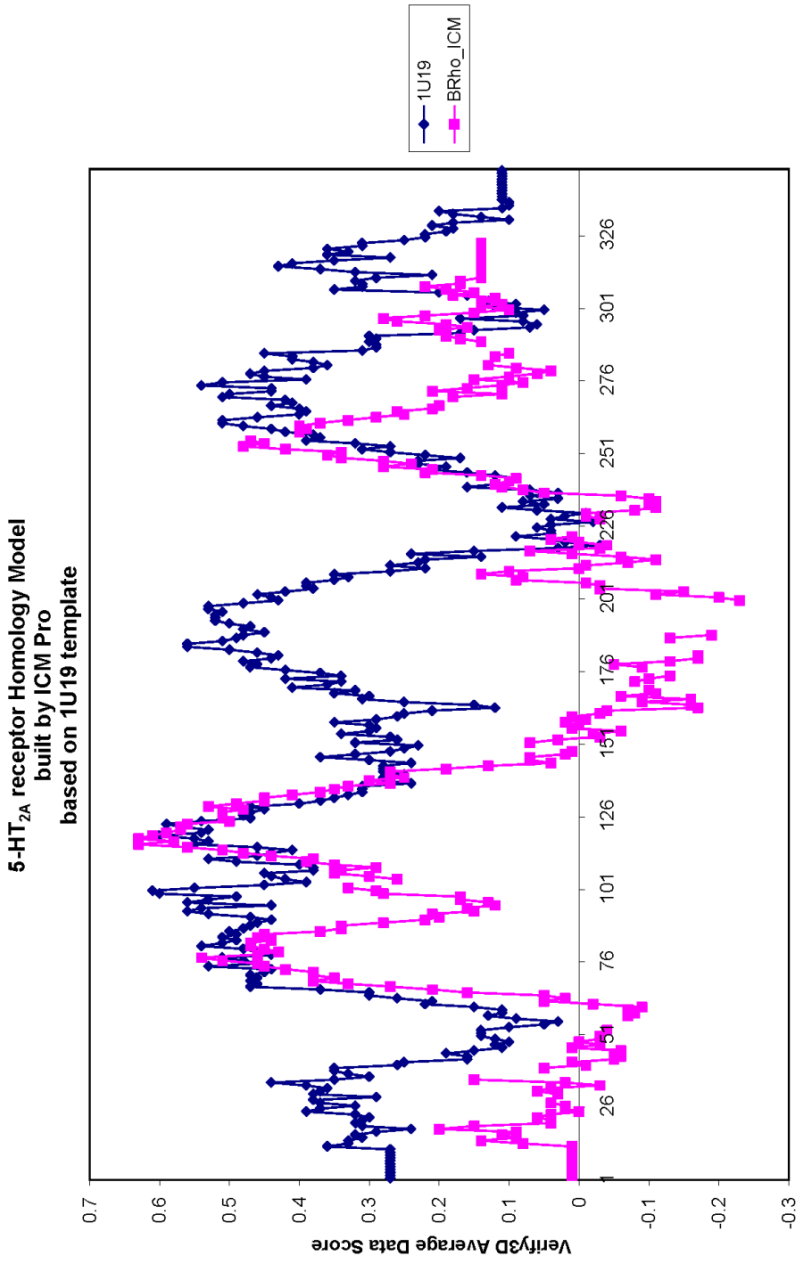

Figure 3.15. Verify3D plots of selected final model BRho_ICM (red) and bovine rhodopsin template 1U19 (blue)

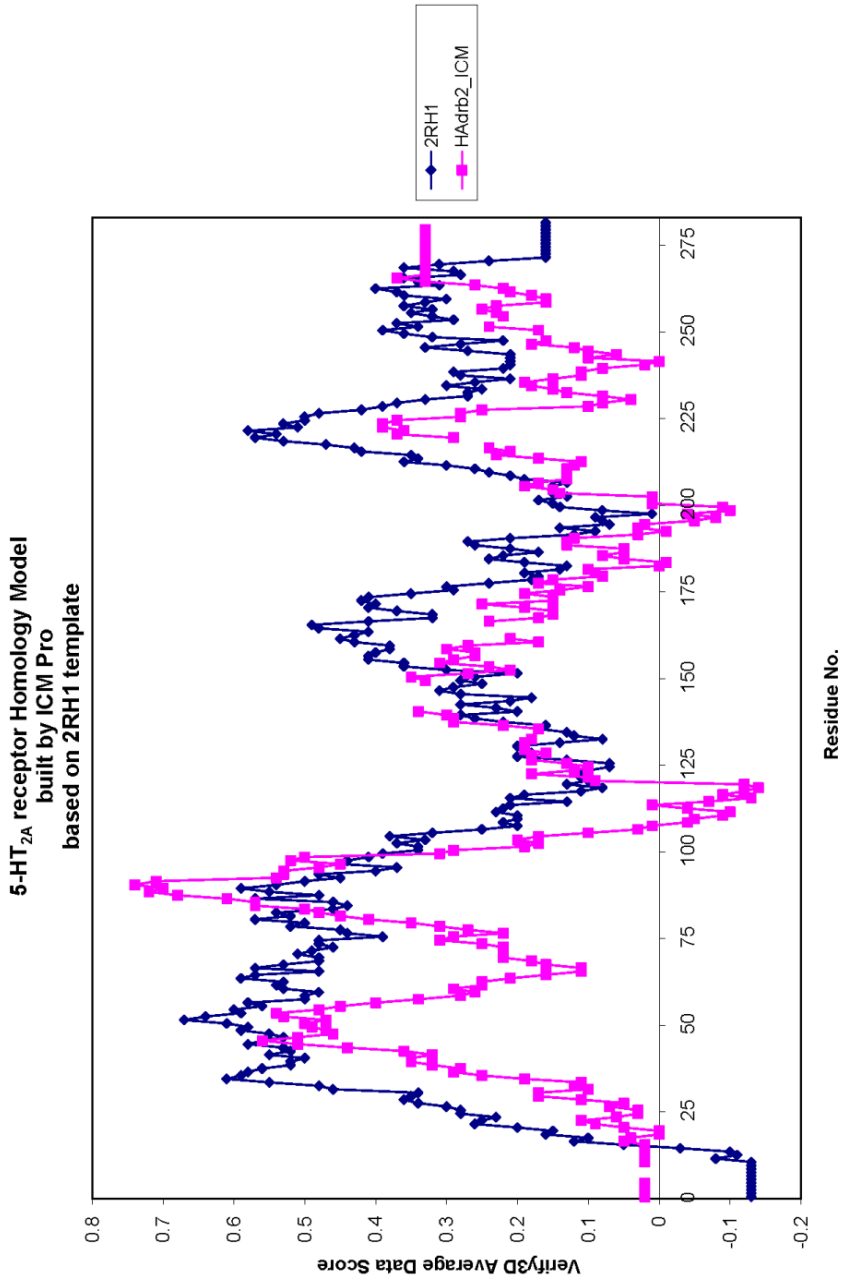

Figure 3.16. Verify3D plots of selected final model HAdrb2_ICM (red) and human β2-adrenoreceptor template 2RH1 (blue)

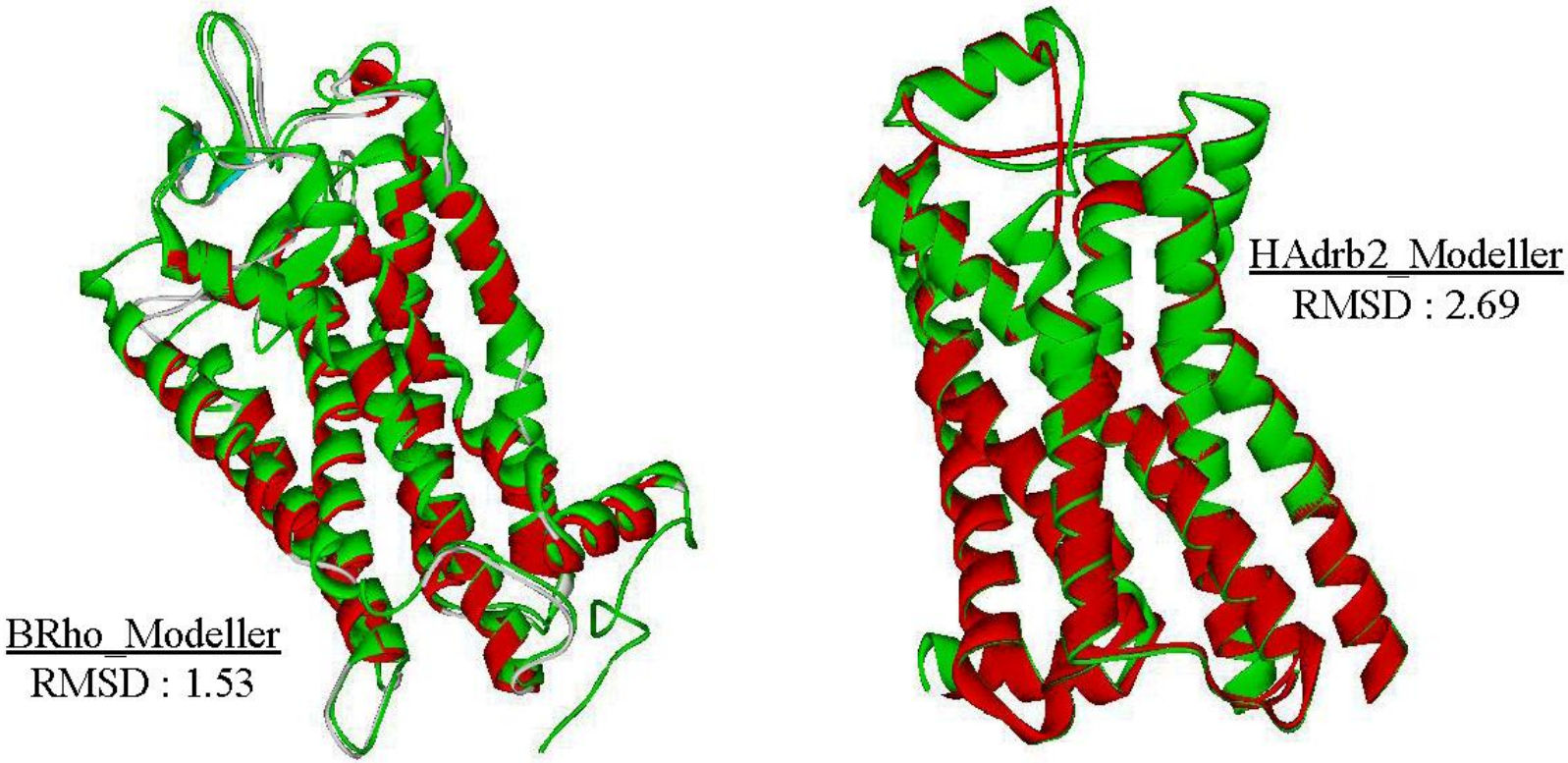

Figure 3.17. RMSD values and structural superposition of Cα trace of BRho_Modeller and HAdrb2_Modeller with respect to their templates

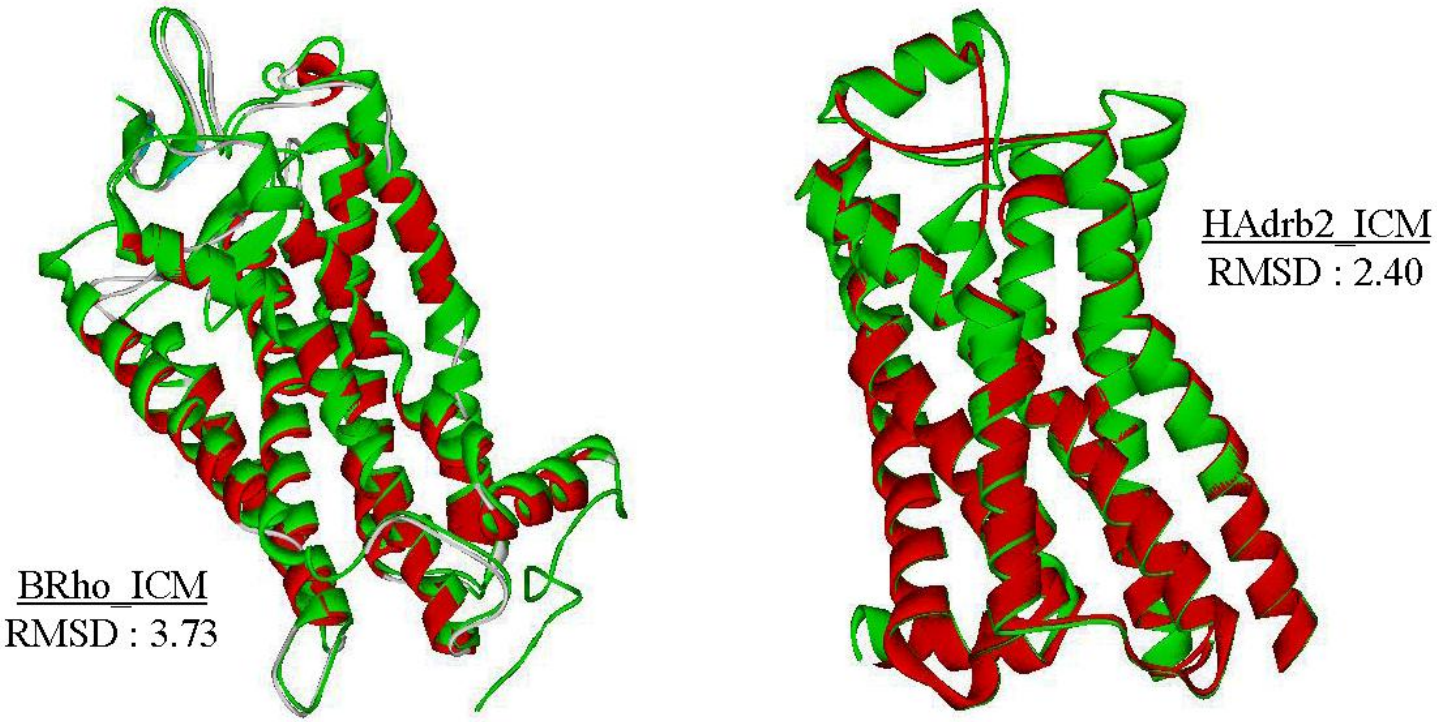

Figure 3.18. RMSD values and structural superposition of Cα trace of BRho_ICM and HAdrb2_ICM with respect to their templates

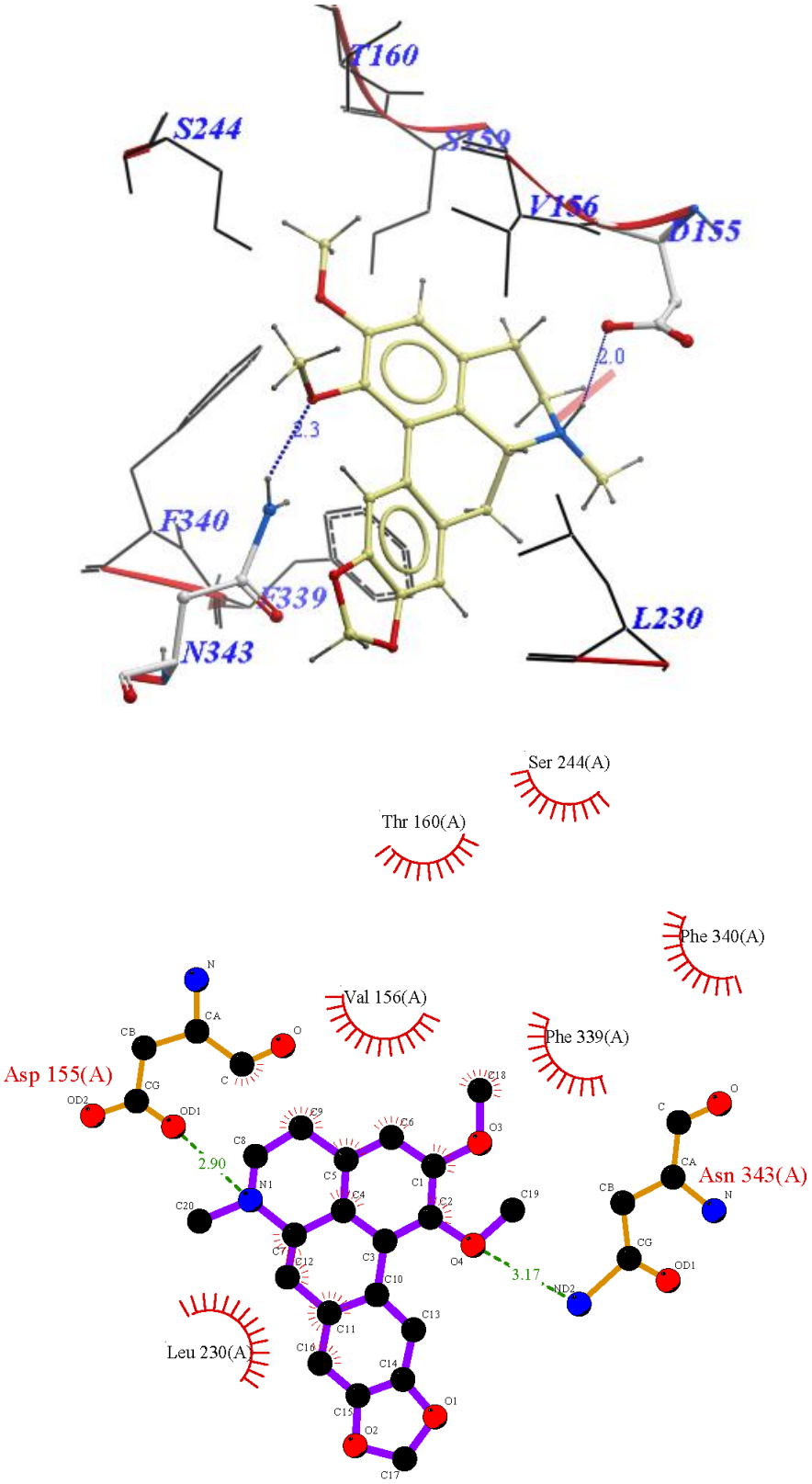

Figure 3.20. Top-ranked GOLD solution and major interactions for nantenine in binding pocket of BRho_Modeller receptor (top); Represented in LigPlot (bottom)

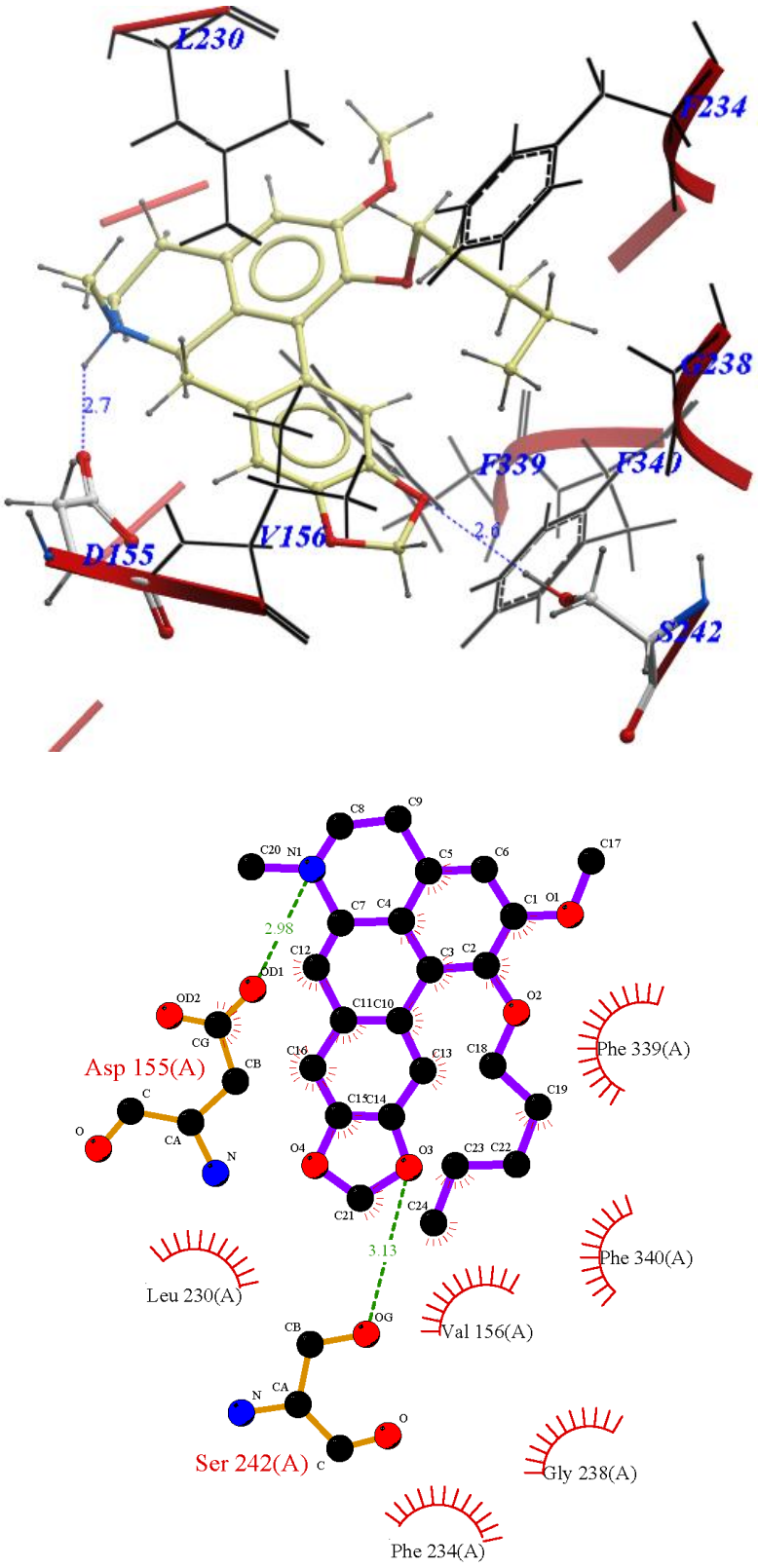

Figure 3.21. Major interactions for analog 20 (top); Represented in LigPlot (bottom)

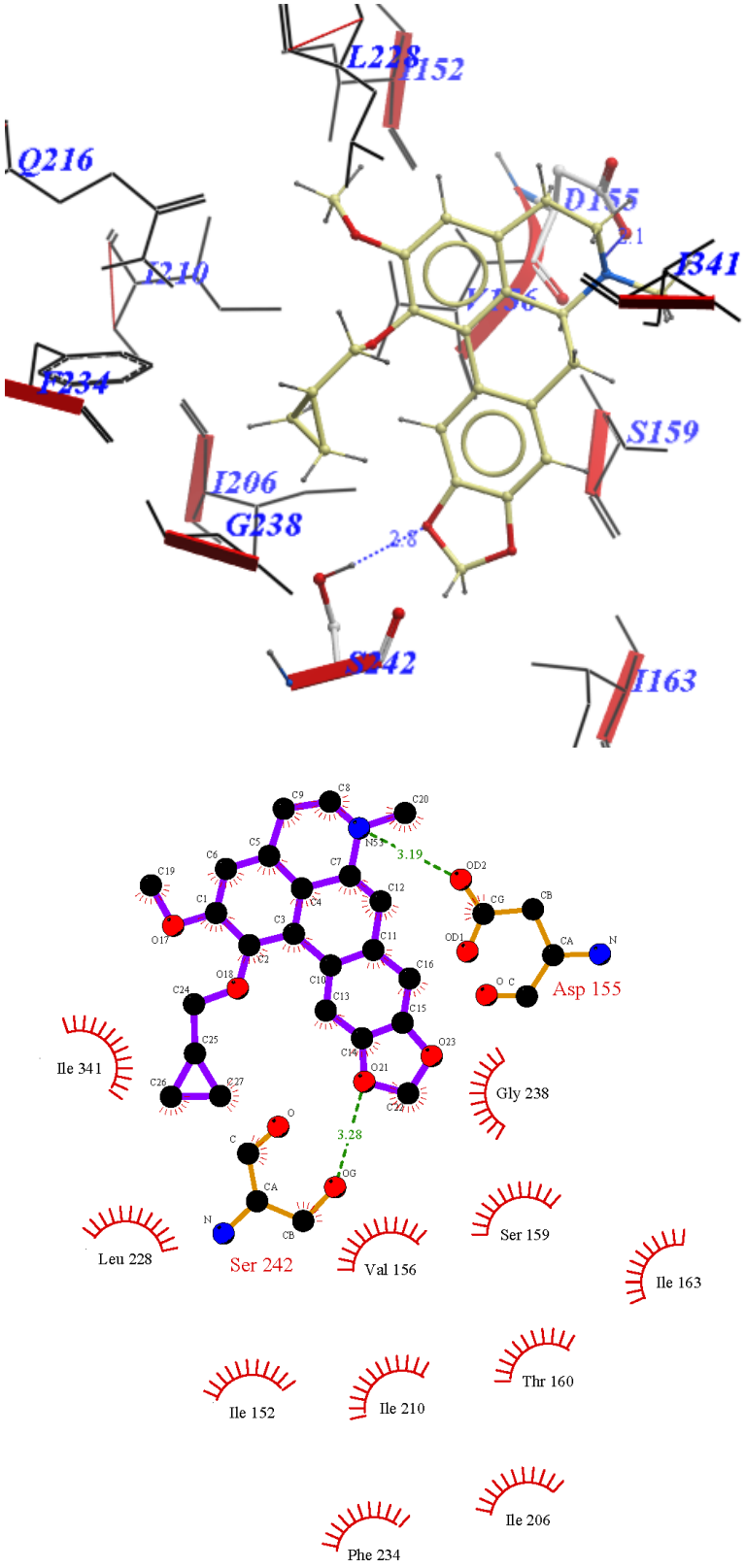

Figure 3.22. Top-scored GOLD complex of analog 21 and BRho_Modeller receptor (top); Represented using LigPlot (bottom)

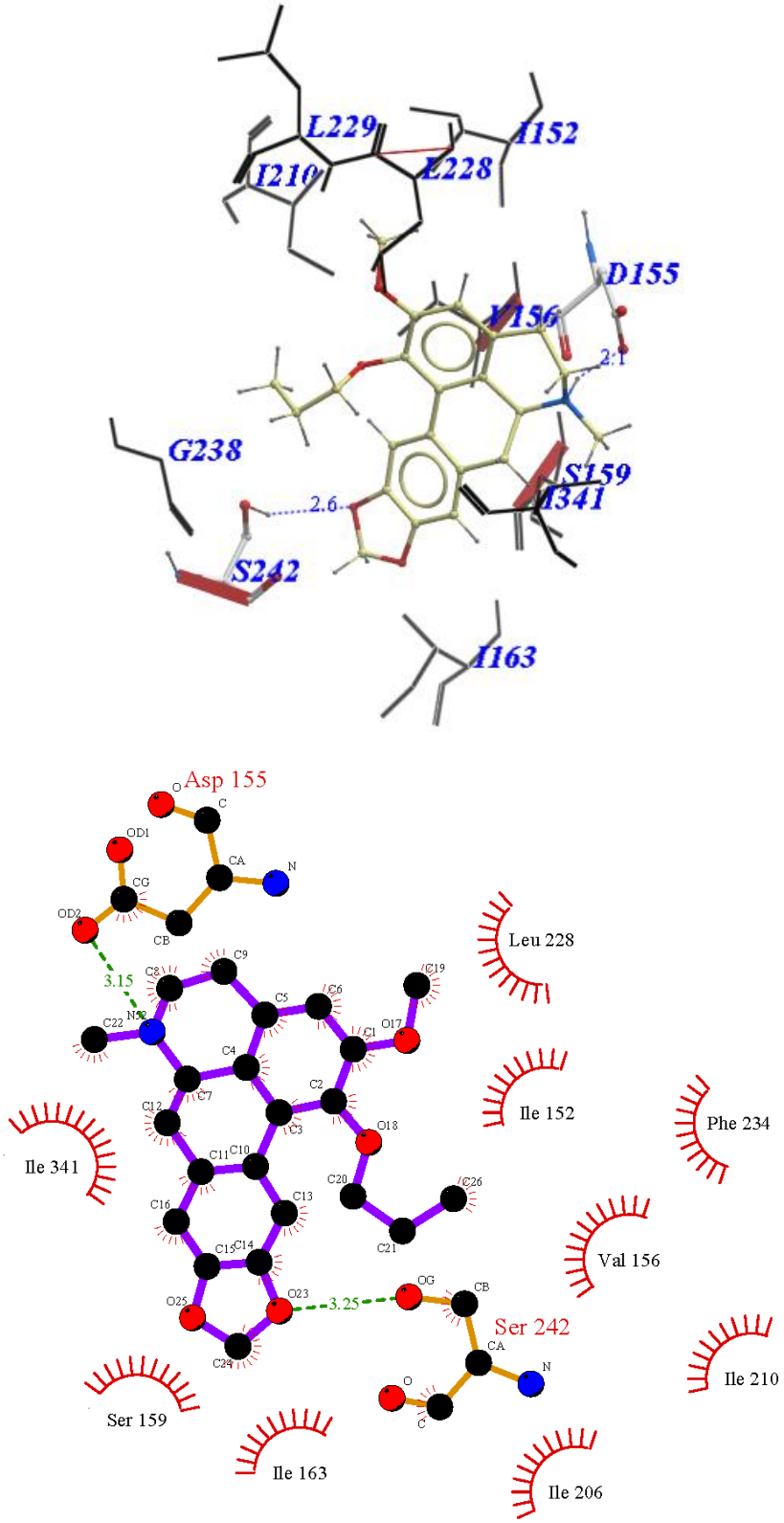

Figure 3.23. Analog 18 in binding cleft of BRho_Modeller receptor (top); LigPlot representation (bottom)

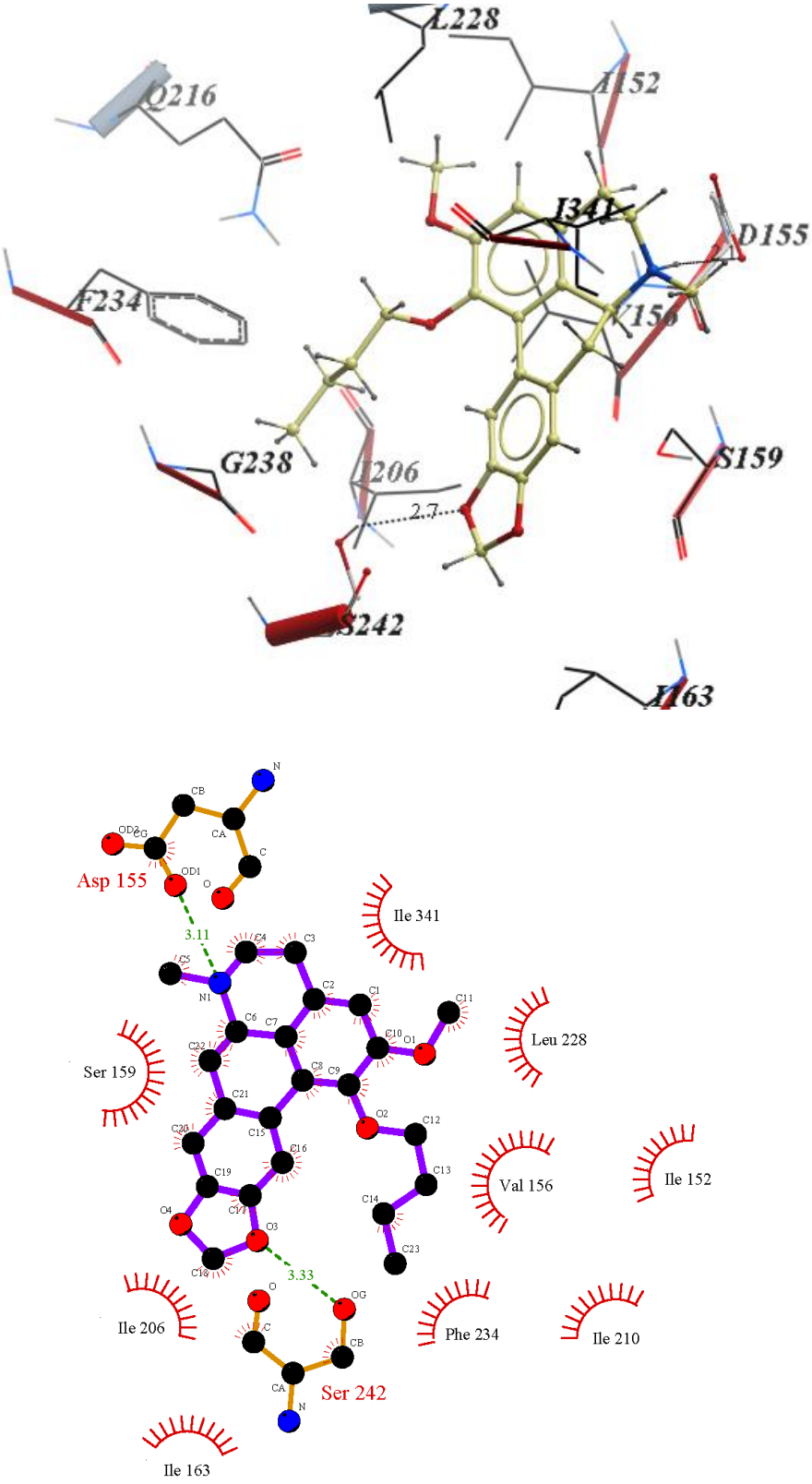

Figure 3.24. Analog 19 in binding cleft of BRho_Modeller receptor (top); LigPlot representation (bottom)

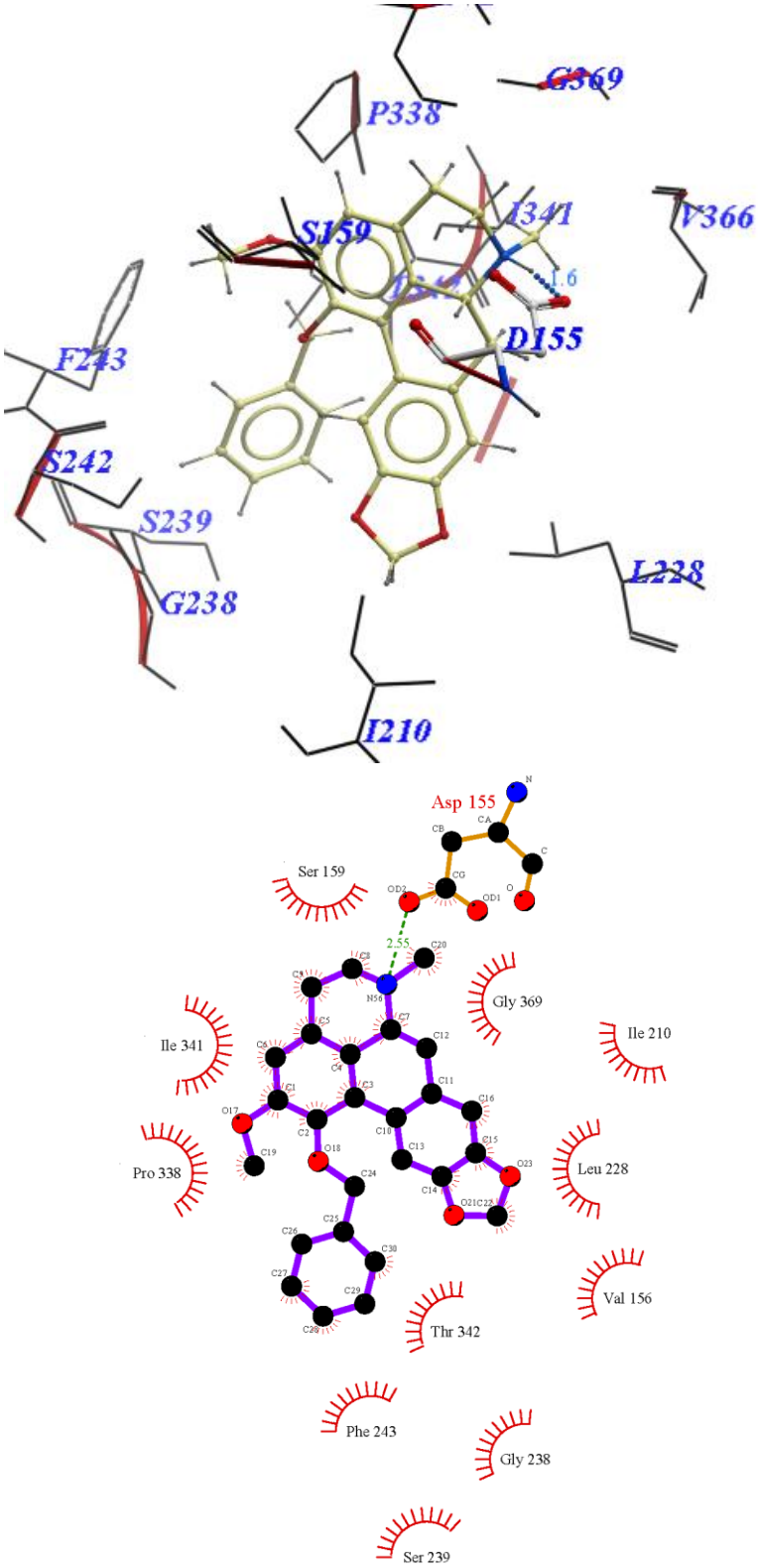

Figure 3.25. Docking pose of analog 22, major interactions and distances (left); Represented by LigPlot (right)

3.6 References

(1) Kroeze, W. K.; Kristiansen, K.; Roth, B. L. *Curr Top Med Chem* **2002**, *2*, 507.

(2) Bojarski, A. J. *Curr Top Med Chem* **2006**, *6*, 2005.

(3) Runyon, S. P.; Mosier, P. D.; Roth, B. L.; Glennon, R. A.; Westkaemper, R. B. *J Med Chem* **2008**, *51*, 6808.

(4) Sanger, D. J.; Soubrane, C.; Scatton, B. *Ann Pharm Fr* **2007**, *65*, 268.

(5) Shelton, R. C.; Papakostas, G. I. *Acta Psychiatr Scand* **2008**, *117*, 253.

(6) Meltzer, H. Y.; Li, Z.; Kaneda, Y.; Ichikawa, J. *Prog Neuropsychopharmacol Biol Psychiatry* **2003**, *27*, 1159.

(7) Levin, E. D.; Slade, S.; Johnson, M.; Petro, A.; Horton, K.; Williams, P.; Rezvani, A. H.; Rose, J. E. *Eur J Pharmacol* **2008**, *600*, 93.

(8) Nic Dhonnchadha, B. A.; Fox, R. G.; Stutz, S. J.; Rice, K. C.; Cunningham, K. A. *Behav Neurosci* **2009**, *123*, 382.

(9) Chaudhary, S.; Pecic, S.; Legendre, O.; Navarro, H. A.; Harding, W. W. *Bioorg Med Chem Lett* **2009**, *19*, 2530.

(10) Aranda, R.; Villalba, K.; Ravina, E.; Masaguer, C. F.; Brea, J.; Areias, F.; Dominguez, E.; Selent, J.; Lopez, L.; Sanz, F.; Pastor, M.; Loza, M. I. *J Med Chem* **2008**, *51*, 6085.

(11) Chambers, J. J.; Nichols, D. E. *J Comput Aided Mol Des* **2002**, *16*, 511.

(12) Leifert, W. R. *G Protein Coupled Receptors in Drug Discovery*; Humana Press: New York, 2009; Vol. 552.

(13) Berman, H. M.; Westbrook, J.; Feng, Z.; Gilliland, G.; Bhat, T. N.; Weissig, H.; Shindyalov, I. N.; Bourne, P. E. *Nucleic Acids Res* **2000**, *28*, 235.

(14) Altschul, S. F.; Madden, T. L.; Schaffer, A. A.; Zhang, J.; Zhang, Z.; Miller, W.; Lipman, D. J. *Nucleic Acids Res* **1997**, *25*, 3389.

(15) Warne, T.; Serrano-Vega, M. J.; Baker, J. G.; Moukhametzianov, R.; Edwards, P. C.; Henderson, R.; Leslie, A. G.; Tate, C. G.; Schertler, G. F. *Nature* **2008**, *454*, 486.

(16) Jaakola, V. P.; Griffith, M. T.; Hanson, M. A.; Cherezov, V.; Chien, E. Y.; Lane, J. R.; Ijzerman, A. P.; Stevens, R. C. *Science* **2008**, *322*, 1211.

(17) Cherezov, V.; Rosenbaum, D. M.; Hanson, M. A.; Rasmussen, S. G.; Thian, F. S.; Kobilka, T. S.; Choi, H. J.; Kuhn, P.; Weis, W. I.; Kobilka, B. K.; Stevens, R. C. *Science* **2007**, *318*, 1258.

(18) Okada, T.; Sugihara, M.; Bondar, A. N.; Elstner, M.; Entel, P.; Buss, V. *J Mol Biol* **2004**, *342*, 571.

(19) Murakami, M.; Kouyama, T. *Nature* **2008**, *453*, 363.

(20) Mobarec, J. C.; Sanchez, R.; Filizola, M. *J Med Chem* **2009**.

(21) Westkaemper, R. B.; Glennon, R. A. *Curr Top Med Chem* **2002**, *2*, 575.

(22) Evers, A.; Hessler, G.; Matter, H.; Klabunde, T. *J Med Chem* **2005**, *48*, 5448.

(23) Sousa, S. F.; Fernandes, P. A.; Ramos, M. J. *Proteins* **2006**, *65*, 15.

(24) Indra, B.; Matsunaga, K.; Hoshino, O.; Suzuki, M.; Ogasawara, H.; Ishiguro, M.; Ohizumi, Y. *Canadian journal of physiology and pharmacology* **2002**, *80*, 198.

(25) Higgins, D. G.; Sharp, P. M. *Gene* **1988**, *73*, 237.

(26) Abagyan R; Totrov M; D., K. *J Comput Chem* **1994**, *15*, 488.

(27) Abagyan, R. A.; Batalov, S. *J Mol Biol* **1997**, *273*, 355.

(28) Baldwin, J. M.; Schertler, G. F.; Unger, V. M. *J Mol Biol* **1997**, *272*, 144.

(29) Sali, A.; Blundell, T. L. *J Mol Biol* **1993**, *234*, 779.

(30) Li, M.; Wang, B. *J Mol Model* **2007**, *13*, 1237.

(31) Morris, A. L.; MacArthur, M. W.; Hutchinson, E. G.; Thornton, J. M. *Proteins* **1992**, *12*, 345.

(32) Colovos, C.; Yeates, T. O. *Protein Sci* **1993**, *2*, 1511.

(33) Eisenberg, D.; Luthy, R.; Bowie, J. U. *Methods Enzymol* **1997**, *277*, 396.

(34) Pontius, J.; Richelle, J.; Wodak, S. J. *J Mol Biol* **1996**, *264*, 121.

(35) Wallace, A. C.; Laskowski, R. A.; Thornton, J. M. *Protein Eng* **1995**, *8*, 127.

(36) Spedding, M.; Newman-Tancredi, A.; Millan, M. J.; Dacquet, C.; Michel, A. N.; Jacoby, E.; Vickery, B.; Tallentire, D. *Neuropharmacology* **1998**, *37*, 769.

(37) Kristiansen, K.; Kroeze, W. K.; Willins, D. L.; Gelber, E. I.; Savage, J. E.; Glennon, R. A.; Roth, B. L. *The Journal of pharmacology and experimental therapeutics* **2000**, *293*, 735.

(38) Choudhary, M. S.; Sachs, N.; Uluer, A.; Glennon, R. A.; Westkaemper, R. B.; Roth, B. L. *Molecular pharmacology* **1995**, *47*, 450.

(39) Choudhary, M. S.; Craigo, S.; Roth, B. L. *Molecular pharmacology* **1993**, *43*, 755.

(40) Klabunde, T.; Evers, A. *Chembiochem* **2005**, *6*, 876.

(41) Bruno, A.; Guadix, A. E.; Costantino, G. *J Chem Inf Model* **2009**, *49*, 1602.

(42) Mobarec, J. C.; Sanchez, R.; Filizola, M. *J Med Chem* **2009**, *52*, 5207.

(43) Dezi, C.; Brea, J.; Alvarado, M.; Ravina, E.; Masaguer, C. F.; Loza, M. I.; Sanz, F.; Pastor, M. *J Med Chem* **2007**, *50*, 3242.

(44) http://www.pdsp.med.unc.edu/.

(45) Wheeler, D. L.; Barrett, T.; Benson, D. A.; Bryant, S. H.; Canese, K.; Chetvernin, V.; Church, D. M.; Dicuccio, M.; Edgar, R.; Federhen, S.; Feolo, M.; Geer, L. Y.; Helmberg, W.; Kapustin, Y.; Khovayko, O.; Landsman, D.; Lipman, D. J.; Madden, T. L.; Maglott, D. R.; Miller, V.; Ostell, J.; Pruitt, K. D.; Schuler, G. D.; Shumway, M.; Sequeira, E.; Sherry, S. T.; Sirotkin, K.; Souvorov, A.; Starchenko, G.; Tatusov, R. L.; Tatusova, T. A.; Wagner, L.; Yaschenko, E. *Nucleic Acids Res* **2008**, *36*, D13.

(46) Thompson, J. D.; Gibson, T. J.; Plewniak, F.; Jeanmougin, F.; Higgins, D. G. *Nucleic Acids Res* **1997**, *25*, 4876.

CHAPTER 4: Nantenine as an acetylcholinesterase inhibitor: SAR, enzyme kinetics and molecular modeling investigations

Abstract

For the second part of the project, nantenine as well as a number of flexible analogs were evaluated for acetylcholinesterase (AChE) inhibitory activity in a microplate spectrophotometric assays based on Ellman's method. It was found that the rigid aporphine core of nantenine and *N*-methyl substituent are important structural requirements for its anticholinesterase activity. Nantenine showed mixed inhibition kinetics in enzyme assays. Molecular docking experiments suggest that nantenine binds preferentially to the catalytic site of AChE but is also capable of interacting with the peripheral anionic site (PAS) of the enzyme thus accounting for its mixed inhibition profile. The aporphine core of nantenine may thus be a useful template for the design of novel PAS or dual-site AChE inhibitors; inhibiting the PAS is desirable for prevention of aggregation of the amyloid peptide Aβ a major causative factor in the progression of Alzheimer's disease (AD).

4.1 Introduction

4.1.1 Alzheimer's Disease

Alzheimer's disease (AD) is an incapacitating condition which afflicts millions of people worldwide. The disease is especially prevalent among the elderly and is associated with severe deficits in cognition and memory.[1-3] The National Institutes of Health predict that there will be 8.5 million Americans with AD by the year 2030.[4] In the early stages patients have impaired cognitive functions and tend to be easily confused. In addition, their performance of daily living activities is significantly reduced.[5] Eventually they will become completely dependent on other people for their everyday care. In advanced stages of AD, dramatic changes in emotional state, psychological well-being and personality are observed.[6,7] In terms of costs, direct (physician visits, acute hospitalization, prescription medications, emergency department visits, etc) and indirect (lost of productivity of patients and also of care-givers), this disease places a heavy economic burden on the US society and economy, with estimated cost of $100 billion annually.[4]

Although there is no cure for the AD caused dementia, there are still several available pharmacologic treatment strategies that can reduce the symptoms of cognitive impairment and slow the disease progression.

The symptoms of AD are presumed to be related to impaired neurotransmission and the degeneration of neurons in the affected brain areas.[8] There are two proposed theories how neurodegeneration in Alzheimer's disease may be caused.

4.1.2 The Amyloid Hypothesis of AD and Treatment Strategies Based on Aβ Biology

The onset and progression of AD is thought to be a consequence of the formation of neuritic plaques via aggregation of the amyloid peptide Aβ.[9-13] According to this hypothesis the primary cause of AD pathogenesis is deposition of amyloid β-peptide, while the rest of the disease process is proposed to be a result of an imbalance between Aβ production and Aβ clearance.[14]

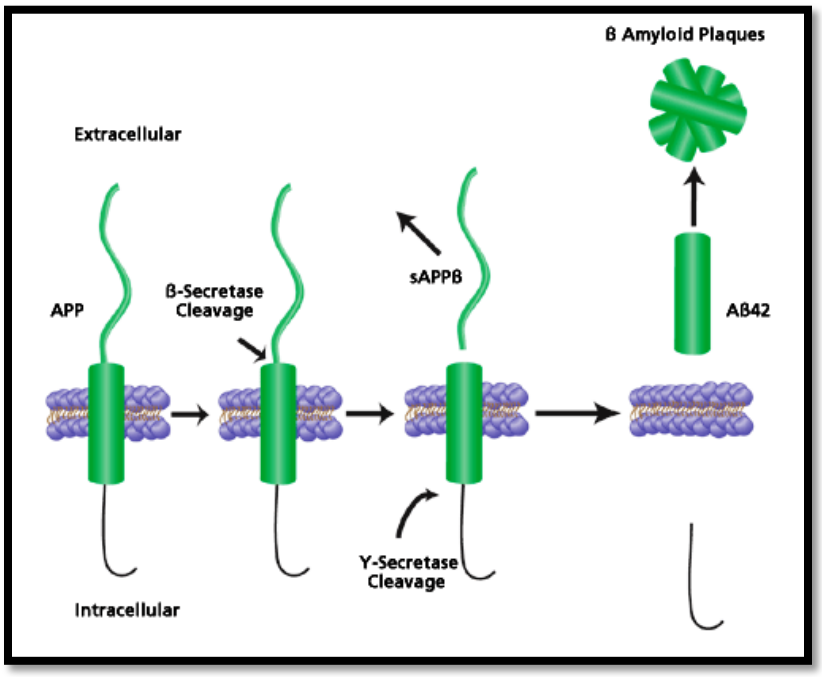

Figure 4.1 Cleavage of Amyloid Precursor Protein. Amyloid precursor protein (APP) is sequentially cleaved first by β-secretase (BACE1) and then by γ-secretase to form soluble amyloid precursor protein β (sAppβ) and the amyloid β42 peptide fragment (Aβ42). The Aβ42 fragments then aggregate and form the extracellular senile plaques common to Alzheimer's disease. (Zharhary et al, *Sigma-Aldrich Corporation*, **2010**)

Amyloid β- peptide is the product of the sequential proteolysis of the membrane anchored amyloid precursor protein (APP),[15,16] first at the N-terminus by β-secretase enzyme (β-site APP cleaving enzyme, aka. BACE1), followed at the C-terminus by one

or more secretase complexes (intramembrane aspartyl proteases) as part of the β-amyloidogenic pathway (Figure 4.1).[17]

Although this hypothesis offers a broad framework to explain the pathogenesis of AD, currently there are several important gaps and weaknesses for amyloid hypothesis.[18-20] The most important objection is that the number of amyloid deposits in the brain does not correlate well with the degree of cognitive impairment. Also some people can have many cortical Aβ deposits without symptoms of AD.[14] Still none of these objections can provide enough evidences to abandon this hypothesis and several broad therapeutic strategies have been proposed.

4.1.2.1 Approaches to Treat AD Based on the Amyloid Hypothesis

The first explored approach was to partially inhibit either one of the two proteases, β- or γ-secretase, that are responsible for generation of Aβ from APP. A lot of studies have been performed to identify potent small-molecule inhibitors that can fit the active site of this enzyme, and still penetrate the blood - brain barrier.[21-23]

Another approach that is already being explored is to enhance the clearance of Aβ from the cerebral cortex, by use of Aβ antibodies that will promote the redistributing the peptide from the brain to the systematic circulation.[24,25] Recently has been reported that clusterin, a secreted molecular chaperone, is involved in clearance of Aβ amyloids. It is also known that the cancer drug Vorinostat stimulates the expression of clusterin.[26]

One of the recent approaches is based on modulating cholesterol homeostasis. In the last 10 years it has been noticed that chronic use of cholesterol-lowering drugs, such

as statins, are associated with a lower incidence of AD.[27-29] The effect of cholesterol on APP processing is poorly understood, but particular advantage of this approach is that statin drugs are generally well tolerated and have been widely prescribed.

It has been noticed that besides senile plaques, AD has one more histopathological hallmark- neurofibrillary tangles.[30] Tangles are intracellular residues of an abnormally phosphorylated protein-tau. Agents capable of preventing the misfolding and sequestration of the protein tau into insoluble fibrillar aggregates are being explored for potential treatment of AD. Recent example of tau aggregation inhibitors are aminothienopyridazine (ATPZ) class of compounds.[31]

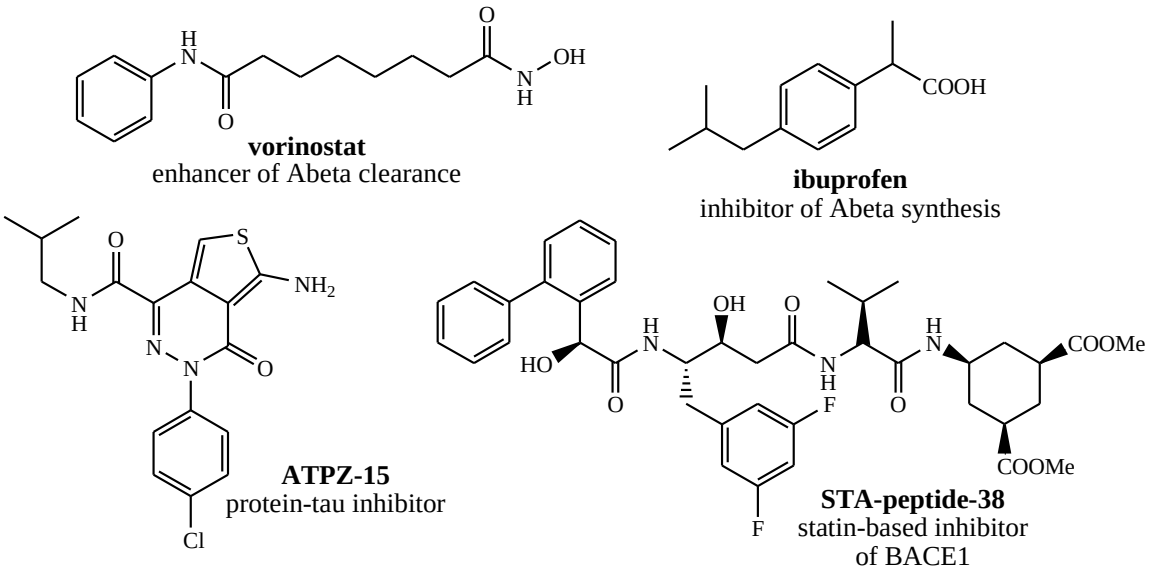

Figure 4.2 Potential therapeutics for treatment of AD based on amyloid hypothesis

Since the progressive accumulation of Aβ will lead to the cellular inflammatory response, a broadened anti-inflammatory strategy has been developed. Epidemiological studies have shown that nonsteroidal anti-inflammatory drugs (eg. ibuprofen) decrease the Aβ42 peptide produced from a variety of cultured cells by as much as 80%.[32] It

seems that this process is not mediated by inhibition of cyclooxygenase (COX) activity although this mechanism has not been proven.

The development of anti-Aβ therapeutics still remains one of the most rational approaches to treat AD, and many clinical trials are under way.

4.1.3 Cholinergic Hypothesis and AChE Inhibitors

Research over the years has supported early hypotheses that a deficit in cholinergic neurotransmission plays a major role in the neurodegeneration associated with the disease.[33,34] Acetylcholine is hydrolytically destroyed in the brain by two cholinesterases, acetylcholinesterase (AChE) and butyrylcholinesterase (BuChE). Several studies have also shown that both, AChE and BuChE, are associated with amyloid plaques.[35,36]

Most current treatments for AD employ compounds which act as inhibitors of acetylcholinesterase which thereby improve cholinergic deficits. Four compounds are commonly prescribed for treatment of AD based on this mechanism of action – galanthamine, tacrine, donepezil and rivastigmine (Figure 4.3).[37,38] Selective inhibition of AChE occurs with galantamine and donepezil, whereas rivastigmine and tacrine inhibit nonselectively both AChE and BuChE.[39] These therapeutics offer short-term improvement in treating symptoms of the disease with modest benefits in slowing decline in behavior, function and cognition associated with the disease.[40-42] All of the approved AChE inhibitors have potentially serious side-effects especially with long-term use, and more efficacious and safer alternatives are desirable.[43-46]

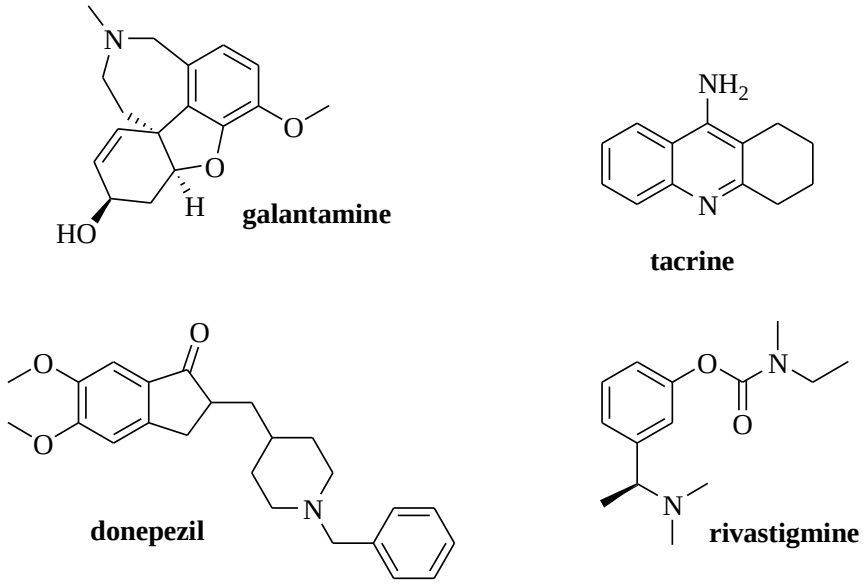

Figure 4.3 Clinically available AChE inhibitors

AChE has two main binding domains, the catalytic site and a peripheral anionic site (PAS).[47-49] There is evidence that AChE facilitates the formation of amyloid fibrils via a set of amino acids located in the vicinity of the PAS and that molecules which bind to the PAS prevent aggregation of the amyloid peptide Aβ (Figure 4.4).[50,51]

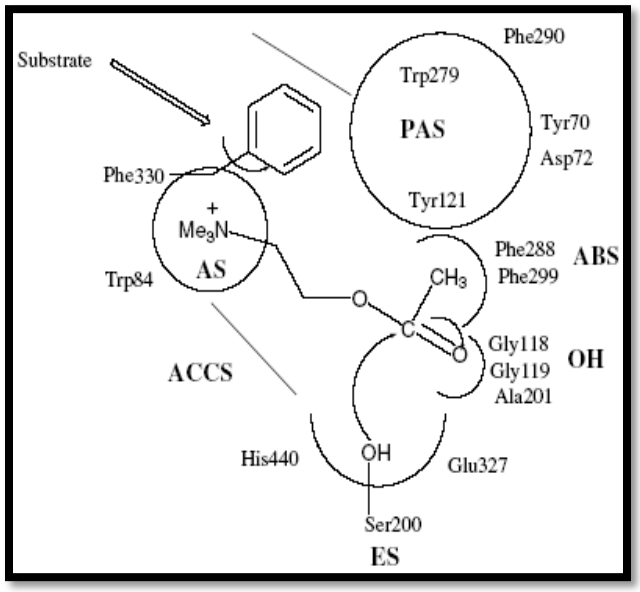

Figure 4.4 The active site and the PAS of AChE
(Zhou et al, *Bioorg Med Chem*, **2008**, *16*, 8011)

Based on these developments, there has recently emerged a new therapeutic strategy which involves the use of molecules (indol-tacrine heterodimers, coumarine analogs, etc) endowed with the ability to bind to the catalytic site and PAS of AChE simultaneously (Figure 4.5).[52-55] Such dual-acting molecules should be more efficacious in decelerating progression of the disease via prevention of Aβ accumulation via PAS inhibition as well as provide the usual palliative cognitive and memory improvements associated with inhibition of the catalytic site of the enzyme.

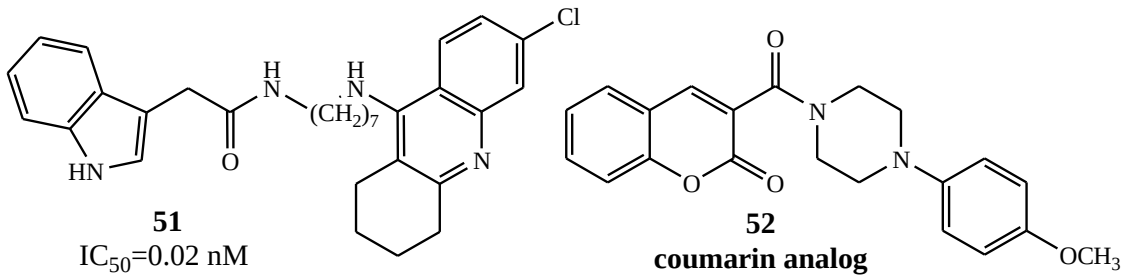

Figure 4.5 Dual binding site AChE inhibitors

4.1.3.1 Aporphines as AChE Inhibitors

As we mentioned in Chaper 1, aporphines are a group of isoquinoline alkaloids that are known to exhibit diverse biological activities (cytoprotective, anti-oxidative, etc).[56,57] Relatively few aporphines have been evaluated as AChE inhibitors. In that regard, a recent report indicated that two aporphinoids **53** and **54** (Figure 4.6) ex *Corydalis turtschaninovii* Besser (Papaveraceae) show moderate activity with IC_{50} values of 27.1 and 48.7 μM respectively.[58] Structurally-related synthetic oxoaporphines and iso-oxoaporphines have been recently reported to possess anticholinesterase activity,

inhibiting the enzyme non-competitively.[59] Also one other aporphine **55** (Figure 4.6) has been reported to have moderate AChE inhibitory activity (34.5% inhibition at 10^{-4} M).[60]

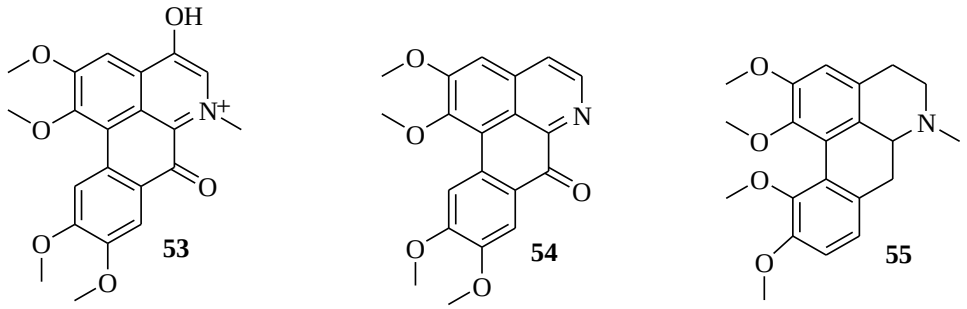

Figure 4.6 Structures of known aporphinoid AChE inhibitors

Very few studies have been conducted to systematically delineate the structure-activity relationships (SAR) of aporphines as AChE inhibitors.

4.1.4 Ellman's Method

Enzyme inhibitory activities of the potential AChE inhibitors can be measured qualitative using a 96-well microplate assay based on Ellman's method.[61] The enzyme hydrolyzes the substrate acetylthiocholine resulting in the product thiocholine which reacts with Ellman's reagent (DTNB) to produce 2-nitrobenzoate-5-mercaptothiocholine and 5-thio-2-nitrobenzoate which can be detected at 405 nm (Scheme 4.1).[62]

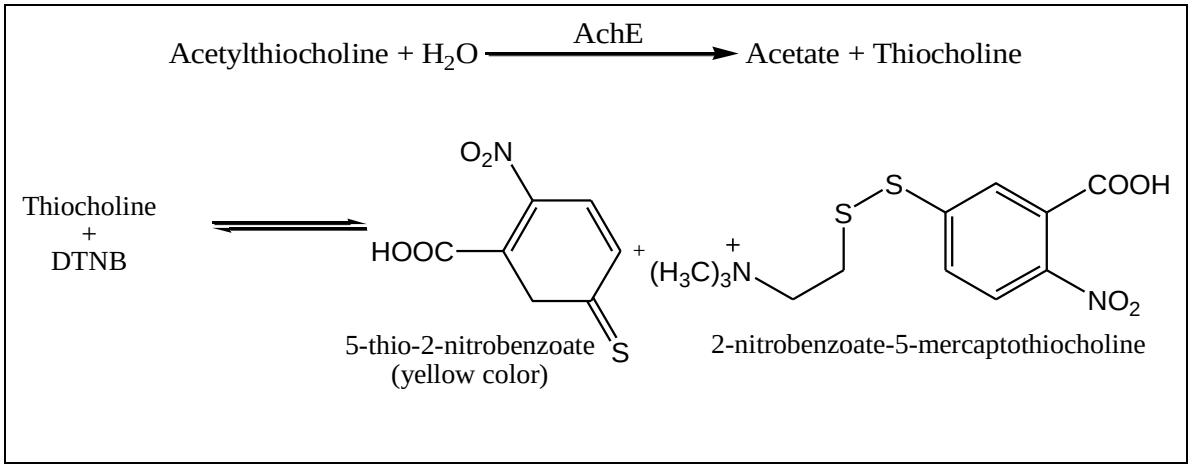

Scheme 4.1 Ellman's method

4.2 Results

4.2.1 SAR study

The structural similarity between nantenine and the aporphines mentioned above prompted us to investigate the anticholinesterase activity of nantenine. We initially compared nantenine with the known AChE inhibitor galanthamine in a TLC anticholinesterase bioautographic assay [63] and found that nantenine showed activity. To understand the mode of inhibition, we also performed enzyme kinetics studies. Since we had already synthesized a library of nantenine analogs (described in detail in Chapter 2) we decided to evaluate them for anticholinesterase activity using a microplate assay.[62]

Nantenine analogs **1-12** (Figure 4.7) will help us to explore the influence of molecular rigidity and the role of *N*-methyl substituent on AChE inhibitory activity of nantenine.

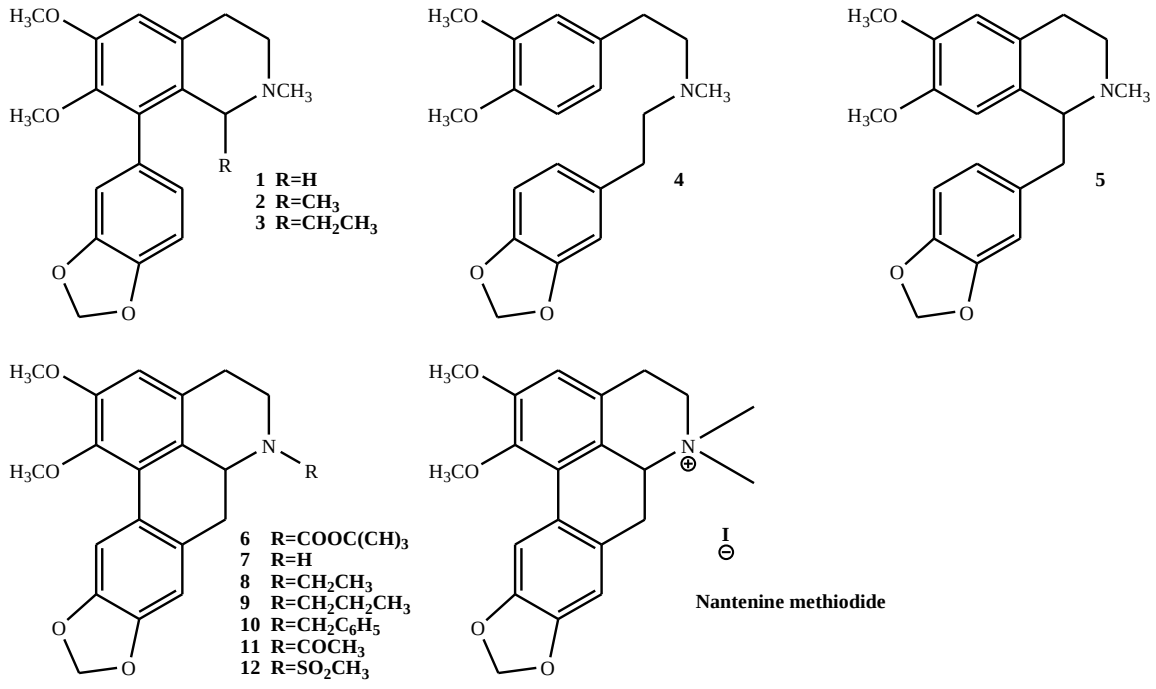

Figure 4.7 Target nantenine analogs

Flexible analogs **1-3** with truncated ring C, will give us information whether the rigid aporphine framework is required for anticholinesterase activity. Analogs **4** and **5**, were prepared also as a part of a set of flexible analogs without C-ring, but biaryl bond of the nantenine is absent, comparing with analogs **1-3**. We were also interested in evaluating these compounds since they are more accessible synthetically, so that any follow-up SAR studies would be facilitated. Nantenine *seco*-ring C analogs **1-3** and flexible analogs **4** and **5** were synthesized as described in Scheme 2.7 and Scheme 2.8 in Chapter 2, respectively.

In this experiment, galanthamine (Figure 4.3) was used as reference standard with an IC_{50} value of 0.53 μM. Previously it has been shown that galanthamine has one non-conventional interaction via its *N*-methyl group with Asp 72 located in the active site of AChE.[64] Given the structural similarities between galanthamine and nantenine, we were interested to find out if the nitrogen atom or *N*-substituents in nantenine played any role in binding to the enzyme. Therefore, we decided to evaluate analogs **6**-**12**.

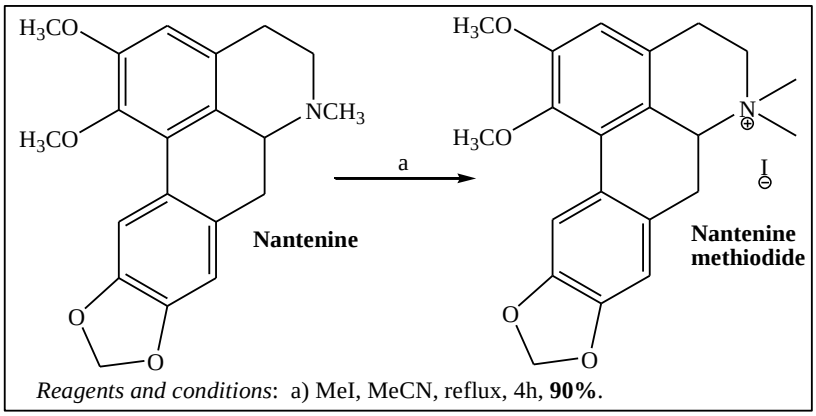

Scheme 4.2 Synthesis of nantenine methiodide

Since the natural ligand, acetylcholine, contains a quaternized nitrogen and also some previous studies concerning achetylcholineserase inhibiting activity have shown that the compounds with a quarternary nitrogen atom have higher inhibitory activity,[65,66]

we decided to prepare and test **nantenine methiodide**. This analog was prepared according to Scheme 4.2 starting from nantenine.

4.2.2 Enzyme Assays

IC_{50} values for nantenine and target nantenine analogs were determined with a microplate assay [62] using lyophilized *Electrophorus electricus* AChE (See Experimental) and based on Ellman's method, and are summarized in Table 4-1.

Table 4-1. AChE inhibitory activity of analogs

Compound	IC_{50} AChE (μM)
Nantenine	1.09 ± 0.17
1	2.63 ± 0.38
2	2.38 ± 0.21
3	11.36 ± 1.85
4	> 100
5	18.06 ± 1.92
6	4.66 ± 0.65
7	>100
8	2.57 ± 0.15
9	> 100
10	> 100
11	> 100
12	> 100
Nantenine methiodide	1.62 ± 0.23
Galanthamine	0.53 ± 0.11

The lead compound nantenine, showed the highest inhibitory activity with an IC_{50} of 1.09 μM. Flexible analogs **1** and **2** were approximately two-fold less active than nantenine, while analog **3** showed almost 10 times decrease in activity. Nantenine analog **5** in which the biaryl bond of nantenine is absent, was 17 times less active than the lead

molecule, while the most flexible analog, analog **4**, had the lowest inhibitory activity among the ring-truncated analogs, being inactive (IC_{50} > 100 μM).

Taking together the results obtained from SAR analysis of this set of compounds, it is apparent that ring C and ring B are required to be intact for anticholinesterase activity. Therefore it appears that the rigid aporphine core of nantenine is an important structural feature for AChE inhibitory activity. We found that replacement of the *N*-methyl group of nantenine with an N-ethyl group (analog **8**) resulted in only a slight decrease in activity. However, the addition of a more bulky benzyl group (analog **10**) resulted in a dramatic reduction in inhibition of the enzyme. The Boc derivative, nantenine analog **9**, and sulfonamide derivative, analog **12**, were also much less active than the nantenine.

Based on the results we obtained, it seems that the *N*-methyl group of nantenine is important for its activity and also suggests that the binding pocket of AChE does not tolerate bulky groups on the basic nitrogen in the aporphine core.

Quarternarization didn`t significantly affect the activity, since we obtained IC_{50} of 1.62 for **nantenine methiodide**.

To determine the mode of inhibition exhibited by nantenine, we then carried out an evaluation of the steady-state kinetics of the enzyme in the presence of nantenine. A double reciprocal (1/V vs 1/[S], Lineweaver-Burk) plot was performed and this indicated mixed inhibition since lines of increasing gradient showed increasing x-intercepts (Figure 4.8).

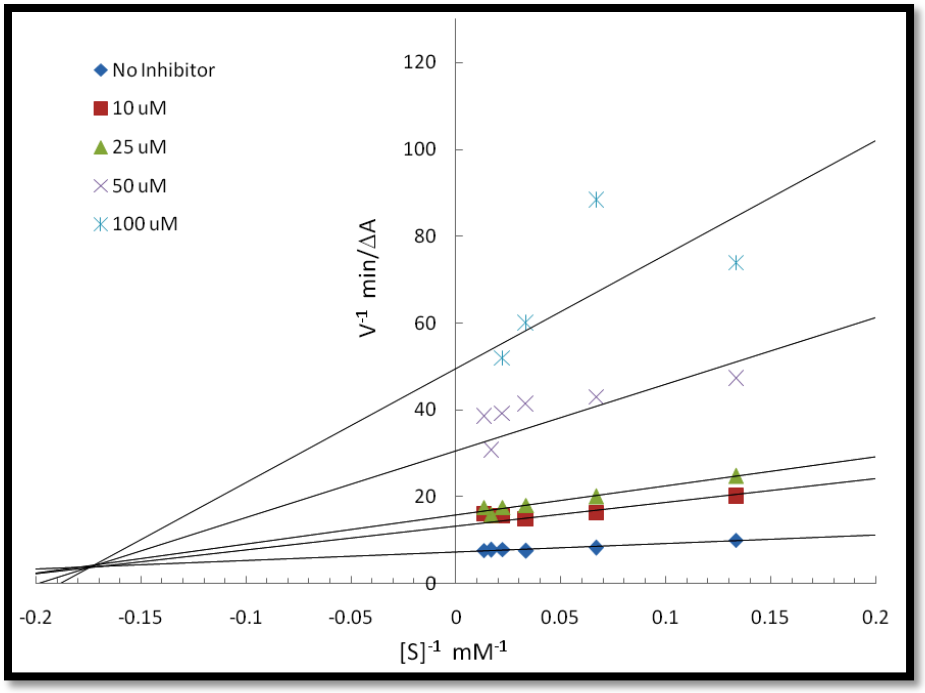

Figure 4.8 Lineweaver-Burk steady-state inhibition plot showing mixed inhibition for nantenine

Figure 4.9 shows a Dixon plot which allowed for calculation of the K_i of nantenine in this assay (18.7 µM).

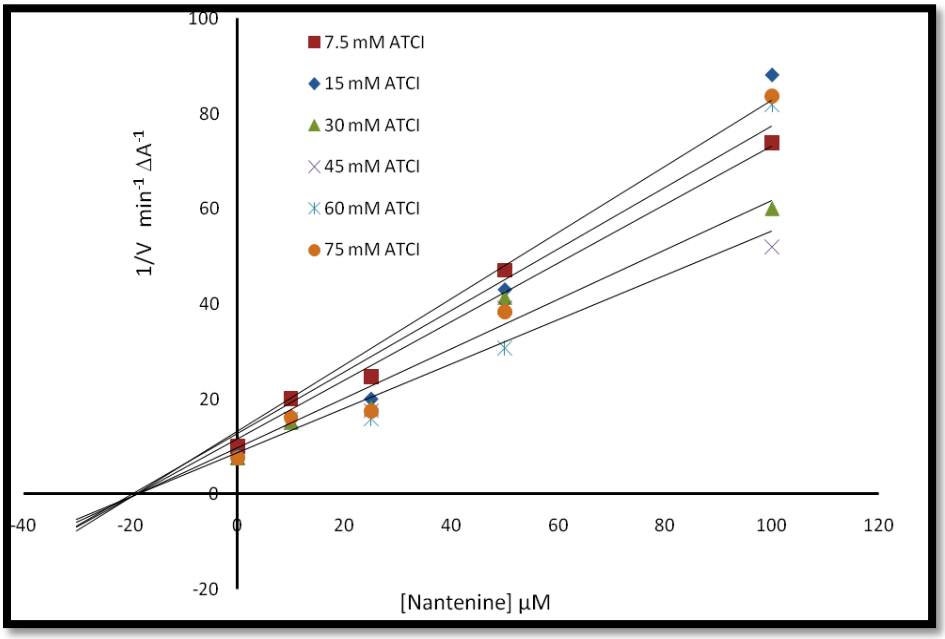

Figure 4.9 Dixon plot. Intercept on the x- axis is $-K_i$

4.2.3 Docking Experiments

To further understand the structural basis for the anti-AChE activity seen in nantenine, molecular docking experiments were performed with the program ICM Pro®.[67] The crystal structure of *Torpedo californica* AChE (*TcAChE*) bound to bis-(5)-tacrine was obtained from Protein Data Bank (PDB)[68] – PDB code 2CMF. Bis-(5)-tacrine was removed and a homology model generated for *Electrophorus electricus* AChE[69] using the homology modeling features of the program (See Appendix: Figure 4.10). Manipulations were performed to allow for identification of binding sites in the homology modeled enzyme. After energy-minimization, nantenine was docked into the identified binding regions of the enzyme. Scoring functions from this docking experiment are reported in Table 4-2.

Table 4-2. ICM docking scores for nantenine and galanthamine in AChE

Pose #	ICM docking scores	Binding site
1	-59.20	Catalytic
2	-55.09	Catalytic
3	-53.90	Catalytic
4	-53.75	PAS
5	-53.56	Catalytic
6	-53.40	Catalytic
7	-52.61	PAS
8	-52.56	PAS
9	-52.31	PAS
10	-51.43	Catalytic
Galanthamine	-59.52	Catalytic

The known catalytic site inhibitor galanthamine was also docked for comparison (*See Appendix*). The docking scores suggest that nantenine may bind preferentially to the catalytic site since the three most favorable conformations are located in this site.

Catalytic site interactions of nantenine: Inspection of the top binding pose in the active site (Figure 4.11) indicates that nantenine interacts with the enzyme via π-π stacking interactions between Trp84 and rings A and D as well as similar interactions between Tyr330 and ring D. Both of these interactions occur in the anionic sub-site[70] region of the enzyme. Of the three amino acid residues in the catalytic triad [71] (His440, Ser200 and Glu327), nantenine interacts only with Ser 200 (via hydrophobic contacts with ring B). Nantenine also shows interactions with Gly118 in the oxyanion hole[72] region of AChE. Other hydrophobic interactions help to stabilize the molecule in the active site. Interactions of nantenine in the catalytic site of the enzyme have been displayed with LigPlot[73] (Figure 4.12) for ease of viewing.

PAS interactions of nantenine: The ICM docking experiments also predicted binding poses for nantenine in the PAS (Figure 4.13). A LigPlot model for the key interactions of pose #4 (Figure 4.14) which indicates that nantenine is stabilized via a hydrogen-bonding interaction between the C2 oxygen atom and the phenolic group of Tyr70 in the PAS. π-π stacking interactions between the aromatic rings of nantenine and Trp279 as well as between Y334 and ring A also seem to be important for binding to the PAS based on inspection of our ICM model.

The ICM models may be used to explain the mode of inhibition exhibited by nantenine; the mixed mode of inhibition is likely due to nantenine binding to both the catalytic site and PAS.

4.3 Discussion

Alzheimer's disease (AD) is a neurodegenerative condition, the onset and progression of which is associated with deficits in cholinergic neurotransmission as well as aggregation of the amyloid peptide Aβ.[1-5] A major biological target for the development of anti-AD drugs is the enzyme acetylcholinesterase. Inhibitors of acetylcholinesterase have proven to be of therapeutic value in the treatment of Alzheimer's disease and have been the front-line approach in this regard.[6,7] This enzyme is known to possess two binding domains: a catalytic site which binds the endogenous neurotransmitter acetylcholine and catalyses its degradation and a peripheral anionic site.[8,9] Clinically available inhibitors have as an integral part of their mode of action the inhibition of the catalytic site of the enzyme. This mode of action of anti-AD drugs is in line with the cholinergic hypothesis of Alzheimer's disease.[10,11] However, current interest is in the identification and development of molecules which potently inhibit both the catalytic site and peripheral anionic site of the enzyme.[12] This dual-site inhibition of the enzyme is beneficial because inhibition of the catalytic site results in improvements in cholinergic deficits while inhibition of the peripheral anionic site prevents aggregation of toxic amyloid peptide Aβ.[13-15] A number of chemical scaffolds have been identified which fit this role, some of which utilize a dimeric design for dual AChE inhibition.[16-18] Our work here indicates that the aporphine scaffold may represent another opportunity to develop novel dual-site AChE inhibitors.

A number of analogs of our lead molecule, nantenine were synthesized and evaluated in an Ellman assay for AChE inhibition. As a positive control in this assays we used known AChE inhibitor galanthamine and we obtained IC_{50} value of 0.53 µM, which

is similar to reported one 0.55 μM.[19] All nantenine analogs were designed to probe *N*-methyl group and structural rigidity of the aporphine core of the lead compound in inhibiting the enzyme. We found that both, the rigidity of nantenine and *N*-methyl group are important structural features for AChE inhibition. Others have found that the less rigid tetrahydroisoquinoline precursors of some aporphines show higher levels of AChE inhibition than the aporphines.[20] These results together suggest that the structural rigidity of aporphines as a group *per se* is not the only determinant of enzyme activity, although in the case of nantenine this rigidity does appear to play a significant role. Nantenine showed mixed inhibition kinetics in our enzyme assays. Interestingly, nantenine was previously shown to be inactive in an AChE assay with rat synaptosomal membrane as the enzyme source.[21] The assay conditions or source of the enzyme may account for the discrepancy in prior and current results.

Our docking experiments suggest that nantenine is capable of binding to both the catalytic site and the PAS of AChE which likely accounts for its mixed mode of inhibition. This study is the first to examine the docking of aporphines and flexible analogs although there is one recent study where docking of structurally related oxoaporphines and oxoisoaporphines was reported.[22] Like nantenine, the molecular modeling experiments suggest that the oxoaporphines and oxoisoaporphines interact with the PAS. In the case of the flexible analogs **1**-**5**, we found that visual inspection of the docked ICM poses seems to be a good method for predicting activity or lack thereof in this series of compounds. However, the top 3 ICM scores for nantenine, **1** and **5** did not show good qualitative correlation with observed inhibitory activities suggesting that the ICM score is not a good predictor of relative AChE inhibitory activity for this series of

compounds. This may be due in part to the occurrence of multiple binding modes for these compounds.

The therapeutic potential of AChE inhibitors has been strengthened by the evidence which shows that besides their role on the improvement in cognitive function, they might also contribute in process of slowing the neurodegeneration in AD patients. It was reported that AChE exerts several other, noncholinergic functions,[23] related to its peripheral anionic site,[24,25] in cell adhesion[26] and differentiation,[27] and some findings also support its role in mediating the processing and deposition of Aβ peptide.[14,28] It is shown that AChE is one of the proteins that colocalizes with Aβ peptide deposits in the brain of AD patients[29] and promotes Aβ fibrillogenesis by forming stable AChE-Aβ complexes.[30] Additionally, it has also been postulated that AChE binds through its peripheral site to the Aβ nonamyloidogenic form and acts as a pathological chaperone inducing a conformational transition to the amyloidogenic form.[14] In considering the design of novel anti-AD drugs, dual inhibition of AChE is a significant strategy to explore, since they might simultaneously enhance the cognitive deficit in AD patients and act as disease modifying agents delaying the amyloid plaque formation.[31]

Nantenine is an interesting lead for such studies. Apart from the dual inhibitory profile, other factors such as blood-brain barrier penetrability will also be important in the future design of nantenine analogs. In that regard, nantenine is perhaps a better lead than some other anti-AChE aporphinoids previously identified (See in Figure 4.6),[32] which predictably will not cross the blood-brain barrier due to its quaternized nitrogen functionality. Other AChE inhibitors that are used for treatment of mild to moderate AD have several serious side effects. Tacrine (Cognex®), for example, the first approved

anticholinesterse agent, has low selectivity and binds to both AChE in brain and periphery, which will result in several muscarinic and nicotinic effects. Additionally, tacrine binds to butyrylcholinesterase with almost the same affinity.[33] Because of its known hepatotoxicity the use of this drug is reduced. Another AChE inhibitor, donepezil (Aricept®) is almost 1000 folds more selective for AChE than for butyrylcholinesterase, and it also exhibits greater affinity for brain AChE than for AChE in the periphery.[34] It has been also shown that this drug has no potential for hepatotoxicity. Still this drug is only aimed for treatment of mild-to-moderate AD. Further pharmacological and pharmacokinetic studies have to be performed on nantenine in order to better understand the possible side effects of this drug. Our findings from previous project, where we screened nantenine for number of various CNS receptors, showed that nantenine has affinity for numerous receptors, which might be the major drawback in development of potential therapeutics for AD treatment based on this molecule. Still the extensive SAR study on this molecule is necessary, since it might reveal which part of nantenine structure can be modified in order to separate the different activities of nantenine.

Our SAR explorations have revealed that the rigid structure of nantenine is important for anticholinesterase activity; increasing molecular flexibility was associated with a decrease in AChE inhibition. The similar findings were also observed for *N*-methyl group- changing of this group led to the significant loss of the anticholinesterase activity. Since the inhibition was of the mixed type, it is perceptible that nantenine binds to both the PAS and the catalytic site. This is corroborated by our molecular docking studies which indicated key H-bond and π-π stacking interactions of nantenine in the PAS.

The aporphine scaffold of nantenine may thus be useful to explore for the synthesis of novel PAS or dual-site AChE inhibitors.

4.4 Experimental

Materials and Methods

Chemistry

General Methods and Instrumentation: High Resolution Electron Impact Mass Spectra (HREIMS) were obtained using an Agilent 6520 Q-TOF instrument. NMR data were collected on a Bruker 500 MHz machine with TMS as internal standard and $CDCl_3$ as solvent unless stated otherwise. Chemical shift (δ) values are reported in ppm and coupling constants in Hertz (Hz). Melting points were obtained on a Mel-Temp capillary electrothermal melting point apparatus. Reactions were monitored by TLC with Analtech Uniplate silica gel G/UV 254 precoated plates (0.2 mm). TLC plates were visualized by UV (254 nm) and by staining with phosphomolybdic acid reagent followed by heating. Flash column chromatography was performed with Silicagel 60 (EMD Chemicals, 230-400 mesh, 0.04-0.063 μm particle size).

Synthesis

Nantenine methiodide. Nantenine (50 mg, 0.15 mmol) was dissolved in acetonitrile (10 ml) and then slowly treated with methyl iodide (0.18 ml, 2.94 mmol). The mixture was refluxed under Ar for 4 h. Acetonitrile was evaporated *in vacuo* providing the crude product which was purified by recrystallization from acetone as a yellow solid (44 mg, 62%): **mp** 202-204 °C. **^{1}H NMR** (500 MHz, DMSO-D_6): δ 7.72 (s, 1H), 6.99 (s, 1H), 6.96 (s, 1H), 6.08 (d, 2H), 4.64 (dd, 1H, J=14.3, 3.0 Hz), 3.85 (s, 3H), 3.79 (m, 1H), 3.78

(m, 1H), 3.62 (s, 3H), 3.52-3.23 (m, 3H), 3.05-2.80 (m, 3H), 2.50 (s, 3H); **^{13}C NMR** (125 MHz, DMSO-D6): δ 152.8, 146.7, 146.6, 144.6, 127.1, 126.3, 124.9, 123.8, 119.5, 111.0, 108.4, 107.7, 101.1, 67.3, 59.8, 55.7, 52.8, 42.8, 28.4, 24.9, 23.1; **HRESIMS** calcd. for $C_{21}H_{24}NO_4$ $[M+H]^+$ 354.1626; found 354.1699.

AChE Inhibition Assay

AChE inhibition was determined using the method of Adsersen et al with ATCI as substrate. In brief, to a 96-well microplate, 25 μL substrate, 15mM ATCI in water, 125 μL 3 mM DTNB in buffer C (50 mM Tris–HCl, pH 8, 0.1M NaCl, 0.02 M $MgCl_2 \cdot 6H_2O$), 72.5 μL buffer B (50 mM Tris–HCl, pH 8, 0.1% bovine serum albumin) and 2.5 μL test compound solution dissolved in DMSO were added and the absorbance was measured seven times at 405 nm every 19 s in a PowerWave 200 Microplate Scanning Spectrophotometer. Then 25 μL AChE (0.22 U/mL in buffer B) were added to the wells and the absorbance was measured again seven times at 405 nm every 19 s. The reaction rate was calculated by GraphPad Prism software version 5.0 and Microsoft Excel. Increase in absorbance due to the spontaneous hydrolysis of substrate was corrected by subtracting the rate of the reaction before adding the enzyme. Percentage inhibition was calculated by comparing the rates for the samples to the blank (2.5 μL DMSO instead of test compound solution). IC_{50} values were calculated by nonlinear regression analysis using GraphPad Prism. Each experiment was done in triplicate.[81]

Docking studies with Nantenine

The binding of the nantenine and *Electrophorus electricus* AChE was examined in silico. All docking studies were performed using Internal Coordinate Mechanics (Molsoft ICM version 3.6-1) package. The ICM score considers several free energy terms such as van

der Waals, hydrogen bonding, Poisson electrostatic desolvation and entropy. ICM sequence-structure alignment is based on ZEGA sequence alignment[82] (Needleman and Wunsch algorithm with zero gap and penalties).

a) Preparation of Homology Model

Since a high-resolution crystal structure of *E. electricus* AChE is not available, the homology model for molecular modeling purposes was built based on the X-ray crystal structure of *Torpedo californica* AChE in complex with bis-(5)-tacrine (PDB code 2CMF) which was obtained from the Protein Data Bank. The tacrine ligand and water molecules present in the pdb file were removed prior to building the model. The sequence of *E. electricus* AChE was aligned with the sequence of *Torpedo californica* AChE, and showed 70% identity. For the sequence alignment step, the following parameters were used:

Alignment Algorithm: ZEGA

Gap Open: 2.4

Gap Extension: 0.15

maxPenalizedGap: 99

This alignment, along with a file containing the atomic coordinates of *Torpedo californica* AChE, was used as an input to the ICM PRO software package to generate the homology model. For the homology model building step the following parameters were used:

3D template: 2CMF

Max loop length: 100

Nterm extension: 1

Cterm extension: 1

Expand gaps by: 1

After energy-minimizing using ICM-PRO, the receptor model was saved and used for docking studies.

b) Generation of ligands

The 2D structure of nantenine (or analogs **1-12** and **nantenine methiodide**) was drawn with ChemDraw Ultra version 9.0 and energy minimized through Chem3D Ultra version 9.0/MOPAC, Job Type: Minimum RMS Gradient of 0.010 kcal/mol and RMS distance of 0.1 Å, and saved as MDL MolFile (*.mol).

c) Docking using Molsoft ICM 3.6-1 program.[83]

To perform ICM small molecule docking the following steps were executed as per program guidelines:

(1) Setup docking project:

(i) The project name was set.

(ii) The enzyme (receptor) was setup: (The receptor molecule was entered in the receptor molecule data entry box, the binding sites were identified by clicking on the "identify binding sites" button. In this way potential ligand binding pockets were identified. After the receptor setup was complete, the program displayed the receptor with selected binding site residues highlighted in yellow x-7stick presentation).

(iii) The binding site was reviewed and adjusted: ICM made a box around the ligand binding site based on the information entered in the receptor setup section. The position of the box encompassed the residues expected to be involved in ligand binding.

(iv) Receptor maps were made: Energy maps of the environment within the docking box were constructed. Flexibility of the receptor residues was set to 4.0.

(2) Docking simulation was executed:

Interactive docking was used to dock nantenine and the other analogs. The molecules were docked in non-chiral mode. The thoroughness level was set to the maximum value of 10. ICM scores were obtained after this procedure.

4.5 Appendix

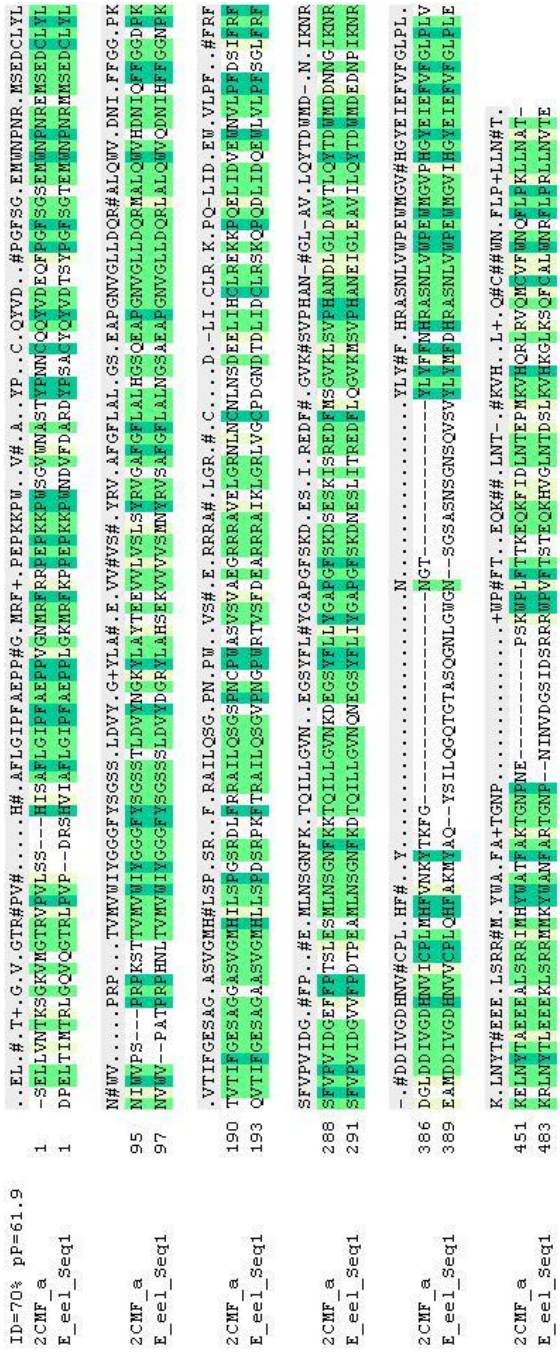

Figure 4.10 ICM Pro sequence alignment of *Electric eel* sequence with the *Torpedo californica* template (PDB: 2CMF)

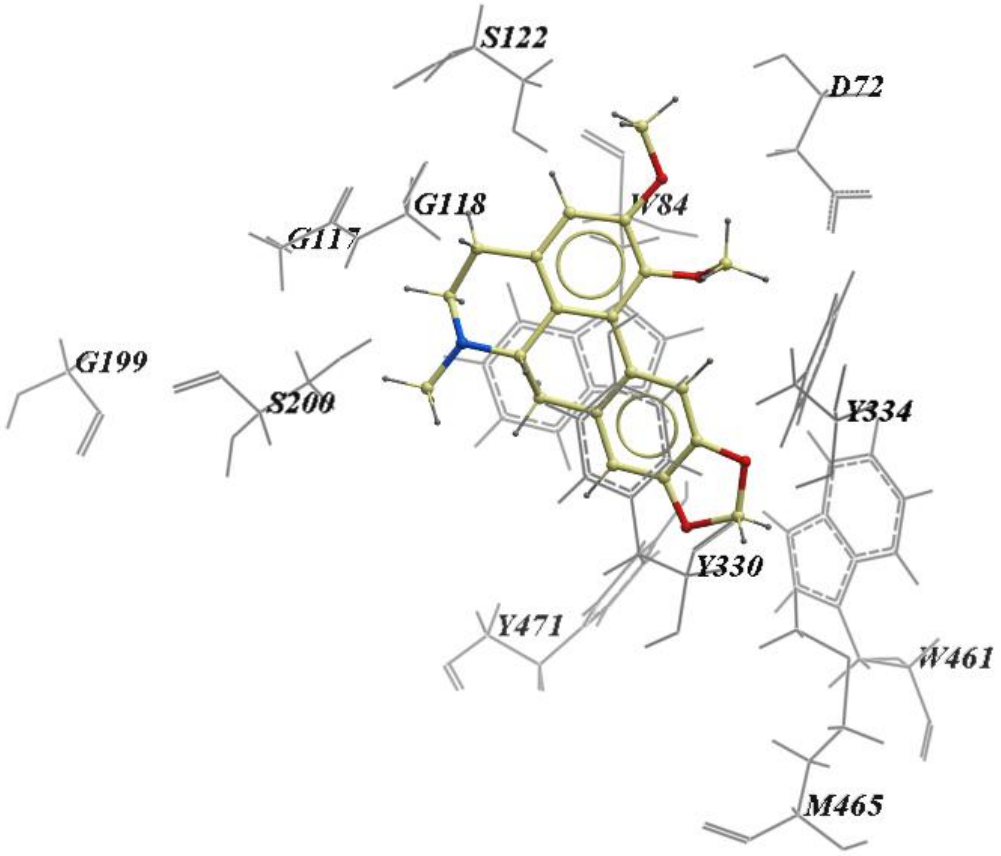

Figure 4.11 ICM model of nantenine in the catalytic site of AChE. Pose shown is for lowest energy conformation (pose #1 in Table 4-2)

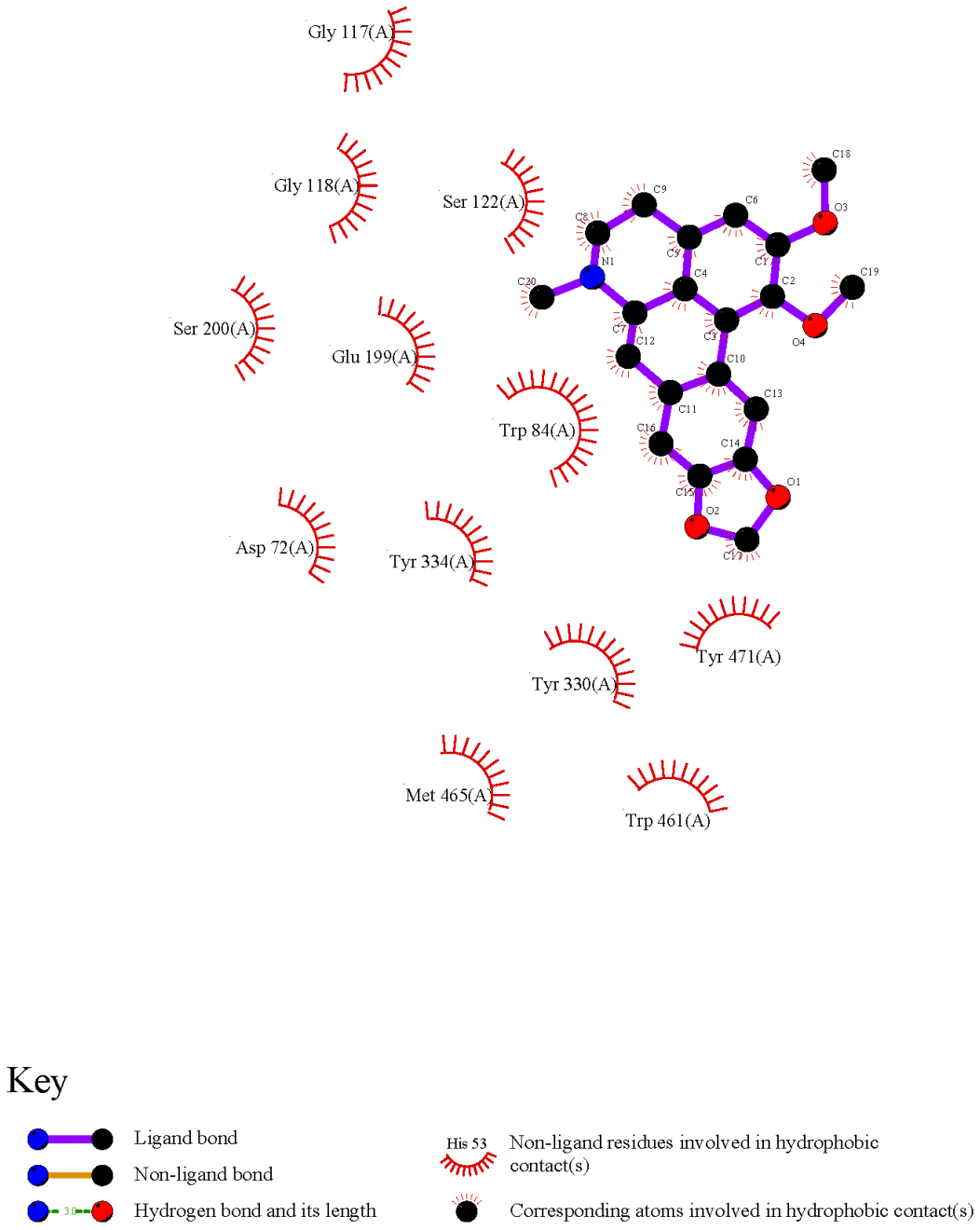

Figure 4.12 LigPlot model of nantenine in the catalytic site of AChE

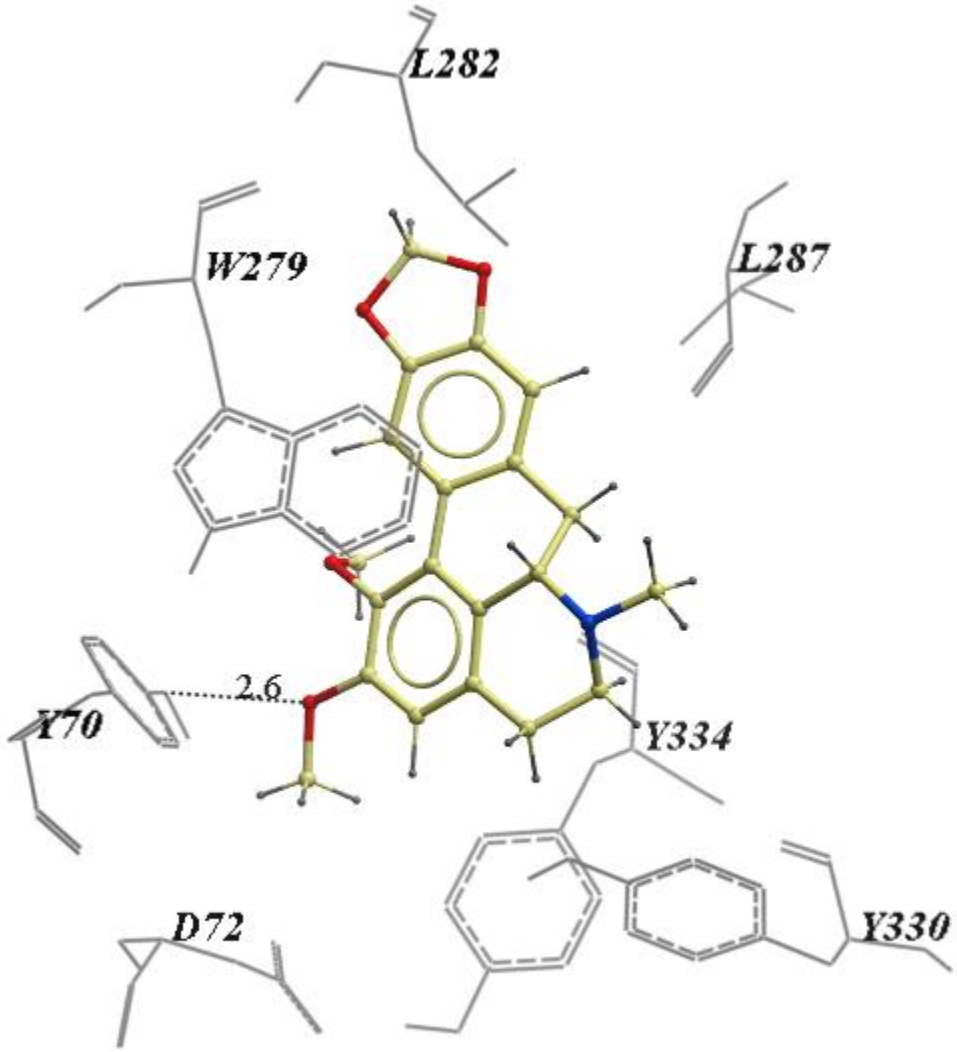

Figure 4.13 ICM model of nantenine in the PAS of AChE. Pose shown is for the lowest energy conformation in the PAS (pose #4 in Table 4-2)

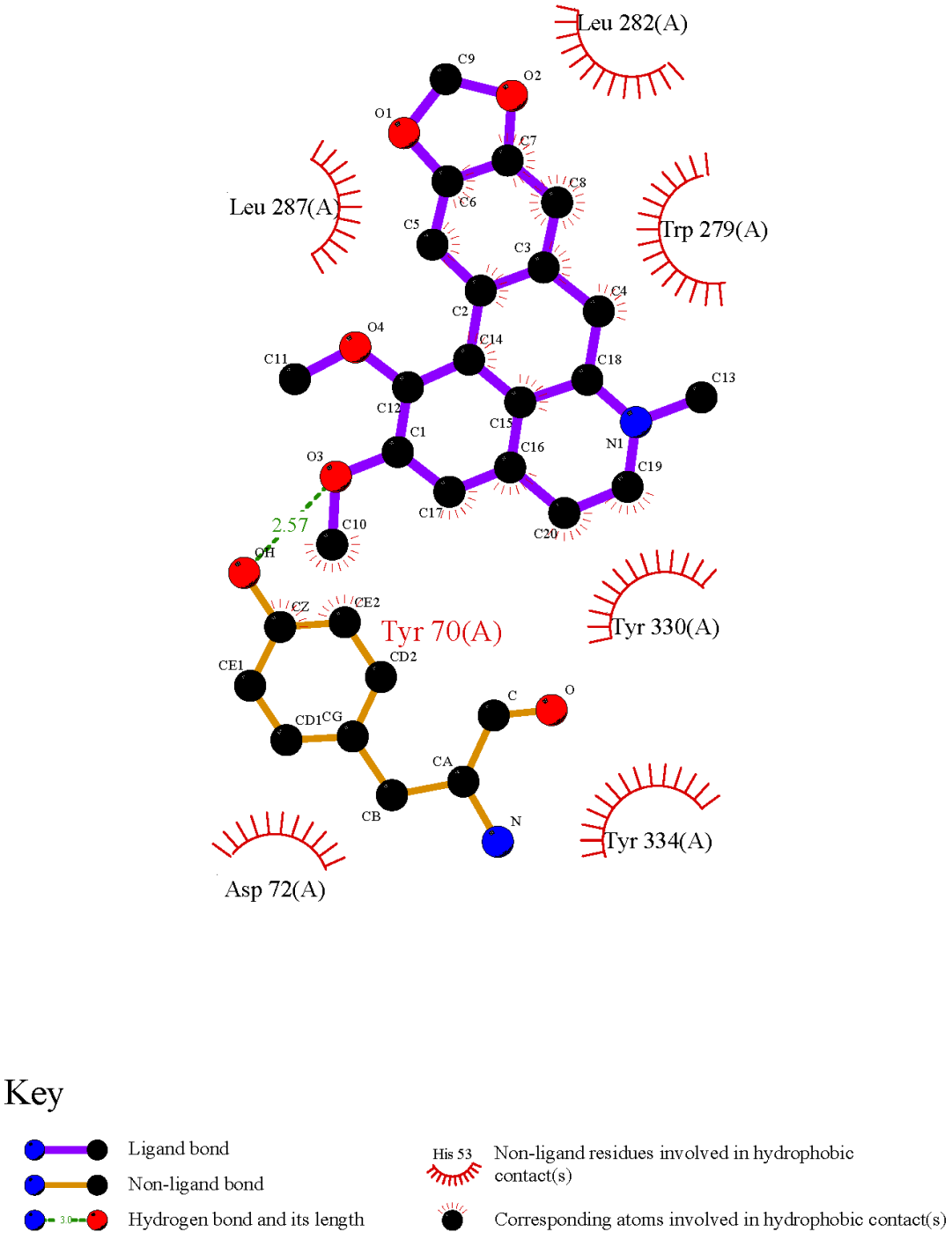

Figure 4.14 LigPlot model of Nantenine in the PAS

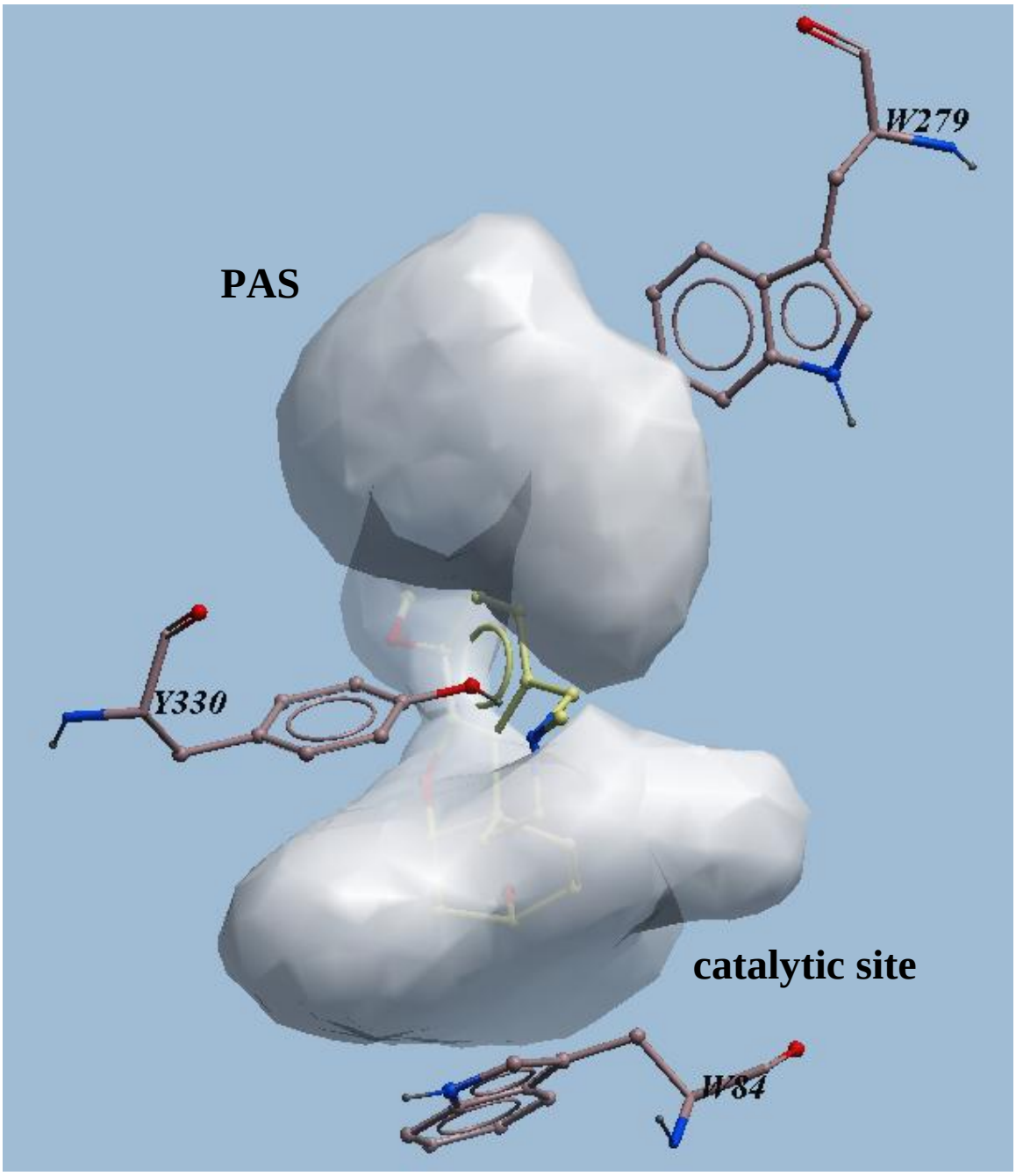

Figure 4.15 ICM model of galanthamine in the binding cleft of AChE

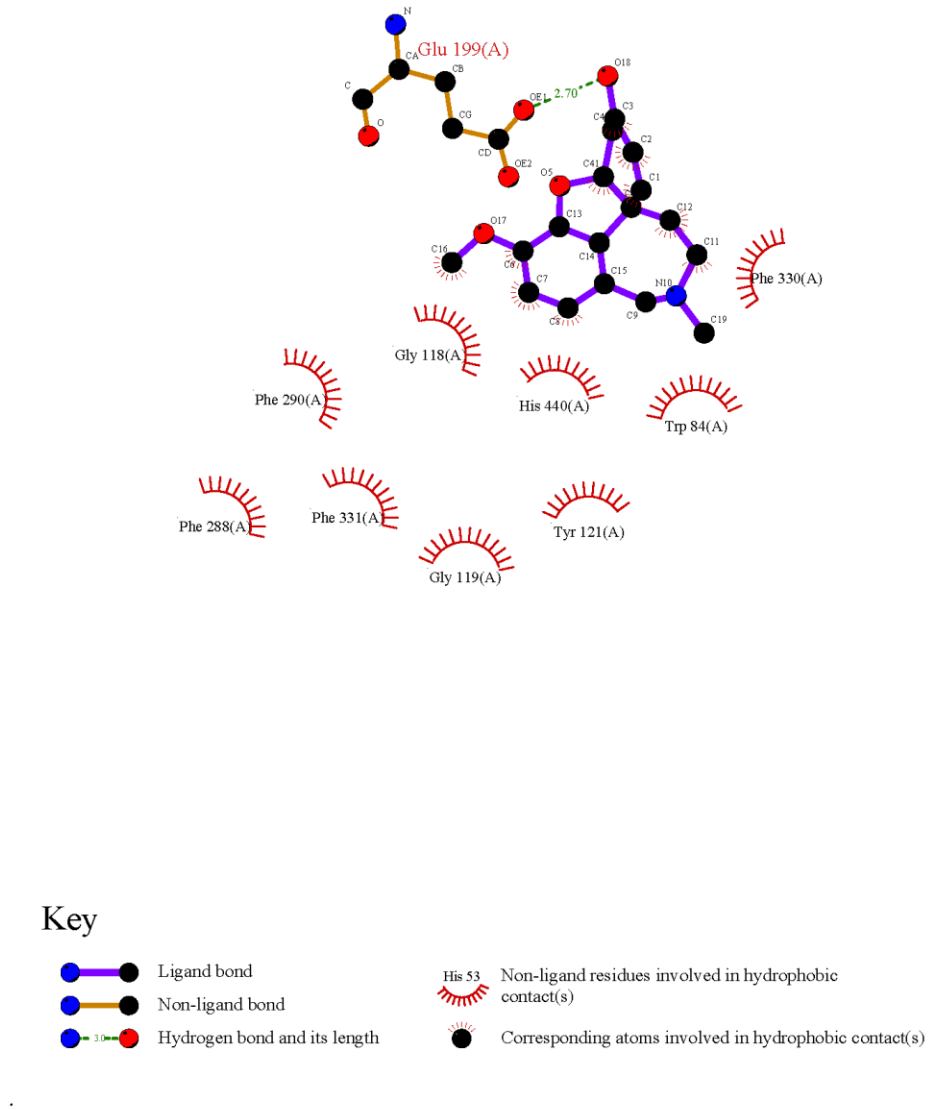

Figure 4.16 LigPlot model of galanthamine in the AChE

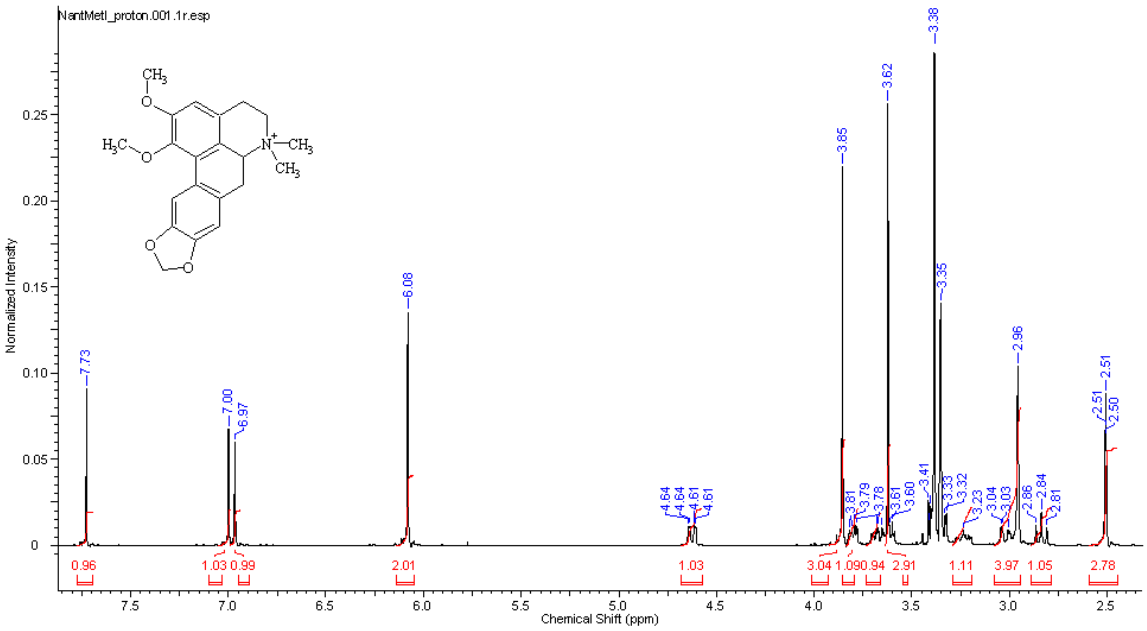

Figure 4.17 ^{1}H NMR (500 MHz, DMSO-D_6) of nantenine methiodide

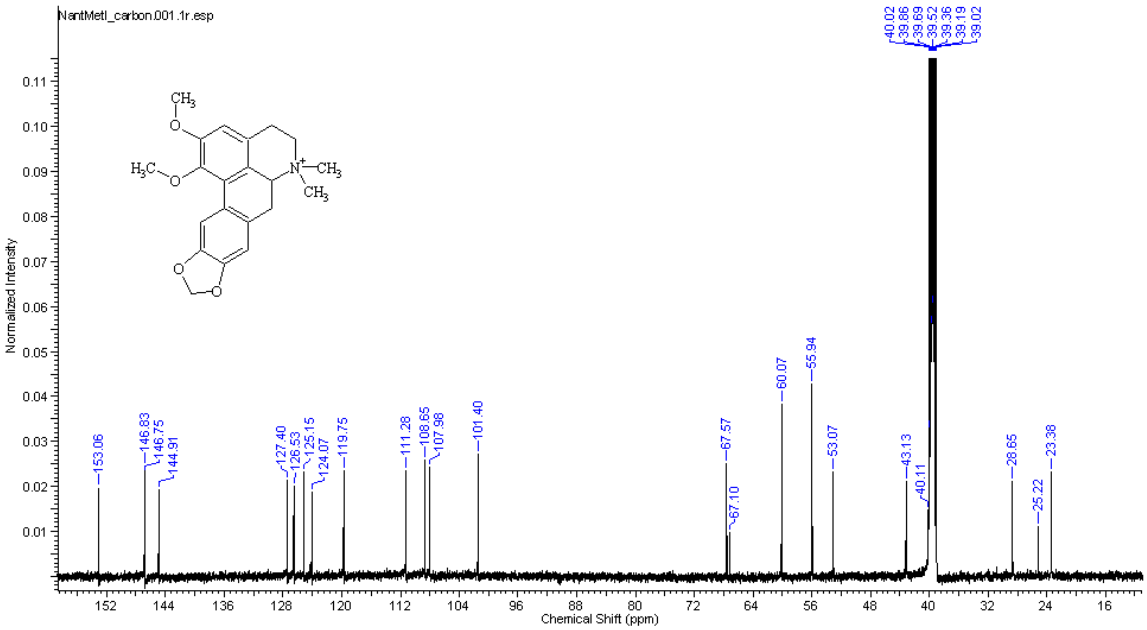

Figure 4.18 ^{13}C NMR (125 MHz, DMSO-D_6) of nantenine methiodide

4.6 References

(1) Corey-Bloom, J. *International psychogeriatrics / IPA* **2002**, *14 Suppl 1*, 51.

(2) Akhondzadeh, S.; Noroozian, M. *IDrugs* **2002**, *5*, 1062.

(3) Backman, L.; Jones, S.; Berger, A. K.; Laukka, E. J.; Small, B. J. *Neuropsychology* **2005**, *19*, 520.

(4) http://www.alzheimers.org/ 2010.

(5) Ellis, J. M. *J Am Osteopath Assoc* **2005**, *105*, 145.

(6) Shimokawa, A.; Yatomi, N.; Anamizu, S.; Torii, S.; Isono, H.; Sugai, Y.; Kohno, M. *Brain and cognition* **2001**, *47*, 423.

(7) Weinshenker, D. *Current Alzheimer research* **2008**, *5*, 342.

(8) Poirier, J. *Int J Clin Pract Suppl* **2002**, 6.

(9) Hardy, J. *J Alzheimers Dis* **2006**, *9*, 151.

(10) Pimplikar, S. W. *The international journal of biochemistry & cell biology* **2009**, *41*, 1261.

(11) Korczyn, A. D. *Alzheimers Dement* **2008**, *4*, 176.

(12) Eckman, C. B.; Eckman, E. A. *Neurologic clinics* **2007**, *25*, 669.

(13) Hardy, J. A.; Higgins, G. A. *Science (New York, N.Y* **1992**, *256*, 184.

(14) Hardy, J.; Selkoe, D. J. *Science (New York, N.Y* **2002**, *297*, 353.

(15) Vassar, R.; Citron, M. *Neuron* **2000**, *27*, 419.

(16) Selkoe, D. J. *Physiol Rev* **2001**, *81*, 741.

(17) Arendt, T. *Neuroscience* **2001**, *102*, 723.

(18) Mehta, N. D.; Refolo, L. M.; Eckman, C.; Sanders, S.; Yager, D.; Perez-Tur, J.; Younkin, S.; Duff, K.; Hardy, J.; Hutton, M. *Ann Neurol* **1998**, *43*, 256.

(19) Games, D.; Adams, D.; Alessandrini, R.; Barbour, R.; Berthelette, P.; Blackwell, C.; Carr, T.; Clemens, J.; Donaldson, T.; Gillespie, F.; et al. *Nature* **1995**, *373*, 523.

(20) Braak, H.; Braak, E. *Acta Neuropathol* **1991**, *82*, 239.

(21) Malamas, M. S.; Erdei, J.; Gunawan, I.; Barnes, K.; Johnson, M.; Hui, Y.; Turner, J.; Hu, Y.; Wagner, E.; Fan, K.; Olland, A.; Bard, J.; Robichaud, A. J. *J Med Chem* **2009**, *52*, 6314.

(22) Hom, R. K.; Fang, L. Y.; Mamo, S.; Tung, J. S.; Guinn, A. C.; Walker, D. E.; Davis, D. L.; Gailunas, A. F.; Thorsett, E. D.; Sinha, S.; Knops, J. E.; Jewett, N. E.; Anderson, J. P.; John, V. *J Med Chem* **2003**, *46*, 1799.

(23) Davis, J. N.; Tung, A.; Chak, S. S.; Ventura, E. E.; Byrd-Williams, C. E.; Alexander, K. E.; Lane, C. J.; Weigensberg, M. J.; Spruijt-Metz, D.; Goran, M. I. *Med Sci Sports Exerc* **2009**, *41*, 1494.

(24) Bard, F.; Cannon, C.; Barbour, R.; Burke, R. L.; Games, D.; Grajeda, H.; Guido, T.; Hu, K.; Huang, J.; Johnson-Wood, K.; Khan, K.; Kholodenko, D.; Lee, M.; Lieberburg, I.; Motter, R.; Nguyen, M.; Soriano, F.; Vasquez, N.; Weiss, K.; Welch, B.; Seubert, P.; Schenk, D.; Yednock, T. *Nat Med* **2000**, *6*, 916.

(25) DeMattos, R. B.; Bales, K. R.; Cummins, D. J.; Dodart, J. C.; Paul, S. M.; Holtzman, D. M. *Proc Natl Acad Sci U S A* **2001**, *98*, 8850.

(26) Nuutinen, T.; Suuronen, T.; Kauppinen, A.; Salminen, A. *Brain Res Rev* **2009**, *61*, 89.

(27) Jick, H.; Zornberg, G. L.; Jick, S. S.; Seshadri, S.; Drachman, D. A. *Lancet* **2000**, *356*, 1627.

(28) Wolozin, B. *Neuron* **2004**, *41*, 7.

(29) Solomon, A.; Kareholt, I.; Ngandu, T.; Wolozin, B.; Macdonald, S. W.; Winblad, B.; Nissinen, A.; Tuomilehto, J.; Soininen, H.; Kivipelto, M. *Neurobiol Aging* **2009**, *30*, 1006.

(30) Scapini, E.; Scheltens, P.; Feldman, H. *Lancet Neurol.* **2003**, *2*, 539.

(31) Ballatore, C.; Brunden, K. R.; Piscitelli, F.; James, M. J.; Crowe, A.; Yao, Y.; Hyde, E.; Trojanowski, J. Q.; Lee, V. M.; Smith, A. B., 3rd *J Med Chem* **2010**, *53*, 3739.

(32) Weggen, S.; Eriksen, J. L.; Das, P.; Sagi, S. A.; Wang, R.; Pietrzik, C. U.; Findlay, K. A.; Smith, T. E.; Murphy, M. P.; Bulter, T.; Kang, D. E.; Marquez-Sterling, N.; Golde, T. E.; Koo, E. H. *Nature* **2001**, *414*, 212.

(33) Sivaprakasam, K. *Current medicinal chemistry* **2006**, *13*, 2179.

(34) Terry, A. V., Jr.; Buccafusco, J. J. *The Journal of pharmacology and experimental therapeutics* **2003**, *306*, 821.

(35) Inestrosa, N. C.; Alvarez, A.; Dinamarca, M. C.; Perez-Acle, T.; Colombres, M. *Curr Alzheimer Res* **2005**, *2*, 301.

(36) Munoz, F. J.; Aldunate, R.; Inestrosa, N. C. *Neuroreport* **1999**, *10*, 3621.

(37) Sabbagh, M. N.; Farlow, M. R.; Relkin, N.; Beach, T. G. *Alzheimer's & Dementia* **2006**, *2*, 118.

(38) Colombres, M.; Sagal, J. P.; Inestrosa, N. C. *Current pharmaceutical design* **2004**, *10*, 3121.

(39) Ballard, C. G. *Eur Neurol* **2002**, *47*, 64.

(40) Hansen, R. A.; Gartlehner, G.; Webb, A. P.; Morgan, L. C.; Moore, C. G.; Jonas, D. E. *Clinical interventions in aging* **2008**, *3*, 211.

(41) Ritchie, C. W.; Ames, D.; Clayton, T.; Lai, R. *Am J Geriatr Psychiatry* **2004**, *12*, 358.

(42) Wagstaff, A. J.; McTavish, D. *Drugs & aging* **1994**, *4*, 510.

(43) Loy, C.; Schneider, L. *Cochrane database of systematic reviews (Online)* **2006**, CD001747.

(44) Heinze, M.; Andreae, D.; Grohmann, R. *Pharmacopsychiatry* **2002**, *35*, 79.

(45) Dunn, N. R.; Pearce, G. L.; Shakir, S. A. *Journal of psychopharmacology (Oxford, England)* **2000**, *14*, 406.

(46) Moller, H. J. *Eur Neuropsychopharmacol* **1999**, *9 Suppl 2*, S53.

(47) Bolognesi, M. L.; Minarini, A.; Rosini, M.; Tumiatti, V.; Melchiorre, C. *Mini reviews in medicinal chemistry* **2008**, *8*, 960.

(48) Cavalli, A.; Bottegoni, G.; Raco, C.; De Vivo, M.; Recanatini, M. *Journal of medicinal chemistry* **2004**, *47*, 3991.

(49) Zhou, X.; Wang, X. B.; Wang, T.; Kong, L. Y. *Bioorg Med Chem* **2008**, *16*, 8011.

(50) Inestrosa, N. C.; Sagal, J. P.; Colombres, M. *Sub-cellular biochemistry* **2005**, *38*, 299.

(51) De Ferrari, G. V.; Canales, M. A.; Shin, I.; Weiner, L. M.; Silman, I.; Inestrosa, N. C. *Biochemistry* **2001**, *40*, 10447.

(52) Bolognesi, M. L.; Cavalli, A.; Valgimigli, L.; Bartolini, M.; Rosini, M.; Andrisano, V.; Recanatini, M.; Melchiorre, C. *Journal of medicinal chemistry* **2007**, *50*, 6446.

(53) del Monte-Millan, M.; Garcia-Palomero, E.; Valenzuela, R.; Usan, P.; de Austria, C.; Munoz-Ruiz, P.; Rubio, L.; Dorronsoro, I.; Martinez, A.; Medina, M. *J Mol Neurosci* **2006**, *30*, 85.

(54) Munoz-Ruiz, P.; Rubio, L.; Garcia-Palomero, E.; Dorronsoro, I.; del Monte-Millan, M.; Valenzuela, R.; Usan, P.; de Austria, C.; Bartolini, M.; Andrisano, V.; Bidon-Chanal, A.; Orozco, M.; Luque, F. J.; Medina, M.; Martinez, A. *Journal of medicinal chemistry* **2005**, *48*, 7223.

(55) Camps, P.; Formosa, X.; Munoz-Torrero, D.; Petrignet, J.; Badia, A.; Clos, M. V. *Journal of medicinal chemistry* **2005**, *48*, 1701.

(56) Cannon, J. G.; Flaherty, P. T.; Ozkutlu, U.; Long, J. P. *J Med Chem* **1995**, *38*, 1841.

(57) Zhang, A.; Zhang, Y.; Branfman, A. R.; Baldessarini, R. J.; Neumeyer, J. L. *J Med Chem* **2007**, *50*, 171.

(58) Hung, T. M.; Na, M.; Dat, N. T.; Ngoc, T. M.; Youn, U.; Kim, H. J.; Min, B. S.; Lee, J.; Bae, K. *Journal of ethnopharmacology* **2008**, *119*, 74.

(59) Tang, H.; Wei, Y. B.; Zhang, C.; Ning, F. X.; Qiao, W.; Huang, S. L.; Ma, L.; Huang, Z. S.; Gu, L. Q. *European journal of medicinal chemistry* **2009**.

(60) Markmee, S.; Ruchirawat, S.; Prachyawarakorn, V.; Ingkaninan, K.; Khorana, N. *Bioorg Med Chem Lett* **2006**, *16*, 2170.

(61) Kiely, J. S.; Moos, W. H.; Pavia, M. R.; Schwarz, R. D.; Woodard, G. L. *Anal Biochem* **1991**, *196*, 439.

(62) Rhee, I. K.; van de Meent, M.; Ingkaninan, K.; Verpoorte, R. *Journal of chromatography* **2001**, *915*, 217.

(63) Marston, A.; Kissling, J.; Hostettmann, K. *Phytochem Anal* **2002**, *13*, 51.

(64) Greenblatt, H. M.; Kryger, G.; Lewis, T.; Silman, I.; Sussman, J. L. *FEBS Lett* **1999**, *463*, 321.

(65) Tang, H.; Wei, Y. B.; Zhang, C.; Ning, F. X.; Qiao, W.; Huang, S. L.; Ma, L.; Huang, Z. S.; Gu, L. Q. *Eur J Med Chem* **2009**, *44*, 2523.

(66) Tang, H.; Ning, F. X.; Wei, Y. B.; Huang, S. L.; Huang, Z. S.; Chan, A. S.; Gu, L. Q. *Bioorg Med Chem Lett* **2007**, *17*, 3765.

(67) Cardozo, T.; Totrov, M.; Abagyan, R. *Proteins: Structure, Function, and Genetics* **1995**, *23*, 403.

(68) Berman, H. M.; Westbrook, J.; Feng, Z.; Gilliland, G.; Bhat, T. N.; Weissig, H.; Shindyalov, I. N.; Bourne, P. E. *Nucleic Acids Res* **2000**, *28*, 235.

(69) Carolan, C. G.; Gaynor, J. M.; Dillon, G. P.; Khan, D.; Ryder, S. A.; Reidy, S.; Gilmer, J. F. *Chem Biol Interact* **2008**, *175*, 293.

(70) Szegletes, T.; Mallender, W. D.; Rosenberry, T. L. *Biochemistry* **1998**, *37*, 4206.

(71) Sussman, J. L.; Harel, M.; Frolow, F.; Oefner, C.; Goldman, A.; Toker, L.; Silman, I. *Science (New York, N.Y* **1991**, *253*, 872.

(72) Harel, M.; Quinn, D. M.; Nair, H. K.; Silman, I.; Sussman, J. L. *Journal of the American Chemical Society* **1996**, *118*, 2340.

(73) Wallace, A. C.; Laskowski, R. A.; Thornton, J. M. *Protein Engineering* **1995**, *8*, 127.

(74) Perry, E. K. *Br Med Bull* **1986**, *42*, 63.

(75) Bartus, R. T.; Dean, R. L.; Pontecorvo, M. J.; Flicker, C. *Ann N Y Acad Sci* **1985**, *444*, 332.

(76) Holzgrabe, U.; Kapkova, P.; Alptuzun, V.; Scheiber, J.; Kugelmann, E. *Expert Opin Ther Targets* **2007**, *11*, 161.

(77) Shen, Y.; Zhang, J.; Sheng, R.; Dong, X.; He, Q.; Yang, B.; Hu, Y. *J Enzyme Inhib Med Chem* **2009**, *24*, 372.

(78) Haviv, H.; Wong, D. M.; Silman, I.; Sussman, J. L. *Curr Top Med Chem* **2007**, *7*, 375.

(79) Dorronsoro, I.; Alonso, D.; Castro, A.; del Monte, M.; Garcia-Palomero, E.; Martinez, A. *Arch Pharm (Weinheim)* **2005**, *338*, 18.

(80) Ribeiro, R. d. A.; De Lores Arnaiz, G. R. *Phytomedicine* **2000**, *7*, 313.

(81) Adsersen, A.; Kjolbye, A.; Dall, O.; Jager, A. K. *Journal of ethnopharmacology* **2007**, *113*, 179.

(82) Abagyan, R. A.; Batalov, S. *J Mol Biol* **1997**, *273*, 355.

(83) Farag, N. A.; Mohamed, S. R.; Soliman, G. A. *Bioorg Med Chem* **2008**, *16*, 9009.

Chapter 5: Bibliography

Chapter 1

(1) Kalant, H. *Cmaj* **2001**, *165*, 917.

(2) Gouzoulis-Mayfrank, E.; Hermle, L.; Kovar, K.; Sass, H. *Fortschr Neurol Psychiatr* **1999**, *67*, 574.

(3) http://www.drugabuse.gov/.

(4) Nichols, D. E.; Oberlender, R. *NIDA research monograph* **1989**, *94*, 1.

(5) Hardman, H. F.; Haavik, C. O.; Seevers, M. H. *Toxicol Appl Pharmacol* **1973**, *25*, 299.

(6) Cuomo, M. J.; Dyment, P. G.; Gammino, V. M. *J Am Coll Health* **1994**, *42*, 271.

(7) Meyer, J. S.; Ali, S. F. *Annals of the New York Academy of Sciences* **2002**, *965*, 373.

(8) http://www.justice.gov/dea/ 2010.

(9) Parrott, A. C. *Psychopharmacology* **2004**, *173*, 234.

(10) Burgess C, O. D. A., Gill M. *Eur Psychiatry* **2000**, *15*, 287.

(11) Nichols, D. E. *Pharmacology & therapeutics* **2004**, *101*, 131.

(12) Ferigolo, M.; Machado, A. G.; Oliveira, N. B.; Barros, H. M. *Revista do Hospital das Clinicas* **2003**, *58*, 332.

(13) Wijetunga, M.; Bhan, R.; Lindsay, J.; Karch, S. *Hawaii Med J* **2004**, *63*, 8.

(14) Karch, S. B. *The Pathology of Drug Abuse*; CRC Press, 1993.

(15) Henry, J. A.; Jeffreys, K. J.; Dawling, S. *Lancet* **1992**, *340*, 384.

(16) Nielsen, S.; Lundemose, J. B.; Simonsen, M. S.; Dragsholt, C. *Ugeskr Laeger* **2001**, *163*, 2253.

(17) Vollenweider, F. X.; Gamma, A.; Liechti, M.; Huber, T. *Neuropsychopharmacology* **1998**, *19*, 241.

(18) Mallick, A.; Bodenham, A. R. *Journal of accident & emergency medicine* **1997**, *14*, 336.

(19) Ricaurte, G. A.; McCann, U. D. *Annals of the New York Academy of Sciences* **1992**, *648*, 371.

(20) Christophersen, A. S. *Toxicol Lett* **2000**, *112-113*, 127.

(21) Boot, B. P.; McGregor, I. S.; Hall, W. *Lancet* **2000**, *355*, 1818.

(22) Colado, M. I.; Granados, R.; O'Shea, E.; Esteban, B.; Green, A. R. *Pharmacology & toxicology* **1999**, *84*, 261.

(23) Parrott, A. C.; Lasky, J. *Psychopharmacology* **1998**, *139*, 261.

(24) Soar, K.; Parrott, A. C.; Fox, H. C. *Psychol Rep* **2004**, *95*, 192.

(25) Robledo, P.; Balerio, G.; Berrendero, F.; Maldonado, R. *Naunyn-Schmiedeberg's archives of pharmacology* **2004**, *369*, 338.

(26) Cottler, L. B.; Womack, S. B.; Compton, W. M.; Ben-Abdallah, A. *Hum Psychopharmacol* **2001**, *16*, 599.

(27) Ricaurte, G. A.; DeLanney, L. E.; Irwin, I.; Langston, J. W. *Brain Res* **1988**, *446*, 165.

(28) Taffe, M. A.; Davis, S. A.; Yuan, J.; Schroeder, R.; Hatzidimitriou, G.; Parsons, L. H.; Ricaurte, G. A.; Gold, L. H. *Neuropsychopharmacology* **2002**, *27*, 993.

(29) Ricaurte, G. A.; Martello, A. L.; Katz, J. L.; Martello, M. B. *The Journal of pharmacology and experimental therapeutics* **1992**, *261*, 616.

(30) McCann, U. D.; Szabo, Z.; Seckin, E.; Rosenblatt, P.; Mathews, W. B.; Ravert, H. T.; Dannals, R. F.; Ricaurte, G. A. *Neuropsychopharmacology* **2005**, *30*, 1741.

(31) Parrott, A. C. *Hum Psychopharmacol* **2001**, *16*, 557.

(32) Slikker, W., Jr.; Ali, S. F.; Scallet, A. C.; Frith, C. H.; Newport, G. D.; Bailey, J. R. *Toxicol Appl Pharmacol* **1988**, *94*, 448.

(33) Green, A. R.; Mechan, A. O.; Elliott, J. M.; O'Shea, E.; Colado, M. I. *Pharmacol Rev* **2003**, *55*, 463.

(34) Sanchez, V.; Camarero, J.; Esteban, B.; Peter, M. J.; Green, A. R.; Colado, M. I. *Br J Pharmacol* **2001**, *134*, 46.

(35) Shankaran, M.; Yamamoto, B. K.; Gudelsky, G. A. *European journal of pharmacology* **1999**, *385*, 103.

(36) Simantov, R.; Tauber, M. *FASEB J* **1997**, *11*, 141.

(37) Mas, M.; Farre, M.; de la Torre, R.; Roset, P. N.; Ortuno, J.; Segura, J.; Cami, J. *The Journal of pharmacology and experimental therapeutics* **1999**, *290*, 136.

(38) Trigo, J. M.; Renoir, T.; Lanfumey, L.; Hamon, M.; Lesch, K. P.; Robledo, P.; Maldonado, R. *Biol Psychiatry* **2007**.

(39) Glennon, R. A.; Young, R. *Pharmacology, biochemistry, and behavior* **2000**, *66*, 483.

(40) Bankson, M. G.; Cunningham, K. A. *Neuropsychopharmacology* **2002**, *26*, 40.

(41) Mazzola-Pomietto, P.; Aulakh, C. S.; Wozniak, K. M.; Hill, J. L.; Murphy, D. L. *Psychopharmacology* **1995**, *117*, 193.

(42) Liechti, M. E.; Vollenweider, F. X. *Hum Psychopharmacol* **2001**, *16*, 589.

(43) Gerra, G.; Zaimovic, A.; Moi, G.; Giusti, F.; Gardini, S.; Delsignore, R.; Laviola, G.; Macchia, T.; Brambilla, F. *Behav Brain Res* **2002**, *134*, 403.

(44) Bubar, M. J.; Cunningham, K. A. *Curr Top Med Chem* **2006**, *6*, 1971.

(45) Cavasotto, C. N.; Orry, A. J.; Abagyan, R. A. *Proteins* **2003**, *51*, 423.

(46) Klabunde, T.; Hessler, G. *Chembiochem* **2002**, *3*, 928.

(47) Attwood, T. K. *Trends Pharmacol Sci* **2001**, *22*, 162.

(48) Bockaert, J.; Pin, J. P. *EMBO J* **1999**, *18*, 1723.

(49) Wess, J. *FASEB J* **1997**, *11*, 346.

(50) Kroeze, W. K.; Kristiansen, K.; Roth, B. L. *Curr Top Med Chem* **2002**, *2*, 507.

(51) Probst, W. C.; Snyder, L. A.; Schuster, D. I.; Brosius, J.; Sealfon, S. C. *DNA Cell Biol* **1992**, *11*, 1.

(52) Lovenberg, T. W.; Erlander, M. G.; Baron, B. M.; Sutcliffe, J. G. *Int Clin Psychopharmacol* **1993**, *8 Suppl 2*, 19.

(53) Saudou, F.; Hen, R. *Neurochem Int* **1994**, *25*, 503.

(54) Gerald, C.; Adham, N.; Kao, H. T.; Olsen, M. A.; Laz, T. M.; Schechter, L. E.; Bard, J. A.; Vaysse, P. J.; Hartig, P. R.; Branchek, T. A.; et al. *EMBO J* **1995**, *14*, 2806.

(55) Plassat, J. L.; Boschert, U.; Amlaiky, N.; Hen, R. *EMBO J* **1992**, *11*, 4779.

(56) Monsma, F. J., Jr.; Shen, Y.; Ward, R. P.; Hamblin, M. W.; Sibley, D. R. *Molecular pharmacology* **1993**, *43*, 320.

(57) Bard, J. A.; Zgombick, J.; Adham, N.; Vaysse, P.; Branchek, T. A.; Weinshank, R. L. *J Biol Chem* **1993**, *268*, 23422.

(58) De Vry, J. *Psychopharmacology* **1995**, *121*, 1.

(59) Grignaschi, G.; Invernizzi, R. W.; Fanelli, E.; Fracasso, C.; Caccia, S.; Samanin, R. *Br J Pharmacol* **1998**, *124*, 1781.

(60) Lemke, T. W., David *Foye`s Principles of Medicinal Chemistry*; Sixth ed., 2008.

(61) Nichols, D. E.; Nichols, C. D. *Chem Rev* **2008**, *108*, 1614.

(62) Roth, B. L. *Ann Clin Psychiatry* **1994**, *6*, 67.

(63) Lummis, S. C. *Biochem Soc Trans* **2004**, *32*, 535.

(64) Farber, L.; Haus, U.; Spath, M.; Drechsler, S. *Scand J Rheumatol Suppl* **2004**, 2.

(65) Bockaert, J.; Claeysen, S.; Compan, V.; Dumuis, A. *Curr Drug Targets CNS Neurol Disord* **2004**, *3*, 39.

(66) Nelson, D. L. *Curr Drug Targets CNS Neurol Disord* **2004**, *3*, 53.

(67) Thomas, D. R. *Pharmacology & therapeutics* **2006**, *111*, 707.

(68) Woolley, M. L.; Marsden, C. A.; Fone, K. C. *Curr Drug Targets CNS Neurol Disord* **2004**, *3*, 59.

(69) Mitchell, E. S.; Neumaier, J. F. *Pharmacology & therapeutics* **2005**, *108*, 320.

(70) Glennon, R. A. *J Med Chem* **2003**, *46*, 2795.

(71) Westkaemper, R. B.; Glennon, R. A. *Curr Top Med Chem* **2002**, *2*, 575.

(72) Bojarski, A. J. *Curr Top Med Chem* **2006**, *6*, 2005.

(73) Greenshaw, A. J. *Trends in pharmacological sciences* **1993**, *14*, 265.

(74) de Wit, R.; Aapro, M.; Blower, P. R. *Cancer Chemother Pharmacol* **2005**, *56*, 231.

(75) Bockaert, J.; Ansanay, H.; Letty, S.; Marchetti-Gauthier, E.; Roman, F.; Rondouin, G.; Fagni, L.; Soumireu-Mourat, B.; Dumuis, A. *C R Acad Sci III* **1998**, *321*, 217.

(76) Corbett, D. F.; Heightman, T. D.; Moss, S. F.; Bromidge, S. M.; Coggon, S. A.; Longley, M. J.; Roa, A. M.; Williams, J. A.; Thomas, D. R. *Bioorg Med Chem Lett* **2005**, *15*, 4014.

(77) Birkett, J. T.; Arranz, M. J.; Munro, J.; Osbourn, S.; Kerwin, R. W.; Collier, D. A. *Neuroreport* **2000**, *11*, 2017.

(78) Hirst, W. D.; Stean, T. O.; Rogers, D. C.; Sunter, D.; Pugh, P.; Moss, S. F.; Bromidge, S. M.; Riley, G.; Smith, D. R.; Bartlett, S.; Heidbreder, C. A.; Atkins, A. R.; Lacroix, L. P.; Dawson, L. A.; Foley, A. G.; Regan, C. M.; Upton, N. *European journal of pharmacology* **2006**, *553*, 109.

(79) Haydar, S. N.; Yun, H.; Andrae, P. M.; Mattes, J.; Zhang, J.; Kramer, A.; Smith, D. L.; Huselton, C.; Graf, R.; Aschmies, S.; Schechter, L. E.; Comery, T. A.; Robichaud, A. J. *J Med Chem* **2010**, *53*, 2521.

(80) Cushing, D. J.; Zgombick, J. M.; Nelson, D. L.; Cohen, M. L. *The Journal of pharmacology and experimental therapeutics* **1996**, *277*, 1560.

(81) Lovenberg, T. W.; Baron, B. M.; de Lecea, L.; Miller, J. D.; Prosser, R. A.; Rea, M. A.; Foye, P. E.; Racke, M.; Slone, A. L.; Siegel, B. W.; et al. *Neuron* **1993**, *11*, 449.

(82) Dewkar, G. K.; Peddi, S.; Mosier, P. D.; Roth, B. L.; Westkaemper, R. B. *Bioorg Med Chem Lett* **2008**, *18*, 5268.

(83) Wishart, G.; Bremner, D. H.; Sturrock, K. R. *Receptors & channels* **1999**, *6*, 317.

(84) Wang, C. D.; Gallaher, T. K.; Shih, J. C. *Molecular pharmacology* **1993**, *43*, 931.

(85) Westkaemper, R. B.; Glennon, R. A. *Pharmacology, biochemistry, and behavior* **1991**, *40*, 1019.

(86) Holtje, H. D.; Batzenschlager, A.; Briem, H.; Bruggmann, J. *Pharmazie in unserer Zeit* **1991**, *20*, 59.

(87) Andersen, K.; Liljefors, T.; Gundertofte, K.; Perregaard, J.; Bogeso, K. P. *Journal of medicinal chemistry* **1994**, *37*, 950.

(88) Mokrosz, J. L.; Strekowski, L.; Duszynska, B.; Harden, D. B.; Mokrosz, M. J.; Bojarski, A. J. *Die Pharmazie* **1994**, *49*, 801.

(89) Klabunde, T.; Evers, A. *Chembiochem* **2005**, *6*, 876.

(90) http://www.pdsp.med.unc.edu/.

(91) Zhang, A.; Zhang, Y.; Branfman, A. R.; Baldessarini, R. J.; Neumeyer, J. L. *J Med Chem* **2007**, *50*, 171.

(92) Shamma, M.; Guinaudeau, H. *Nat Prod Rep* **1986**, *3*, 345.

(93) Anakabe, E. *Synthesis* **2004**, *7*, 1093.

(94) Mahiou, V.; Roblot, F.; Hocquemiller, R.; Cave, A.; Rojas de Arias, A.; Inchausti, A.; Yaluff, G.; Fournet, A.; Angelo, A. *J Nat Prod* **1994**, *57*, 890.

(95) Munoz, V.; Sauvain, M.; Mollinedo, P.; Callapa, J.; Rojas, I.; Gimenez, A.; Valentin, A.; Mallie, M. *Planta Med* **1999**, *65*, 448.

(96) Cassels, B. K. A., M.; Cognet, P.; Speisky, H *Pharmacol. Res.* **1995**, *31*, 103.

(97) Loghin, F.; Chagraoui, A.; Asencio, M.; Comoy, E.; Speisky, H.; Cassels, B. K.; Protais, P. *Eur J Pharm Sci* **2003**, *18*, 133.

(98) Zhelyazkova-Savova, M. D.; Zhelyazkov, D. K. *J Pharm Pharmacol* **2003**, *55*, 125.

(99) Wang. B.H.; Lu, Z. X. P., G.-M. *Planta Med.* **1997**, *63*, 494.

(100) Orhana, I.; Ozcelik, B.; Karaoglu, T.; Sener, B. *Z Naturforsch C* **2007**, *62*, 19.

(101) Tang, H.; Wei, Y. B.; Zhang, C.; Ning, F. X.; Qiao, W.; Huang, S. L.; Ma, L.; Huang, Z. S.; Gu, L. Q. *Eur J Med Chem* **2009**, *44*, 2523.

(102) Protais, P.; Arbaoui, J.; Bakkali, E. H.; Bermejo, A.; Cortes, D. *J Nat Prod* **1995**, *58*, 1475.

(103) Gao, Y.; Zong, R.; Campbell, A.; Kula, N. S.; Baldessarini, R. J.; Neumeyer, J. L. *J Med Chem* **1988**, *31*, 1392.

(104) Schaus, J. M.; Titus, R. D.; Foreman, M. M.; Mason, N. R.; Truex, L. L. *J Med Chem* **1990**, *33*, 600.

(105) Sobarzo-Sanchez, E. M.; Arbaoui, J.; Protais, P.; Cassels, B. K. *J Nat Prod* **2000**, *63*, 480.

(106) Neumeyer, J. L. *Synthesis and Structure-Activity Relationships of Aporphines as Dopamine Receptor Agonists and Antagonists*; Springer-Verlag: Berlin, 1985.

(107) Baldessarini, R. J.; Marsh, E. R.; Kula, N. S.; Zong, R.; Neumeyer, J. L. *European journal of pharmacology* **1994**, *254*, 199.

(108) Cannon, J. G.; Mohan, P.; Bojarski, J.; Long, J. P.; Bhatnagar, R. K.; Leonard, P. A.; Flynn, J. R.; Chatterjee, T. K. *J Med Chem* **1988**, *31*, 313.

(109) Cannon, J. G.; Moe, S. T.; Long, J. P. *Chirality* **1991**, *3*, 19.

(110) Csutoras, C.; Zhang, A.; Zhang, K.; Kula, N. S.; Baldessarini, R. J.; Neumeyer, J. L. *Bioorg Med Chem* **2004**, *12*, 3553.

(111) Linnanen, T.; Brisander, M.; Unelius, L.; Sundholm, G.; Hacksell, U.; Johansson, A. M. *J Med Chem* **2000**, *43*, 1339.

(112) Linnanen, T.; Brisander, M.; Mohell, N.; Johansson, A. M. *Bioorg Med Chem Lett* **2001**, *11*, 367.

(113) Hayes, M. W.; Fung, V. S.; Kimber, T. E.; O'Sullivan, J. D. *Med J Aust* **2010**, *192*, 144.

(114) Tsukiyama, M.; Ueki, T.; Yasuda, Y.; Kikuchi, H.; Akaishi, T.; Okumura, H.; Abe, K. *Planta Med* **2009**, *75*, 1393.

(115) Barrera, C.; Ericsson, D.; Suarez, C.; Enrique, L. *Biochemical Systematics and Ecology* **2009**, *37*, 522.

(116) Correa, J. E.; Rios, C. H.; del Rosario Castillo, A.; Romero, L. I.; Ortega-Barria, E.; Coley, P. D.; Kursar, T. A.; Heller, M. V.; Gerwick, W. H.; Rios, L. C. *Planta Med* **2006**, *72*, 270.

(117) Shoji, N.; Umeyama, A.; Takemoto, T. *Journal of pharmaceutical sciences* **1984**, *73*, 568.

(118) Indra, B.; Matsunaga, K.; Hoshino, O.; Suzuki, M.; Ogasawara, H.; Ohizumi, Y. *European journal of pharmacology* **2002**, *437*, 173.

(119) Fantegrossi, W. E.; Godlewski, T.; Karabenick, R. L.; Stephens, J. M.; Ullrich, T.; Rice, K. C.; Woods, J. H. *Psychopharmacology* **2003**, *166*, 202.

(120) Fantegrossi, W. E.; Kiessel, C. L.; Leach, P. T.; Van Martin, C.; Karabenick, R. L.; Chen, X.; Ohizumi, Y.; Ullrich, T.; Rice, K. C.; Woods, J. H. *Psychopharmacology* **2004**, *173*, 270.

(121) Peroutka, S. J.; Lebovitz, R. M.; Snyder, S. H. *Science (New York, N.Y* **1981**, *212*, 827.

(122) Indra, B.; Matsunaga, K.; Hoshino, O.; Suzuki, M.; Ogasawara, H.; Ishiguro, M.; Ohizumi, Y. *Canadian journal of physiology and pharmacology* **2002**, *80*, 198.

(123) Chambers, J. J.; Nichols, D. E. *Journal of computer-aided molecular design* **2002**, *16*, 511.

(124) Wall, S. C.; Gu, H.; Rudnick, G. *Molecular pharmacology* **1995**, *47*, 544.

(125) Rothman, R. B.; Baumann, M. H.; Dersch, C. M.; Romero, D. V.; Rice, K. C.; Carroll, F. I.; Partilla, J. S. *Synapse* **2001**, *39*, 32.

(126) Sprague, J. E.; Brutcher, R. E.; Mills, E. M.; Caden, D.; Rusyniak, D. E. *Br J Pharmacol* **2004**, *142*, 667.

(127) Bexis, S.; Docherty, J. R. *Br J Pharmacol* **2008**, *153*, 591.

(128) Liechti, M. E.; Saur, M. R.; Gamma, A.; Hell, D.; Vollenweider, F. X. *Neuropsychopharmacology* **2000**, *23*, 396.

(129) Blessing, W. W.; Seaman, B.; Pedersen, N. P.; Ootsuka, Y. *J Neurosci* **2003**, *23*, 6385.

(130) Shioda, K.; Nisijima, K.; Yoshino, T.; Kuboshima, K.; Iwamura, T.; Yui, K.; Kato, S. *Neurotoxicology* **2008**, *29*, 1030.

(131) Schmidt, A. W.; Lebel, L. A.; Howard, H. R., Jr.; Zorn, S. H. *European journal of pharmacology* **2001**, *425*, 197.

(132) Verrico, C. D.; Miller, G. M.; Madras, B. K. *Psychopharmacology* **2007**, *189*, 489.

(133) Schmidt, C. J. *The Journal of pharmacology and experimental therapeutics* **1987**, *240*, 1.

(134) Malberg, J. E.; Sabol, K. E.; Seiden, L. S. *The Journal of pharmacology and experimental therapeutics* **1996**, *278*, 258.

(135) Aguirre, N.; Ballaz, S.; Lasheras, B.; Del Rio, J. *European journal of pharmacology* **1998**, *346*, 181.

(136) Mortensen, O. V.; Kristensen, A. S.; Wiborg, O. *J Neurochem* **2001**, *79*, 237.

(137) Berger, U. V.; Gu, X. F.; Azmitia, E. C. *European journal of pharmacology* **1992**, *215*, 153.

(138) Bordet, R.; Thomas, P.; Dupuis, B. *Am J Psychiatry* **1998**, *155*, 1346.

(139) Maurer, H. H.; Bickeboeller-Friedrich, J.; Kraemer, T.; Peters, F. T. *Toxicol Lett* **2000**, *112-113*, 133.

(140) Tucker, G. T.; Lennard, M. S.; Ellis, S. W.; Woods, H. F.; Cho, A. K.; Lin, L. Y.; Hiratsuka, A.; Schmitz, D. A.; Chu, T. Y. *Biochem Pharmacol* **1994**, *47*, 1151.

(141) Oesterheld, J. R.; Armstrong, S. C.; Cozza, K. L. *Psychosomatics* **2004**, *45*, 84.

(142) Upreti, V. V.; Eddington, N. D. *Journal of pharmaceutical sciences* **2008**, *97*, 1593.

(143) Bexis, S.; Docherty, J. R. *Br J Pharmacol* **2009**, *158*, 259.

(144) Morphy, R.; Rankovic, Z. *J Med Chem* **2006**, *49*, 4961.

Chapter 2

(1) Fantegrossi, W. E.; Kiessel, C. L.; Leach, P. T.; Van Martin, C.; Karabenick, R. L.; Chen, X.; Ohizumi, Y.; Ullrich, T.; Rice, K. C.; Woods, J. H. *Psychopharmacology* **2004**, *173*, 270.

(2) Indra, B.; Matsunaga, K.; Hoshino, O.; Suzuki, M.; Ogasawara, H.; Ishiguro, M.; Ohizumi, Y. *Canadian journal of physiology and pharmacology* **2002**, *80*, 198.

(3) Indra, B.; Matsunaga, K.; Hoshino, O.; Suzuki, M.; Ogasawara, H.; Ohizumi, Y. *European journal of pharmacology* **2002**, *437*, 173.

(4) Kupchan, S. M.; Liepa, A. J. *Journal of the American Chemical Society* **1973**, *95*, 4062.

(5) Hoshino, O.; Suzuki, M.; Ogasawara, H. *Heterocycles* **2000**, *52*, 751.

(6) Hara, H.; Komoriya, S.; Miyashita, T.; Hoshino, O. *Tetrahedron: Asymmetry* **1995**, *6*, 1683.

(7) Landais, Y.; Robin, J. P. *Tetrahedron* **1992**, *48*, 7185.

(8) Gottlieb, L.; Meyers, A. I. *J. Org. Chem* **1990**, *55*, 5659.

(9) Kita, Y.; Arisawa, M.; Gyoten, M.; Nakajima, M.; Hamada, R.; Toma, H.; Takada, T. *J Org Chem* **1998**, *63*, 6625.

(10) Herrero, M. T.; Tellitu, I.; Dominguez, E.; Hernandez, S.; Moreno, I.; SanMartin, R. *Tetrahedron* **2002**, *58*, 8581.

(11) Anakabe, E. *Synthesis* **2004**, *7*, 1093.

(12) Moreno, I.; Tellitu, I.; Etayo, J.; SanMartin, R.; Dominguez, E. *Tetrahedron* **2001**, *57* 5403.

(13) Pingaew, R.; Ruchirawat, S. *Synlett* **2007**, *15*, 2363.

(14) Zalan, Z.; Martinek, T.; Lazar, L.; Fulop, F. *Tetrahedron* **2003**, *59*, 9117.

(15) Lafrance, M.; Gorelsky, S. I.; Fagnou, K. *Journal of the American Chemical Society* **2007**, *129*, 14570.

(16) Campeau, L. C.; Parisien, M.; Leblanc, M.; Fagnou, K. *Journal of the American Chemical Society* **2004**, *126*, 9186.

(17) Garcia-Cuadrado, D.; de Mendoza, P.; Braga, A. A.; Maseras, F.; Echavarren, A. M. *Journal of the American Chemical Society* **2007**, *129*, 6880.

(18) Lafrance, M.; Lapointe, D.; Fagnou, K. *Tetrahedron* **2008**, *64*, 6015.

(19) Chaudhary, S.; Pecic, S.; Legendre, O.; Harding, W. W. *Tetrahedron Lett* **2009**, *50*, 2437.

(20) Moreno-Manas, M. R., A.; Suau, R. *Tetrahedron* **2004**, *60*, 5725.

(21) Ahmed F. Abdel-Magid; Kenneth G. Carson; Bruce D. Harris; Cynyhia A. Maryanoff; Shah, R. D. *J. Org. Chem.* **1996**, *61*, 3849.

(22) Bermejo, A.; Andreu, I.; Suvire, F.; Leonce, S.; Caignard, D. H.; Renard, P.; Pierre, A.; Enriz, R. D.; Cortes, D.; Cabedo, N. *Journal of medicinal chemistry* **2002**, *45*, 5058.

(23) Chambers, J. J.; Nichols, D. E. *Journal of computer-aided molecular design* **2002**, *16*, 511.

(24) Julie A. McCarron, V. W. P. *Journal of Labelled Compounds and Radiopharmaceuticals* **2003**, *46*, 1127.

(25) Rao, N. S. K. L., Shoei-Sheng *Journal of the Chinese Chemical Society* **2000**, *47*, 1227.

(26) Chaudhary, S.; Pecic, S.; Legendre, O.; Navarro, H. A.; Harding, W. W. *Bioorg Med Chem Lett* **2009**, *19*, 2530.

(27) http://www.pdsp.med.unc.edu/.

(28) Leifert, W. R. *G Protein Coupled Receptors in Drug Discovery*; Humana Press: New York, 2009; Vol. 552.

(29) Schmidhammer, H.; Jennewein, H. K.; Krassnig, R.; Traynor, J. R.; Patel, D.; Bell, K.; Froschauer, G.; Mattersberger, K.; Jachs-Ewinger, C.; Jura, P.; et al. *J Med Chem* **1995**, *38*, 3071.

(30) Fantegrossi, W. E.; Godlewski, T.; Karabenick, R. L.; Stephens, J. M.; Ullrich, T.; Rice, K. C.; Woods, J. H. *Psychopharmacology* **2003**, *166*, 202.

(31) Nash, J. F. *Life sciences* **1990**, *47*, 2401.

(32) Fantegrossi, W. E.; Ullrich, T.; Rice, K. C.; Woods, J. H.; Winger, G. *Psychopharmacology* **2002**, *161*, 356.

(33) Liechti, M. E.; Saur, M. R.; Gamma, A.; Hell, D.; Vollenweider, F. X. *Neuropsychopharmacology* **2000**, *23*, 396.

(34) Indra, B.; Tadano, T.; Nakagawasai, O.; Arai, Y.; Yasuhara, H.; Ohizumi, Y.; Kisara, K. *Life sciences* **2002**, *70*, 2647.

(35) Blessing, W. W.; Seaman, B.; Pedersen, N. P.; Ootsuka, Y. *J Neurosci* **2003**, *23*, 6385.

(36) Shioda, K.; Nisijima, K.; Yoshino, T.; Kuboshima, K.; Iwamura, T.; Yui, K.; Kato, S. *Neurotoxicology* **2008**, *29*, 1030.

(37) Zhang, A.; Zhang, Y.; Branfman, A. R.; Baldessarini, R. J.; Neumeyer, J. L. *J Med Chem* **2007**, *50*, 171.

(38) Cannon, J. G.; Flaherty, P. T.; Ozkutlu, U.; Long, J. P. *J Med Chem* **1995**, *38*, 1841.

(39) Yasuda, M.; Yamashita, T.; Kojima, R.; Shima, K. *Heterocycles* **1996**, *43*.

(40) Yasuda, M.; Hamasuna, S.; Yamano, K.; Kubo, J.; Shima, K. *Heterocycles* **1992**, *34*, 965.

(41) Suau, R.; Lopez-Romero, J. M.; Rico, R. *Tetrahedron Lett* **1996**, *37*, 9357.

(42) Ramana, M. M. V.; Prashant, V. P. *Tetrahedron Lett* **1996**, *37*, 1671.

(43) Kupchan, S. M.; Liepa, A. J.; Kameswaran, V.; Bryan, R. F. *Journal of the American Chemical Society* **1973**, *95*, 6861.

(44) Deslongchamps, P. *Stereoelctronic Effect in Organic Chemistry*; Pergamon Press: Oxford, 1983.

(45) Sha, C. K.; Young, J. J.; Yeh, C. P.; Chang, S. C.; Wang, S. L. *Journal of Organic Chemistry* **1991**, *56*, 2694.

(46) Mavandadi, F.; Pilotti, A. *Drug Discov Today* **2006**, *11*, 165.

(47) Kappe, C. O.; Dallinger, D. *Nat Rev Drug Discov* **2006**, *5*, 51.

(48) Lindh, J.; Enquist, P. A.; Pilotti, A.; Nilsson, P.; Larhed, M. *J Org Chem* **2007**, *72*, 7957.

(49) Arvela, R. K.; Leadbeater, N. E. *J Org Chem* **2005**, *70*, 1786.

(50) Datta, G. K.; Vallin, K. S.; Larhed, M. *Mol Divers* **2003**, *7*, 107.

(51) Walla, P.; Kappe, C. O. *Chem Commun (Camb)* **2004**, 564.

(52) Legendre, O.; Pecic, S.; Chaudhary, S.; Zimmerman, S. M.; Fantegrossi, W. E.; Harding, W. W. *Bioorg Med Chem Lett* **2010**, *20*, 628.

(53) Liu, Z.; Chen, X.; Yu, L.; Zhen, X.; Zhang, A. *Bioorg Med Chem* **2008**, *16*, 6675.

(54) Cannon, J. G.; Mohan, P.; Bojarski, J.; Long, J. P.; Bhatnagar, R. K.; Leonard, P. A.; Flynn, J. R.; Chatterjee, T. K. *J Med Chem* **1988**, *31*, 313.

(55) Neumeyer, J. L. *Synthesis and Structure-Activity Relationships of Aporphines as Dopamine Receptor Agonists and Antagonists*; Springer-Verlag: Berlin, 1985.

(56) Martin, G. R.; Humphrey, P. P. *Neuropharmacology* **1994**, *33*, 261.

(57) Porter, R. H.; Benwell, K. R.; Lamb, H.; Malcolm, C. S.; Allen, N. H.; Revell, D. F.; Adams, D. R.; Sheardown, M. J. *Br J Pharmacol* **1999**, *128*, 13.

(58) Newton, R. A.; Phipps, S. L.; Flanigan, T. P.; Newberry, N. R.; Carey, J. E.; Kumar, C.; McDonald, B.; Chen, C.; Elliott, J. M. *J Neurochem* **1996**, *67*, 2521.

(59) Jerman, J. C.; Brough, S. J.; Gager, T.; Wood, M.; Coldwell, M. C.; Smart, D.; Middlemiss, D. N. *European journal of pharmacology* **2001**, *414*, 23.

(60) Kenakin, T. *ACS Chem Biol* **2009**.

(61) Lloyd-Williams, F.; Giralt, E. *Chem Soc Rev* **2001**, *30*, 145.

(62) Runyon, S. P.; Mosier, P. D.; Roth, B. L.; Glennon, R. A.; Westkaemper, R. B. *J Med Chem* **2008**, *51*, 6808.

(63) Aranda, R.; Villalba, K.; Ravina, E.; Masaguer, C. F.; Brea, J.; Areias, F.; Dominguez, E.; Selent, J.; Lopez, L.; Sanz, F.; Pastor, M.; Loza, M. I. *J Med Chem* **2008**, *51*, 6085.

(64) Meltzer, H. Y.; Matsubara, S.; Lee, J. C. *Psychopharmacol Bull* **1989**, *25*, 390.

(65) Roth, B. L.; Tandra, S.; Burgess, L. H.; Sibley, D. R.; Meltzer, H. Y. *Psychopharmacology* **1995**, *120*, 365.

(66) Wisniewski, H. M.; Vorbrodt, A. W.; Wegiel, J. *Annals of the New York Academy of Sciences* **1997**, *826*, 161.

(67) Thomas, T.; Bryant, M.; Clark, L.; Garces, A.; Rhodin, J. *Microvasc Res* **2001**, *61*, 28.

(68) Rhodin, J. A.; Thomas, T. *Microcirculation* **2001**, *8*, 207.

(69) Chodobski, A.; Szmydynger-Chodobska, J. *Microsc Res Tech* **2001**, *52*, 65.

(70) Petty, M. A.; Lo, E. H. *Prog Neurobiol* **2002**, *68*, 311.

(71) Lipinski, C. A.; Lombardo, F.; Dominy, B. W.; Feeney, P. J. *Adv Drug Deliv Rev* **2001**, *46*, 3.

(72) Reichel, A. *Curr Drug Metab* **2006**, *7*, 183.

(73) Zhang, A.; Csutoras, C.; Zong, R.; Neumeyer, J. L. *Organic letters* **2005**, *7*, 3239.

(74) Csutoras, C.; Zhang, A.; Zhang, K.; Kula, N. S.; Baldessarini, R. J.; Neumeyer, J. L. *Bioorg Med Chem* **2004**, *12*, 3553.

(75) Bhal, S. K.; Kassam, K.; Peirson, I. G.; Pearl, G. M. *Mol Pharm* **2007**, *4*, 556.

(76) Lemke, T. W., David *Foye`s Principles of Medicinal Chemistry*; Sixth ed., 2008.

(77) Ringdahl, B.; Chan, R. P. K.; Craig, C.; Cava, M. P.; Shamma, M. *J. Nat. Prod.* **1981**, *44*, 80.

Chapter 3

(1) Kroeze, W. K.; Kristiansen, K.; Roth, B. L. *Curr Top Med Chem* **2002**, *2*, 507.

(2) Bojarski, A. J. *Curr Top Med Chem* **2006**, *6*, 2005.

(3) Runyon, S. P.; Mosier, P. D.; Roth, B. L.; Glennon, R. A.; Westkaemper, R. B. *J Med Chem* **2008**, *51*, 6808.

(4) Sanger, D. J.; Soubrane, C.; Scatton, B. *Ann Pharm Fr* **2007**, *65*, 268.

(5) Shelton, R. C.; Papakostas, G. I. *Acta Psychiatr Scand* **2008**, *117*, 253.

(6) Meltzer, H. Y.; Li, Z.; Kaneda, Y.; Ichikawa, J. *Prog Neuropsychopharmacol Biol Psychiatry* **2003**, *27*, 1159.

(7) Levin, E. D.; Slade, S.; Johnson, M.; Petro, A.; Horton, K.; Williams, P.; Rezvani, A. H.; Rose, J. E. *Eur J Pharmacol* **2008**, *600*, 93.

(8) Nic Dhonnchadha, B. A.; Fox, R. G.; Stutz, S. J.; Rice, K. C.; Cunningham, K. A. *Behav Neurosci* **2009**, *123*, 382.

(9) Chaudhary, S.; Pecic, S.; Legendre, O.; Navarro, H. A.; Harding, W. W. *Bioorg Med Chem Lett* **2009**, *19*, 2530.

(10) Aranda, R.; Villalba, K.; Ravina, E.; Masaguer, C. F.; Brea, J.; Areias, F.; Dominguez, E.; Selent, J.; Lopez, L.; Sanz, F.; Pastor, M.; Loza, M. I. *J Med Chem* **2008**, *51*, 6085.

(11) Chambers, J. J.; Nichols, D. E. *J Comput Aided Mol Des* **2002**, *16*, 511.

(12) Leifert, W. R. *G Protein Coupled Receptors in Drug Discovery*; Humana Press: New York, 2009; Vol. 552.

(13) Berman, H. M.; Westbrook, J.; Feng, Z.; Gilliland, G.; Bhat, T. N.; Weissig, H.; Shindyalov, I. N.; Bourne, P. E. *Nucleic Acids Res* **2000**, *28*, 235.

(14) Altschul, S. F.; Madden, T. L.; Schaffer, A. A.; Zhang, J.; Zhang, Z.; Miller, W.; Lipman, D. J. *Nucleic Acids Res* **1997**, *25*, 3389.

(15) Warne, T.; Serrano-Vega, M. J.; Baker, J. G.; Moukhametzianov, R.; Edwards, P. C.; Henderson, R.; Leslie, A. G.; Tate, C. G.; Schertler, G. F. *Nature* **2008**, *454*, 486.

(16) Jaakola, V. P.; Griffith, M. T.; Hanson, M. A.; Cherezov, V.; Chien, E. Y.; Lane, J. R.; Ijzerman, A. P.; Stevens, R. C. *Science* **2008**, *322*, 1211.

(17) Cherezov, V.; Rosenbaum, D. M.; Hanson, M. A.; Rasmussen, S. G.; Thian, F. S.; Kobilka, T. S.; Choi, H. J.; Kuhn, P.; Weis, W. I.; Kobilka, B. K.; Stevens, R. C. *Science* **2007**, *318*, 1258.

(18) Okada, T.; Sugihara, M.; Bondar, A. N.; Elstner, M.; Entel, P.; Buss, V. *J Mol Biol* **2004**, *342*, 571.

(19) Murakami, M.; Kouyama, T. *Nature* **2008**, *453*, 363.

(20) Mobarec, J. C.; Sanchez, R.; Filizola, M. *J Med Chem* **2009**.

(21) Westkaemper, R. B.; Glennon, R. A. *Curr Top Med Chem* **2002**, *2*, 575.

(22) Evers, A.; Hessler, G.; Matter, H.; Klabunde, T. *J Med Chem* **2005**, *48*, 5448.

(23) Sousa, S. F.; Fernandes, P. A.; Ramos, M. J. *Proteins* **2006**, *65*, 15.

(24) Indra, B.; Matsunaga, K.; Hoshino, O.; Suzuki, M.; Ogasawara, H.; Ishiguro, M.; Ohizumi, Y. *Canadian journal of physiology and pharmacology* **2002**, *80*, 198.

(25) Higgins, D. G.; Sharp, P. M. *Gene* **1988**, *73*, 237.

(26) Abagyan R; Totrov M; D., K. *J Comput Chem* **1994**, *15*, 488.

(27) Abagyan, R. A.; Batalov, S. *J Mol Biol* **1997**, *273*, 355.

(28) Baldwin, J. M.; Schertler, G. F.; Unger, V. M. *J Mol Biol* **1997**, *272*, 144.

(29) Sali, A.; Blundell, T. L. *J Mol Biol* **1993**, *234*, 779.

(30) Li, M.; Wang, B. *J Mol Model* **2007**, *13*, 1237.

(31) Morris, A. L.; MacArthur, M. W.; Hutchinson, E. G.; Thornton, J. M. *Proteins* **1992**, *12*, 345.

(32) Colovos, C.; Yeates, T. O. *Protein Sci* **1993**, *2*, 1511.

(33) Eisenberg, D.; Luthy, R.; Bowie, J. U. *Methods Enzymol* **1997**, *277*, 396.

(34) Pontius, J.; Richelle, J.; Wodak, S. J. *J Mol Biol* **1996**, *264*, 121.

(35) Wallace, A. C.; Laskowski, R. A.; Thornton, J. M. *Protein Eng* **1995**, *8*, 127.

(36) Spedding, M.; Newman-Tancredi, A.; Millan, M. J.; Dacquet, C.; Michel, A. N.; Jacoby, E.; Vickery, B.; Tallentire, D. *Neuropharmacology* **1998**, *37*, 769.

(37) Kristiansen, K.; Kroeze, W. K.; Willins, D. L.; Gelber, E. I.; Savage, J. E.; Glennon, R. A.; Roth, B. L. *The Journal of pharmacology and experimental therapeutics* **2000**, *293*, 735.

(38) Choudhary, M. S.; Sachs, N.; Uluer, A.; Glennon, R. A.; Westkaemper, R. B.; Roth, B. L. *Molecular pharmacology* **1995**, *47*, 450.

(39) Choudhary, M. S.; Craigo, S.; Roth, B. L. *Molecular pharmacology* **1993**, *43*, 755.

(40) Klabunde, T.; Evers, A. *Chembiochem* **2005**, *6*, 876.

(41) Bruno, A.; Guadix, A. E.; Costantino, G. *J Chem Inf Model* **2009**, *49*, 1602.

(42) Mobarec, J. C.; Sanchez, R.; Filizola, M. *J Med Chem* **2009**, *52*, 5207.

(43) Dezi, C.; Brea, J.; Alvarado, M.; Ravina, E.; Masaguer, C. F.; Loza, M. I.; Sanz, F.; Pastor, M. *J Med Chem* **2007**, *50*, 3242.

(44) http://www.pdsp.med.unc.edu/.

(45) Wheeler, D. L.; Barrett, T.; Benson, D. A.; Bryant, S. H.; Canese, K.; Chetvernin, V.; Church, D. M.; Dicuccio, M.; Edgar, R.; Federhen, S.; Feolo, M.; Geer, L. Y.; Helmberg, W.; Kapustin, Y.; Khovayko, O.; Landsman, D.; Lipman, D. J.; Madden, T. L.; Maglott, D. R.; Miller, V.; Ostell, J.; Pruitt, K. D.; Schuler, G. D.; Shumway, M.; Sequeira, E.;

Sherry, S. T.; Sirotkin, K.; Souvorov, A.; Starchenko, G.; Tatusov, R. L.; Tatusova, T. A.; Wagner, L.; Yaschenko, E. *Nucleic Acids Res* **2008**, *36*, D13.

(46) Thompson, J. D.; Gibson, T. J.; Plewniak, F.; Jeanmougin, F.; Higgins, D. G. *Nucleic Acids Res* **1997**, *25*, 4876.

Chapter 4

(1) Corey-Bloom, J. *International psychogeriatrics / IPA* **2002**, *14 Suppl 1*, 51.

(2) Akhondzadeh, S.; Noroozian, M. *IDrugs* **2002**, *5*, 1062.

(3) Backman, L.; Jones, S.; Berger, A. K.; Laukka, E. J.; Small, B. J. *Neuropsychology* **2005**, *19*, 520.

(4) http://www.alzheimers.org/ 2010.

(5) Ellis, J. M. *J Am Osteopath Assoc* **2005**, *105*, 145.

(6) Shimokawa, A.; Yatomi, N.; Anamizu, S.; Torii, S.; Isono, H.; Sugai, Y.; Kohno, M. *Brain and cognition* **2001**, *47*, 423.

(7) Weinshenker, D. *Current Alzheimer research* **2008**, *5*, 342.

(8) Poirier, J. *Int J Clin Pract Suppl* **2002**, 6.

(9) Hardy, J. *J Alzheimers Dis* **2006**, *9*, 151.

(10) Pimplikar, S. W. *The international journal of biochemistry & cell biology* **2009**, *41*, 1261.

(11) Korczyn, A. D. *Alzheimers Dement* **2008**, *4*, 176.

(12) Eckman, C. B.; Eckman, E. A. *Neurologic clinics* **2007**, *25*, 669.

(13) Hardy, J. A.; Higgins, G. A. *Science (New York, N.Y* **1992**, *256*, 184.

(14) Hardy, J.; Selkoe, D. J. *Science (New York, N.Y* **2002**, *297*, 353.

(15) Vassar, R.; Citron, M. *Neuron* **2000**, *27*, 419.

(16) Selkoe, D. J. *Physiol Rev* **2001**, *81*, 741.

(17) Arendt, T. *Neuroscience* **2001**, *102*, 723.

(18) Mehta, N. D.; Refolo, L. M.; Eckman, C.; Sanders, S.; Yager, D.; Perez-Tur, J.; Younkin, S.; Duff, K.; Hardy, J.; Hutton, M. *Ann Neurol* **1998**, *43*, 256.

(19) Games, D.; Adams, D.; Alessandrini, R.; Barbour, R.; Berthelette, P.; Blackwell, C.; Carr, T.; Clemens, J.; Donaldson, T.; Gillespie, F.; et al. *Nature* **1995**, *373*, 523.

(20) Braak, H.; Braak, E. *Acta Neuropathol* **1991**, *82*, 239.

(21) Malamas, M. S.; Erdei, J.; Gunawan, I.; Barnes, K.; Johnson, M.; Hui, Y.; Turner, J.; Hu, Y.; Wagner, E.; Fan, K.; Olland, A.; Bard, J.; Robichaud, A. J. *J Med Chem* **2009**, *52*, 6314.

(22) Hom, R. K.; Fang, L. Y.; Mamo, S.; Tung, J. S.; Guinn, A. C.; Walker, D. E.; Davis, D. L.; Gailunas, A. F.; Thorsett, E. D.; Sinha, S.; Knops, J. E.; Jewett, N. E.; Anderson, J. P.; John, V. *J Med Chem* **2003**, *46*, 1799.

(23) Davis, J. N.; Tung, A.; Chak, S. S.; Ventura, E. E.; Byrd-Williams, C. E.; Alexander, K. E.; Lane, C. J.; Weigensberg, M. J.; Spruijt-Metz, D.; Goran, M. I. *Med Sci Sports Exerc* **2009**, *41*, 1494.

(24) Bard, F.; Cannon, C.; Barbour, R.; Burke, R. L.; Games, D.; Grajeda, H.; Guido, T.; Hu, K.; Huang, J.; Johnson-Wood, K.; Khan, K.; Kholodenko,

D.; Lee, M.; Lieberburg, I.; Motter, R.; Nguyen, M.; Soriano, F.; Vasquez, N.; Weiss, K.; Welch, B.; Seubert, P.; Schenk, D.; Yednock, T. *Nat Med* **2000**, *6*, 916.

(25) DeMattos, R. B.; Bales, K. R.; Cummins, D. J.; Dodart, J. C.; Paul, S. M.; Holtzman, D. M. *Proc Natl Acad Sci U S A* **2001**, *98*, 8850.

(26) Nuutinen, T.; Suuronen, T.; Kauppinen, A.; Salminen, A. *Brain Res Rev* **2009**, *61*, 89.

(27) Jick, H.; Zornberg, G. L.; Jick, S. S.; Seshadri, S.; Drachman, D. A. *Lancet* **2000**, *356*, 1627.

(28) Wolozin, B. *Neuron* **2004**, *41*, 7.

(29) Solomon, A.; Kareholt, I.; Ngandu, T.; Wolozin, B.; Macdonald, S. W.; Winblad, B.; Nissinen, A.; Tuomilehto, J.; Soininen, H.; Kivipelto, M. *Neurobiol Aging* **2009**, *30*, 1006.

(30) Scapini, E.; Scheltens, P.; Feldman, H. *Lancet Neurol.* **2003**, *2*, 539.

(31) Ballatore, C.; Brunden, K. R.; Piscitelli, F.; James, M. J.; Crowe, A.; Yao, Y.; Hyde, E.; Trojanowski, J. Q.; Lee, V. M.; Smith, A. B., 3rd *J Med Chem* **2010**, *53*, 3739.

(32) Weggen, S.; Eriksen, J. L.; Das, P.; Sagi, S. A.; Wang, R.; Pietrzik, C. U.; Findlay, K. A.; Smith, T. E.; Murphy, M. P.; Bulter, T.; Kang, D. E.; Marquez-Sterling, N.; Golde, T. E.; Koo, E. H. *Nature* **2001**, *414*, 212.

(33) Sivaprakasam, K. *Current medicinal chemistry* **2006**, *13*, 2179.

(34) Terry, A. V., Jr.; Buccafusco, J. J. *The Journal of pharmacology and experimental therapeutics* **2003**, *306*, 821.

(35) Inestrosa, N. C.; Alvarez, A.; Dinamarca, M. C.; Perez-Acle, T.; Colombres, M. *Curr Alzheimer Res* **2005**, *2*, 301.

(36) Munoz, F. J.; Aldunate, R.; Inestrosa, N. C. *Neuroreport* **1999**, *10*, 3621.

(37) Sabbagh, M. N.; Farlow, M. R.; Relkin, N.; Beach, T. G. *Alzheimer's & Dementia* **2006**, *2*, 118.

(38) Colombres, M.; Sagal, J. P.; Inestrosa, N. C. *Current pharmaceutical design* **2004**, *10*, 3121.

(39) Ballard, C. G. *Eur Neurol* **2002**, *47*, 64.

(40) Hansen, R. A.; Gartlehner, G.; Webb, A. P.; Morgan, L. C.; Moore, C. G.; Jonas, D. E. *Clinical interventions in aging* **2008**, *3*, 211.

(41) Ritchie, C. W.; Ames, D.; Clayton, T.; Lai, R. *Am J Geriatr Psychiatry* **2004**, *12*, 358.

(42) Wagstaff, A. J.; McTavish, D. *Drugs & aging* **1994**, *4*, 510.

(43) Loy, C.; Schneider, L. *Cochrane database of systematic reviews (Online)* **2006**, CD001747.

(44) Heinze, M.; Andreae, D.; Grohmann, R. *Pharmacopsychiatry* **2002**, *35*, 79.

(45) Dunn, N. R.; Pearce, G. L.; Shakir, S. A. *Journal of psychopharmacology (Oxford, England)* **2000**, *14*, 406.

(46) Moller, H. J. *Eur Neuropsychopharmacol* **1999**, *9 Suppl 2*, S53.

(47) Bolognesi, M. L.; Minarini, A.; Rosini, M.; Tumiatti, V.; Melchiorre, C. *Mini reviews in medicinal chemistry* **2008**, *8*, 960.

(48) Cavalli, A.; Bottegoni, G.; Raco, C.; De Vivo, M.; Recanatini, M. *Journal of medicinal chemistry* **2004**, *47*, 3991.

(49) Zhou, X.; Wang, X. B.; Wang, T.; Kong, L. Y. *Bioorg Med Chem* **2008**, *16*, 8011.

(50) Inestrosa, N. C.; Sagal, J. P.; Colombres, M. *Sub-cellular biochemistry* **2005**, *38*, 299.

(51) De Ferrari, G. V.; Canales, M. A.; Shin, I.; Weiner, L. M.; Silman, I.; Inestrosa, N. C. *Biochemistry* **2001**, *40*, 10447.

(52) Bolognesi, M. L.; Cavalli, A.; Valgimigli, L.; Bartolini, M.; Rosini, M.; Andrisano, V.; Recanatini, M.; Melchiorre, C. *Journal of medicinal chemistry* **2007**, *50*, 6446.

(53) del Monte-Millan, M.; Garcia-Palomero, E.; Valenzuela, R.; Usan, P.; de Austria, C.; Munoz-Ruiz, P.; Rubio, L.; Dorronsoro, I.; Martinez, A.; Medina, M. *J Mol Neurosci* **2006**, *30*, 85.

(54) Munoz-Ruiz, P.; Rubio, L.; Garcia-Palomero, E.; Dorronsoro, I.; del Monte-Millan, M.; Valenzuela, R.; Usan, P.; de Austria, C.; Bartolini, M.; Andrisano, V.; Bidon-Chanal, A.; Orozco, M.; Luque, F. J.; Medina, M.; Martinez, A. *Journal of medicinal chemistry* **2005**, *48*, 7223.

(55) Camps, P.; Formosa, X.; Munoz-Torrero, D.; Petrignet, J.; Badia, A.; Clos, M. V. *Journal of medicinal chemistry* **2005**, *48*, 1701.

(56) Cannon, J. G.; Flaherty, P. T.; Ozkutlu, U.; Long, J. P. *J Med Chem* **1995**, *38*, 1841.

(57) Zhang, A.; Zhang, Y.; Branfman, A. R.; Baldessarini, R. J.; Neumeyer, J. L. *J Med Chem* **2007**, *50*, 171.

(58) Hung, T. M.; Na, M.; Dat, N. T.; Ngoc, T. M.; Youn, U.; Kim, H. J.; Min, B. S.; Lee, J.; Bae, K. *Journal of ethnopharmacology* **2008**, *119*, 74.

(59) Tang, H.; Wei, Y. B.; Zhang, C.; Ning, F. X.; Qiao, W.; Huang, S. L.; Ma, L.; Huang, Z. S.; Gu, L. Q. *European journal of medicinal chemistry* **2009**.

(60) Markmee, S.; Ruchirawat, S.; Prachyawarakorn, V.; Ingkaninan, K.; Khorana, N. *Bioorg Med Chem Lett* **2006**, *16*, 2170.

(61) Kiely, J. S.; Moos, W. H.; Pavia, M. R.; Schwarz, R. D.; Woodard, G. L. *Anal Biochem* **1991**, *196*, 439.

(62) Rhee, I. K.; van de Meent, M.; Ingkaninan, K.; Verpoorte, R. *Journal of chromatography* **2001**, *915*, 217.

(63) Marston, A.; Kissling, J.; Hostettmann, K. *Phytochem Anal* **2002**, *13*, 51.

(64) Greenblatt, H. M.; Kryger, G.; Lewis, T.; Silman, I.; Sussman, J. L. *FEBS Lett* **1999**, *463*, 321.

(65) Tang, H.; Wei, Y. B.; Zhang, C.; Ning, F. X.; Qiao, W.; Huang, S. L.; Ma, L.; Huang, Z. S.; Gu, L. Q. *Eur J Med Chem* **2009**, *44*, 2523.

(66) Tang, H.; Ning, F. X.; Wei, Y. B.; Huang, S. L.; Huang, Z. S.; Chan, A. S.; Gu, L. Q. *Bioorg Med Chem Lett* **2007**, *17*, 3765.

(67) Cardozo, T.; Totrov, M.; Abagyan, R. *Proteins: Structure, Function, and Genetics* **1995**, *23*, 403.

(68) Berman, H. M.; Westbrook, J.; Feng, Z.; Gilliland, G.; Bhat, T. N.; Weissig, H.; Shindyalov, I. N.; Bourne, P. E. *Nucleic Acids Res* **2000**, *28*, 235.

(69) Carolan, C. G.; Gaynor, J. M.; Dillon, G. P.; Khan, D.; Ryder, S. A.; Reidy, S.; Gilmer, J. F. *Chem Biol Interact* **2008**, *175*, 293.

(70) Szegletes, T.; Mallender, W. D.; Rosenberry, T. L. *Biochemistry* **1998**, *37*, 4206.

(71) Sussman, J. L.; Harel, M.; Frolow, F.; Oefner, C.; Goldman, A.; Toker, L.; Silman, I. *Science (New York, N.Y* **1991**, *253*, 872.

(72) Harel, M.; Quinn, D. M.; Nair, H. K.; Silman, I.; Sussman, J. L. *Journal of the American Chemical Society* **1996**, *118*, 2340.

(73) Wallace, A. C.; Laskowski, R. A.; Thornton, J. M. *Protein Engineering* **1995**, *8*, 127.

(74) Perry, E. K. *Br Med Bull* **1986**, *42*, 63.

(75) Bartus, R. T.; Dean, R. L.; Pontecorvo, M. J.; Flicker, C. *Ann N Y Acad Sci* **1985**, *444*, 332.

(76) Holzgrabe, U.; Kapkova, P.; Alptuzun, V.; Scheiber, J.; Kugelmann, E. *Expert Opin Ther Targets* **2007**, *11*, 161.

(77) Shen, Y.; Zhang, J.; Sheng, R.; Dong, X.; He, Q.; Yang, B.; Hu, Y. *J Enzyme Inhib Med Chem* **2009**, *24*, 372.

(78) Haviv, H.; Wong, D. M.; Silman, I.; Sussman, J. L. *Curr Top Med Chem* **2007**, *7*, 375.

(79) Dorronsoro, I.; Alonso, D.; Castro, A.; del Monte, M.; Garcia-Palomero, E.; Martinez, A. *Arch Pharm (Weinheim)* **2005**, *338*, 18.

(80) Ribeiro, R. d. A.; De Lores Arnaiz, G. R. *Phytomedicine* **2000**, *7*, 313.

(81) Adsersen, A.; Kjolbye, A.; Dall, O.; Jager, A. K. *Journal of ethnopharmacology* **2007**, *113*, 179.

(82) Abagyan, R. A.; Batalov, S. *J Mol Biol* **1997**, *273*, 355.

(83) Farag, N. A.; Mohamed, S. R.; Soliman, G. A. *Bioorg Med Chem* **2008**, *16*, 9009.